UNCLASSIFIED

ORNL
MASTER COPY

ORNL-2384
Health and Safety
TID-4500 (13th ed. Rev.)

HEALTH PHYSICS DIVISION

ANNUAL PROGRESS REPORT

FOR PERIOD ENDING JULY 31, 1957

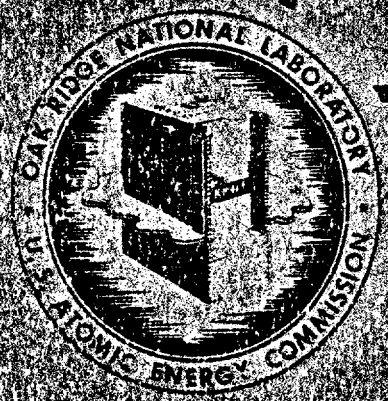

OAK RIDGE NATIONAL LABORATORY
OPERATED BY
UNION CARBIDE NUCLEAR COMPANY
A Division of Union Carbide and Carbon Corporation
POST OFFICE BOX X · OAK RIDGE, TENNESSEE

ChemRisk Document No. 720

UNCLASSIFIED

Printed in USA. Price $3.50 cents. Available from the
Office of Technical Services
U. S. Department of Commerce
Washington 25, D. C.

LEGAL NOTICE

This report was prepared as an account of Government sponsored work. Neither the United States, nor the Commission, nor any person acting on behalf of the Commission

A. Makes any warranty or representation, express or implied, with respect to the accuracy, completeness, or usefulness of the information contained in this report, or that the use of any information, apparatus, method, or process disclosed in this report may not infringe privately owned rights; or

B. Assumes any liabilities with respect to the use of, or for damages resulting from the use of any information, apparatus, method, or process disclosed in this report.

As used in the above, "person acting on behalf of the Commission" includes any employee or contractor of the Commission to the extent that such employee or contractor prepares, handles or distributes, or provides access to, any information pursuant to his employment or contract with the Commission.

25

ORNL-2384
ERRATA

HEALTH PHYSICS DIVISION ANNUAL PROGRESS REPORT

FOR PERIOD ENDING JULY 31, 1957

Please make the following corrections in your copy of the subject report.

Page 18, Table 13. Values in column labeled "Soil" should read 1.32×10^5
7.13×10^4
3.56×10^4
3.04×10^4

Page 20, Figure 10, Dwg. 24790. In all cases, read "mites" for "units."

Page 36, Table 29. Title should read "Gamma Spectrometric Analyses of Tree Material (Microcuries per Gram of Dry Weight).

Page 94, Equation 5. The symbol "me^2" in the formula should be changed to "m^2e^2."

Page 100, Figure 47. The symbol "$\longleftarrow\delta_{1/2} = 0.19\%\longrightarrow$" should be moved upward to a T value of 2.2%.

Page 101, Figure 49. Label on right hand curve should be "$T/\delta_{1/2}$." Also, right hand ordinate scale should be designated "$T/\delta_{1/2}$."

UNCLASSIFIED

ORNL-2384
Health and Safety
TID-4500 (13th ed. Rev.)

Contract No. W-7405-eng-26

HEALTH PHYSICS DIVISION ANNUAL PROGRESS REPORT

For Period Ending July 31, 1957

K. Z. Morgan, Director

DATE ISSUED

NOV 11 1957

OAK RIDGE NATIONAL LABORATORY
Operated by
UNION CARBIDE NUCLEAR COMPANY
A Division of Union Carbide and Carbon Corporation
Post Office Box X
Oak Ridge, Tennessee

UNCLASSIFIED

Semiannual reports previously issued by the Health Physics Division are as follows:

ORNL-1596	Period Ending July 31, 1953
ORNL-1684	Period Ending January 31, 1954
ORNL-1763	Period Ending July 31, 1954
ORNL-1860	Period Ending January 31, 1955
ORNL-1942	Period Ending July 31, 1955
ORNL-2049	Period Ending January 31, 1956
ORNL-2151	Period Ending July 31, 1956

ORNL-2384
Health and Safety
TID-4500 (13th ed. Rev.)

INTERNAL DISTRIBUTION

1. C. E. Center
2. Biology Library
3. Health Physics Library
4–6. Central Research Library
7. Reactor Experimental Engineering Library
8–24. Laboratory Records Department
25. Laboratory Records, ORNL R.C.
26. L. B. Emlet (K-25)
27. J. P. Murray (Y-12)
28. A. M. Weinberg
29. J. A. Swartout
30. E. D. Shipley
31. E. J. Murphy
32. M. L. Nelson
33. K. Z. Morgan
34. S. C. Lind
35. A. S. Householder
36. C. S. Harrill
37. C. E. Winters
38. A. H. Snell
39. E. H. Taylor
40. W. H. Jordan
41. T. A. Lincoln
42. A. Hollaender
43. F. L. Culler
44. D. W. Cardwell
45. D. Phillips
46. M. T. Kelley
47. E. E. Anderson
48. R. S. Livingston
49. C. P. Keim
50. K. E. Cowser
51. C. D. Susano
52. L. B. Farabee
53. F. J. Davis
54. R. J. Morton
55. C. E. Haynes
56. Hugh F. Henry (K-25)
57. E. G. Struxness
58. W. E. Cohn
59. H. H. Hubbell
60. D. E. Arthur
61. J. Neufeld
62. M. L. Randolph
63. P. M. Reyling
64. G. C. Williams
65. M. J. Skinner
66. J. C. Hart
67. T. H. J. Burnett
68. W. J. Lacy
69. M. J. Cook
70. G. S. Hurst
71. T. E. Bortner
72. J. A. Lane
73. R. W. Johnson
74. H. P. Yockey
75. C. E. Clifford
76. J. L. Gabbard
77. R. A. Charpie
78. G. E. Boyd
79. A. C. Upton
80. L. C. Emerson (Y-12)
81. D. M. Davis
82. P. E. Brown
83. E. D. Gupton
84. J. C. Ledbetter
85. R. L. Clark
86. G. C. Cain
87. L. C. Johnson
88. W. Ogg
89. O. D. Teague
90. E. L. Sharp
91. E. J. Kuna
92. H. H. Abee
93. C. R. Guinn
94. A. D. Warden
95. E. B. Wagner
96. C. C. Sartain
97. J. R. Muir
98. J. A. Auxier
99. M. F. Fair
100. S. I. Auerbach
101. G. W. Royster, Jr.
102. R. R. Dickison
103. J. D. McLendon
104. F. W. Sanders
105. F. C. Maienschein
106. W. J. Boegly, Jr.
107. F. L. Parker
108. W. E. Lotz

109. B. Fish
110. M. B. Edwards
111. F. M. Empson
112. R. D. Birkhoff
113. R. H. Ritchie
114. J. A. Harter
115. W. G. Stone
116. J. S. Cheka
117. P. N. Hensley
118. R. W. Peelle
119. ORNL – Y-12 Technical Library, Document Reference Section

EXTERNAL DISTRIBUTION

120. C. P. Straub, Public Health Service, Robert A. Taft Sanitary Engineering Center
121. R. M. Collier, University of Florida
122. Physics and Engineering Group, Balcones Research Center, RFD 4, Box 189, Austin, Texas
123. R. F. Bacher, California Institute of Technology
124. G. E. Thoma, USAF
125. H. J. McAlduff, AEC, Oak Ridge
126. Vanderbilt University (Physics Library)
127. Massachusetts Institute of Technology (Department of Electrical Engineering)
128. University of California (Gerhard Klein)
129. R. M. Richardson, U.S. Geological Survey, 2-C P. O. Building, Knoxville, Tennessee
130. C. V. Theis, U.S. Geological Survey, Box 433, Albuquerque, New Mexico
131. Lola Lyons, Librarian, Olin Industries, Inc., East Alton, Illinois
132. Jack Story, Health Physicist, North Carolina State College, Raleigh, North Carolina
133. J. H. Ebersole, USSS Nautilus, c/o Fleet Post Office, New York, New York
134. David S. Smith, Health and Safety Division, U.S. Atomic Energy Commission, Chicago Operations Office, P. O. Box 59, Lemont, Illinois
135. Division of Research and Development, AEC, ORO
136. S. C. Sigoloff, USAF, The Radiobiological Laboratory, University of Texas and U.S. Air Force, Austin, Texas
137. Robert Wood, Department of Physics, Memorial Center, 444 E. 68th St., New York 21, New York
138. Robert E. Yoder, Harvard School of Public Health, 55 Shattuck Street, Boston, Massachusetts
139. John Wolfe, Division of Biology and Medicine, U.S. Atomic Energy Commission, Washington, D.C.
140. Orlando Park, Department of Biology, Northwestern University, Evanston, Illinois
141. Eugene Odum, Department of Zoology, University of Georgia, Athens, Georgia
142. W. T. Ham, Medical College of Virginia, Richmond, Virginia
143. F. H. W. Noll, Department of Physics, Berea College, Berea, Kentucky
144. S. R. Bernard, Committee on Mathematical Biology, University of Chicago, 5741 Drexel Avenue, Chicago 37, Illinois
145. B. G. Saunders, Bosscha Laboratory, University of Indonesia, Djalan, Ganeca 10, Bandung, Indonesia
146. Herbert E. Stokinger, Bureau of State Service, Department of Health Education and Welfare, Penn 14 Broadway, Cincinnati 2, Ohio

147–722. Given distribution as shown in TID-4500 (13th ed. Rev.) under Health and Safety category (100 copies – OTS)

CONTENTS

APPLIED RADIOBIOLOGY 1
Distribution and Excretion of Uranium in Man 1
Ecological Research 10
Maximum Permissible Concentration Studies 39
Analysis of Human Tissue for Trace Elements 44
Spectrographic Analysis of Normal Human Tissue 49
The Determination of Alkali and Alkaline Earth Elements in Normal Human Tissue by Flame Photometry 49
WASTE DISPOSAL RESEARCH 52
Development of Analytical Methods 52
Chemical Decontamination of Fuel Process Wastes 58
Disposal of High-Level Wastes by Sintering 58
Disposal into Geologic Structures 69
Soil Disposal of Intermediate-Level Wastes 71
RADIATION DOSIMETRY 89
Dosimetry Applications 89
Physics of Tissue Damage 91
Theoretical Physics of Dosimetry 92
Experimental Physics of Dosimetry 97
Instrument Research 108
EDUCATION, TRAINING, AND CONSULTATION 118
PUBLICATIONS 119
PAPERS 122
LECTURES 126

HEALTH PHYSICS DIVISION ANNUAL PROGRESS REPORT

APPLIED RADIOBIOLOGY

E. G. Struxness

DISTRIBUTION AND EXCRETION OF URANIUM IN MAN

S. R. Bernard
G. J. Dodson
M. B. Edwards
L. B. Farabee
B. R. Fish
N. L. Gillum
W. E. Lotz
J. R. Muir
G. W. Royster, Jr.
F. W. Sanders

Experimental Body Burden Counter

A device to measure directly the body burden of enriched uranium in a small live animal has been designed and constructed. It will be used to measure the amount of enriched uranium remaining in an animal at various times after injection. The present counter is designed to measure the body burden of mice or rats. If the first model is successful, subsequent models will be constructed for use on larger animals.

The principle of operation is based on the irradiation of the animal by a thermal neutron beam of relatively low flux. This causes fissioning of a portion of the U^{235} present in the animal. The fast fission neutrons are moderated in graphite and detected by BF_3 counters, which are shielded from the thermal neutron beam. The count rate (fission rate) is proportional to the amount of U^{235} present. It is hoped that amounts from 0.025 to 1.0 μc of enriched uranium in a mouse can be measured.

The present apparatus, shown in Fig. 1, consists of a cube of AGHT graphite (44 × 44 × 40 in.) containing a Po-Be neutron source at its bottom center. Another cube of graphite (40 × 40 × 28 in.) wrapped in 0.025-in. cadmium sheet rests on top of the source cube. The upper cube has an open, cadmium-lined, vertical chimney (8 × 8 × 28 in.) through its center. The animal is placed in this chimney. The detectors are placed in the upper cube also; 12 BF_3 tubes are placed on the sides of a square around the chimney. The electronic equipment consists of a high-voltage supply, an A1A preamplifier, an A1 linear amplifier, scalers, and a timer.

Testing is under way to determine the optimum positions for the counter tubes, animal, and neutron source. Neutron flux measurements are being made at various points in the apparatus. Future improvements must increase the primary irradiating flux while minimizing the background from the Po-Be source.

Digital Computer

The Garwood procedure[1] for fitting nonlinear curves as previously described by Cornell[2] and Bernard *et al.*[3] has been applied to linear combinations of exponentials. The method programed for the Oracle[4] and applied to uranium distribution and excretion data was found to be unstable.[3]

---

[1] F. Garwood, *Biometrika* 32, 46–58 (1941).

[2] R. G. Cornell, *A New Estimation Procedure for Linear Combinations of Exponentials*, ORNL-2120 (June 21, 1956).

[3] S. R. Bernard *et al.*, *Fitting Linear Combinations of Exponentials to Human Uranium-Excretion Data*, ORNL-2364 (to be published).

[4] S. R. Bernard *et al.*, *HP Semiann. Prog. Rep. July 31, 1956*, ORNL-2151, p 12.

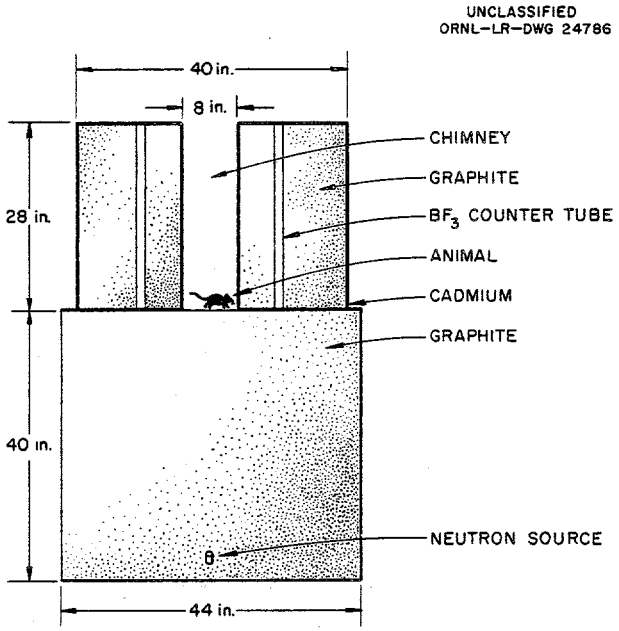

Fig. 1. Enriched-Uranium Body-Burden Counter.

An expedient suggested by Lucas,[5] in which the instability might be mitigated by directly inhibiting the amount of change required of the parameters, is now being investigated.

An iterative method for fitting nonlinear curves has been derived by Fish.[6] The method may be used to fit multiple exponentials as well as other types of functions, including mixed series. Although, in general, the procedure requires a greater number of iterations for convergence than do some other methods, it has the advantages of extreme stability and superior speed in performing each iteration. The procedure does not give the maximum likelihood estimates; however, an expedient[5] to improve the estimate is being investigated.

Application of the Analog Computer to Distribution and Excretion Models

An attempt has been made to analyze the human uranium excretion data of the Boston patients on the basis of a four-compartment model[7] with the addition of a second blood compartment to represent a nondiffusible protein-UO_2 complex. The diffusible-nondiffusible model was first treated with the exchange rates linear, and then in successive trials these rates were allowed to be proportional to various powers of the concentration of uranium in the blood. Although the excretion curve for each patient could be fitted better by using the added compartment, the parameters necessary for a fit for the data of one patient showed little relation to those for other patients. This result implied that, in order for the model to fit the data, a materially different set of parameters would have to be assumed for the data of each patient. In addition, the predicted blood content curve did not agree with the pattern shown by the measured values. It was concluded that, although such a diffusible-nondiffusible phase may have been operating, the effect was not great enough to account for the different excretion patterns of the patients.

An examination of the blood data revealed no apparent nonlinearity of sufficient magnitude to account for the excretion patterns. Also, the initial excretion rate became a progressively lower percentage of the injected dose as the injected dose increased. The postulation of a saturable pathway[8] between blood and urine offers a possibility of explaining all the excretion and blood data under one model; however, only preliminary work has been done on this model. Figure 2 shows an approximate solution for one set of data based upon average distribution and excretion parameters derived from a different and independent set of data[9] (Rochester patients). The apparent departure of the data from the predicted excretion toward the lower right hand side of the graph represents a period of abnormal body function just prior to the expiration of the patient. Because of the promise shown by this saturable model, further work is being done toward improving the present estimate of the parameters and testing the model.

Influence of Cortisone on the Deposition of Uranium

It has been shown that uranium concentrates in the proximal convoluted tubules of the kidney, and it is for this reason that the kidney is considered to be the critical organ for uranium toxicity. A

[5]H. L. Lucas, North Carolina State College, Raleigh, N. C., oral communication, January 1957.

[6]B. R. Fish, *Non-Linear Curve Fitting by Data Fractionation* (in manuscript).

[7]S. R. Bernard and E. G. Struxness, *A Study of the Distribution and Excretion of Uranium in Man — An Interim Report*, ORNL-2304 (June 4, 1957).

[8]B. R. Fish, "Practical Applications of an Analog Computer to Analysis of Distribution and Excretion Data," *Proceedings of the Third Annual Health Physics Society Meeting, Pittsburgh, Pa., June 17–19, 1957* (to be published).

[9]E. G. Struxness, *Health Physics Progress Report July 1, 1953–December 31, 1953*, Y-1074 (Oct. 29, 1954).

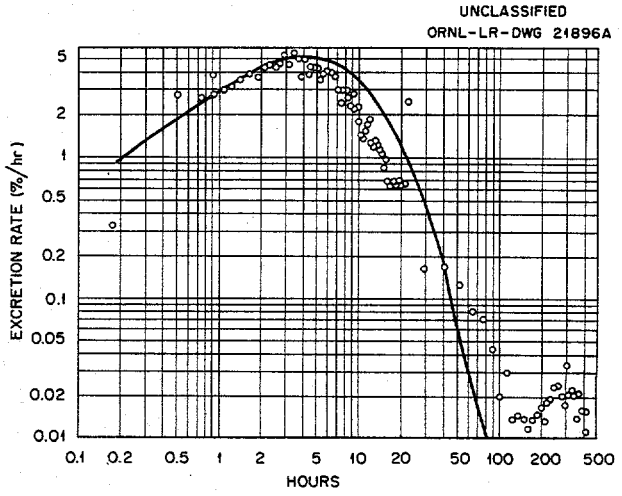

Fig. 2. Saturated Model for Case of Patient B-VI.

means of eliminating or preventing the accumulation of uranium in the kidney might be of some therapeutic significance in industrial accidents.

Lotz, Comar, and Rust[10] have found an increased deposition of Ca^{45} in the proximal convoluted tubules of rats treated with parathyroid extract. In addition the above authors found that the administration of cortisone to the parathyroid-treated animals prevented or markedly lowered the accumulation of Ca^{45} in the kidney.

Since calcium and uranium behave similarly in the body, it was felt that likewise cortisone treatment might prevent the accumulation of uranium in the kidney.

Eighteen rats were used to test the hypothesis. The experimental animals were given 12.5 mg of cortisone daily for five days prior to the injection of U^{235}, while the control animals received intramuscular injections of saline solution. Subsequently, all animals received 1 μc of U^{235} either intravenously or intraperitoneally and were sacrificed after 2 or 24 hr as indicated in Table 1. The data shown in Table 1 indicate that cortisone did not reduce the deposition of U^{235} in the kidney, but, conversely, increased the deposition.

Metabolic and Pathologic Studies of Orally Administered U^{233}

Fifty-two mice were used in an experiment to determine the uptake, distribution, and retention of U^{233} and to study the pathologic effects to the gastrointestinal tract from daily ad libitum ingestion of U^{233} via the drinking water. The drinking water contained 0.04 μc/ml of U^{233}. It was determined that the mice drank an average of 3 ml/day; thus, the U^{233} dose per mouse was 0.12 μc/day. Ten mice which had received U^{233} and three control mice were killed at each of four intervals of 30 days (30, 60, 90, and 120 days). The average amounts of U^{233} present in the gastrointestinal tract, bone, and kidney are shown in Table 2. The dose rate to the organ was calculated in rem/week except in the cases of kidney and bone; for these organs the mass was not determined.

Histological inspection of the gastrointestinal tract and kidneys revealed no signs of radiation damage from U^{233} at the 90- and 120-day intervals.

Quantitative Tests of Inhalation Apparatus

The uranium-fume inhalator shown in Fig. 3 and described previously[11] has undergone quantitative tests. Eight mongrel dogs were exposed and sacrificed within an hour after the inhalation exposure. Also, to test the validity of the method for predicting the amount of fume retained, seven sham experiments were performed with the apparatus. In the sham experiments, an electrostatic precipitator backed with a CWS charcoal cannister (to absorb ozone) was inserted in the line between the breathing valve and the aerosol container (Fig. 3). In this arrangement the dog breathes through the electrostatic precipitator, and the amount of uranium collected on the precipitator can be compared with the amount it is predicted the dog would inhale. To predict the amount the concentration of the aerosol in units of disintegrations/min/liter is multiplied by the volume of air breathed. However, the concentration is not

[10] W. E. Lotz, C. L. Comar, and J. H. Rust (in manuscript).

[11] S. R. Bernard *et al.*, *HP Semiann. Prog. Rep. July 31, 1956*, ORNL-2151, p 1–4.

Table 1. The Influence of Cortisone on the Accumulation of U^{235} in the Kidney of the Rat

Treatment	Number of Rats	Injection Route	Sacrifice Time (hr)	Average Amount of U^{235} in Kidneys (d/min)
Control	4	Intravenous	2	44,600
Cortisone	4	Intravenous	2	55,150
Control	3	Intraperitoneal	24	13,988
Cortisone	3	Intraperitoneal	24	18,577
Control	2	Intravenous	24	16,646
Cortisone	2	Intravenous	24	27,498

Table 2. Distribution of U^{233} in Mice Following Continuous Intake at a Rate of 0.12 μc/day for 120 Days

Organ	Microcuries Present (qf_2)*	Microcuries per Gram of Critical Organ	rem/week**
Stomach	0.0009	0.002	36
Small intestine	0.001	0.001	18
Large intestine	0.009	0.03	536
Caecum	0.002	0.008	143
Bone	0.0005		
Kidney	0.00005		
Total	0.013		

*q = body burden, f_2 = fraction in critical organ of that in total body.

**rem/week = $qf_2\left(\frac{\Sigma\, E(\mathrm{RBE})N}{2.8 \times 10^{-3}}\right)$, $\Sigma\, E(\mathrm{RBE})N = 50$, m = mass of critical organ, in grams.

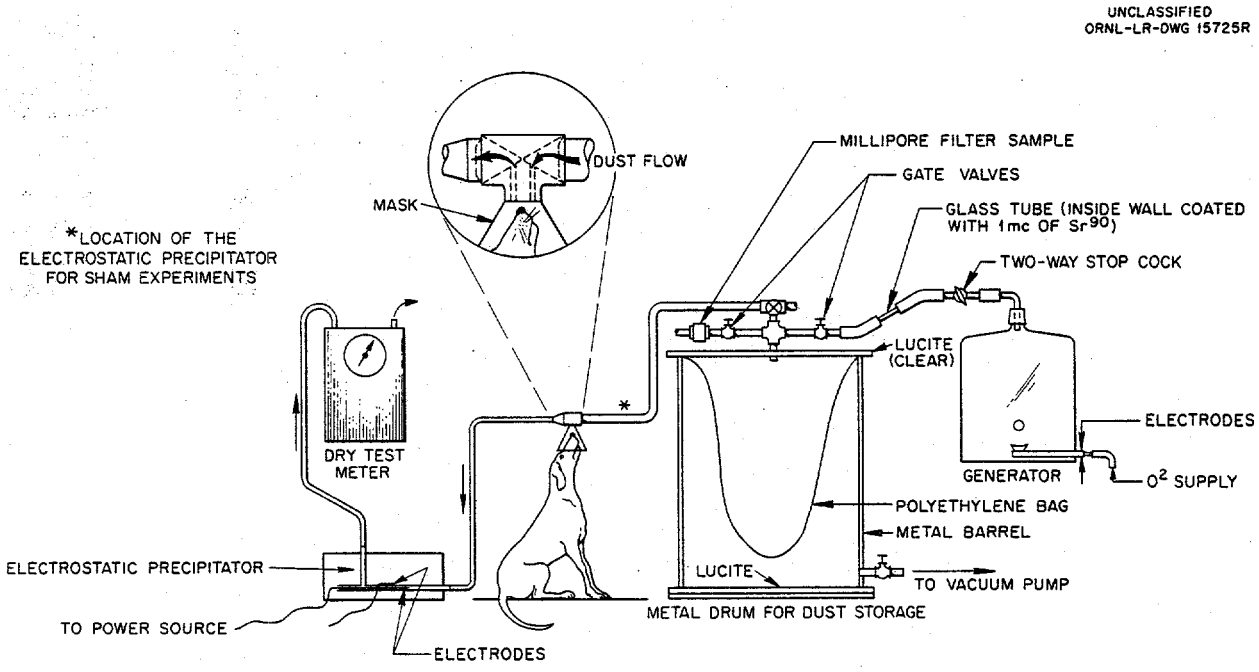

Fig. 3. Schematic Drawing of Inhalation Apparatus.

constant during the period of inhalation, and thus a numerical integration is performed. In Fig. 4 there appears an example of the procedure. A plot of the concentration values vs the liters of air inhaled is shown together with the average concentration over the interval of exposure (which interval is usually a 10-min period). Multiplying the liters breathed in the interval by the concentration in the interval and summing over the three intervals gives the amount inhaled. Table 3 gives the results of the seven sham experiments. Appearing in the first and second columns are, respectively, the disintegrations per minute (d/min) predicted and the d/min found on the precipitator.

The last column lists the ratios of these values. The mean value of these ratios is 0.915.

In the experiments with the eight mongrel dogs, the dogs were permitted to breathe the aerosol for approximately 30 to 40 min and the total d/min inhaled was obtained by the numerical integration of the concentration values. The total amount inhaled was then multiplied by 0.915, the factor determined in the sham experiments. Table 4 presents the data obtained in these experiments. Appearing in column 1 are the d/min inhaled, while column 2 shows the d/min exhaled, that is, the amount of uranium in exhaled air collected on the electrostatic precipitator. The differences between the values in column 1 and column 2 are the amounts retained, and these are shown in column 4. These values are compared with those

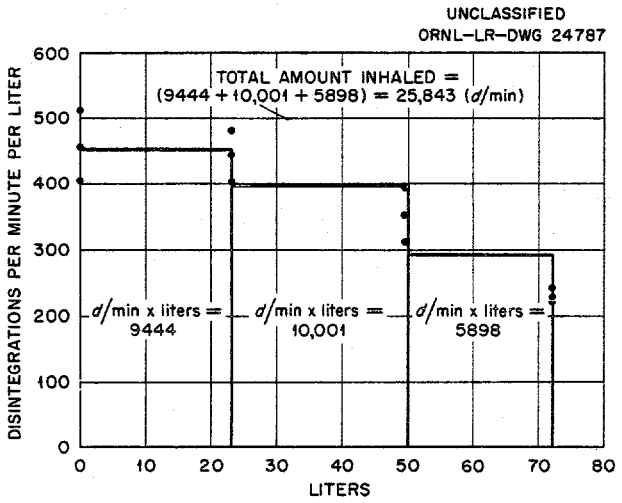

Fig. 4. Sample Calculation of Amount of Uranium Fume Inhaled.

Table 3. Results of Sham Tests

Amount Predicted (d/min)	Amount Found on Electrostatic Precipitator (d/min)	Ratio: d/min Found / d/min Predicted
27,624	27,096	0.981
144,190	143,286	0.994
68,947	63,582	0.922
22,254	19,777	0.889
7,866	7,207	0.916
52,990	44,100	0.832
37,730	32,775	0.869
	av	0.915

Table 4. Predicted Retention of Uranium Fumes in Dogs

Dog No.	(1) Predicted Amount Inhaled (d/min)	(2) Measured Amount Exhaled (d/min)	(3) Per Cent Exhaled	(4) Predicted Amount Retained, Col 1 – Col 2 (d/min)	(5) Measured Amount in Organ and Tissues (d/min)	(6) Ratio: Observed d/min / Predicted d/min
10	260,800	219,500	84.2	41,300	17,000	0.41
11	84,900	73,100	86.1	11,800	18,600	1.57
12	30,400	22,200	73.0	8,200	5,200	0.63
13	181,900	154,800	85.1	27,100	13,700	0.51
14	197,700	163,000	82.4	34,000	16,900	0.49
25	227,000	179,000	78.9	48,000	45,200	0.94
27	53,600	36,200	67.5	17,400	26,200	1.51
29	50,600	38,200	75.5	12,400	18,600	1.49
Av			79.1			0.944

listed in column 5, the d/min measured in the organs and tissues. Note that the average ratios of the measured d/min to the predicted d/min appear in column 6; these ratios range from 0.41 to 1.57, the average being 0.944. It is believed that the wide variation in values can be attributed to errors in the method of determining the total amount inhaled, and additional experiments are under way to test the validity of this method.

Column 3 of Table 4 lists the per cent of the dose which was exhaled; the average value is 79.1%. This is greater than the 25% which is listed in Handbook 52 (ref 12) and in the ICRP recommendations[13] and which is presently employed in the computation of maximum permissible concentrations. However, Handbook 52 and ICRP assume a mean particle size of 1 μ (ref 14). The mean particle size of the uranium fume is 0.36 μ. Lung retention – or, more precisely, lung deposition – is known to be a function of particle size. Maximum deposition occurs upon inhalation of aerosols whose particle size is 1 μ; lower deposition is found for smaller, for example, 0.4 μ, particles.[15] Thus, in part, the discrepancy in per cent exhaled can be attributed to the difference in particle sizes. Another factor contributing to the discrepancy is the error in the method of determining the total amount inhaled. Hence, the 80% exhaled lacks the desired significance until these errors can be resolved.

Table 5 presents the measured amount of enriched uranium in the organs and tissues of these eight mongrel dogs expressed in per cent of inhaled uranium. Wide variation in deposition in organs and tissues are noted to occur. On the average, the lungs contain 9.3% of the inhaled dose, while the gastrointestinal tract (trachea, esophagus, stomach, and intestines) contains 4.2% and the whole carcass averages 5.7%. These data also can be compared with the values listed in Handbook 52 and with the ICRP recommendations as shown in Table 6. Note that differences occur between the recommended values and the uranium-fume experiments. However, this is no cause for alarm since uranium fume cannot be said to be a representative compound furnishing inhalation exposure. There are no measurements of the deposition at the end of one day of exposure, but experiments are under way to obtain this data.

Pilot Studies of Excretion of Uranium During Exposure

Inhalation of Enriched Uranium Fumes. – Two dogs were administered enriched uranium fumes once per week for a period of five weeks. They were housed in metabolism cages during the course of the experiment, and samples of urine and feces were collected and measured for uranium. Urine specimens were collected from 8:00 AM to 8:00 AM the following day. All feces voided in the same period were taken to represent a daily elimination. Therefore, the measured uranium contained in each of the specimens roughly corresponds to a daily rate of uranium excretion. Figure 5 shows a plot of the measured d/min/day contained in feces and urine plotted vs time. Also, the predicted retained dose is plotted as arrows on the graph. The feces samples contain more uranium than do the urine specimens. Levels of uranium in urine and feces tend to decrease with time after inhalation exposure ceases. The possibilities for contamination of urine with uranium in the feces are real in this experiment and present a difficult problem. Additional experiments are being carried out and attempts to minimize the cross contamination are being made.

Ingestion of Uranium Oxide. – Two dogs were administered insoluble oxides of uranium once per week for a period of eight weeks and were housed in metabolism cages during the course of the experiment for the purpose of collecting urine and feces. The same procedure for collecting urine and feces specimens described above was followed. One dog received U_3O_8, while the other received UO_2. The oxides were weighed and then mixed with Hill's dog food in a Waring Blendor and given to the animal at feeding time. The average weekly dose was 11.1×10^6 d/min for dog 15 ingesting U_3O_8, and 8.7×10^6 d/min for dog 16 ingesting UO_2. Figure 6 shows the amounts of uranium excreted per day in the urine and feces of these two

[12] U.S. National Bureau of Standards, *Maximum Permissible Amounts of Radioisotopes in the Human Body and Maximum Permissible Concentrations in Air and Water*, Handbook 52 (1953), Superintendent of Documents, Washington 25, D. C.

[13] International Congress of Radiology, "Recommendations of the International Commission of Radiological Protection," *Brit J. Radiol. Suppl. 6*, (1955).

[14] K. Z. Morgan, personal communication.

[15] J. H. Brown *et al.*, *Am. J. Public Health* 40, 450–459 (1950).

Table 5. Tentative Distribution of Enriched Uranium in Dogs 1 hr After Inhalation of Metal Fumes

Dog No.	10	11	12	13	14	25	27	29	
Inhaled dose, d/min	260,800	84,900	30,400	181,900	197,700	227,000	53,600	50,600	
Body tissue, per cent of inhaled dose present in organ or tissue									Average
Blood	0.3	5.0*	2.8*	1.5*	0.3				2.0*
Skeleton						0.7	7.8		4.3
Kidneys (2)	0.03	0.1	0.1	0.1	0.07	0.1	0.1		0.1
Trachea	0.03	0.2	0.1	0.07	0.6	0.02	0.06	0.07	0.1
Esophagus	0.03	0.4	0.3	0.4	0.4	0.2	0.1	0.07	0.2
Stomach	2.4	0.2	3.2	0.5	0.2	0.004	6.6	2.6	2.0
Intestines	0.08	4.3	0.3	0.9	0.05	0.5	0.3	8.1	1.8
Lungs (2)	3.0	11.0	9.6	3.2	6.5	10.5	9.1	21.1	9.3
Liver	0.02	0.1	0.05	0.01	0.01	0.06			0.04
Spleen	0.01	0.2	0.01	0.04	0.002	0.01	0.02		0.04
Salivary glands (2)			0.005						0.005
Thyroid glands					0.02				0.02
Lymph glands					0.01				0.01
Skin, body						2.1*	8.4*		5.3*
Skin, head						1.1	8.4	3.5	4.3
Head						3.6	2.7	1.1	2.5
Nasal washings	0.7	0.4	0.5	0.8	0.2				0.5
Carcass						0.9	10.5		5.7
Fetus				0.03					0.03
Urine							0.03		0.03
Total	6.5	21.9	17.0	7.5	8.5	19.9	49.0	36.6	20.9

*Believed to be contaminated.

Table 6. Comparison Between ICRP Recommendations and Dog Data

Distribution	Uranium (%)			
	Readily Soluble Compounds		Other Uranium Compounds	
	ICRP	Dog Data	ICRP	Dog Data, U Fumes
Exhaled	25	Not tested	25	80
Deposited in upper respiratory tract and subsequently swallowed	50	Not tested	50	4
Deposited in lungs (lower respiratory passages)	25	Not tested	25*	10
Deposited in all organs other than above	0	Not tested	0	6

*Of this, half is eliminated from the lungs and swallowed in the first 24 hr, making a total of 62½% swallowed. The remaining 12½% is retained in the lungs with a half life of 120 days, it being assumed that this portion is taken up into body fluids.

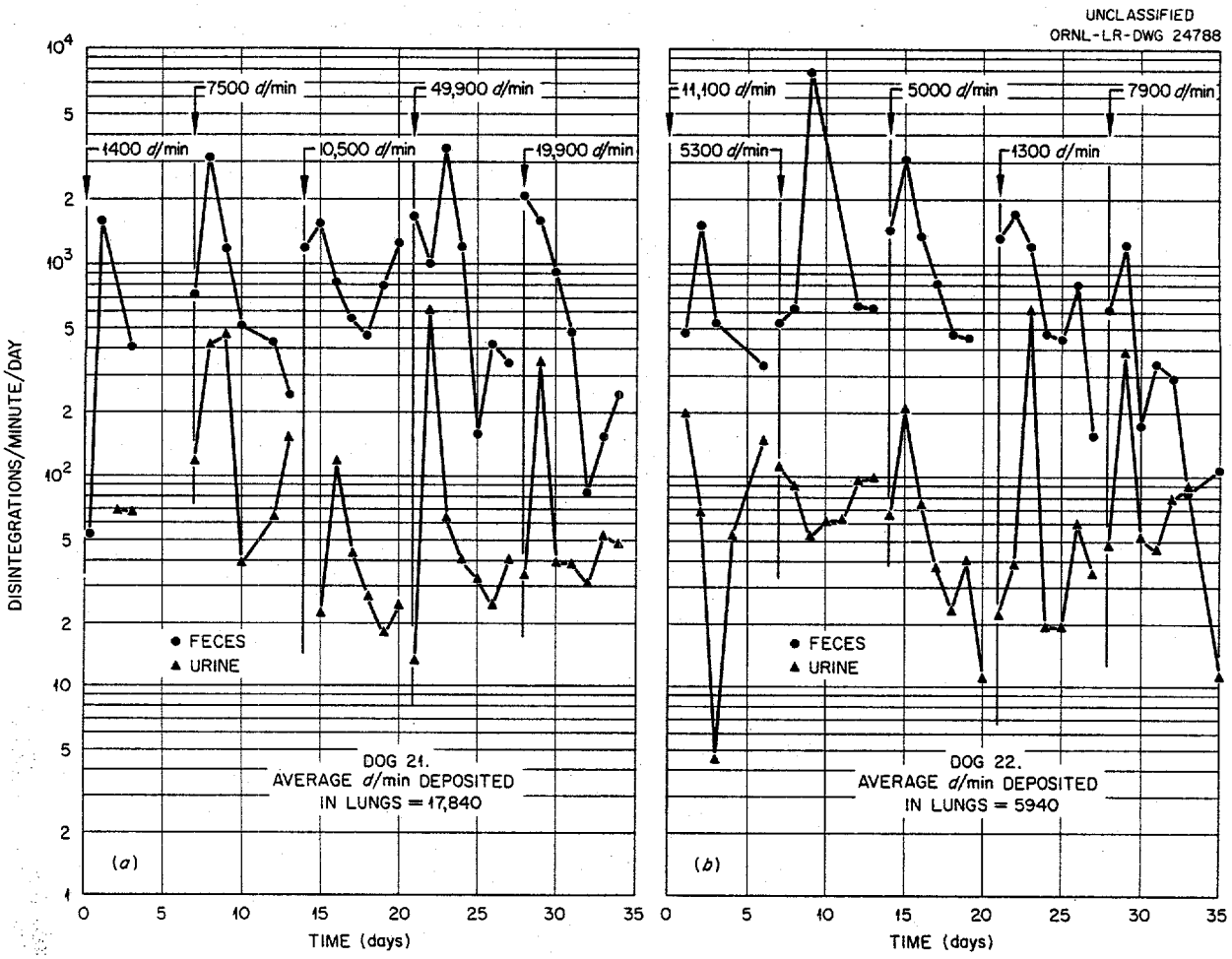

Fig. 5. Fecal and Urinary Excretion of Uranium During and After Inhalation of Enriched Uranium Fumes.

dogs. Note that the levels of uranium in the feces drop precipitously with time, exhibiting a decrease by a factor of 10^5 at the end of one week. Uranium levels in urine fluctuate, and they are noted to be low, relative to the levels in the feces. The ratio of d/min/day excreted in urine to d/min/day excreted in feces, the so-called urinary to fecal ratio, is lower by one or more orders of magnitude than that observed in the inhalation experiments.

Bioassay Techniques

An analytical procedure has been developed for the determination of uranium alpha activity in urine. This new technique is based on the use of a strongly basic anion exchange resin to remove the uranyl chloride complex from the urine solution. The chief advantage of this procedure is that urine can be used directly, thereby eliminating the laborious task of oxidizing the urine sample which is necessary in uranium urinalysis procedures currently in use. The eluted uranium can be evaporated and transferred directly to a stainless steel planchet for counting. The method is simple to carry out in ordinary laboratory operations, and requires no special equipment.

Kraus and Nelson[16] have demonstrated that a number of metal ions, including uranium, form stable complexes in a strong hydrochloric acid medium and this complex can be removed from the solution on an anion exchange resin. The adsorbability of uranium on the resin rises steeply with increasing HCl concentrations to a distribution

[16] K. A. Kraus and F. Nelson, *Proc. Intern. Conf. Peaceful Uses Atomic Energy, Geneva, 1955* **7**, 113 (1956).

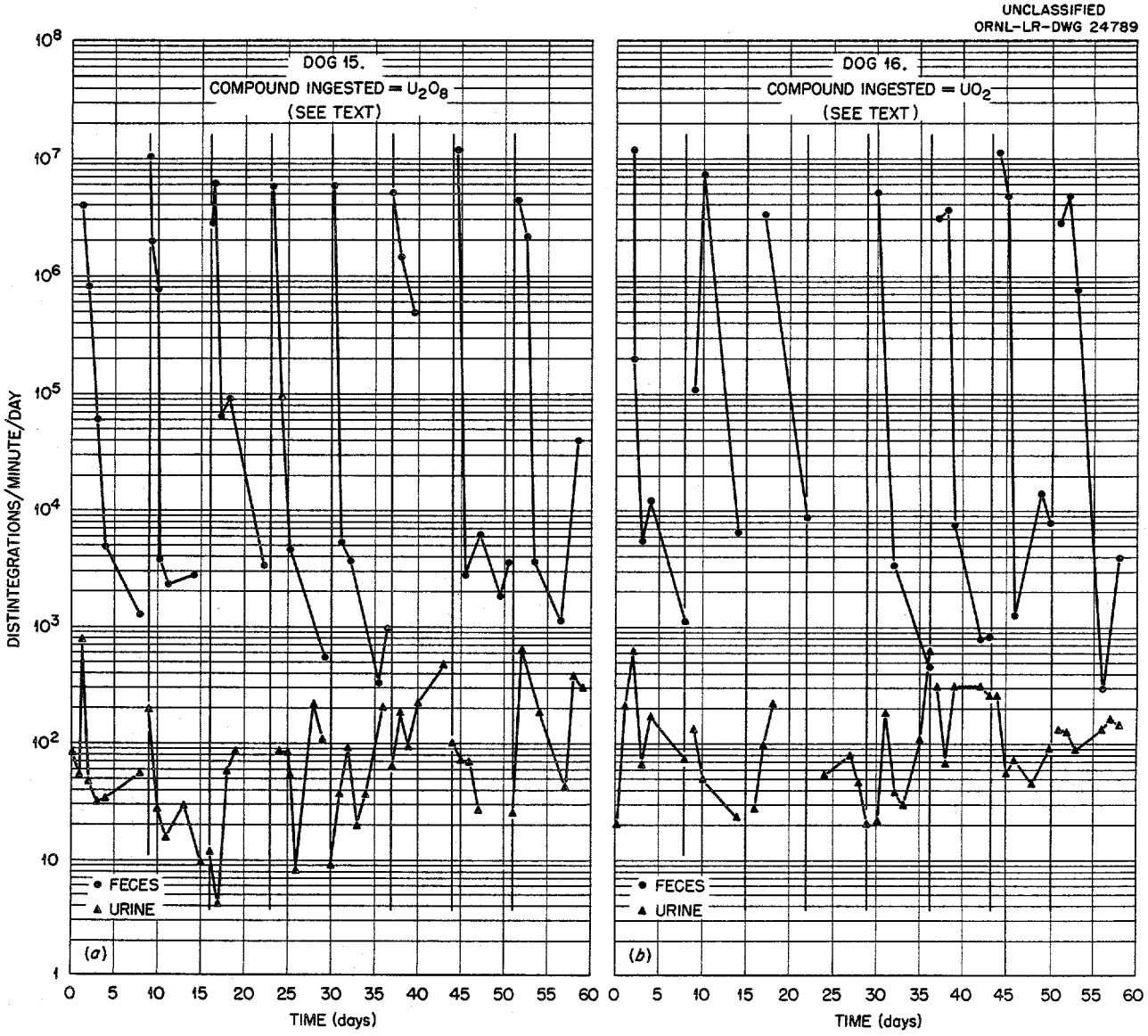

Fig. 6. Fecal and Urinary Excretion of Uranium During and After Ingestion of Insoluble Compounds of Uranium.

coefficient of about 1800 at 9 *M* HCl, and about one-half this value at 6 *M* HCl. Since the potassium of the urine would tend to precipitate as KCl in HCl concentrations greater than 7 *M*, the urine feed solution is made up to 6 *M* in HCl prior to being passed over the resin column.

The column is a cylindrical glass tubing 0.9 cm inside diameter and 6 in. in length. The bottom is fitted with a one-way stopcock in a one-hole rubber stopper with glass wool over the stopper to hold the resin bed. A 5-in. pyrex funnel fitted to the top with rubber tubing serves as a reservoir for the feed, wash, and eluting solutions. The column was charged with 1.5 g of Dowex 1, × 10 (10% divinyl benzene), 100 to 200 mesh, air dried (3-ml volume). The resin is conditioned by passing 25 ml of 6 *M* HCl through the resin column. The urine feed solution is prepared in 6 *M* HCl by adding concentrated HCl equal in volume to the urine sample. This urine feed solution is put over the resin column at a flow rate of 6 ± 2 ml/min/cm^2 of resin bed. The residual inorganic salts are washed from the resin with 50 ml of 6 *M* HCl. The effluent and wash solutions are discarded. The uranium is then eluted from the resin with 50 ml of 0.5 *N* HCl at a flow rate of

3 ± 1 ml/min/cm^2. The eluate is evaporated to dryness at a temperature slightly below the boiling point. Any residual trace of organic matter can be destroyed by adding about 3 ml of concentrated HNO_3 and heating to dryness. The final residue is dissolved in about 0.5 ml of 1 *N* HNO_3 and is transferred with a pipette to a stainless steel planchet. The liquid is evaporated under an infrared lamp, and the planchet is flamed to a dull red heat. The alpha activity can be determined in either a scintillation or a gas flow proportional counter.

The average recovery in 26 experimental runs using 100-ml urine samples "spiked" with U^{233} tracer was 89.8% ± 2.4. Although this procedure was designed to analyze 100 ml of urine, the recovery in samples of twice this size is equally as good.

ECOLOGICAL RESEARCH

R. M. Anderson
S. I. Auerbach
D. A. Crossley, Jr.
C. Krauth
C. J. Rohde, Jr.
A. Broseghini[17]
H. Conner[17]
M. D. Engelmann[17]
E. R. Graham[17]
H. F. Howden[18]
J. B. Lackey[19]

The purpose of the ecology program is to obtain information on the effects of the release of radioactive fission products on man's environments. These data are needed for the resolution of three major hazard problems in the atomic energy field; namely, radioactive waste disposal, reactor site selection and associated hazards, and weapons fallout. The ecology program has two interrelated phases which are:

1. Applied environmental studies. – These include determinations of concentration and distribution in the different components of the environment (such as fresh water, soils, plants, and animals) of the fission products generally considered to be of greatest hazard. The data developed by these studies are needed for the design of safe and economical methods of disposing of large volumes of low- and intermediate-level radioactive wastes, since the extent of a nuclear power program will be determined in part by the costs and hazards of the waste disposal. These data also will be useful for the selection of safe reactor sites as well as for the determination of practical insurance liability on individual reactors.

2. Long-range environmental studies. – This program includes long-range field studies in areas which will have a rise in the background of radioactivity and which have some degree of assurance of a long period of use. Included in this phase of investigation are studies of fluctuations of plant and animal populations, plant and animal successions, soil formation, food chains, mineral cycles, and microclimates. These data not only will complement the applied environmental studies but will provide information needed for evaluation of the effects of radioactivity on the various ecosystems which comprise the biosphere.

White Oak Lake Bed Studies

In October 1955, White Oak Lake, an impoundment which had served as a final holdup basin for the Laboratory's low-level radioactive wastes, was drained. The alluvial material which comprised the bottom of the lake contained various amounts and kinds of transported soil and subsoil material, all of which had come in contact with solutions containing mixed fission products. Draining was done slowly so that nearly all the alluvial material remained, leaving a bare, silty area (Fig. 7).

In February 1956, a photographic record of changes in the appearance of the bed due to revegetation was started. This revegetation occurred rapidly. Among the invading species were smartweed (*Polygonum*) and sedge (*Juncus, Cyperus*). By June 1956 most of the bed was covered. The dominant species was *Polygonum lapathifolium*.

Initial studies were concerned primarily with determining the yield and productivity of this newly developing community. Ten 1-m square quadrats were harvested in June and five quadrats each in July and August. The data are summarized in Table 7. The yield in terms of pounds per acre of the dominant plants (smartweed-sedge) compares very favorably with that of the highest yield agricultural crops.

For long-term studies the lake bed was divided into two areas, refered to as the upper lake and lower lake. The upper lake portion is that part lying northeast of the line ab where White Oak Creek flows diagonally across the lake bed from the south shore to the north shore (Fig. 7). The

[17] Temporary employee.

[18] ORINS research participant.

[19] Consultant, University of Florida.

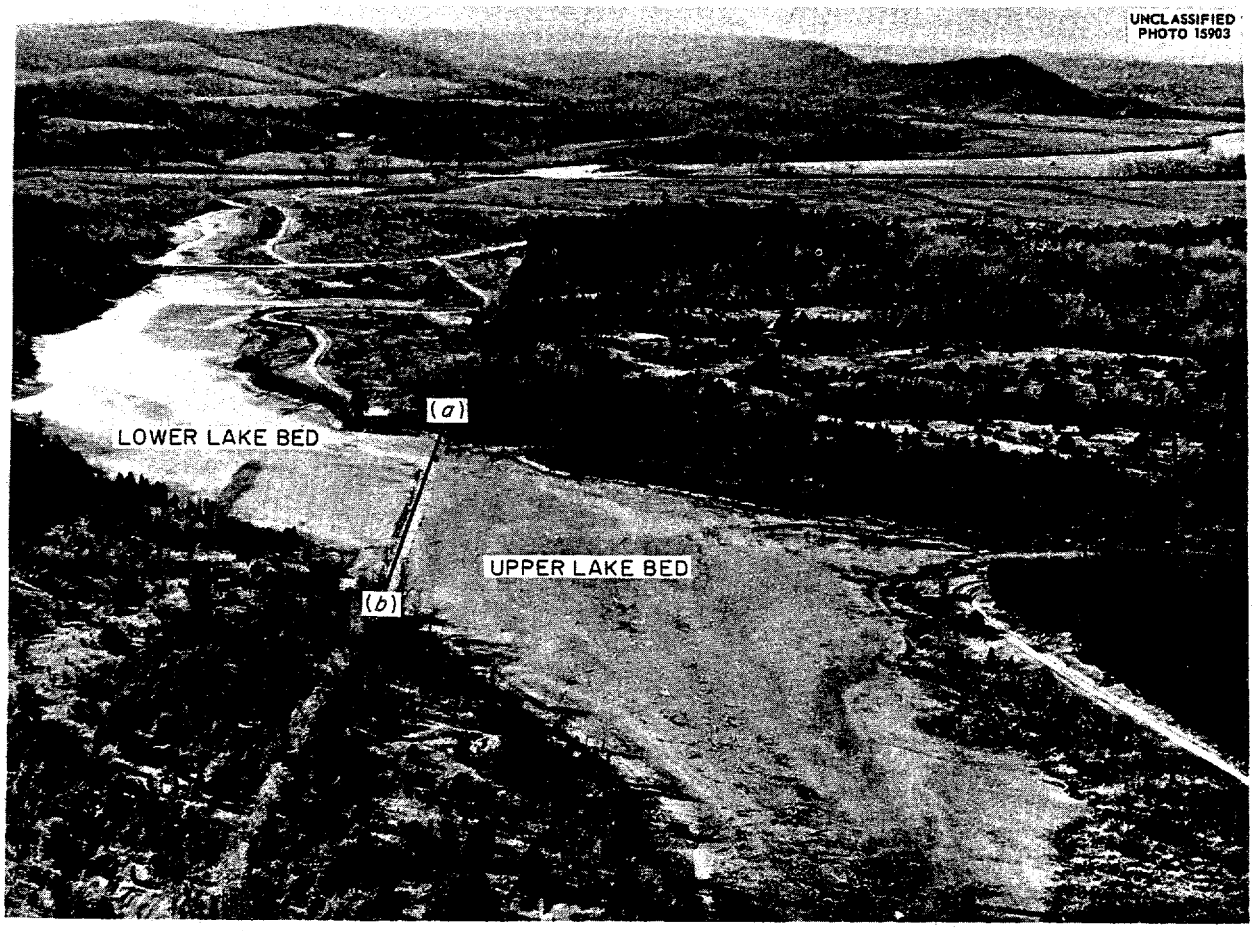

Fig. 7. Aerial Photograph of White Oak Lake Bed, Showing Condition of the Bed Immediately Following Drainage of the Lake in October 1955.

Table 7. Standing Crop and Productivity of the Pioneer Biota on White Oak Lake Bed in the Spring to Summer of 1956

Biota	Harvest Date	Days of Growth	Dry Weight (g/m^2)	Dry Weight (lb/acre)	Dry Weight (g/m^2/day)
Smartweed-sedge	6-20-56	61	572.8	5110.0	9.4
Sedge-sedge	6-20-56	61	402.2	3588.0	6.6
Smartweed-sedge	7-19-56	90	985.4	8792.0	10.9
Smartweed-sedge	9-11-56	143	1105.0	9859.0	7.7
Herbivore insects				6.7	
Predator insects				0.66	
Average Yield and Productivity for U.S. 1943–1952 for Comparison					
Alfafa		150	495	4420	3.30
Clover-timothy		80	316	2820	3.95
Green grain		75	269	2400	3.59

lower lake is that portion of the lake bed lying southwest of that line.

In addition to a topographic separation, the two areas differed in their background radiations. Background radiation at the surface of the soil ranged from 5 to 35 mrad/hr in the lower lake area and from 10 to 120 mrad/hr in the upper lake area. These differences are related to the deposition of materials by White Oak Creek and its flow patterns across the lake bottom. Not only are the materials laid down first in the upper lake area, but the creek in that part is not confined to its normal channel. Figure 8, taken in October 1956 after a period of flooding, shows the creek to be flowing through the upper lake bed in two channels in addition to the normal one. Also the upper lake receives radionuclides seeping from the ORNL waste pits which are immediately adjacent to the upper lake (part of the pit area can be seen in the lower right hand corner of Figs. 7 and 8).

Most of the studies during the first year were confined to the lower lake area. To facilitate sampling and provide a basis for detailed comparisons of vegetation through time, three acres of the lower lake were surveyed and a grid subdivided into 10- by 10-m squares was staked on this area.

Soil Samples. – The first set of soil samples was taken along transects which were parallel to the old dam site, one at the lower end, one in the middle, and one at the upper end of the lake. The samples were taken at 50-ft intervals along the transects and at three depths, namely, samples "a" at 6 in., samples "b" at 12 in., and samples "c" at 18 in. The samples were air-dried and analyzed for radioactivity and per cent base saturation.

The second set of samples was taken from the center of the area. These consisted of six surface

Fig. 8. Aerial Photograph of White Oak Lake Bed, Taken in October 1956 After a Period of Flooding.

samples (0 to 6 in.) and three subsoil samples (near 15 in., 26 in., and 32 in.). These samples were analyzed for general soil properties.

The third set of soil samples was taken in relation to the air dose rate as determined by ionization-chamber measurements made at a level of 3 ft above the surface of the soil. The areas chosen showed air dose rates of 12, 25, 75, and 120 mr/hr. A composite sample of the surface soil (0 to 6 in.) was taken from each area.

A fourth sample which consisted of a single composite sample of surface soil was taken from the downtown section of the city of Oak Ridge. This sample was used as a control and was taken from a recently excavated area in which *Polygonum lapathifolium* was growing.

Plant Samples. – The upper leaves of several plants (*Polygonum lapathifolium*) were harvested from each of the sample areas. The samples were oven-dried (60°C) overnight, cut into small pieces, and stored for subsequent analysis. A composited plant sample was taken from the downtown section of Oak Ridge and used as a control.

Methods. – The soil samples were air-dried and examined for radioactivity by placing 1 g of the soil on the second shelf of an end-window Geiger-Mueller counter with a counting efficiency of 5%. The pH in water was determined by mixing 5 g of soil and 5 ml of deionized water and determining the pH with a glass electrode. The salt pH (Schofield and Taylor[20]) was determined by adding 5 ml of 0.01 *M* $CaCl^2$ to 5 g of soil and determining the pH with the glass electrodes. Total carbonate was determined by the Hutchinson and MacLennon method.[21] The organic matter and soluble phosphate were determined by methods outlined by Graham.[22] Total hydrogen was determined by the Woodruff method.[23] Weak acid (0.1 *N* HCl) extracts were prepared by leaching 50 g of soil with 500 ml of the acid. The concentration of potassium, sodium, and calcium in the weak acid extraction was determined with the flame photometer. The magnesium was determined with a modified thiazol yellow method.[22]

Saturation extracts of the soil were prepared and analyzed for potassium and calcium. The pH–$\frac{1}{2}$ pCa values of the extracts were calculated as outlined by Woodruff.[23] Analysis for the chloride ion was made with the silver–silver chloride electrode. The SO_4 anion was determined by the method of Steinbergs,[24] and the NO_3 ion was determined by the Bray method.[25]

All extracts were analyzed for Sr^{90} by the methods outlined by Kahn,[26] and for Cs^{137} by methods outlined by Farabee.[27] In order to extract the total amount of radioactive Sr contained in the soil, the soil was boiled in 1 *M* HNO_3, centrifuged, and then treated with a second lot of acid. The HNO_3 acid extracts were then analyzed for strontium following the method outlined by Kahn. In order to extract the total amount of radioactive cesium the soil was treated with hot 9 *M* H_2SO_4; two treatments will remove the total amount of radioactive cesium in the soil.[26] The sulfuric acid extracts were taken to dryness and the radioactive cesium determined by the method as outlined by Farabee.[27]

Plant samples were digested with nitric and perchloric acids and analyzed for sodium, potassium, and calcium with the flame photometer. The total phosphorus and total nitrogen were determined by conventional methods. Magnesium was determined by the thiazol yellow method. Nitrate nitrogen was determined by making first a water extract of the dried plant material and then following the Bray method.[25] The plant samples were digested and analyzed for Sr^{90} and Cs^{137} by methods outlined by Kahn[26] and Farabee.[27]

Soil Properties. – The data on soil water pH, salt pH, and gross beta activity (Table 8) show the soil of the disposal area to be heterogeneous. The beta activity of the soils varied from zero to 1313 counts/min/g. The average value for "a" sample was 223 counts/min/g; for "b" 78 counts/min/g; and for "c" 24 counts/min/g. The samples of soil which had activities greater

[20] R. E. Schofield and W. A. Taylor, *Soil Sci. Soc. Am. Proc.* 19, 164–167 (1955).

[21] C. S. Piper, *Soil and Plant Analysis*, Interscience, New York, 1950.

[22] E. R. Graham, *Testing Missouri Soils*, Missouri Agr. Expt. Sta. Circular 345, p 1–23 (March 1950).

[23] C. M. Woodruff, *Soil Sci. Soc. Am. Proc.* 19, 167–171 (1955).

[24] A. Steinbergs, *Analyst* 80, 457–461 (1955).

[25] R. H. Bray, *Soil Sci.* 60, 219–221 (1945).

[26] B. Kahn, *Procedures for the Analysis of Some Radionuclides Adsorbed on Soil*, ORNL-1951 (Sept. 28, 1955).

[27] L. B. Farabee, personal communication.

Table 8. Distribution of Radioactivity, pH, and salt pH of the White Oak Lake Bed Soils

Lower Transect				Middle Transect				Upper Transect			
Sample No.	Gross β (counts/min/g)*	pH Soil and H_2O	pH Soil and Salt	Sample No.	Gross β (counts/min/g)*	pH Soil and H_2O	pH Soil and Salt	Sample No.	Gross β (counts/min/g)*	pH Soil and H_2O	pH Soil and Salt
1 a**	5	6.23	5.82	1 a	54	6.25	5.90	1 a	554	7.58	7.42
b	61	6.98	6.62	b	3	6.42	6.00	b	151	6.47	6.48
c	18	7.05	6.62	c	0	6.60	6.12	c	42	6.15	5.80
2 a	128	6.83	6.58	2 a	11	5.85	5.35	2 a	196	7.03	6.20
b	1	6.18	5.80	b	1	5.88	5.38	b	4	5.90	5.68
c	9	6.77	6.41	c	26	6.23	5.68	c	34	6.18	5.92
3 a	10	5.42	5.12	3 a	30	6.20	5.73	3 a	257	7.63	6.15
b	2	5.62	5.43	b	23	6.95	6.40	b	10	6.30	5.97
c	0	5.95	5.50	c	12	7.28	6.63	c	37	6.35	6.43
4 a	406	7.96	7.58	4 a	16	5.82	5.27	4 a	317	7.20	7.16
b	24	7.72	7.38	b	832	7.38	7.00	b	28	6.06	6.25
c	0	6.45	6.17	c	7	5.87	5.29	c	9	6.80	6.47
5 a	89	7.25	7.08	5 a	52	7.20	7.08	5 a	98	6.52	6.32
b	20	7.26	7.07	b	74	8.13	7.72	b	22	6.42	6.26
c	0	6.85	6.34	c	1	6.73	6.40	c	7	7.08	6.58
6 a	623	7.82	7.65	6 a	28	6.15	6.63	6 a	636	8.13	7.92
b	337	8.18	7.82	b	1	7.10	6.45	b	317	7.26	7.18
c	55	7.89	7.57	c	0	7.15	6.60	c	77	6.77	6.86
7 a	199	7.60	7.08	7 a	550	7.75	7.63	7 a	5	6.47	6.02
b	0	7.22	6.75	b	159	7.85	7.60	b	1	6.31	5.73
c	2	7.12	6.45	c	45	7.78	7.43	c	6	6.28	5.73
8 a	1313	7.68	7.20	8 a	8	7.17	6.62	8 a	37	6.52	6.14
b	10	6.24	6.12	b	5	6.64	6.14	b	17	6.32	6.00
c	225	6.63	6.58	c	6	6.35	5.87	c	10	6.31	5.82
								9 a	36	7.18	6.90
								b	4	6.88	6.48
								c	0	6.72	6.32
								10 a	344	7.76	7.34
								b	2	6.84	6.26
								c	8	6.80	6.28
								11 a	6	6.26	5.67
								b	3	6.42	5.90
								c	2	6.60	6.13

*Over-all counting efficiency 5%.

**a = soil depth 5–7 in.
b = soil depth 11–13 in.
c = soil depth 17–19 in.

than 250 counts/min/g were found to have pH values above 7.0. The reason for the high pH values could have been that eroded dolomitic limestone or calcareous shales of the area were mixed and deposited in the area. Soil samples showing salt pH of less than 6.0 had a beta activity of less than 54 counts/min/g.

The general soil chemistry of the area is shown in Tables 9 and 10. The surface soil consists of a complex mixture of gravel, sand, and clay. Most of the soil is low in organic matter. The percentage of organic matter was higher in the lower subsoil samples. This could be the result of silt and sand from the early construction work done at the Laboratory being carried into the area and deposited over the natural soil. Soluble phosphorus as extracted with Bray's[28] No. 2 reagent was found to be low in relation to the values published by Bray and which are necessary for good yields of common farm crops. Weak acid extract measurements of potassium ranged from a low of 0.12 milliequivalents (meq) per 100 g (94 lb/acre) to a high of 0.43 meq per 100 g (335 lb/acre). The range for magnesium was 0.6 to 5.5 meq per 100 g. The calcium removed by leaching was greater than 50 meq per 100 g in the samples containing carbonates. A more normal value of calcium for the unsaturated soil was 11 meq per 100 g. The highest value found for exchangeable hydrogen was 2.0 meq per 100 g.

The saturation extract analyses revealed relatively high concentrations of nitrate and sulfate ions and a low concentration of chloride ions. The concentration of potassium and calcium found in the saturation extracts when substituted in Woodruff's equation[23] $[\Delta F = RT \ln (K/\sqrt{Ca})]$ yielded values which ranged from −3490 to −5150. According to Woodruff[23] these values, when related to plant growth, represent a calcium-rich, potash-deficient system.

The results of the radiochemical analyses (Table 11) revealed values ranging from 0.00092 to 0.00039 μc per 100 g for Sr^{90} and 0.00025 to 0.00520 μc per 100 g for Cs^{137} as calculated from the saturation extracts and the bulk density of the soil. The 0.1 *N* HCl extracts showed values which ranged from 0.029 to 0.064 μc per 100 g for Sr^{90}, and from 0.0036 to 0.0069 μc per 100 g for Cs^{137}. The range obtained for Sr^{90} on treating the soil with 1 *M* hot HNO_3 was 0.036 to 0.060 μc per 100 g. These values were near those obtained by leaching the soil with 0.1 *N* acid, which suggests that the total active strontium of the soil is held in water-soluble and weak-acid-extractable forms. The treatment with 9 *M* hot H_2SO_4 showed a range of Cs^{137} activity from 0.33 to 2.55 μc per 100 g. The latter values are very much greater than those obtained by leaching with 0.1 *N* acid, which indicates that most of the Cs^{137} is held in mineral combinations which would be considered non-exchangeable.

The chemical composition of the leaves as shown in Table 12 revealed that the plants of the area were high in total nitrogen and nitrogen as nitrate when compared to the controls. The high nitrate level of the area is a result of the use of nitric acid in the chemical processing of reactor fuel elements. With the exception of phosphorus, the control plants contained lower amounts of the elements tested than did the plants from the White Oak Lake bed area. The control sample contained no measurable amount of sodium while the plants from the 75 and 120 mr/hr air-dose-rate regions contained 0.041% sodium and the plants from the 12 and 25 mr air-dose-rate regions contained 0.004% sodium. This was to be expected, since the extractable sodium was much higher in the soil from the area of high air dose rate.

Sr^{90} Uptake. — The plant samples ranged in Sr^{90} content from 0.057 to 0.178 μc per 100 g of dry plant material. It has been suggested that the available calcium content of the soil acts as a regulator of the amount of Sr^{90} absorbed by the plants. This concept would, no doubt, be true in instances where there was a marked difference in the level of exchange calcium. Since the soils of the area all have a high calcium level, especially in the zone of high radioactivity, as shown by the salt pH values (pH−½ pCa, Schofield and Taylor[29]) and the saturation extract pK−½ pCa, this concept will not explain the observed difference in Sr^{90} content of the plants of the area.

The data in Table 11 show the saturation extract method for Sr^{90} to be more related to the plant content of Sr^{90} than the other methods used in this investigation. The samples collected from the areas of high dose rate as shown in Table 11

[28] R. H. Bray, chap 2, p 53–86 in *Diagnostic Techniques for Soils and Crops*, (ed. H. B. Kitchen) American Potash Institute, Washington, 1948.

[29] R. E. Schofield and W. A. Taylor, *Soil Sci. Soc. Am. Proc.* 19, 164–167 (1955).

Table 9. Properties of the Soils of the White Oak Lake Bed Area

	Gross β (counts/min/g)*	Bulk Density	Organic Matter (%)	Soluble Phosphate P_2O_5 (lb/acre)	Weak Acid Extracts, meq per 100 g of Soil					pH		Deionized Water Saturation Extract			
					K	Mg	Ca	H	Na	Soil H_2O	Soil Salt	$\Delta F = RT \ln \frac{K}{\sqrt{Ca}}$	ppm Cl	ppm SO_4	ppm NO_3
Surface soil samples, 0–6 in.															
A	1512		2.0	26	0.30	2.9	50+	0.0	0.65	7.90**	7.65				
B	829		2.1	19	0.43	2.9	50+	0.0	0.56	7.90**	7.70				
C	216		1.5	19	0.30	1.4	41	0.0	0.53	7.55	7.32	−3840	3	42	62
D	89		1.5	13	0.21	0.6	18	2.0	0.30	6.01	5.61	−3840	6	>100	10
E	12	1.6	0.8	13	0.14	0.6	8	1.0	0.17	6.11	5.84	−4030	3	18	53
F	9	1.6	0.6	19	0.14	1.1	9	1.0	0.17	6.05	5.82	−5030	2	5	52
Subsoil samples, in.															
15	4	1.5	1.2	41	0.12	1.2	10	1.5	0.20	6.80	6.52	−4960	2	8	9
26	0	1.3	2.9	22	0.16	1.0	13	1.0	0.22	7.20	6.72	−5150	2	2	5
32	2	1.2	2.4	45	0.24	1.3	13	1.0	0.22	6.44	6.40	−5140	2	4	8

*Over-all counting efficiency 5%.

**Sample A contained 7.05% carbonate.
Sample B contained 4.30% carbonate.

Table 10. Properties of the Surface Soil of the Areas Sampled According to Air Dose Rate

Sample (mr/hr)	Organic Matter (%)	Free $CaCO_3$ (%)	Soluble P_2O_5 (lb/acre)	Weak Acid Extracts (meq per 100 g of Soil)					pH		Free Carbonate (%)	Deionized Water Saturation Extract			
				K	Mg	Ca	H	Na	Soil H_2O	Soil Salt		$\Delta F = RT \ln \frac{K}{\sqrt{Ca}}$	ppm		
													Cl	SO_4	NO_3
12	1.8	0.5	30	0.12	1.6	14	*	0.13	7.12	7.00	0.50	-4187	5	42	60
25	2.7	2.3	40	0.25	4.3	42	*	0.52	7.68	7.40	2.30	-3928	5	63	63
75	2.9	2.7	38	0.33	5.5	56	*	1.08	7.72	7.57	2.7	-3683	12	103	82
120	2.9	2.6	48	0.41	5.4	59	*	2.25	7.58	7.51	2.6	-3492	13	61	73
Control	0.7	1.0	43	0.25	1.2	17	*	0.25	7.60	7.33	1.0	-4201	11	49	4

*Not analyzed.

Table 11. Strontium-90 and Cesium-137 Content of Soil Extracts and *Polygonum lapathifolium*

Sample (mr/hr)*	Soil Extracts						*Polygonum lapathifolium* (μc/100 g)	
	Deionized Water Saturation Extract (μc/100 g)		0.1 *N* HCl Leaching Extract (μc/100 g)		Hot** 1 *M* HNO_3 (μc/100 g)	Hot 9 *M* H_2SO_4 (μc/100 g)		
	Sr^{90}	Cs^{137}	Sr^{90}	Cs^{137}	Sr^{90}	Cs^{137}*	Sr^{90}	Cs^{137}
12	0.00092	0.00025	0.029	0.0036	0.037	0.33	0.178	0.262
25	0.00054	0.00520	0.064	0.0038	0.060	1.74	0.171	0.334
75	0.00039	0.00039	0.055	0.0069	0.040	2.55	0.057	0.216
120	0.00043	0.00078	0.035	0.0041	0.036	2.44	0.069	0.133

*Lack of correlation between air dose rates and total Cs^{137} content is due to the presence of other gamma emitters such as Co^{60} and $Ru\text{-}Rh^{106}$, which are known to be present, but for which analyses were not made at the time.

**Hot – heated to boiling.

Table 12. Chemical Composition of *Polygonum lapathifolium* Leaves from the Disposal Area and from a Nonradioactive Area Near Oak Ridge

Sample (mr/hr)	Per Cent						
	Na	K	Ca	Mg	P	N	N as NO_3
12	0.004	1.59	0.93	0.26	0.226	3.3	0.13
25	0.005	2.00	1.30	0.32	0.324	4.4	0.21
75	0.041	1.84	1.01	0.32	0.330	3.8	0.05
120	0.038	1.72	0.80	0.32	0.258	3.2	0.04
Control	0.001	1.44	0.52	0.29	0.241	2.4	0.00

revealed lower Sr^{90} content in both the saturation extract and in the plants. This may be explained by the fact that the soil of this area contained appreciable amounts of extractable sodium, which would depress the activity of strontium in the system and result in a lower uptake of Sr^{90}. The difference in sodium level is also evident in the results of the plant analysis as shown in Table 12.

The value of 64 d/sec/g of Sr^{90} in the leaves of bean plants grown on the alkaline calcareous soil of Yucca Flat by Romney *et al.*[30] corresponds well with the average value of 0.119 μc/100 g obtained for the leaves of the *Polygonum lapathifolium* growing on the disposal area. This is to be expected, since the radioactive soil of the low-level-waste area was dominated by zones of alkaline-calcareous conditions.

Cs^{137} Uptake. – The plant samples of the area ranged in Cs^{137} content from a low of 0.133 to a high of 0.334 μc per 100 g of dry plant material. It has been reported by Menzel[31] that the uptake of Cs^{137} was inversely proportional to the level of exchange potassium in the soil. The results of this investigation supports those of Menzel. The available potassium was determined by analyzing the weak acid extracts for potassium concentration and expressing results in milliequivalents per 100 g of dry soil and also by analyzing the concentration of potassium and calcium in the saturation extracts and relating these values to plants by using Woodruff's equation.[32] As shown in Tables 10 and 11 the low concentrations of Cs^{137} in the plants were associated with high extractable potassium levels (0.33 and 0.41 meq of potassium per 100 g of soil) and with the high potassium values found by using the saturation extract method. The analysis of the soil for Cs^{137} by the methods used in this investigation resulted in values which could not be related to the amounts absorbed by the plants.

The concentration of Cs^{137} taken up by *Polygonum lapathifolium* was higher than that of Sr^{90}. This is to be expected since the soil is moderately potassium-deficient and extremely calcium-rich. The best soil indication of the potassium deficiency is shown by the potassium and the calcium contents of the saturation extracts. An average value of −3820 calcium was found for the $\Delta F = RT \ln (K/\sqrt{Ca})$ relationship. According to Woodruff[32] a value of −4000 calcium represents a severe potassium-deficient, calcium-rich situation; and a value of −3500 calcium represents a moderate deficiency.

It seemed of interest to compare these data with that obtained in fallout investigations.[33] By utilizing the information contained in Tables 10, 11, and 12 the Sr^{90} data were converted into "Sunshine Units." These data are presented in Table 13. Because of the striking contrast of these data with that of fallout (fallout "Sunshine Units" typically range from 1 to 75) together with the relative paucity of data on uptake of Sr^{90} by plants grown under natural conditions, it seemed that the White Oak Lake bed offered a unique opportunity for obtaining pertinent information. Accordingly, in the latter part of the year an agricultural plot was prepared in a portion of the upper lake bed. Intensive analysis of the chemical properties of the soil are under way and four varieties of corn are being grown on the plot.

Field Studies on Arthropods

A program of field studies on arthropods has been initiated, with the basic aspects oriented towards investigations of populations and of the food web,

[30] E. M. Romney *et al.*, *Effects of Calcium and Strontium on Plant Uptake of Sr^{90} and Stable Strontium from Nutrient Solutions and Soils*, UCLA-374 (July 15, 1956).

[31] R. G. Menzel, *Soil Sci.* 77, 419–425 (1954).

[32] C. M. Woodruff, *Soil Sci. Soc. Am. Proc.* 19, 167–171 (1955).

[33] E. A. Martell, *Strontium-90 Concentration Data for Biological Materials, Soils, Waters, and Air Filters*, AECD-3763 (Dec. 1, 1955).

Table 13. Soil and Plant (*Polygonum lapathifolium*) Concentrations of Sr^{90} in Relation to Calcium Concentrations

Sample (mr/hr)	"Sunshine Units" $\left(\frac{1\ m\mu c\ of\ Sr^{90}}{1000\ g\ of\ Ca}\right)$	
	Soil	Plant
12	1.32×10^5	1.91×10^5
25	71.3×10^4	1.31×10^5
75	35.6×10^4	5.64×10^4
100	30.4×10^4	8.62×10^4

and the applied studies concerned with the passage and dissemination of radionuclides through these components of the ecosystem.

Use of Berlese Extraction Apparatus. – A widely used method for the recovery of small animals from soil samples employs the Berlese apparatus, which utilizes heat to drive animals from the samples through funnels into collecting tubes. Conventional metal funnels with light bulbs as a heat source were compared with a high-gradient apparatus[34] for relative effectiveness. The high-gradient apparatus (Fig. 9) utilizes Nichrome resistance wire for heat and is entirely enclosed; air may be forced through the container. Thus the apparatus is relatively insulated from changes in laboratory temperatures and relative humidities.

[34] A. MacFadyen, *J. Animal Ecol.* 22, 65–77 (1953).

Soil samples were taken in round cores, $2\frac{5}{8}$ in. in diameter by 3 in. high; all samples included the ground surface. After being weighed, the samples were placed in the two types of apparatus for one week. Arthropods recovered during this time were counted.

Counts of microarthropods disclosed no significant differences in effectiveness between the two types of funnels. Table 14 shows the number of animals recovered in one such experiment. The stability of the laboratory climate (maintained at 75 ± 2°F and 50 ± 5% relative humidity) probably accounts for the relative success of the more conventional type of apparatus. Yields were relatively constant over the temperature range 35 to 45°C. Partial results of day-to-day counts from two samples are shown in Fig. 10. Usually the collembolans and other insects are recovered

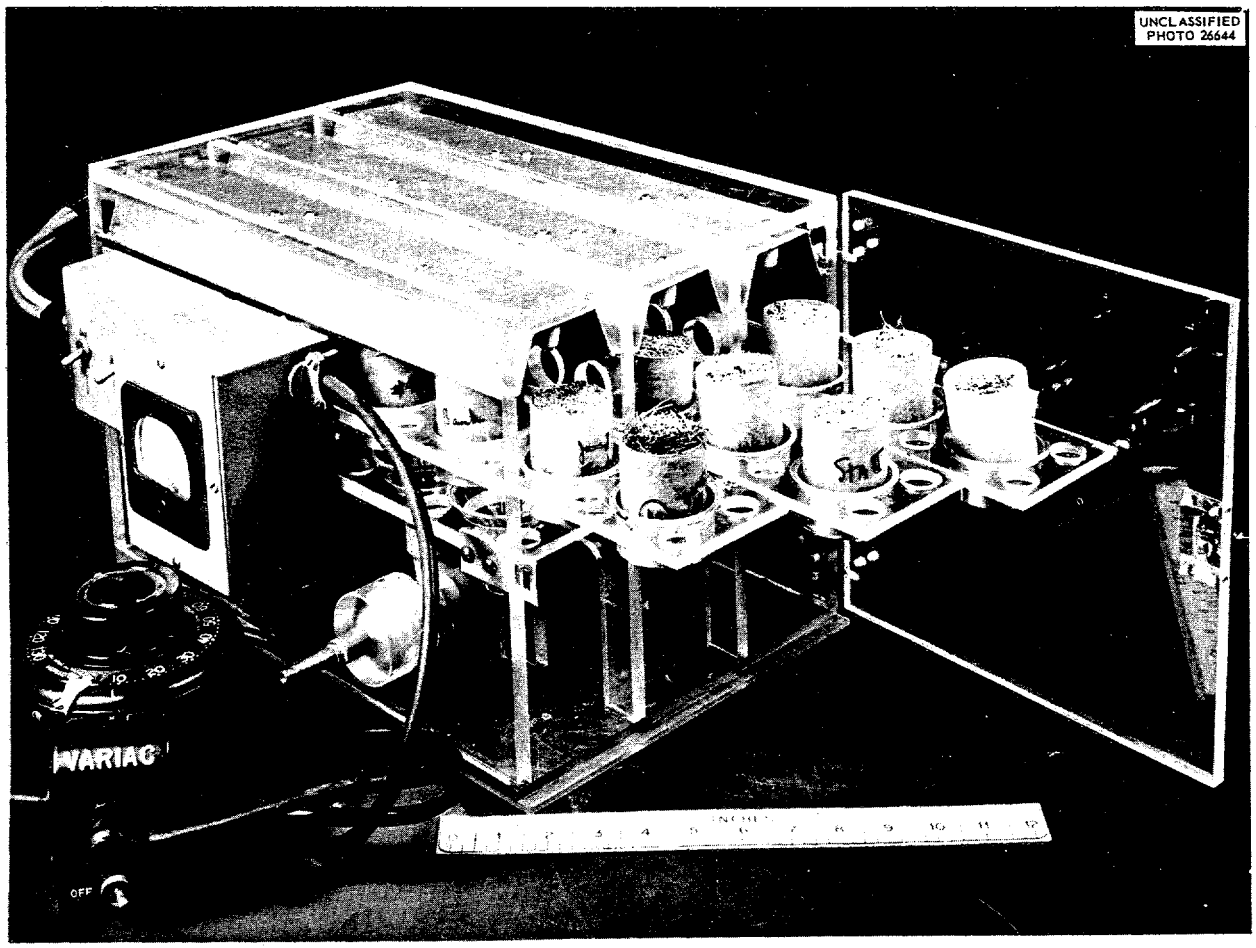

Fig. 9. High-Gradient Berlese Funnel Apparatus Used to Extract Microarthropods from Soil Samples.

Table 14. Total Numbers of Microarthropods Recovered in Two Different Berlese Apparatuses – Several Replicates

Conventional Funnel		High-Gradient Apparatus
60-w Bulb	40-w Bulb	
190	136	162
132	153	94
106	346	106
Total 428	635	490
Av 142.7	211.7	122.5

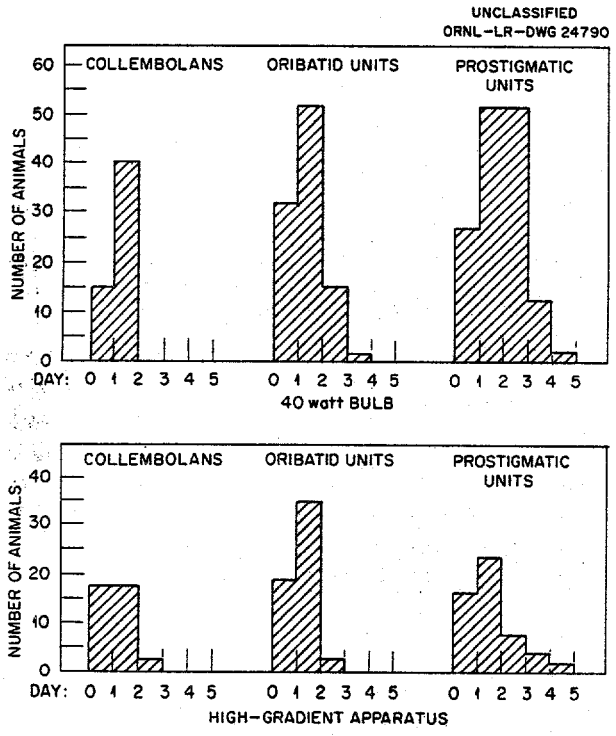

Fig. 10. Day-to-Day Recoveries of Soil Animals in Two Types of Berlese Funnels (Unreplicated).

in the first two or three days, oribatid and mesostigmatic mites (not shown) are collected within three or four days, and the prostigmatic mites require five days or more. For general studies the seven-day period of operation seems adequate.

The number of arthropods per sample usually varied independently of the weight of the sample. This seems to indicate that a majority of the animals occur in the top portion (1½ to 2 in.) of the soil, so that weight differences due to varying amounts of deeper soil collected have little effect. However, one series of samples from White Oak Lake bed showed a negative relationship of numbers of soil animals to weight of sample, the lighter samples containing more mites. Possibly the heavier samples were too tightly packed, destroying the passageways through which the animals could escape. Such a negative relationship has not recurred in additional samples.

Microarthropods of White Oak Lake Bed. – In October 1956 a sampling regimen for soil microarthropods was begun on White Oak Lake bed. Samples taken during this period were intended to show the kinds and numbers of arthropods which had invaded the lake bed soils, differences between areas, and the general winter composition of the lake bed soil fauna. One-square-meter quadrats were located in smartweed-sedge areas in the lower, middle, and upper parts of the lake bed (the designations "lower" and "middle" here refer to lower and upper parts of the general lower lake area). These quadrats were sampled in October, January, and May. The upper lake quadrat proved excessively moist and was not sampled after October.

From these samples the numbers of soil arthropods per square meter have been estimated by extrapolation (Table 15). The most abundant animals are collembolans of the family Entomobryidae and mites of the families Tarsonemidae and Eupodidae. The total numbers as shown in Table 15 show a greater abundance in the lower lake, and little change with time in both areas during the sampling period.

The areas of the lake may be compared as to their progress in soil arthropod succession by comparing ratios of the number of species to the total number of individuals in these areas (Table 16). This ratio is an indication of the diversity of the areas sampled. It is seen that the middle area of the lake supported a more diverse fauna than did either the lower or the upper areas. This probably indicated that the middle lake area is in a more advanced stage of succession than are the other two areas. Corroborative evidence may be obtained from Table 15 by noting the greater numbers of eremaeid and acarid mites from the middle lake area; these mites are associated with litter.

From the foregoing data a picture of some of the dynamics of this developing ecosystem may be

Table 15. Soil Arthropods of White Oak Lake Bed: Estimates of Number per Square Meter (Each Figure Based on 5 Samples)

	Lower Lake			Middle Lake		
	October	January	May	October	January	May
Insecta						
Entomobryidae	1,300	700	9,400	1,000	5,200	1,400
Sminthuridae	1,900	3,200	0	700	0	400
Miscellaneous	700	1,000	2,000	300	1,700	600
Acarina						
Eupodidae	22,400	2,700	16,100	8,100	1,400	5,700
Tarsonemidae	7,900	36,800	2,900	5,400	8,100	1,000
Phytoseiidae	1,600	300	2,600	2,000	1,900	3,200
Eremaeidae	1,300	300	1,400	1,000	1,000	5,500
Scutacaridae	2,500	600	2,800	900	300	400
Acaridiae	0	300	300	700	600	0
Miscellaneous	100	0	0	700	600	0
Total	39,700	45,900	37,500	26,600	21,400	18,200

Table 16. Soil Arthropods of White Oak Lake: Ratios of Number of Species to Total Number of Individuals (Each Figure Based on Five Samples)

	October	January	May
Lower lake area	0.04	0.03	0.04
Middle lake area	0.09	0.07	0.08
Upper lake area	0.02		

proposed. Invading arthropods may be divided into three groupings on the basis of their appearance and abundance on the lake bed as follows:

Group 1 – Tarsonemidae, Entomobryidae, and Sminthuridae (feeders on decaying plant materials and fungi, tolerant of moist conditions).

Group 2 – Eupodidae (probably phytophagous) and Phytoseiidae (predators).

Group 3 – Acaridae, Eremaeidae (feeders on plant remains), Scutacaridae (arthropod parasites), and miscellaneous predators.

The January sampling was done after considerable moisture had accumulated on the lake bed; this seems to have had the effect of setting back the succession of soil arthropods, as evidenced by a buildup of tarsonemid populations and a drop in most groups. The May samples show a buildup of the more specialized groups of mites.

As plant and soil succession continues, the eremaeids and relatives, the prostigmate predators, and various specialized mites may be expected to increase their numbers at the expense of the tarsonemids and eupodids. While there are indications of such changes in the data presented in Table 15, there are certainly other factors involved in these data as well.

Further work will be oriented towards following the succession of soil arthropod species on the lake bed, estimation of populations of dominant animals, and analysis of these animals for radionuclides.

Insect Fauna of White Oak Lake Bed. – In addition to the microarthropod sampling, a series of samples of the macroarthropod fauna was begun in the summer of 1956. Objectives are to ascertain the species of insects present on the major vegetational types (smartweed, sedge, and willow) of the lake bed, to examine biomass relationships

among these arthropods, and to determine the uptake and transfer of radionuclides in these levels of the food web.

The principal method of sampling used during this period for insects on vegetation was the sweep net; other sampling methods are now being investigated. A subcircular insect net with a diameter of about 14 in. and a 4-ft handle was swept rapidly through the vegetation under study. Ten such sweeps were taken in rapid succession; the insects thus collected were killed in a cyanide jar and returned to the laboratory for counting. Preliminary estimates indicate that ten such sweeps yield a number of insects which roughly approximates the number found on one square meter of vegetation.

The distribution of insect species on the lake bed vegetation closely follows the distribution of plant species. That insect species are strongly associated with vegetation type is shown for the insect order Hemiptera in Table 17. Species of *Lygus* and *Arhyssus* occur predominantly on smartweed with few individuals on sedge; *Jalysus* and *Crius* occur exclusively on smartweed. On sedge, *Geocoris* occurs primarily and *Cymus* and *Sinea* exclusively. Of these insects all are herbivores except *Spinea*, which is predaceous. About one-third of the insects found on the lake bed vegetation belong to the Hemiptera.

Such specificity is not obvious in some orders. Some species of Diptera (flies) and Hymenoptera (bees and wasps) are not clearly associated with type of vegetation.

As plant succession continues on the lake bed, a succession of insects follows. In Table 18 the number of species of three orders of insects found in 1956 and 1957 is given. The number of species is not necessarily a good characterization of change. As shown, the order Hemiptera is represented by 20 species in both 1956 and 1957; however, 65% of the species taken in 1957 were not taken in 1956. Much of this change in species composition is due to the appearance of new plants (particularly willow) on the lake bed in 1957.

Preliminary biomass data are given in Table 19. Biomass (dry weight of organisms) is widely used as a measure of productivity for a given area. Also, comparisons of groups and areas based on biomass estimations are more meaningful than those based on numbers of animals alone. The data given in Table 19 are preliminary. Not only is replication necessary, but a thorough understanding of seasonal dynamics must be achieved before

Table 17. Illustration of Specificity of Herbivorous Insects on Vegetation

Numbers of insects of the order Hemiptera taken on White Oak Lake Bed Vegetation (totals of 6 samples taken August 2 to September 4, 1956)

	Vegetation Type				
	Short Smartweed Inshore	Tall Smartweed Inshore	Tall Smartweed Center	Short Sedge	Tall Sedge
Lygus lineolaris, adults	117	99	109	11	10
Lygus lineolaris, nymphs	71	79	134	0	3
Arhyssus lateralis	17	17	24	6	8
Geocoris punctipes	5	11	13	63	75
Cymus sp.	0	0	0	6	39
Sinea spinipes (predator)	0	0	0	7	8
Jalysus wickhami	2	7	1	0	0
Crius insidiosus	1	7	2	0	0
Miscellaneous Hemiptera	20	8	11	11	15

Table 18. Change in Insect Species Composition from 1956 to 1957
White Oak Lake Bed

	Number of Species Present, 1956	Number of Species Present, 1957	Per Cent of Species New, 1957
Homoptera	17	32	66
Hemiptera	20	20	65
Coleoptera	37	40	55

Table 19. Biomass Relationships of Insects of White Oak Lake Bed
(Unreplicated Samples)

	Weight of Herbivores (g)	Weight of Predators (g)	Ratio: Weight of Herbivore / Weight of Predator
1956 (50 sweep samples)			
August 13	0.6365	0.1563	4.1
August 20	0.4815	0.0851	5.7
August 27	1.3981	0.0475	29.5
1957 (20 sweep samples)			
June 18			
Smartweed	0.5256	0.0613	8.6
Sedge	0.0608	0.0739	0.8
Willow	0.0907	0.0241	3.8

these data may be realistically interpreted. However, good biomass data are essential for studies of the transfer of radionuclides through the food web.

Samples of these insects have been counted with Geiger-Mueller and with gamma scintillation equipment. Thus far, counts have been low and no estimates have been made of kinds or concentrations of radionuclides present in the insects.

Laboratory Studies on Arthropods

Effects of Gamma Radiation on Collembola Population Growth. – Relatively little work has been done on the effects of ionizing radiations on populations, in contrast to the considerable body of work devoted to their effects, physiological and genetic, on individuals. Because of the interest of this Laboratory in the disposal of low-level radioactive wastes into the soil, some research emphasis is being placed on radiation effects on populations of different soil arthropods. The Collembola, which are small, primitive, ametabolous, wingless insects, were chosen because they are abundant in soil, where they play a role in the breakdown of organic materials in the biological cycle of soil formation. Also, they are easily reared in the laboratory, have a short life cycle, and will multiply rapidly. The species used in

these studies was *Proisotoma minuta* Tull.,[35] which is a ubiquitous form known from North America, Europe, and Australia.

The effects of radiation on population growth rate were examined in these experiments. Increase in population size was measured by bidaily counts of individuals at food points and by counts of total numbers at the termination of the experiment. If the magnitude of the doses used reduced the numbers, this reduction could be construed to be an effect on the future potential of the population. Since certain important internal population parameters such as age distribution, longevity, and sex ratios were not known, and since these experiments were carried through only about three generations, only a crude index of the effect on the intrinsic rate of increase can be obtained.

The experiments were started with 61 reproducing population units of 10 individuals each. Three doses of gamma radiation from a Co^{60} source totaling 3000 r, 5000 r, and 7000 r were given in single exposures (at a dose rate of 19 r/sec) to these units. Sixteen replicates were used for each dose level; the remaining 13 were not irradiated. The experiments were terminated at periods of time ranging from 16 to 30 days at which time the individuals were sacrificed and counted. At the end of the experiments 42,504 individuals were present.

There was a significant difference ($P = 0.001$) in the total numbers between the control and irradiated populations. The means of the populations appear to be linearly related to dose. A negative linear regression was significant at greater than 0.001 probability, while the deviations from linearity were not significant. Means of the bidaily sample counts with their standard errors are given in Table 20. An analysis of variance shows that differences between the control populations and those populations receiving 5000 and 7000 r are significant; similiarly the differences between those receiving 3000 and 7000 r were significant. However, the differences between the controls and those populations receiving 3000, between 3000 and 5000 r, or between 5000 and 7000 r were not significant.

The bidaily counts at food points show that all the population units had an initial threshold period followed by the typical phase of exponential growth (Fig. 11). The effect of radiation seems to be chiefly one of lengthening the threshold period. When this lag phase has been passed, the population (with the possible exception of those units given 7000 r) then proceeds to multiply at the control rate. Until asymptotic levels are approached by all experimental cultures, the total at any sampling point in time prior to reaching the plateau reflects the lag effect.

[35]The authors thank D. L. Wray, Division of Entomology, North Carolina Department of Agriculture for the identification of this species.

Table 20. Means of Sample Counts Taken Every Two Days After Irradiation

Days Postirradiated	Control Mean (N_i = 13)	3000-r Mean (N_i = 16)	5000-r Mean (N_i = 16)	7000-r Mean (N_i = 16)
2	26.7 ± 9.66	28.0 ± 7.43	21.5 ± 5.35	23.0 ± 5.03
4	36.0 ± 7.68	25.2 ± 5.62	21.1 ± 4.55	26.6 ± 5.90
6	50.6 ± 14.43	37.5 ± 9.46	28.1 ± 5.88	27.5 ± 6.27
8	39.2 ± 9.87	28.7 ± 5.34	23.1 ± 3.48	21.6 ± 3.17
10	57.5 ± 12.50	47.8 ± 10.21	39.6 ± 9.40	25.2 ± 4.33
12	87.0 ± 24.65	76.2 ± 15.57	55.0 ± 11.68	25.8 ± 4.15
14	115.8 ± 26.41	121.3 ± 23.76	78.1 ± 13.45	53.0 ± 8.52
16	111.8 ± 25.22	103.8 ± 19.26	78.6 ± 12.92	60.2 ± 8.22
Grand means	65.6 ± 6.89	58.6 ± 5.62	43.2 ± 3.74	33.52 ± 2.39

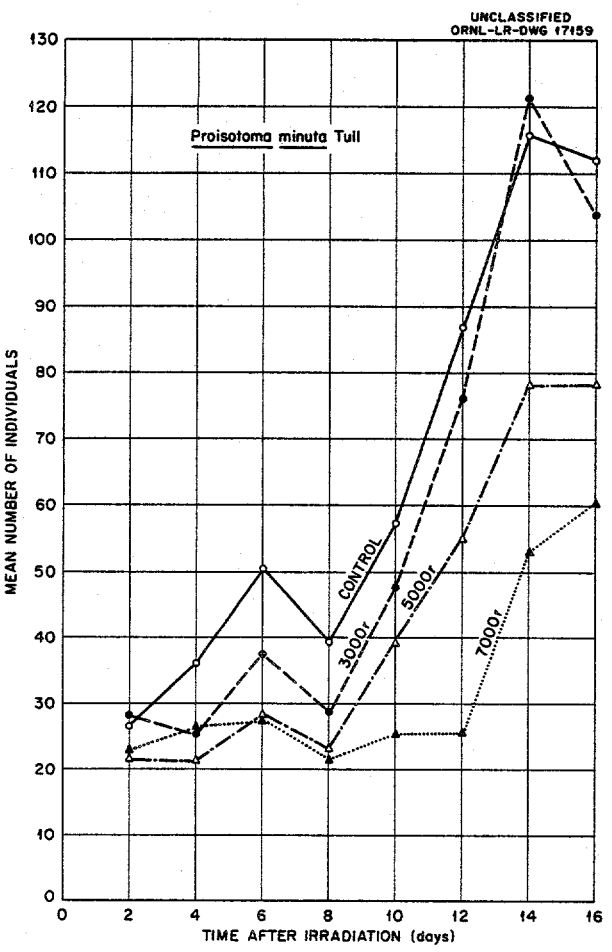

Fig. 11. The Effect of Acute Gamma Radiation on Growth of Collembola Population Units as Shown by Bidaily Counts of Individuals at Feeding Points.

Radiation Effects on *Trogoderma sternale* Jayne. – This study was an extension of work begun in 1955 on the comparative effects of radiation on various species of forest Coleoptera.[36] The first species investigated, *Onthophagus texanus* Schaffer, belongs to that large group of beetles which possesses relatively fixed habits, together with a low reproductive capacity. In contrast, *Trogoderma* is labile in its food needs and has a high reproductive potential.

Gamma radiation from a Co^{60} source delivering 19 r/sec was used to irradiate 1600 larvae of *T. sternale*. Each of two series received doses of 1, 2, 3, 4, 5, 6, and 10 thousand r, one series receiving the total dose in one treatment, the second receiving $\frac{1}{5}$ of the dose each day for 5 days.

Differences in population size at the various dose levels and differences in larval development time are summarized in Table 21. Figure 12 depicts the number of original larvae still present in each of the populations six months after irradiation, There was no immediate mortality in any of the replicates. Some of the larvae in each series survived the 10,000-r dose for at least four months but did little feeding and actually became smaller in size. Doses from 1000 to 4000 r delayed development to the adult stage but did not entirely inhibit reproduction.

Fractionation of the dose seems to have increased the total dose required for sterilization. The *Trogoderma* receiving an instantaneous dose of 5000 r were unable to reproduce; a fractionated dose of 6000 r was needed to produce this same effect. Also, Fig. 12 gives an indication that fractionated doses have less effect upon transformation of larvae than do single doses. At 10,000 r (Table 21) fractionation of the dose had a lesser effect on the larvae than did a single dose. However, differences in fractionation vs single-dose effects on population size below the sterilization level were not evident.

From these data it is impossible to detect differences between fractionated and single dosages at the lower levels because of the large variation among replicates. It should be emphasized that the experiments measure not only sterility of individuals but sterility of populations as well so that many additional factors are introduced. For example, in *Trogoderma* the females usually emerge a week or so before the males. If the female life span is shortened, perhaps by the effects of irradiation, the female may die before the male has emerged, having the same result as sterilization. This appeared to be one of the factors affecting the variations in population sizes and serves to illustrate that not just one factor, such as sterilization of individuals, should be considered, but that all of the ecological aspects need be investigated when considering the effects of radiation on population survival.

Reduction in population size at the lower levels of radiation may not have been due to sterility as

[36] S. I. Auerbach *et al.*, *HP Semiann. Prog. Rep. Jan. 31, 1956*, ORNL-2049, p 5.

Table 21. Effects of Dose and Exposure on Time of Transformation of Larvae and on Fertility as Expressed by Number of Individuals

All replicates were started with 50 larvae

Dose	Single Exposure				Fractionated 5-Day Exposure			
	Original Larvae After 2 Months	Original Larvae After 6 Months	Number of F_1 Larvae in 2 Months	Number of F_1 and F_2 Larvae in 6 Months	Original Larvae After 2 Months	Original Larvae After 6 Months	Number of F_1 Larvae in 2 Months	Number of F_1 and F_2 Larvae in 6 Months
Control								
a	38	0	331	820	11	0	569	700
b	45	0	64	553	22	0	555	824
1000 r								
a	37	16	176	486	24	15	178	485
b	40	18	20	225	20	0	196	588
2000 r								
a	38	28	136	358	26	14	22	79
b	45	17	20	122	25	13	5	54
3000 r								
a	35	27	178	286	21	17	86	434
b	40	15	63	288	34	12	20	28
4000 r								
a	40	26	4	49	23	18	4	48
b	42	22	0	0	29	21	4	7
5000 r								
a	46	31	0	0	27	19	32	192
b	43	30	0	0	24	14	0	0
6000 r								
a	38	14*	0	0	21	14	0	0
b	39	14*	0	0	25	18	0	0
10,000 r								
a	5*	0*	0	0	42	3*	0	0
b	8*	0*	0	0	30	2*	0	0

*Mortality causing reduction in numbers before pupation.

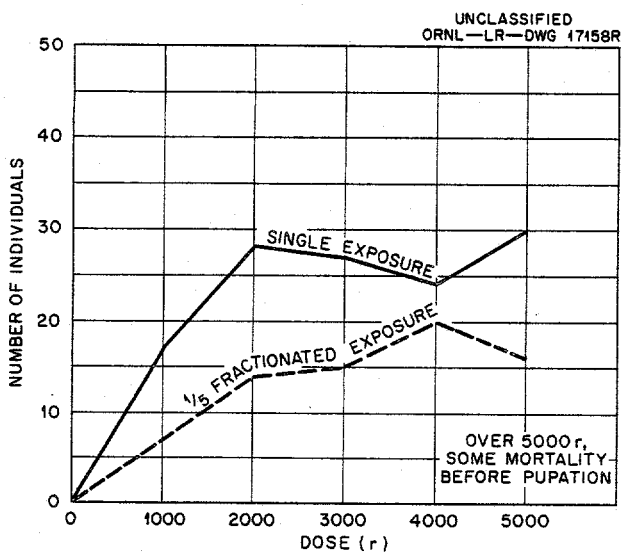

Fig. 12. Effects of Single and Fractionated Exposures on Transformation of Larvae. Numbers of untransformed larvae remaining after six months.

much as to lessened vitality, a suggestion originally proposed by Whiting and Bostian.[37] Less frequent matings and slightly shortened adult life span might be a factor in reducing the reproductive potential of any insect species. In *T. sternale* these effects may be magnified owing to the timing of the appearance of adults. It was noted, particularly in the 3000- and 4000-r treatments, that the females often died before the males emerged, an event which eliminated reproduction as effectively as sterilization.

Radiation Effects on Two Mite Species. – In a previous report[38] studies on the effect of gamma radiation upon the mite *Caloglyphus* were detailed. The hatchability of eggs was the criterion used as a measure of radiation effect. At exposures below 5000 r, no effects were observed in irradiated females; however, such doses induced a temporary sterility in irradiated males.

During the current period the effects of higher exposures on both males and females of *Caloglyphus* were determined. Figure 13 presents the results of these experiments.

Caloglyphus males have been irradiated at 4000-, 5000-, and 8000-r gamma doses. At the lower doses fertility approaches that of controls on the fifth day of postirradiation pairing. At 8000 r, hatchability ranges from 19 to 36% of normal during the first three days of mating. This is the period of highest egg production under normal conditions. Fertility appears to return to normal near the eighth to tenth day of pairing.

That the return of fertility in the male is real and not a function of egg decline in the female was tested in a separate series of experiments. Males irradiated at 5000 r received a virgin female every third day. Results show that sterility is temporary and fertility returns to the male on the fifth day. Effects of irradiation upon female *Caloglyphus* are slight at 8000 r but are more marked at 12000 r (Table 22).

Caloglyphus serves as prey for a predatory species of mite, *Fuscuropoda*. In these mites, the median incubation period for eggs is seven days, compared to 40 hr for *Caloglyphus*. *Fuscuropoda* requires approximately 40 days to complete its life cycle; that of *Caloglyphus* is completed in 6 to 7 days.

In experiments paralleling those on *Caloglyphus*, eggs of *Fuscuropoda* of maximum 24 hr age were irradiated with gamma doses ranging from 100 to 3000 r (Fig. 14). Complete lethality occurs beginning with 2000 r. The 24-hr eggs were used, since eggs of this age were irradiated in *Caloglyphus* experiments. However, *Fuscuropoda* eggs at 24 hr age have completed only about one-seventh of their development, while *Caloglyphus* eggs have completed about half their development at 24 hr age. Therefore, in a series of experiments *Fuscuropoda* eggs of 84 hr age were irradiated; these eggs should have completed about half their development. Hatchability is virtually unaffected in dosages to 3000 r (Fig. 14).

Waste-Pit-Area Studies

Uptake of Fission Product Seepage by Vegetation. – Monitoring of the core wells located within and around the margin of the ORNL waste pit area indicated that seepage containing Ru^{106} and free nitrates had migrated from the pits through the Conasauga shale directly and by means of ground fissures for some distance. Because of

[37] A. R. Whiting and C. H. Bostian, *Genetics* 16, 659–680 (1931).

[38] S. I. Auerbach *et al.*, *HP Semiann. Prog. Rep. July 31, 1956*, ORNL-2151, p 16.

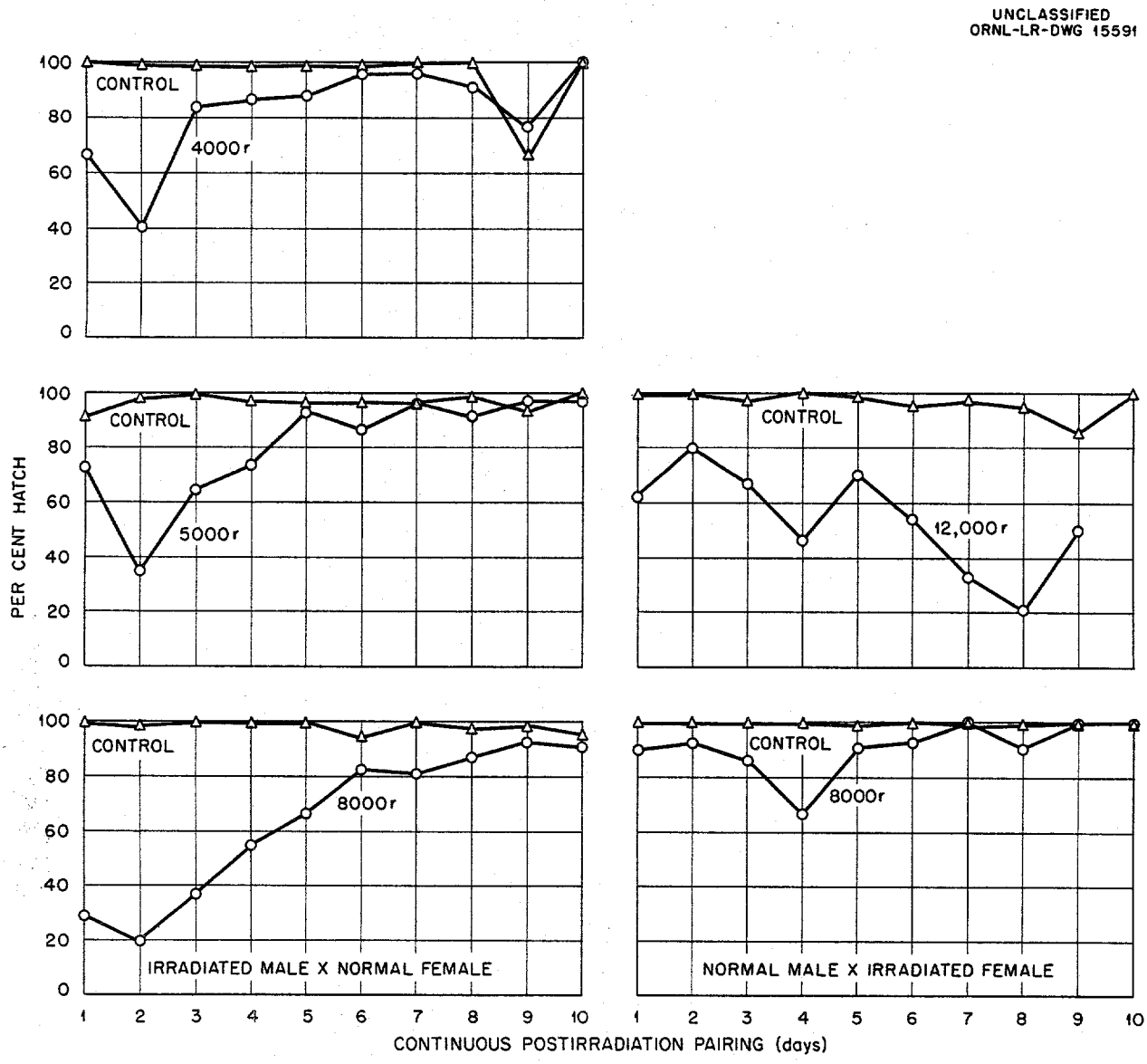

Fig. 13. Radiation-induced Sterility in *Caloglyphus*.

evidence that the trees and other vegetation were taking up radioactive materials, it was felt that a more detailed study of the uptake of radionuclides by trees in the vicinity was necessary. Primary objectives were (1) to determine the specific activity of Ru^{106} in tree components and ground litter; (2) to ascertain if Ru^{106} and other fission products were being concentrated; (3) to compare the geographical distribution of radionuclides in the trees and ground litter with that obtained from core well data.

Initially a series of samples were taken from 15 species of trees mainly located at the outer margin of radionuclide distribution as indicated by well data (Table 23). In most cases these trees were approximately 300 to 500 ft from the pits proper. As shown in Fig. 15 the sampled trees tend to fall into two groups. Those east of the

Table 22. Hatchability of Eggs from Female *Caloglyphus* Irradiated at 12,000 r

Ten virgin irradiated females paired with ten virgin males; two pairs of virgin adults as controls.

Day	Experimental			Control		
	Total Eggs	Total Hatch	Per Cent Hatch	Total Eggs	Total Hatch	Per Cent Hatch
1	197	120	60.9	81	81	100
2	341	273	80.0	44	44	100
3	178	119	66.8	116	113	97.4
4	258	121	46.8	105	105	100
5	72	51	70.8	119	117	98.3
6	26	14	53.8	40	38	95.0
7	30	10	33.3	43	42	97.6
8	14	3	21.4	21	20	95.2
9	4	2	50.0	14	12	85.7
10	0			12	12	100

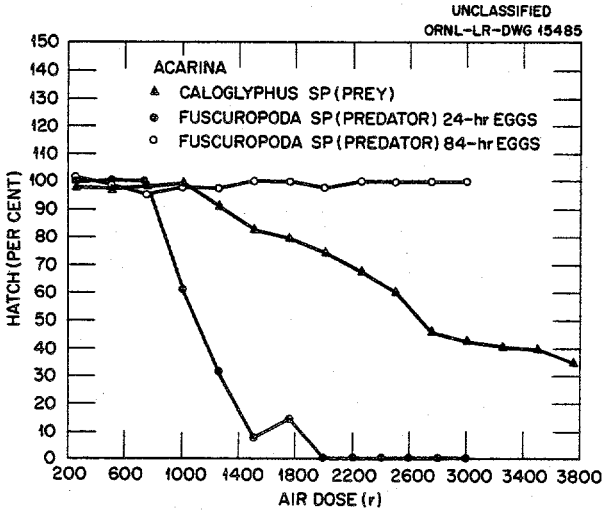

Fig. 14. Effects of Gamma Irradiation upon Hatchability of Eggs of *Fuscuropoda* Species. Effects upon *Caloglyphus* eggs included for comparison.

pits are generally located along the drainage line which is commonly referred to as the "east seep," while those west of the pits are mainly along the drainage known as the "west seep." Eleven species were sampled along each seep with seven species duplicated in each series.

Preliminary sampling included bark at 2 to 5 ft above the ground, twigs at various heights, and litter from beneath the trees. The first samples were taken before the trees had begun to leaf and were analyzed for gross beta activity (Table 24). These prevernal data provided a basis for comparison with subsequent samples taken in various stages of foliation. On the basis of gross radioactivity 12 of the trees were selected for systematic study over an extended period. These trees were evenly divided between the east and west sides of the pit area. They were sampled on April 24 and May 23, in addition to the initial samples taken before April 3.

Leaves and twigs were collected by means of a pruning device at heights of 4, 8, 16, and 20 ft from the ground. The samples were dried at 60 to 70°C for periods ranging from 18 to 40 hr and then ground in a Wiley mill to pass a 20- or 40-mesh screen. Portions ranging in weight from 30 to 60 mg were mounted on 1-in. watch glasses and analyzed for gross beta activity by counting on the second shelf of an end-window G-M counter. The activity was then converted to a standard weight of 1 g of dry material. Next the samples were ashed at 500 to 550°C for 18 to 40 hr depending on the constituency of the material. Ash percentages were determined, and approximately 20 mg of ash was analyzed for gross beta activity. These activities were converted to a dry weight basis by the following: (activity per gram of

Table 23. Names and Locations of Trees Sampled for Radionuclides

Tree No.	Common Name	Scientific Name	Location	
			Direction	Near Well No.
1	Short leaf pine	*Pinus virginiana* Mill.	NE	101
2	Scrub pine	*Pinus echinata* Mill.	SE	118
3	Scrub pine	*Pinus echinata* Mill.	SW	100 (across road)
4	Short leaf pine	*Pinus virginiana* Mill.	S	92
5	Short leaf pine	*Pinus virginiana* Mill.	SW	120
6	White pine	*Pinus strobus* L.	W	120
7	Dogwood	*Cornus florida* L.	W	105
8	Scrub pine	*Pinus echinata* Mill.	NW	74 (across road)
9	Black locust	*Robina Pseudo-Acacia* L.	SE	100 (fork of road)
10	Sassafras	*Sassafras variifolium* Ktze	NW	85 (across road)
11	Sweet gum	*Liquidamber Styraciflua* L.	N	95
12	Sycamore	*Platanus occidentalis* L.	NW	106
13	Sycamore	*Platanus occidentalis* L.	NW	106
14	Red cedar	*Juniperus virginiana* L.	SE	116 (across road)
15	Sycamore	*Platanus occidentalis* L.	SE	84
16	Sweet gum	*Liquidamber styraciflua* L.	SE	83
17	Elderberry	*Sambucus canadensis* L.	E	83
18	Black willow	*Salix nigra* Marsh.	N	83
19	Black walnut	*Juglans nigra* L.	S	84
20	Tulip poplar	*Liriodendron Tulipifera* L.	W	95 (across seep)
21	Black willow	*Salix nigra* Marsh.	NE	84
22	Red cedar	*Juniperus virginiana* L.	E	106
23	Red cedar	*Juniperus virginiana* L.	S	106
24	White pine	*Pinus strobus* L.	S	106
25	Scrub pine	*Pinus echinata* Mill.	N	106
26	Scrub pine	*Pinus echinata* Mill.	NE	106
27	Tulip poplar	*Liriodendron Tulipifera* L.	N	117
28	Red maple	*Acer rubrum* L.	N	106
29	Black willow	*Salix nigra* Marsh.	S	97
30	Red maple	*Acer rubrum* L.	S	97
31	Red maple	*Acer rubrum* L.	S	97
32	Red maple	*Acer rubrum* L.	E	97
33	Pokeberry	*Phytolacca americana*	S	83 (edge of road)
34	Sycamore	*Platanus occidentalis* L.	NW	85
35	Dogwood	*Cornus florida* L.	E	97 (across fence)
36	Pokeberry	*Phytolacca americana*	W	117 (edge of road)
37	Sweet gum	*Liquidamber styraciflua* L.	NW	92

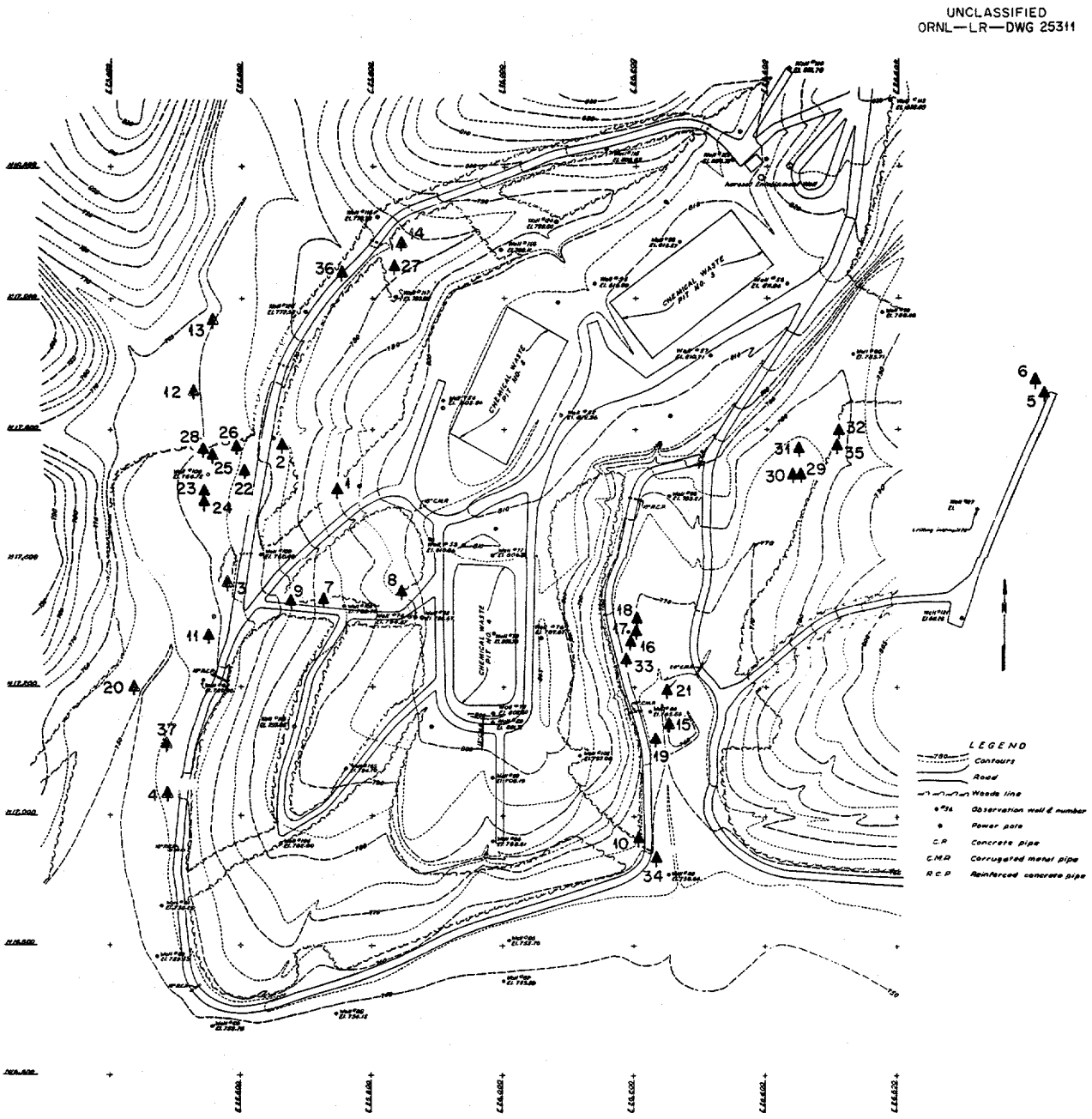

Fig. 15. Locations of Trees Sampled for Radionuclides.

ash × per cent ash)/100. The results are listed in Tables 25 and 26.

The specific activity of Ru^{106} was obtained by using ash and converting to a dry weight basis. A weighed sample of ash was dissolved with 2 to 4 ml concentrated nitric acid during which time the flask was simultaneously cooled in an ice bath to minimize the loss of Ru^{106} by volatilization. Following this, the analysis was performed according to standard procedures.[39] The ruthenium precipitate was collected on a tared filter disk, dried, weighed, and mounted on a 1-in. watch glass

[39] R. E. Druschel, "Ruthenium Activity in Aqueous or Organic Solutions," Method No. 2 21731 (3-2-54) *ORNL Master Analytical Manual.*

Table 24. Gross Activity of Tree Samples in Disintegrations per Minute per Gram Dry Weight

Theoretical dry weight values calculated from ash weight. All samples taken prior to April 3.

Tree No.*	Bark	Litter	Twig	Leaves	Cone or Seeds	Flower
5	0	900	0	0	0	
6	400	2,700	0	0		
7	1000	3,900				
8	500					
9	500	2,000				
10	1100	12,400				
11	0	1,000				
12	56 at 5 ft 2380 at 2 ft	2,200		0		
13	3500 at 5 ft 30 at 2 ft	3,530				
14	450		280	220		
15	1500	14,900	3390			
16	370	4,480				
17			1060	1660		
18	390		300			
19	200		0			
20	136	2,280	370			
21	400		310			
22	175	140				
23				2420		
24	130	950		360		
25				1630		
26	90	2,800		770	1430	250
27	0	1,300	0			
28	60			1000		
29	2200	1,800				
30	1200					
31	625		1250	1250	1250	
32	1250	7,400		1250		
33						
34			690	3000		
35			250	450		930
36			500	620		
37		600	100	1850		

*See Fig. 1.

Table 25. Gross Activity of Monitor Trees Along East Seep at Different Sample Periods

Values calculated from ash activity data

Tree No.	Type Sample	Sample Period, 4-3-57* (dpm/g dry wt)	Height of Sample (ft)	Sample Period, 4-24-57 (dpm/g dry wt)	Sample Period, 5-23-57 (dpm/g dry wt)
10	Bark	88			
	Litter	7800			
	Twigs		16	150	110
			20	160	210
	Leaves		16	1,800	110
			20	175	490
15	Bark	440			
	Litter	1500			
	Twigs	220	8	850	3,200
			12	5,300	600
			16	10,000	5,700
			20	9,300	7,500
	Leaves		8	1,200	2,450
			12	1,900	2,440
			16	1,500	1,850
			20	2,150	3,000
16	Bark	380			
	Litter	4500			
	Twigs	710	8		24,000
			12	1,680	24,000
			16	1,350	14,400
			20		9,200
	Leaves		8		180,000
			12	7,200	203,000
			16	5,600	230,000
			20		145,000
34	Twigs		8		930
			12		750
			16	690	750
			20		910
	Leaves		8		4,340
			12		3,380
			16	3,000	3,000
			20		3,100

*These samples were taken on or prior to this date, which was before leafing.

Table 26. Gross Activity of Monitor Trees Along West Seep at Different Sampling Periods

Values calculated from ash activity data

Tree No.	Type Sample	Sample Period, 4-3-57* (dpm/g dry wt)	Height of Sample (ft)	Sample Period, 4-24-57 (dpm/g dry wt)	Sample Period, 5-23-57 (dpm/g dry wt)
20	Bark	140			
	Litter	2280			
	Twigs		12	110	140
			16	110	
			20	160	150
	Leaves		12	1251	220
			16	125	
			20	380	490
24	Bark	140			
	Litter	950			
	Twigs		4	540	
			8	440	750
			12	390	
	Leaves		4	1440	
			8	1200	2800
			12	2300	
26	Bark	88			
	Litter	2800			
	Cones	250			
	Dead Leaves	1400			
	Twigs		8	980	1190
			12	560	850
			16	840	1480
			20	460	1300
	Leaves		8	2540	3550
			12	2300	3000
			16	5100	4000
			20	1640	5150

*These samples were taken on or prior to this date, which was before leafing.

and counted on the second shelf of an end-window G-M counter.

Ruthenium-106 accounted for 90 to 95% of the total activity of the ash in most of the samples. Consistently lower percentages were found in about 20% of all the samples. Of these only two or three were low due to incomplete oxidation in the distillation step of the process. The consistently low percentage of the total activity due to Ru^{106} in the remainder of the 20% suggested the presence of other radionuclides. These were analyzed with the 20-channel gamma spectrometer.[40] The litter beneath trees 15 and 26 showed measurable concentrations of Cs^{137} and Co^{60}. The Cs^{137} data were confirmed by analyzing these

[40] Work performed by Radiochemistry Group of S. A. Reynolds, Analytical Chemistry Division.

samples radiochemically. A second set of leaf and twig samples from six trees, including 15 and 26, were also scanned with the spectrometer. Cobalt-60 was detected in all samples. Cesium-137 was not present in significant concentrations. The specific activities of Ru^{106} in monitor trees are summarized in Tables 27 and 28. Also, kinds and concentrations of nuclides in monitor trees, as detected by gamma spectrometry, are given in Table 29.

On an individual tree, the height from which the sample was taken had little effect on its activity. Both twig and leaf samples of tree No. 10 showed more activity in higher samples, but this was not consistent throughout the group of trees. The litter samples taken prior to April 3

Table 27. Specific Activity (Microcuries per Gram of Dry Weight) of Ru^{106} in the Monitor Trees Along East Seep at Different Sampling Periods

Tree No.	Type Sample	Sample Period, 4-3-57* (μc/g dry wt)	Height of Sample (ft)	Sample Period, 4-24-57 (μc/g dry wt)	Height of Sample (ft)	Sample Period, 5-23-57 (μc/g dry wt)
10	Bark	1.7×10^{-5}				
	Litter	3.0×10^{-3}				
	Twigs		16	1.6×10^{-5}	16	3.0×10^{-5}
	Leaves		16	2.8×10^{-3}**	16	2.0×10^{-6}
15	Bark	2.0×10^{-4}				
	Litter	3.8×10^{-3}				
	Twigs	5.0×10^{-5}	8	3.4×10^{-4}	8	1.7×10^{-3}
			12	2.2×10^{-3}		
			16	4.3×10^{-3}		
			20	3.9×10^{-3}**	20	3.0×10^{-3}
	Leaves		8	5.1×10^{-4}	8	1.0×10^{-3}
			12	5.7×10^{-4}	12	9.8×10^{-4}
			16	5.7×10^{-4}	16	2.6×10^{-3}
			20	8.2×10^{-4}	20	1.3×10^{-3}
16	Litter	1.5×10^{-3}				
	Twigs	9.8×10^{-5}	8			
			12		12	1.2×10^{-2}
			16			
			20			
	Leaves		8		8	8.9×10^{-2}
			12	2.0×10^{-3}**	12	9.6×10^{-2}
			16	3.5×10^{-4}	16	1.1×10^{-1}
			20		20	6.9×10^{-2}
34	Twigs		16	2.2×10^{-4}	16	3.2×10^{-4}
	Leaves		16	7.2×10^{-4}**	16	1.4×10^{-3}

*These samples all taken on or prior to this date, which was before budding.

**Analyzed by gamma spectrometry.

Table 28. Specific Activity (Millicuries per Gram of Dry Weight) of Ru^{106} in the Monitor Trees Along West Seep at Different Sampling Periods

Tree No.	Type Sample	Sample Period, 4-3-57* (μc/g dry wt)	Height of Sample (ft)	Sample Period, 4-24-57 (μc/g dry wt)	Height of Sample (ft)	Sample Period, 5-23-57 (μc/g dry wt)
20	Bark	1.9×10^{-4}				
	Litter	2.1×10^{-4}				
	Twigs	2.4×10^{-5}				
	Leaves		20	6.1×10^{-5}	20	4.0×10^{-5}
24	Bark	6.2×10^{-5}				
	Litter	1.2×10^{-4}				
	Leaves	4.3×10^{-5}	4	5.42×10^{-5}		
			8	2.8×10^{-4}**	8	1.1×10^{-3}
26	Bark	6.2×10^{-5}				
	Litter	9.6×10^{-4}				
	Cones	1.6×10^{-5}				
	Twigs				16	4.0×10^{-4}
	Leaves	2.54×10^{-4}	12	8.3×10^{-4}	8	8.8×10^{-4}
			16	1.2×10^{-3}**	12	1.2×10^{-3}
			20	4.8×10^{-4}	16	8.3×10^{-4}
					20	1.9×10^{-3}

*These samples were taken on or prior to this date, which was before leafing.
** Analyzed by gamma spectrometry.

Table 29. Gamma Spectrometic Analyses of Tree Material (Millicuries per Gram of Dry Weight)

Tree No.	Type and Height (ft) of Example	Sampling Period, 4-3-57*			Sampling Period, 4-24-57		
		Ru^{106}	Co^{60}	Cs^{137}	Ru^{106}	Co^{60}	Cs^{137}
10	Leaves, 20				2.8×10^{-3}	3.9×10^{-5}	3.9×10^{-5}
15	Litter	2.2×10^{-3}	8.7×10^{-5}	6.5×10^{-4}			
	Twig, 20				2.9×10^{-3}	9.1×10^{-5}	4.6×10^{-5}
16	Leaves, 12				2.0×10^{-3}	1.1×10^{-4}	4.3×10^{-5}
24	Leaves, 8				2.8×10^{-4}	7.1×10^{-5}	1.8×10^{-5}
26	Litter	3.5×10^{-4}	9.7×10^{-5}	2.9×10^{-4}			
	Leaves, 16				1.2×10^{-3}	1.6×10^{-4}	8.1×10^{-5}
34	Leaves, 16				7.2×10^{-4}	7.2×10^{-5}	3.6×10^{-5}

*These samples were taken on or prior to this date, which was before leafing.

had more activity than did any of the samples from the trees. Activities of leaf and twig samples were higher than bark, sap, or flower samples.

Leaf and twig samples taken through time show that activities in these tissues are approaching litter values. Approximately a tenfold increase in activity accumulated in leaves and twigs during the sampling periods. Tree No. 16 (east seep) shows concentrations of ruthenium greater than the litter values for that tree. This tree has now died; salt concentrations at the base seem responsible for the death of the tree.

Comparisons of trees from the two seeps show that trees of the east seep generally have more activity than do those of the west seep. Tree No. 10 (east seep) would appear to be an exception; however, this tree is on an elevation and is considerably higher than other trees on the seep. Gross measurements of seep water show more activity in the east seep than in the west seep.

Along each seep, trees nearer the head of the seep show more activity. While this is logical, the small number of trees sampled and the presence of additional factors must be considered. It is possible that the relationship is fortuitous.

Inadequate replication of tree species sampled makes it impossible to compare trees for differences in uptake between species. It is notable, however, that different species of trees differ in uptake of ruthenium by no more than a factor of ten. Extremes are the low values for tree No. 10 (on an elevation) and the high values for tree No. 16 (now dead, in high salt concentration). While differences between species of trees probably exist, these differences do not seem to be great.

No explanation is offered for the presence of Cs^{137} in some samples. This nuclide has not been detected in the seep water. It seems possible that the trees may concentrate Cs^{137} from undetected trace amounts in seep water, but this hypothesis requires confirmation before it may be seriously advanced.

Uptake of Ru^{106} and Co^{60} from Seep Water by Bean Plants. – The unexpected occurrence of Cs^{137} in trees in the ORNL Waste Pit area led to an experiment in which bean plants grown in uncontaminated soil were watered with liquid obtained from seeps in the waste pit area. If Cs^{137} is present in seep water in trace concentrations, it is possible that this nuclide may be concentrated to detectable levels by plants. Beans were chosen because of their rapid growth and ability to tolerate the high nitrates present in the seep water.

At the conclusion of the experiment no Cs^{137} could be detected in the bean plants, the soils in which the plants were grown, nor the seep waters used. However, Ru^{106} and Co^{60} were present in these materials. The data from this experiment are of interest for comparison with the tree data.

For the experiment ten flower pots were used. Each pot received 3 kg of an uncontaminated shale-earth mixture. Five beans were planted in each pot. These pots were then divided into two groups of five each; one group received water dipped from the east seep at the ORNL waste pits, the other received water from the west seep. Three hundred milliliters of water were added to each pot at two-day intervals (usually). The experiment was terminated after 28 days.

During the course of the experiment it became obvious that plants receiving the east-seep water were growing less successfully than those receiving the west-seep water. As shown in Fig. 16 east-seep plants were smaller and of a darker color than west-seep plants. Measurements with a G-M survey meter showed considerably more activity in pots receiving east-seep water.

At the termination of the experiment a composite sample of each of the seep waters was prepared and analyzed;[41] results of the analyses are given in Table 30. Analyses[41] were performed on soils from pots Nos. 9 and 12 (east seep) and Nos. 1 and 2 (west seep) (see Table 31). Bean plants from these pots were divided into roots, stems, and leaves, and these materials were analyzed[41] (Table 32).

The chemical analyses of the composite water samples and of the soils at termination of the experiment show concentrations of some elements which are high by agricultural standards. An unfavorable balance of nutrient materials probably accounts for the failure of beans receiving east-seep water to grow well. It seems likely that had

[41] Analytical Chemistry Division performed the radionuclide analyses by gamma spectrometry (Radiochemistry Group) and the chemical analyses (Service Group).

Fig. 16. Bean Plants (3 Weeks of Age) Grown in Similar Soils but Watered from Two Different Seeps from ORNL Waste Pits. Pots in the front row were provided with east-seep water; those in the back row, west-seep water.

Table 30. Analysis of Composite Samples of Seep Water (in mg/ml, Except pH and Activity)

	East Seep	West Seep
NO_3	6.94	1.86
NH_3	0.1	0.1
Na	1.63	0.26
Ca	0.82	0.27
Cl	0.36	0.05
SO_4^{--}	0.49	0.08
Total solids	13.75	3.38
pH	7.0	7.7
Activity, $\mu c/ml$		
Ru^{106}	2.25×10^{-2}	2.70×10^{-3}
Co^{60}	4.50×10^{-4}	9.01×10^{-5}

the experiment been prolonged, plants in all pots would have showed signs of this chemical imbalance.

Soils in the flower pots appear to have retained most of the Ru^{106} added in the seep water. As each pot contained 3 kg of soil, the values in Table 31 for Ru^{106} may be extrapolated to 30 μc in pot No. 12 and 60 μc in pot No. 9 (east seep). A total of 3300 ml of east-seep water by extrapolation from Table 30 should have contained about 75 μc of Ru^{106}. Similar calculations for west-seep water show concentrations of 4 and 10 μc in pots 1 and 2, respectively, each of which received about 9 μc of Ru^{106}.

Activity in the plants was present in roots, stems, and leaves. Stems consistently showed less activity than did roots or leaves, as shown in Table 32. The ratio of plant to soil values on a per gram basis, as shown in Table 32, seem to indicate only that Ru^{106} is absorbed by plants.

Table 31. Analysis of Soils at Termination of Experiment

	Pot No. 9 (East-Seep Water)	Pot No. 2 (West-Seep Water)
NO_3	0.45%	0.09%
NH_3	0.02%	0.02%
Na	0.70%	0.88%
Ca	873 ppm	853 ppm
Cl^-	57 ppm	41 ppm
SO_4^{--}	0.12%	293 ppm
pH	4.9	4.5
Activity, $\mu c/g$		
Ru^{106}	2.06×10^{-2} (pot No. 12: 1.02×10^{-2})	3.27×10^{-3} (pot No. 1: 1.48×10^{-3})
Co^{60}	6.89×10^{-4} (pot No. 12: 3.40×10^{-4})	2.82×10^{-5} (pot No. 1: 8.87×10^{-5})

These values are not so large as to indicate concentration. Similar conclusions for Co^{60} seem to be indicated. Plant activity values for Ru^{106} are of a similar magnitude as those obtained from trees in the waste pit area.

Aquatic Studies. – Biological surveys of the Clinch River above White Wing Bridge showed almost no suspended organisms. Surveys of the embayments from that point to the Watts Bar Dam showed a very large species list, with large numbers often in bloom proportions. Several samples from each of three other lakes, taken at different intervals revealed the same species list, substantially. These waters all contain enough phosphorus and nitrogen for bloom support. The remaining pool in the White Oak Lake bed is consistently muddy, and has had few organisms and relatively few species. Its water has had a very low gross beta count. Concentrated algae from the Clinch embayment into which it enters have had gross beta counts several hundred times greater. A bloom from an embayment near the Gallaher bridge also showed an accumulation of radioactivity. Algae from the seepage areas at the disposal pits, and from the sedimentation basin have shown gross beta counts up to 400,000 per minute per gram of dried algae. Both areas contain many organisms, but the seepage areas have few species. Exposure of mixed dense cultures from the seepage areas to Co^{60} radiation up to 32,000 r indicates that chemical and osmotic factors are the factors limiting growth and not radiation. However, limitation may be due to continuous exposure to radiation as high as 20 mr/hr. A complete treatment of these results will be published as a separate ORNL report.

MAXIMUM PERMISSIBLE CONCENTRATION STUDIES

M. J. Cook
M. R. Ford
F. G. Karioris[42]
J. M. Kohn
K. Z. Morgan
J. R. Muir
W. S. Snyder

Internal Dose Handbook Revisions

The National[43] and International[44] Handbooks on Internal Dose are being revised and will be submitted to the respective subcommittees for review. Biological data are included for 98 stable elements in the total body and in the principal organs of deposition. For 227 radionuclides maximum permissible concentration (MPC) values for occupational exposure are calculated for the total body and the gastrointestinal (GI) tract and the other principal organs of deposition (these principal organs vary from one to six in number). A comparison in the number of elements for which MPC values are listed in the handbooks and in the revisions is given in Table 33.

[42] F. G. Karioris, Physics Department, Marquette University, summer employee.

[43] U.S. National Bureau of Standards, *Maximum Permissible Amounts of Radioisotopes in the Human Body and Maximum Permissible Concentrations in Air and Water*, Handbook 52 (1953), Superintendent of Documents, Washington 25, D. C.

[44] International Congress of Radiology, "Recommendations of International Commission of Radiological Protection," *Brit J. Radiol., Suppl. 6*, 23–29 (1955).

Table 32. Ru^{106} and Co^{60} Activity in Bean Plants

Source of Activity	Pot No.	Nature of Sample	Ru^{106} ($\mu c/g$)	Ratio: $\frac{\mu c/g, \text{ plant}}{\mu c/g, \text{ soil}}$	Co^{60} ($\mu c/g$)	Ratio: $\frac{\mu c/g, \text{ plant}}{\mu c/g, \text{ soil}}$
East-seep water	9	Roots	1.02×10^{-1}	4.95		
		Stems	0.97×10^{-1}	4.70	2.44×10^{-4}	0.35
		Leaves	1.50×10^{-1}	7.28	7.48×10^{-4}	2.20
	12	Roots	1.38×10^{-1}	13.53	3.45×10^{-3}	10.15
		Stems	1.00×10^{-1}	9.80	2.35×10^{-3}	6.91
		Leaves	1.42×10^{-1}	13.97	4.73×10^{-3}	13.91
West-seep water	1	Roots	3.09×10^{-2}	20.88		
		Stems	1.10×10^{-2}	7.43		
		Leaves	2.23×10^{-2}	15.07		
	2	Roots	1.42×10^{-3}	0.43		
		Stems	0.51×10^{-3}	0.16		
		Leaves	1.45×10^{-3}	0.44		

Table 33. Number of Elements or Radionuclides for Which Exposure Data Are Given in Internal Dose Handbooks

	Handbook 52 (NCRP)	ICRP	Revisions
Stable elements		86	98
Radionuclides	70	86	227

Number of Values of Body Burden, q, and MPC Given in Internal Dose Handbooks

	Handbook 52 (NCRP)			ICRP			Revisions		
	q	MPC_{air}	MPC_{water}	q	MPC_{air}	MPC_{water}	q	MPC_{air}	MPC_{water}
Values for critical organ (other than GI tract)	76	76	76	100	100	100	920	920	920
Values for GI tract					86	86		227*	227*

*Although MPC values are given in the revised handbooks only for the critical portion of the GI tract, values were calculated for four segments (stomach, small intestine, upper large intestine, and lower large intestine) for each of the 227 radionuclides. These additional values are available upon request.

At the present time there are two basic standards by which MPC values are calculated. (1) From the long-term exposures of the radium-dial painters and the patients of radium therapy, 0.1 μg of Ra^{226} deposited in the body has been set as the maximum permissible body burden and this exposure level has been adopted as the basic standard of reference for other bone-seeking radionuclides. At this level no pathology in the bone has been reported. From the recent studies of Norris *et al.*[45] the estimate of the per cent of radium daughter products retained in the bone has been reduced from 55% to 30%. Assuming a relative biological effectiveness (RBE) of 10 for alphas, 0.1 μg of deposited Ra^{226} + 30% daughter products will deliver 0.56 rem/week to the bone. Therefore, based on Ra^{226} the internal RBE dose rate resulting from a maximum permissible body burden of a bone-seeking radionuclide corresponds to 0.56 rem/week. (2) The second basic standard is 0.3 rem/week of RBE dose to the critical organ unless the critical organ is the total body, the gonads, bone, thyroid, or skin. If the total body or the gonads are the critical body organs the maximum permissible RBE dose rate is 0.1 rem/week. If the thyroid or the skin are the critical body organs the maximum permissible RBE dose rate is 0.6 rem/week. In the revised handbooks the limiting RBE dose rate is 0.1 rem/week in the case of 43 radionuclides for which the total body is the critical body organ. In no cases are the gonads taken as the critical body organ for occupational exposure, and only values for occupational exposure are given in the internal dose handbooks. Also, in the revised handbooks 0.6 rem/week is the limiting RBE dose rate for three radionuclides for which thyroid is the critical body organ and for two radionuclides for which skin is the critical body organ.

In the present handbooks the biological half life generally has been determined by assuming that the burden in the critical body organ decreases exponentially. From studies of the burdens in the critical body organ for Sr^{90}, Pu^{239}, Ra^{226}, and U^{238} as they decrease following a single intake, it is apparent that the long-term retention of these radionuclides is expressed most satisfactorily by a power function of the time since they were taken into the body. Therefore, in the revised handbooks the power function is applied in obtaining MPC and q values for these radionuclides.

The current MPC values were calculated for an occupational exposure of 70 years, but in the new editions the exposure time has been reduced from 70 to 50 years, which is more realistic and yet a sufficiently conservative value.

In the revisions the gastrointestinal tract is the critical organ for 70% of the ingested radionuclides and 50% of the inhaled radionuclides.

Distribution of Sr^{90} + Y^{90} in Mice. – Laboratory work has been completed for the experiment to determine the biophysical factors used in the calculation of the MPC values[42,43] for Sr^{90} + Y^{90}. Ninety-eight mice were divided into two groups. Group I received a single oral administration of radiostrontium while Group II was permitted to drink Sr^{90}-contaminated water ad libitum. It was anticipated that the parameters deduced from the single administration results would permit prediction of the body burden due to continuous feeding as in the case of Co^{60} (ref 46). The organization of the experiment, analytical methods, and the data for Group I have been reported.[47,48] This is a report of the results of ad libitum feeding of Group II.

The accumulation of Sr^{90} in the skeleton of the mouse after various intervals of ad libitum feeding on contaminated water is shown in Fig. 17 with the details of the data being given in Table 34. Eight groups of 10 young adult mice were used to determine the average skeletal burden after 4, 8, 14, 25, 50, 70, 100, and 150 days of continuous feeding. Two groups of 9 animals sacrificed after 10 and 35 days of feeding were considerably older at the start of the experiment and showed a significantly lower uptake. The body weight of the animals increased with age and showed a mean standard deviation of 5.9% of the average for each group. The skeletal burdens and their standard deviations are reported in columns 9 and 11, respectively, of Table 34. The average standard deviation is 17.7% of the mean skeletal burden.

---

[45] W. P. Norris *et al.*, *Am. J. Roentgenol. Radium Therapy Nuclear Med.* 73, 785–802 (1955).

[46] M. J. Cook, K. Z. Morgan, and A. G. Barkow, *Am. J. Roentgenol. Radium Therapy Nuclear Med.* 75, 1177–1187 (1956).

[47] M. J. Cook, F. G. Karioris, and K. Z. Morgan, *HP Semiann. Prog. Rep. Jan. 31, 1956*, ORNL-2049, p 17–18.

[48] M. J. Cook, F. G. Karioris, and K. Z. Morgan, *HP Semiann. Prog. Rep. July 31, 1956*, ORNL-2151, p 12–16.

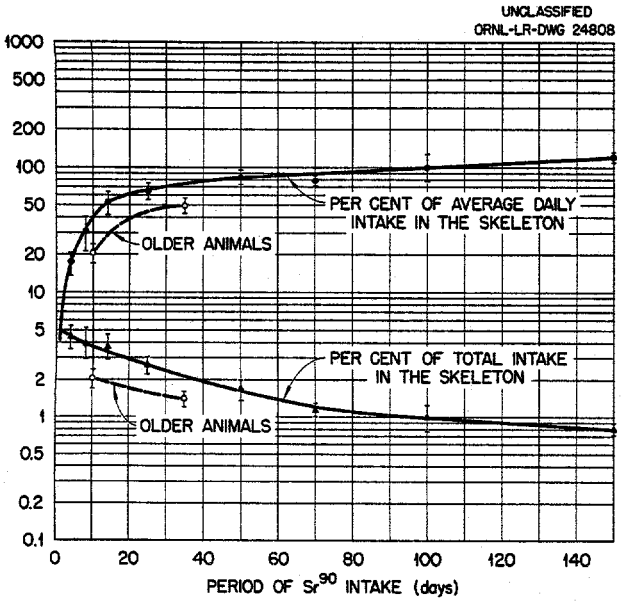

Fig. 17. Accumulation of Sr^{90} in the Skeleton of the Mouse After Various Intervals of ad Libitum Feeding on Contaminated Water. Data points show standard deviation.

The skeletal burden increases rapidly for about 15 days (Fig. 17) and may seem to equilibrate after approximately 70 days in the manner reported for rats.[49] However, the rapid rise is not consistent with the concept of a single biological half life of 200 days[50] and offers some supporting evidence for the current practice of expressing the body burden of Sr^{90} as a multiple exponential or as a power function of time. For example, see Comar and Wasserman.[51] Biological half lives for strontium in sheep range from 0.5 to 1200 days.

The increase in skeletal burden after 50 days is considered significant and may, in part, be attributable to growth of the animals during the experiment. In support of this hypothesis, Fig. 18

[49] W. J. Gross, J. F. Taylor, and J. C. Watson, *Some Factors Influencing the Metabolism of Radio-strontium by Animals*, UCLA-274 (Jan. 6, 1954).

[50] J. G. Hamilton, *Revs. Modern Phys.* 20, 718–728 (1948).

[51] C. L. Comar and R. H. Wasserman, *Progress in Nuclear Energy, Series VI, Biological Sciences*, p 181, McGraw-Hill, New York, 1956.

Table 34. Sr^{90}-Y^{90} Skeletal Burden in Mice After ad Libitum Feeding

Days of ad Libitum Feeding	Number of Mice	Concentration (mc/ml)	Average Rate of Intake (ml/day)	Age of Mice at Start (days)	Weight of Mice at Sacrifice (g)	Standard Error,* Weight	Standard Deviation,** Weight	Skeletal Burden, Average (Per Cent Daily Intake)	Standard Error	Standard Deviation	Skeletal Burden (Per Cent Total Intake)
4	10	1.0	3.65	76	20.15	±0.39	1.22	17.58	±1.14	3.60	4.39
8	10	1.0	3.45	61	19.07	±0.29	0.91	30.88	±3.04	9.60	3.86
14	10	1.0	3.70	61	19.87	±0.39	1.24	52.34	±3.54	11.21	3.74
25	10	0.05	4.56	69	21.26	±0.07	0.21	63.96	±2.75	8.69	2.56
50	10	0.05	4.63	79	21.21	±0.36	1.13	82.87	±3.65	11.54	1.66
70	10	0.05	4.08	42	22.91	±0.42	1.33	78.28	±1.81	5.71	1.12
100	10	0.05	4.26	82	23.56	±0.42	1.34	98.82	±7.68	24.28	0.99
150	10	0.05	3.76	110	24.23	±0.80	2.52	120.53	±6.58	20.80	0.80
					Older Animals						
10	9	0.05	4.53	121	22.77	±0.32	1.01	20.53	±0.98	2.93	2.05
35	9	0.05	4.57	129	23.62	±0.74	2.35	48.82	±2.14	6.43	1.39

*Standard error = Standard deviation/$\sqrt{N}$

**Standard deviation = $\sqrt{\frac{(\Sigma x^2) - (\Sigma x)^2/N}{(N-1)}}$

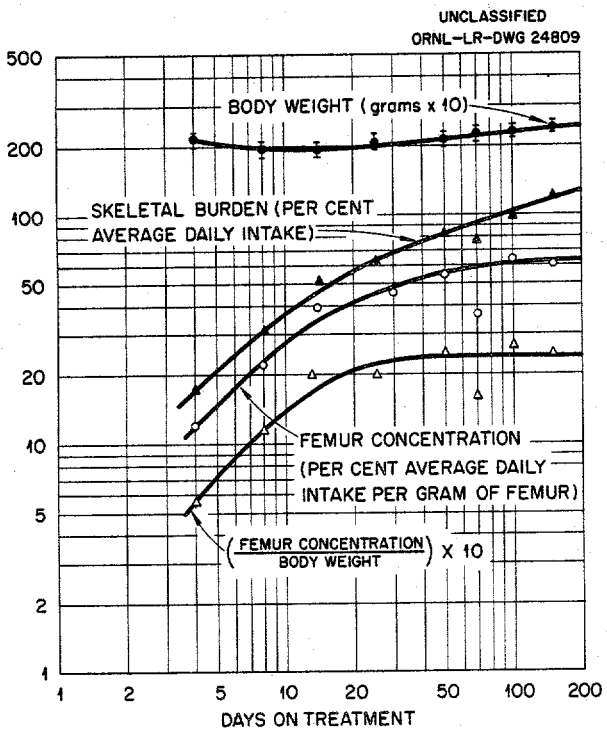

Fig. 18. The Influence of Growth and Aging on Sr^{90} Skeletal Burden due to Continuous Feeding on Contaminated Water.

shows the skeletal burden, the concentration in the femur, and the weight of the animals at the time of sacrifice. The ratio of femur concentration (per cent of average daily intake in the femur/gram of femur) to body weight increases very slowly, if at all, after 50 days. Aging factors must of necessity influence any long-term experiment and the skeletal burden reflects not only the increase in size, but the increased mineralization with age.

The concentrations in tissues (per cent of average daily intake in the tissue/gram of tissues) after various times of ad libitum feeding are given in Table 35 and plotted in Fig. 19. Concentrations in soft tissues appear to have reached a constant value earlier than four days and maintain this value throughout the 150 days of the experiment. Concentration in the femur increases slowly, if at all, after 50 days and at no time is greater than six times that of the lower alimentary tract with contents. The values for blood, liver, spleen, muscle, and gonads are of the same order of magnitude. Except for bone, concentrations in the tissues of the older animals were not significantly different from those in the younger animals.

The manner in which the total body burden is distributed in several organs at various times after ad libitum feeding of contaminated water is shown in Fig. 20. The values plotted were obtained by determining the total body burden as the sum of the activities in the organs and calculating the fraction of the total body burden in each organ. For simplicity of presentation, the entire GI tract and contents are grouped together; the remaining viscera are grouped together; and the muscle, pelt, and blood are plotted individually. Total activity in muscle and blood was determined from the measured concentration in these tissues and the body weight of the animals, assuming that muscle and blood are 40 and 7.5% of body weight, respectively. Other organs were analyzed *in toto*.

After 50 days of continuous feeding, 88% of the total body burden is in the skeleton, 10% is in the GI tract, and approximately 2% is in the remainder of the animal. Although it may not be statistically significant, there seems to be a trend for the fraction of body burden taken by the skeleton, GI tract, and pelt to remain constant and for the muscle, viscera, and blood fractions to decrease with time after 50 days.

The greatest part of the burden attributed to the GI tract is actually in the contents, and, if the contents of the GI tract were ignored in determining body burden, the skeleton would have about 95% of the body burden for all times greater than 4 days. The study of the body burden distribution after a single administration[52] has shown that at any time after 3 days, 95% of the total body burden is in the skeleton.

Although the experiment was not designed to study nutritional factors, analyses of the food and bones[53] were made and are shown in Table 36. Because of the errors inherent in the analysis, the limited number of samples used, and the estimations of the rates of intake and mass of total skeleton, the probable error in each determination is of the order of 25% of the value reported. Probable error limits for the quotients were formed in the usual manner from the probable error in the individual measurements.

---

[52] M. J. Cook, F. G. Karioris, and K. Z. Morgan, *HP Semiann. Prog. Rep. July 31, 1956*, ORNL-2151, p 12.

[53] Analyses were done by I. H. Tipton, Physics Department, University of Tennessee.

Table 35. Concentration of Sr^{90} (Per Cent Daily Intake per Gram) in Various Organs of Mouse After Continuous ad Libitum Feeding

Age of Mice at Start (days)	76	61	61	69	79	42	82	110	121	129
Organ	Days of Continuous Feeding									
	4	8	14	25	50	70	100	150	10	35
Femur	11.36	22.03	39.75	42.50	55.9	36.8	63.0	61.0	28.8	24.7
Sigmoid	16.5	16.7	15.2	15.9	11.7	3.36	12.4	9.2	22.0	19.8
Large intestine	7.70	8.30	6.47	9.51	7.35	6.26	6.5	10.2	11.3	11.8
Small intestine	0.76	0.93	0.635	0.637	0.563	0.465	0.990	1.68	1.16	1.69
Stomach	0.39	0.98	0.614	0.633	0.918	0.392	0.860	0.610	1.78	1.30
Blood	0.076	0.06	0.089	0.054	0.124	0.042	0.075	0.100	0.059	0.047
Liver	0.023	0.026	0.025	0.025	0.026	0.015	0.022	0.032	0.041	0.022
Spleen	0.037	0.028	0.049	0.062	0.068	0.015	0.014	0.060	0.021	0.034
Kidney	0.028	0.084	0.110	0.060	0.056	0.034	0.040	0.077	0.050	0.068
Heart	0.049	0.036	0.053	0.055	0.127	0.007		0.040	0.053	0.044
Lungs	0.075	0.089	0.147	0.120	0.113	0.077	0.100	0.102	0.073	0.067
Gonads	0.051	0.060	0.053	0.099	0.072	0.041	0.040	0.071	0.047	0.050
Brain	0.039	0.049	0.066	0.089	0.192	0.064	0.052	0.059	0.076	0.044
Muscle	0.062	0.078	0.195	0.078	0.673	0.033	0.040	0.046	0.220	0.055
Fat	0.030	0.034	0.032	0.026	0.097	0.004	0.013	0.010	0.085	0.018
Pelt	0.056	0.20	0.20	0.38	1.05	0.233	0.003	0.340	0.272	0.249

The isotopic ratios Sr/Ca, Sr^{90}/Ca, and Sr^{90}/Sr in the intake diet are not equal, within limits, to the corresponding ratios in the bone. If a preferential utilization factor[51] is defined as $(Sr/Ca)_{intake}/(Sr/Ca)_{bone}$, a value of about 1.7 ± 0.8 is obtained in the case of the stable strontium. This checks fairly well with the work of Pecher[54] in which 1.7 times as much Ca^{45} as Sr^{89} was retained after intravenous injection in mice. Comar, Whitney, and Lengemann[55] report a factor of 3.6 for growing rats.

The ratio of Sr^{90}/Sr in bone is probably less than the corresponding ratio in the diet and may indicate that equilibrium has not been reached after 150 days of feeding. It is quite probable, however, that the bone concentration has reached at least one-half of the equilibrium value.

ANALYSIS OF HUMAN TISSUE FOR TRACE ELEMENTS

M. J. Cook
E. L. Grove[56]
K. K. McDaniel
I. H. Tipton[57]

To date, tissues have been received from 10 cities in the United States from approximately 225 autopsies, and during the past year over 1000 samples were prepared for analysis. The spectrographic data of human tissue from four of these

[54]C. Pecher, *Proc. Soc. Exptl. Biol. Med.* 46, 86–91 (1941).

[55]C. L. Comar, I. B. Whitney, and F. W. Lengemann, *Proc. Soc. Exptl. Biol. Med.* 88, 232–236 (1955).

[56]Consultant, University of Alabama.

[57]Consultant, University of Tennessee.

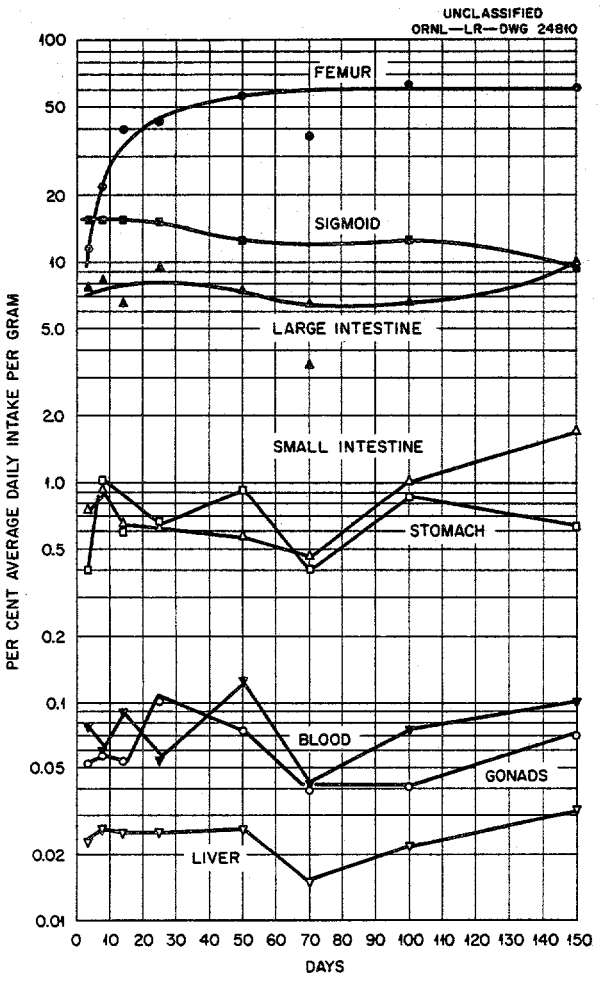

Fig. 19. Strontium-90 Concentration in Tissues of Mouse With ad Libitum Feeding on Contaminated Water. Analyses of portions of gastrointestinal tract include contents at time of sacrifice.

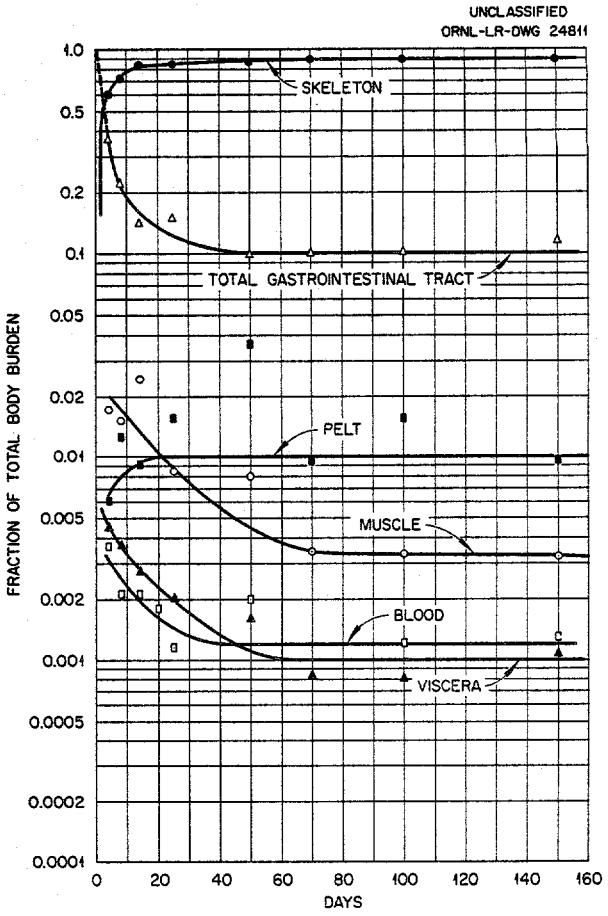

Fig. 20. Strontium-90 Body Burden Distribution with ad Libitum Feeding. Gastrointestinal tract includes contents at time of sacrifice.

United States cities are summarized briefly in Table 37. Because the amount of data is great, central files reports have been issued to include the results on all tissues received from each city. The methods of collection, preparation, and spectrographic analysis, and the data on tissues from three cities have been issued.[58–61] Analyses of tissues from a fourth city have been finished and a report will be issued soon.[62]

To supplement the spectrographic data the same tissues are analyzed by flame photometry for sodium and potassium. For flame photometry the tissues are prepared as for spectrographic determinations, and are sent to the Chemistry Division, University of Alabama. The sodium and potassium

[58] I. H. Tipton *et al., Progress Report: Spectrographic Analysis of Tissues for Trace Elements, July 1, 1955 Through December 31, 1955,* ORNL CF-56-3-60.

[59] I. H. Tipton *et al., Methods of Collection, Preparation and Spectrographic Analysis of Human Tissues,* ORNL CF-57-2-2 (Feb. 28, 1957).

[60] I. H. Tipton *et al., Spectrographic Analysis of Normal Human Tissue from Dallas, Texas,* ORNL CF-57-2-3 (Feb. 28, 1957).

[61] I. H. Tipton *et al., Spectrographic Analysis of Normal Human Tissue from Miami, Florida,* ORNL CF-57-2-4 (Feb. 28, 1957).

[62] I. H. Tipton *et al., Spectrographic Analysis of Normal Human Tissue from Baltimore, Maryland,* (to be published as ORNL CF memorandum).

Table 36. Isotopic Ratios in Mice After 150 Days ad Libitum Feeding

Analyses, ±25%

	Per Cent in Ash	
	Ca	Sr
Food (5.9% ash)	16.0	0.13
Bone (25% ash)	25.0	0.12
Water	0.0035	0.00001

Intake Rates, ±25% (g/day)	
Food	2.5
Water	4.0
Ca	24×10^{-3}
Sr	0.19×10^{-3}
Sr^{90}	1.4×10^{-9}

Bone Content, ±25% (g)	
Ca	100.0×10^{-3}
Sr	0.48×10^{-3}
Sr^{90}	1.7×10^{-9}

Isotopic Ratios After 100–150 Days

$(Sr/Ca)_{intake} = 8.1 \pm 2.8 \times 10^{-3}$

$(Sr^{90}/Ca)_{intake} = 5.9 \pm 2.1 \times 10^{-8}$

$(Sr^{90}/Sr)_{intake} = 7.3 \pm 2.6 \times 10^{-6}$

$(Sr/Ca)_{bone} = 4.8 \pm 1.7 \times 10^{-3}$

$(Sr^{90}/Ca)_{bone} = 1.7 \pm 0.6 \times 10^{-8}$

$(Sr^{90}/Sr)_{bone} = 3.5 \pm 1.2 \times 10^{-6}$

Preferential Utilization Factors

$$\frac{(Sr/Ca)_{intake}}{(Sr/Ca)_{bone}} = 1.7 \pm 0.8$$

$$\frac{(Sr^{90}/Ca)_{intake}}{(Sr^{90}/Ca)_{bone}} = 3.5 \pm 1.7$$

$$\frac{(Sr^{90}/Sr)_{intake}}{(Sr^{90}/Sr)_{bone}} = 2.1 \pm 1.0$$

data in Table 38 are supplementary to the spectrographic data presented elsewhere.[58]

For neutron activation analysis, samples of liver, kidney, spleen, lung, bone, ovary, and testis were dried and sent to the Analytical Chemistry Division, ORNL.

In addition to studying tissues from the United States, arrangements have been made whereby human tissue is received from foreign countries. These tissues are preserved in metal-free formalin, which prior to use was analyzed spectrographically for trace elements. Generally ten tissues – aorta,

Table 37. Human Tissue Data from the U.S.A.

Element	Principal Organ of Deposition	f_2*	Number of Tissues Analyzed	Concentration (μg/g of Wet Tissue)		Average Value
				Lowest Value	Highest Value	
Al	Lung	0.15	102	1.7	120	24
Ba	Bone	0.7	99	0.11	10	1.2
Cd	Kidney	0.15	102	10	77	32
Ca	Bone	0.99	99	9000	85,000	36,500
Cr	Lung	0.05	102	0.005	1.27	0.13
Co	Liver	0.5	102	<0.025	1.3	0.34
Cu	Liver	0.15	102	3.3	28	8.7
Cu	Brain	0.1	94	1.32	11.5	5.7
Ga	Lung	0.95	102	<0.01	0.054	0.02
Au	Aorta		75	<0.07	1.5	0.4
Fe	Spleen	0.015	97	21	1,360	330
Pb	Bone	0.7	99	0.14	45	6.6
Mg	Bone	0.5	99	190	2,100	990
Mn	Liver	0.35	102	0.56	3.7	1.3
Mn	Pancreas	0.01	95	0.39	2.6	1.14
Mo	Liver	0.9	102	0.3	2.6	1.2
Ni	Intestines	0.03	94	<0.2	1.0	0.23
Ag	Liver	0.1	102	<0.001	0.11	0.02
Sr	Bone	0.95	99	1.1	65	18
Sn	Intestines	0.03	94	<0.03	3.4	0.4
Ti	Lungs	0.2	102	0.2	14.4	2.9
V	Intestines	0.5	94	<0.002	0.14	0.09
Zn	Prostate	0.0009	27	25	380	108
Zn	Bone	0.2	99	12	170	70
Cs	Muscle	0.8	91			0.06 (composited sample)

Other Tissues Analyzed					Additional Elements Studied			
Adrenal glands	Heart	Skin	Thyroid	Uterus	Sb	B	P	Na
Breast	Larynx	Stomach	Tongue	Vagina	As	La	K	Tl
Diaphragm	Omentum	Testis	Trachea		Be	Li	Rb	Zr
Esophagus	Ovary	Thymus	Urinary Bladder		Bi	Nb	Ru	

*f_2 – fraction of the element in the organ of that in the total body.

Table 38. Sodium and Potassium Data Supplementary to That Presented in ORNL-CF-56-3-60 (ref 57)

Tissue	Element	Average Per Cent by Analysis	Per Cent Deviation
Aorta	Na	13.8	3.99
	K	9.84	0.965
Brain	Na	9.72	0.617
	K	19.4	0.258
Esophagus	Na	19.7	0.508
	K	18.2	0
Heart	Na	11.7	1.71
	K	25.5	1.57
Large intestine	Na	14.2	1.41
	K	21.2	0
Small intestine	Na	12.7	2.36
	K	22.4	0.670
Kidney	Na	18.4	0.815
	K	28.0	0.893
Liver	Na	10.8	2.16
	K	19.6	2.89
Lung	Na	17.4	1.44
	K	17.5	1.14
Muscle	Na	5.28	0.852
	K	28.0	0.893
Pancreas	Na	10.4	0.481
	K	22.2	1.13
Prostate	Na	14.6	0.911
	K	17.9	1.68
Spleen	Na	6.99	0.572
	K	24.5	0.543
Stomach	Na	15.3	1.96
	K	19.2	1.82
Testis	Na	17.3	1.73
	K	17.3	1.35
Thyroid	Na	19.4	0.773
	K	13.3	2.26
Urinary bladder	Na	16.7	0
	K	19.8	0.505

bone, brain, heart, kidney, liver, lung, gonads, pancreas, and spleen – from each of ten autopsies were received from the following:

Africa – Orange Free State, Usumbura, Nigeria, and Kampala
Egypt – Cairo
Hawaii – Honolulu
China – Hong Kong
Japan – Tokyo, Chiba, and Kyoto
Phillipines – Manila
Thailand – Bangkok
Switzerland – Bern
Formosa – Taipeh
India – Bombay and Vellore
Lebanon – Beyrouth
Alaska (only 2 autopsies).

Preliminary data are presented in Fig. 21 for Cd, Sr, Cu, Pb, and Zn in the kidney. Similar data are available for other elements and other body organs.

SPECTROGRAPHIC ANALYSIS OF NORMAL HUMAN TISSUE

Subcontract No. 380
Physics Department
University of Tennessee

Work authorized by this subcontract includes quantitative, spectrographic determinations of 40 minor and trace elements in dry ash samples of normal human tissue. Autopsy tissues from selected metropolitan centers in this country and abroad are obtained by medical officers and shipped to ORNL for storage and preparation. The objective is to determine the concentration and distribution of minor and trace elements in "standard man" for application to limits of permissible internal exposure and internal dosimetry.

During the past year approximately 50,000 spectrographic determinations were made on tissues from 100 autopsies of instantaneous, accidental death in three cities of the United States, and from collection centers in Africa, Switzerland, and Alaska. Significant differences in trace element distribution were found in African natives. A summary report of these results is in preparation.

THE DETERMINATION OF ALKALI AND ALKALINE EARTH ELEMENTS IN NORMAL HUMAN TISSUE BY FLAME PHOTOMETRY

Subcontract No. 1084
School of Chemistry
University of Alabama

Work under this subcontract, initiated in February 1957, includes quantitative determinations of sodium and potassium in the same samples of normal human tissue described above. It is also planned to extend or develop analytical procedures by flame photometry for other specific elements such as lithium, rubidium, and strontium (within the limits of flame spectrophotometry) as a check on the spectrographic determinations of these elements.

During the brief period since the subcontract was established, work has been performed on the adaptation of a flame photometric procedure for lithium in ores and ceramic materials developed by the University of Alabama School of Chemistry and the U.S. Bureau of Mines to the elements sodium and potassium in ashed tissue samples.

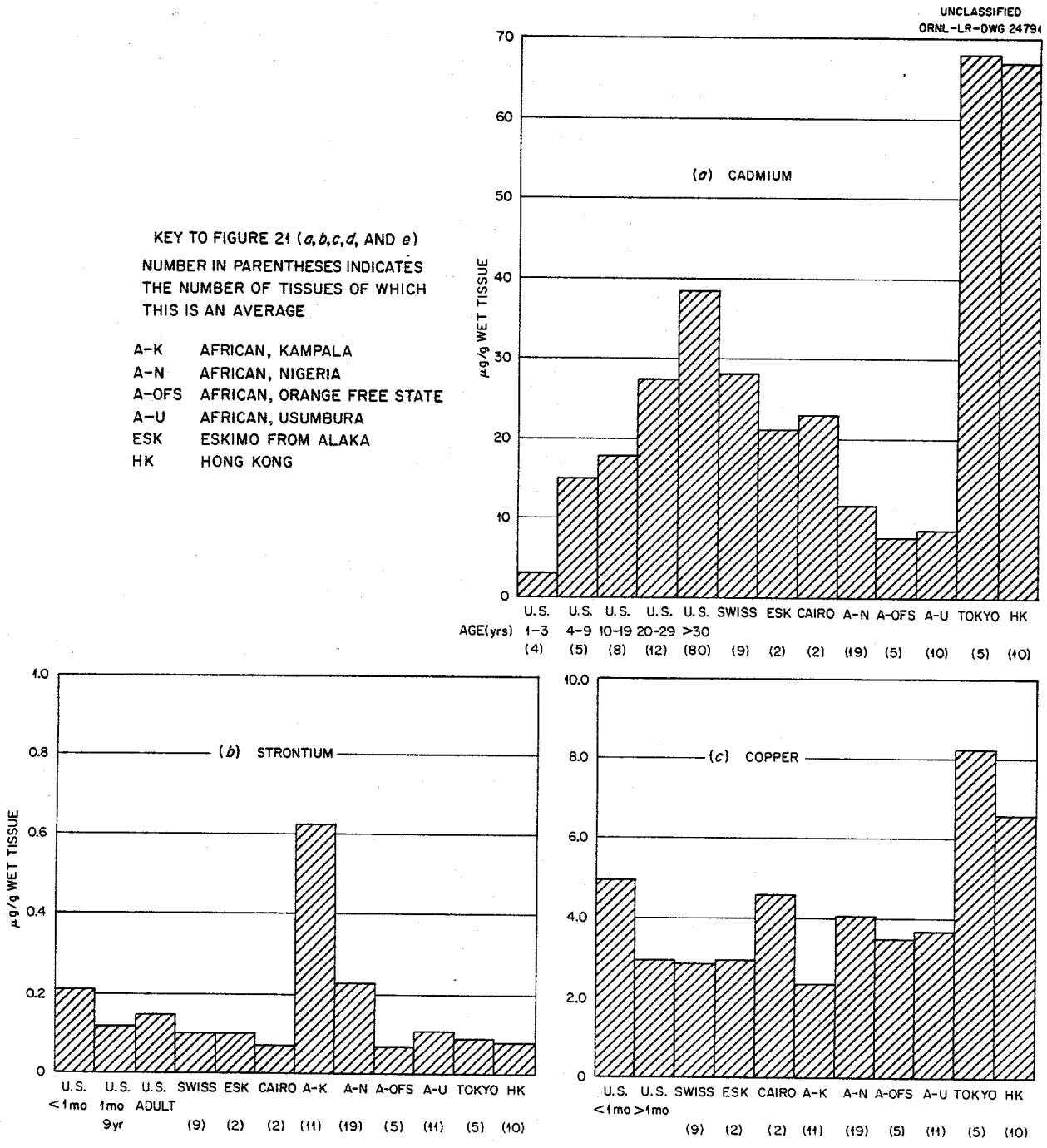

Fig. 21. Preliminary Spectrographic Analyses of Various Elements in the Kidney by Country. (*a*) Cadmium; (*b*) Strontium; (*c*) Copper.

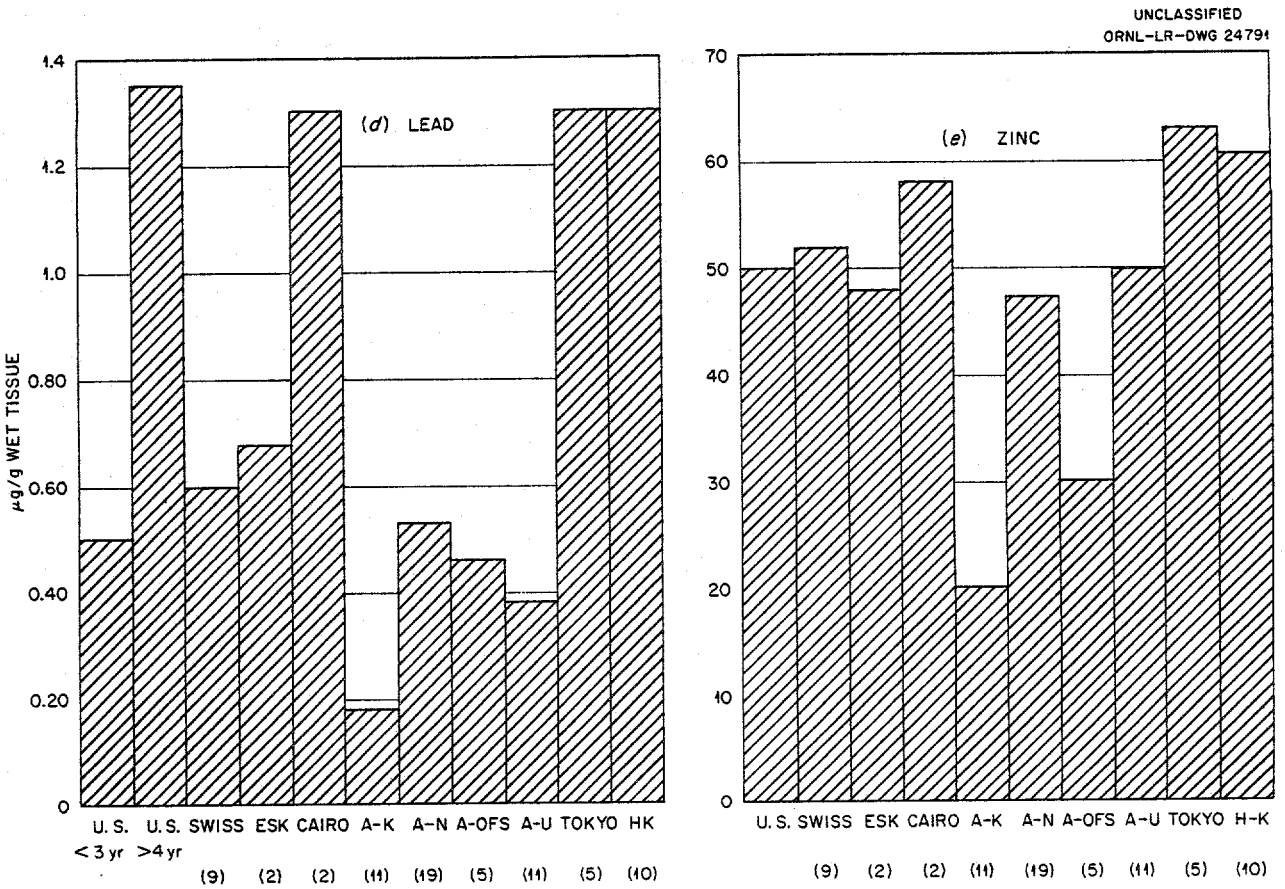

Fig. 21. Preliminary Spectrographic Analyses of Various Elements in the Kidney by Country. (*d*) Lead; (*e*) Zinc.

WASTE DISPOSAL RESEARCH

E. G. Struxness R. J. Morton

DEVELOPMENT OF ANALYTICAL METHODS

B. Kahn (USPHS) E. R. Eastwood
H. L. Krieger (USPHS) G. G. Robeck (USPHS)
R. E. Yoder

Condensation Nuclei Meter

To generate homogeneous dioctyl phthalate (DOP) aerosols in a La Mer type aerosol generator,[1] it is necessary to provide a source of condensation nuclei. Fused sodium chloride heated to a temperature of 500°C will deliver to an air stream passing over the salt surface a large number of condensation nuclei.

The size of DOP droplets produced by condensation of DOP vapor on the salt nuclei is a function of nuclei concentration. The concentration of salt nuclei is determined by the rate of air flow over the fused salt and the salt temperature. It is desirable to be able to predict the size of aerosol droplets as a function of nuclei concentration by the use of a calibrated nuclei meter.

The nuclei concentration increases as the temperature of the salt increases and as the air flow rate over the salt surface decreases,[2] Figs. 22 and 23, respectively.

Figure 24 is a photograph of sodium chloride condensation nuclei produced at a salt temperature of 585°C, and Fig. 25 is a photograph of condensation nuclei produced at a salt temperature of 700°C. The chained nuclei shown in Fig. 25 will not produce a homogeneous aerosol because they are too large (5 μ) and nonuniform, whereas nuclei of individual crystals will produce aerosols 98% homogeneous with respect to size.

Analysis of Water

Low levels of radioactive cesium, strontium, cerium, and cobalt have been determined by concentration from liter volumes by cation exchange resins and then purifying by standard radiochemical techniques.[3] The radionuclides and their carriers are absorbed on various resins from 0.001 *M* hydrochloric solutions and then eluted with 20 to 25 ml of strong hydrochloric or nitric acid. The quantity of resin needed depends on the amount of calcium in the water. When analyzing water containing very low concentrations of radionuclides, it is desirable to process blanks to

[1] E. E. Grassel, *Construction of a La Mer Type Thermal Aerosol Generator for Radioactive Compounds*, ORNL CF-54-3-46 (April 1954).

[2] B. E. Prince and V. C. Vaughan, *Study of the Linearity and Accuracy of the GE Condensation Nuclei Meter*, KT 249 (Oct. 19, 1956).

[3] B. Kahn, E. R. Eastwood, and W. J. Lacy, *Use of Ion Exchange Resins to Concentrate Radionuclides for Subsequent Analysis*, ORNL-2321 (June 17, 1957).

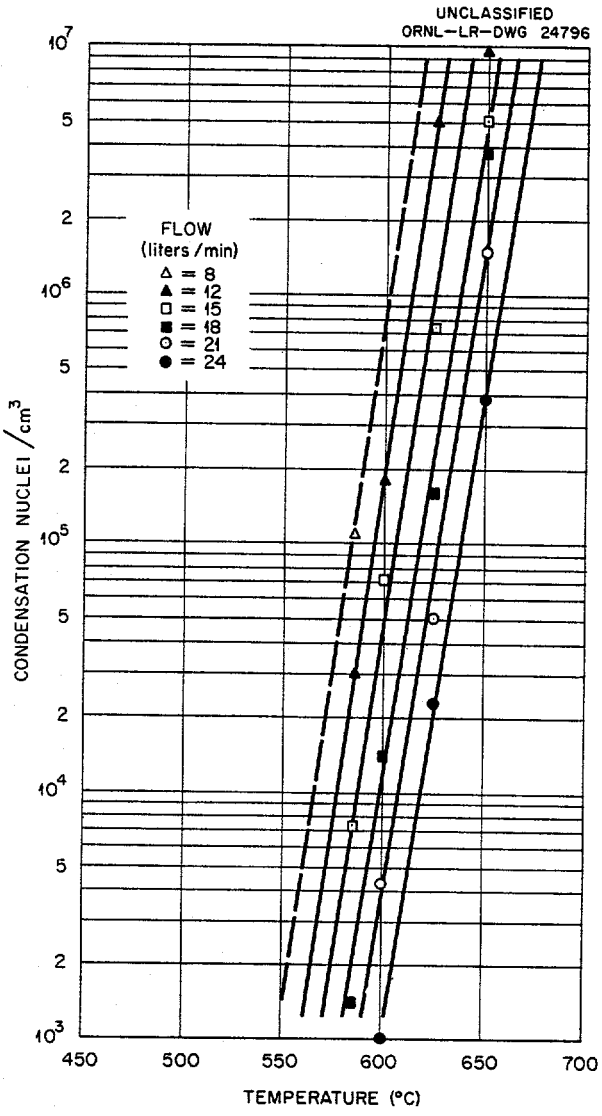

Fig. 22. Aerosol Concentration vs Temperature.

eliminate the error caused by the use of slightly contaminated reagents. Sensitivity of detection has been increased by this method from approximately 10^{-6} to 10^{-8} $\mu c/ml$. The method has been used to perform radiochemical analyses of ORNL Settling Basin and Clinch River waters. It is believed that with proper preparations of the sample and correct choice of ion exchange resin this concentration procedure may be applied to a large number of radionuclides.

To increase further the consistency and sensitivity of strontium detection a 10-liter water sample was concentrated on 25 g of Dowex 50 resin. In addition to acidifying slightly the water sample before concentration on the resin, Versene was added to the influent to decrease the amount of calcium retained on the resin, and the resin was

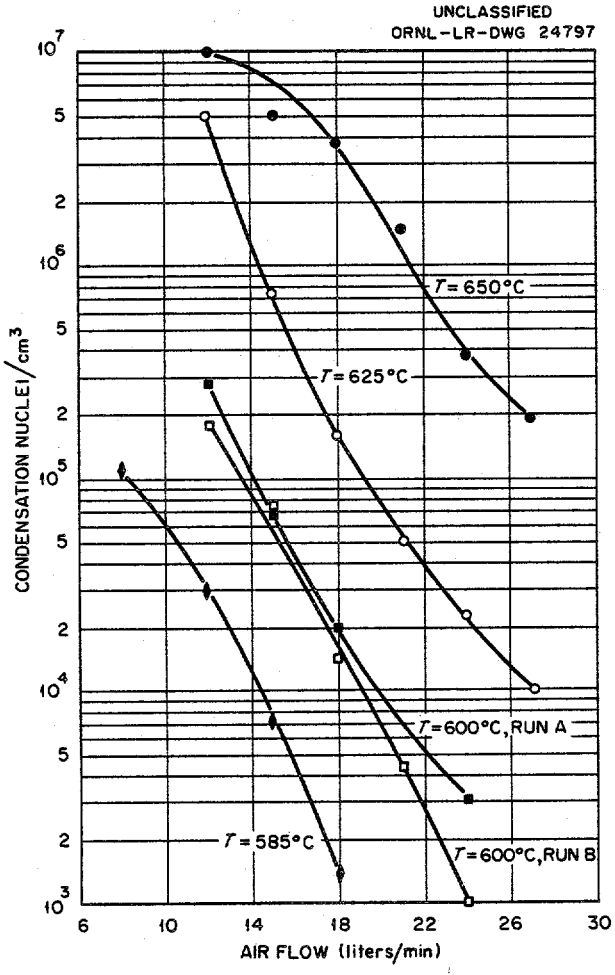

Fig. 23. Aerosol Concentration vs Air Flow Rate.

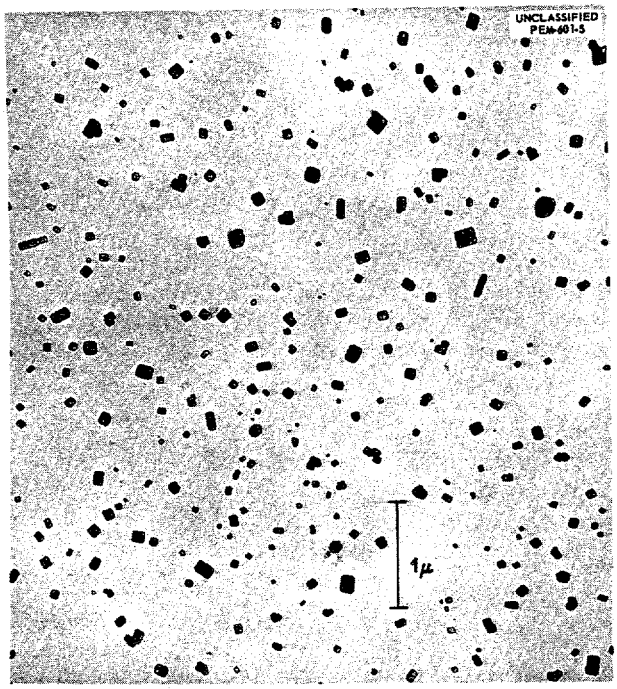

Fig. 24. Sodium Chloride Condensation Nuclei Produced at 585°C. 25,000X. Reduced 46%.

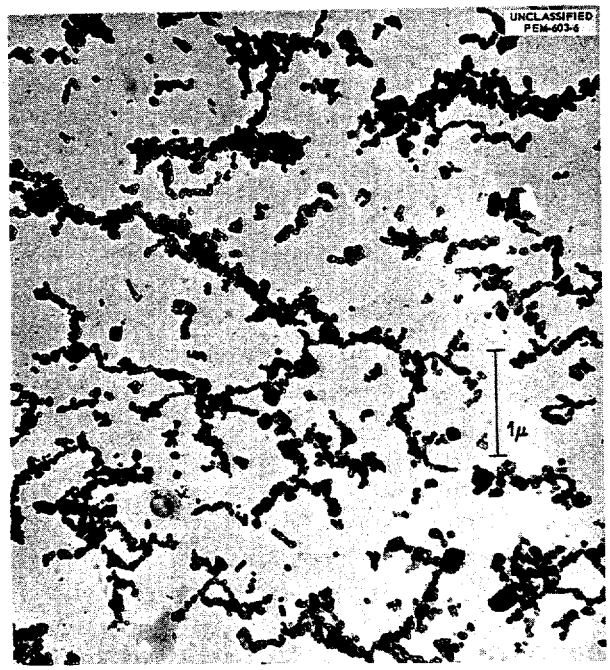

Fig. 25. Chained Sodium Chloride Condensation Nuclei Produced at 700°C. 25,000X. Reduced 45%.

also washed with a 1% Versene solution. However, after the usual purification of the strontium, approximately 1 mg of calcium accompanied the strontium, whether or not the Versene was used. After the strontium was leached from the resin with a 14 *M* nitric acid solution, it was precipitated with fuming nitric acid and then purified as before.

The determination of ruthenium is complicated by the fact that radioactive ruthenium may be in various chemical forms and may not interchange completely with the ruthenium carrier which is added. With the use of Ru^{106} tracer in the trichloride form to test a procedure consisting in oxidizing the ruthenium to RuO_4 with $KMnO_4$ in dilute H_2SO_4 and distilling the RuO_4 into 15 ml of 6 *M* NaOH, it was found that its fractional recovery was equal to that of the carrier. However, only a small fraction of Ru^{106} in other chemical forms was recovered in this manner. The other forms of ruthenium were obtained either in ground water which contained anionic or nonionic ruthenium from the ORNL pits, or by boiling ruthenium with iron metal in 1.6 *M* $Al(NO_3)_3$ solution. To obtain better interchange between carrier and tracer, the distillation step was preceded by oxidation with $KMnO_4$ in boiling KOH solution, as reported by Ruff and Vidic.[4] Both the ruthenium carrier and tracer were oxidized to RuO_4^{--}, and no ruthenium was distilled from the boiling solution. The completeness of the oxidation depends on the concentration of KOH and the time of boiling, as indicated in Table 39. Suitable conditions are the addition of 112 g of KOH and 1 g of $KMnO_4$ to a liter of water and a 2-hr boiling period.

After the oxidation to RuO_4^{--} the solution was cooled, and 100 ml of H_2SO_4 was added slowly. The ruthenium was then distilled by boiling the acid solution for 15 min. The ruthenium was dissolved in 15 ml of 6 *M* NaOH, precipitated as RuO_2 by adding ethanol, dissolved in HCl, and reduced to the metal with magnesium. All values of Table 39 were obtained by comparing the ruthenium activity, corrected for loss in the procedure, with the initial Ru^{106} activity.

Since interchange between the radioactive cobalt in the ORNL intermediate-level waste and the

[4] O. Ruff and E. Vidic, *Z anorg. u. allgem. Chem.* 136, 49 (1924).

Table 39. Determination of Ru^{106} in 1-Liter Volumes of Water

Solution Containing Tracer	Conditions for Carrier-Tracer Interchange	Tracer Activity Recovered (counts/min)	Tracer Activity Added (counts/min)	Per Cent Tracer Recovered
Chloride solution	100 ml H_2SO_4, 1.0 g $KMnO_4$, 15 min	113,400	115,000	98.6
	28 g KOH, 1.0 g $KMnO_4$, 60 min	114,400	115,000	99.5
Boiled $Al(NO_3)_3$ solution	100 ml H_2SO_4, 1.2 g $KMnO_4$, 15 min	31,300	76,750	41
	28 g KOH, 1.2 g $KMnO_4$, 30 min	74,100	76,750	97
Ground water	100 ml conc H_2SO_4, 1.2 g $KMnO_4$, 15 min	8,660	127,800	7
	28 g KOH, 1.2 g $KMnO_4$, 30 min	79,200	127,800	62
	28 g KOH, 1.2 g $KMnO_4$, 60 min	100,900	118,500	85
	56 g KOH, 1.2 g $KMnO_4$, 120 min	108,500	123,400	88
	112 g KOH, 1.0 g $KMnO_4$, 120 min	121,000	123,400	98.0
	168 g KOH, 1.0 g $KMnO_4$, 120 min	121,100	122,400	98.9
	112 g KOH, 1.0 g $KMnO_4$, 60 min	118,400	122,400	97

cobalt carrier is incomplete in the cobaltinitrite precipitation now in use, the procedure was revised.

The sample is acidified with hydrochloric acid, cobalt nitrate is added as carrier, and the solution is dried and heated until the black oxide is formed. The cobalt is then dissolved in at least 7 ml of hot 6 *M* hydrochloric acid and neutralized with potassium hydroxide, and 1 ml of acetic acid and 2 ml of potassium nitrate (1 g/ml) are added to precipitate potassium cobaltinitrite. The cobalt is then purified and recovered in the usual manner.

The results of low-level radiochemical analyses of the Clinch River water sampled on December 12, 1956, are given in Table 40. Duplicate runs demonstrated reproducibility; however, it was extremely difficult to get these results on background-level or low-level samples because of the contamination usually present in a research laboratory. The procedures used for concentrating 1000-ml samples were precipitation with H_3PO_4 for zirconium and niobium, boiling and volatilization with $KMnO_4$ for ruthenium, and adsorption on resin and acid leaching for cesium, strontium, and the rare earths. The concentrated fission products were then purified and determined by modified radiochemical procedures. Also included in Table 40 are the gross beta count rates, which were obtained by evaporating a liter or less of these samples to dryness. Both strontium and the trivalent rare earths (including yttrium) were present in the river water as far as mile 4.6, suggesting the presence of Sr^{90} and Y^{90}.

As a further check on the effectiveness and reproducibility of the low-level analytical methods, another series of Clinch River water samples was collected on March 1. Since the December series showed some unexplained peaks in the downstream activity, floats were used this time to aid in determining the flow-time and cross-channel dispersion after the confluence of White Oak Creek. Although the winds intermittently had an adverse effect on the floats, it was possible to sample regularly the same stream of waste as it flowed and dispersed downstream. The results of duplicate analyses listed in Table 41 again indicate that the above procedures will give reproducibility for levels of radioactivity as low as 10^{-9} $\mu c/ml$.

Analysis of Soils and River Bottom Mud

The feasibility of determining the critical fission products in soil that has been subjected to high temperatures was studied. Samples were prepared by absorbing from aqueous solutions the radioactive tracers Cs^{137}, Sr^{89}, Ce^{144}, or Zr-Nb^{95} on local shale which had been dried at 110°C and then powdered. The shale containing the radionuclides was washed with water, dried by centrifuging, and then heated in a muffle furnace at 1000°C for 1 hr. The results indicate that the tracers are relatively firmly fixed to the soil at 1000°C but not at 110°C.

The following procedures were used to remove the tracers from the shale:

1. cesium – heated 5 g of soil in platinum crucible with 50 ml of HF to dryness, then leached the soil with 35 ml of 6 *M* HCl, heating and stirring for 5 min; repeated the leaching twice with 10-ml portions of 6 *M* HCl,
2. cerium, strontium, trivalent rare earths, and yttrium – heated 5 g of soil in platinum crucible with 50 ml of HF to dryness; to residue added 1 ml of concentrated HNO_3 and 5 ml of $HClO_4$ and heated nearly to dryness; leached the soil with 35 ml of 1 *M* HCl, heating and stirring for 5 min; repeated the leaching twice with 10-ml portions of 1 *M* HCl,
3. zirconium and niobium – heated 5 g of soil in platinum crucible with 50 ml of HF nearly to dryness, then leached the soil with 35 ml of 1 *M* HCl, heating and stirring for 5 min; repeated the leaching twice with 10 ml of 1 *M* HCl, adding one drop of HF to each leach,
4. ruthenium – in a platinum crucible, heated 5 g of soil, 2 ml of Ru carrier, and 50 ml of HF containing 1 g of $NH_2OH{\cdot}HCl$ almost to dryness; added 10 ml of $HClO_4$ and transferred soil to a ruthenium still with 1 ml of concentrated HNO_3 and 3 ml of H_2O; heated about 5 min to remove the HF, and distilled into 20 ml of 6 *M* NaOH.

The radiochemical procedures following these digestions were identical to those described elsewhere.[5]

---

[5] B. Kahn, *Procedures for the Analysis of Some Radionuclides Adsorbed on Soil*, ORNL-1951 (Sept. 28, 1955).

Table 40. Fission Product Activity in Clinch River Water Collected December 12, 1956

Samples counted on first shelf of end-window G-M counter
Count rate expressed in terms of count per minute per liter of water, counts/min/l
Activity expressed in terms of 10^{-9} $\mu c/ml$[a]

Source[b]	Time Collected	Gross Beta (counts/min/l)	Cesium		Cerium		Trivalent Rare Earths + Yttrium		Ruthenium		Strontium	
			Count	Activity	Count	Activity	Count	Activity	Count	Activity	Count	Activity
White Oak Creek at dam	1:00 PM	32,965	1398	3400	3504	4700	8250	16,000	14,492	21,000	9474	25,000
			1435		3553		8761		12,995		9378	
Clinch River, mile 19.4[c]	11:45 AM	137	7.6	14	14.6	19	33.3	61	86	140	22	52
			4.2		13.6		31.2		91		17	
14.0	11:00 AM	139	0.5	3.0	17.4	22	85	160	24	36	56	150
			1.8		15.8		84		22		58	
10.4	10:40 AM	22	1.0	3.0	2.8	7	18	31	5	11	18	52
			1.3		7.8		15		8		21	
4.6	3:00 PM	15	0.4	1.0	2.0	3	12	24	5	7	15	40
			0.8		2.9		13		4		14	
Tap water (background)			0.0	2.0	0.0	1	0	1	5	6	3	7
			1.6		0.8		1		3		2	

[a] Factors used to convert from counts/min/l to 10^{-9} $\mu c/ml$ are: Cs, 2.4; Ce, 1.3; trivalent rare earths Y, 1.9; Rn, 1.5; Sr, 2.6.

[b] It had rained several hours before as well as during sampling, thus samples were very turbid and allowed to settle before they were analyzed. Zirconium and niobium results were all near or at background levels.

[c] This sample location is 1.4 miles below confluence of White Oak Creek and Clinch River.

Table 41. Fission Product Activity in Clinch River Water Collected March 1, 1957

Samples counted on first shelf of end-window G-M counter
Count rate expressed in terms of counts per minute per liter of water, counts/min/l
Activity expressed in terms of 10^{-9} $\mu c/ml$*
All samples were allowed to settle for several days before being analyzed
Zirconium and niobium results were all near or at background levels

Source	Time Collected	Gross Beta (counts/min/l)	Cesium		Cerium		Trivalent Rare Earths + Yttrium		Ruthenium		Strontium	
			Count	Activity	Count	Activity	Count	Activity	Count	Activity	Count	Activity
White Oak Creek**	9:18 AM	10,065	324 307	760	292 289	390	1529 1453	2820	6860 7122	10,700	1382 1281	3540
Clinch River, mile 18.8	11:00 AM	60	6.9 11.4	22	1.4 0.0	1.0	8.8 8.9	17	104 86	145	15.2 12.0	36
16.8	12:30 PM	27	1.2 2.3	4.0	2.3 2.7	3.0	1.1 4.5	5.0	20.5 26.9	36	0.9 3.2	6.0
15.3	1:15 PM	34	5.9 8.9	18	4.0 1.1	3.0	5.4 5.0	10.0	24.7 23.5	37	2.5 4.9	10.0
13.3	2:30 PM	48	0.0 0.0	0	2.4 1.2	2.0	3.2 3.6	6.0	32.9 28.3	47	0.0 6.5	9.0
Tap water (background)			0.0 0.0	0	0.0 0.0	0	0.0 0.9	1.0	1.7 3.2	4	0.0 3.2	4.0

*For conversion factors, see Table 40.

**This sample location was at confluence of White Oak Creek and Clinch River at mile 20.8.

The Environs Group of the Applied Health Physics Section, in cooperation with the Analytical Chemistry Division, whose personnel performed the radiochemical analyses, has for the third consecutive year used the procedures developed by Kahn[6] in determining the concentrations of radionuclides on bottom muds of the Clinch and Tennessee Rivers. A report on these determinations is being prepared by the Applied Health Physics Section.

The major activities found are listed in Table 42. The Fort Loudon Lake samples should not contain activity from ORNL, and thus are an indication of contamination introduced during or after collection. Radioactive cesium and cobalt have increased considerably in the rivers since last year, while the other radionuclides have increased only slightly.

CHEMICAL DECONTAMINATION OF FUEL PROCESS WASTES

H. L. Krieger (USPHS) B. Kahn (USPHS)
G. G. Robeck (USPHS)

Solvent Extraction

The efficiency of a number of amines and organophosphorus compounds in extracting the major fission products from a synthetic reactor waste was compared to that of tributyl phosphate (TBP) (ref 7). Table 43 indicates that tridecylphosphine oxide is approximately as effective as TBP in the concentrations used. The other extractants are less effective for extracting the fission products, but the difference in cerium and yttrium extraction of some of them suggests that they may be used in the separation of the rare earths. An indication of the difference with which the various rare earths are extracted into tri-*n*-octyl amine is given in Table 44.

Cocrystallization and Scavenging Precipitation

Radioactive cesium from the synthetic waste solution was removed by means of cocrystallization with potassium and ammonium alum.[8,9] High cesium removals can be obtained, as shown in Table 45, while Table 46 indicates little removal of the other radionuclides, with the exception of strontium. Rimshaw[10] has demonstrated that the cesium can then be separated from the potassium alum, and thus be obtained in a small volume.

Another method for decontaminating the synthetic waste was proposed, based on Diban preparation[11] and the aluminum purification methods used in the aluminum industry. The procedure consists in drying the acid aluminum nitrate waste, removing and recovering the nitric acid as nitrous oxide at approximately 200°C, and then dissolving the aluminum oxide in sodium hydroxide. The insoluble hydroxides of the fission products are removed by a scavenging precipitation, and then the hydrated aluminum oxide is recovered from the solution by crystallization. The caustic solution, containing the residual fission products, is either purified on an ion exchange column or directly re-used. Tracer studies indicated one undesirable effect, namely, some ruthenium activity was carried on the nitrous oxide gas. Solution of the heated aluminum oxide cake resulting from 1 liter of the acid 1.6 *M* aluminum nitrate waste was complete in 120 g of sodium hydroxide plus 280 ml of water.

DISPOSAL OF HIGH-LEVEL WASTES BY SINTERING

W. J. Boegly L. Hemphill
M. A. Cobble B. L. Houser
F. M. Empson O. H. Myers
R. E. Yoder

Development of Ceramic Mixtures

The development of ceramic materials and refined clays for sintering media has been continued by the Ceramics Laboratory, Metallurgy Division.

[6] B. Kahn, *Anal. Chem.* 28, 216 (1956).

[7] G. E. Robeck *et al.*, *HP Semiann. Prog. Rep. July 31, 1956*, ORNL-2151, p 35.

[8] A. T. Gresky, *The Recovery of Cs^{137} from ORNL Radiochemical Waste*, ORNL-742 (Jan. 8, 1951).

[9] S. J. Rimshaw, *Sanitary Engineering Aspects of the Atomic Energy Industry. A Seminar Sponsored by the AEC and the Public Health Service, Held at the Robert A. Taft Engineering Center, Cincinnati, Ohio, Dec. 6–9, 1955*, TID-7517(Pt. Ia), p 303.

[10] A. F. Rupp, *Proc. Intern. Conf. Peaceful Uses Atomic Energy, Geneva, 1955* 14, 68–84 (1956).

[11] I. R. Higgins and R. G. Wymer, *Diban-Ion Exchange Waste Disposal Scheme. I*, ORNL-1984 (Nov. 10, 1955).

Table 42. Radionuclide Composition of River Muds for 1954, 1955, and 1956

Source as to River Mileage	Activity in Units of 10^{-6} μc/g of Dried Mud*																	
	Cesium (as Cs-Ba^{137})			Strontium (as Sr^{90})			Cerium (as Ce-Pr^{144})			Trivalent Rare Earths + Yttrium (as Y^{90})			Ruthenium (as Ru-Rh^{106})			Cobalt (as Co^{60})		
	1954	1955	1956	1954	1955	1956	1954	1955	1956	1954	1955	1956	1954	1955	1956	1954	1955	1956
Fort Loudoun Lake**	2	2	5	2	1.4	1.3	1	1.7	3	2	1.7	3	1	0.5	3	4	0.0	1.0
Clinch River,																		
mile 21.5	2	5		2			2	4		2	3		1			4	2	
19.1	11	7	116	5		4	5	6	24	2	3	7	8		5	12		26
16.3	28	21	208	6	4	7	7	21	37	4	5	11	5	4	8	19	18	39
15.2	21	34	268	6		9	7	33	56	4	7	15	4		11	21		59
14.0	23	29	115	5	4	4	9	22	20	4	6	7	6	4	6	21	23	29
11.0	21	34	144	6	4	6	8	31	41	5	16	19	3	5	7	20	25	37
8.3	23	39	244	3	4	6	5	34	48	4	24	19	5	5	10	22	29	50
5.7	25	29	266	4	4	6	8	40	56	8	11	18	5	8	8	29	26	52
4.7	23			4			7			5			5			26		
2.6	15			3			4			5			5			20		
1.1	25	25	257	3	3	6	5	31	44	5	9	15	3	4	10	22	21	46
Tennessee River,																		
mile 571	2			2			1			2			3			4		
563	8	7	73	2	0.1	3	1	13	15	3	6	6	2	3	4	8	7	11
553	13			2			1			2			2			6		
544	5			2			1			2			2			7		
532	8	11	32	4	0.4	3	2	15	8	4	7	4	1	4	3	7	13	7
510	2			3			1			3			1			4		
492	5		20	2		2	2		6	2		3	1		2	5		4
475	5	2	14	2	0.3	2	1	4	4	2	6	1.8	1	1.2	3	5	4	6
White Oak Lake	24,100			2420			30,800			2860			1280			21,000		

*Gross beta counts/min/g are available, but cannot readily be converted to μc/g.

**(Background) – Tennessee River, mile 603.

Table 43. Solvent Extraction of Fission Products from an Acid 1.6 *M* $Al(NO_3)_3$ Solution by Various Solvents (Volume Ratio, Aqueous/Organic = 10:1)

Fission Product	Per Cent Activity Extracted by Solvent After Two Passes*				
	Primene $R(CH_3)_2\ CNH_2$	Tri-*n*-octyl Amine	Di-2-ethylhexyl Phosphoric Acid	Tridecyl Phosphine Oxide	TBP
Aged Ru^{106}	11	53	6	60.2	82.4
Fresh Ru^{106}		14		2.0	
Zr^{95}-Nb^{95}	20	22	94.4	88.5	87.2
Nb^{95}	21	34			36.7
Y^{91}	0	0	96.0	98.9	99.3
Ce^{144}	5	62	20	98.2	99.0
Sr^{89}	0	0	0	0	0

*Reagent dilution: Primene – 1/2 volumes with benzene; di-2-ethylhexyl phosphoric acid – equal volume with benzene; tri-*n*-octyl amine – equal volume with benzene; tridecyl phosphine oxide – 1 g dissolved in 1.0 ml of benzene; tributyl phosphate – 100%.

Table 44. Solvent Extraction of the Rare Earths from an Acid 1.6 *M* $Al(NO_3)_3$ Solution by Four 15-min Passes with Tri-*n*-octyl Amine

Volume ratio aqueous/organic = 10:1

Pass No.	Per Cent Activity Extracted *per Pass* with Tri-*n*-octyl Amine				
	La^{140}	Ce^{144}	Pm^{147}	Eu^{155}	Y^{91}
1	23.8	21.0	3.2	2.9	0.7
2	29.5	28.5	6.8	4.4	5.1
3	35.2	25.7	20.4	13.2	1.4
4	36.1	30.9	22.7	15.1	0.4

Attapulite and bentonite type clays have been mixed with mixed fission products and fired at temperatures ranging from 400 to 800°C. Preliminary results on leaching of the fired mixtures are listed in Table 47. Representative samples of the above mixtures are being studied by means of x-ray and differential thermal analysis in an attempt to correlate fission product retention with crystal structure and phase changes. In general all of the above materials exhibit a smaller percentage weight loss (13.4%) than does mix No. 15 (ref 12) and yield greater volume reduction values.

The material balance studies of mix No. 15 clinkers have been completed, and the results are presented in Table 48.

[12]For a description of mix No. 15 see T. V. McVay, R. L. Hammer, and M. P. Haydon, *Sanitary Engineering Aspects of the Atomic Energy Industry. A Seminar Sponsored by the AEC and the Public Health Service, Held at the Robert A. Taft Engineering Center, Cincinnati, Ohio, Dec. 6–9, 1955*, TID-7517(Pt. Ib), p 336.

Table 45. Cesium-137 Removals in Two Consecutive Passes on 100-ml Acid 1.6 *M* $Al(NO_3)_3$ Solution

Stirring time: 1 hr
Temperature: 0°C

Pass	Cesium Carrier Added (mg)	Grams of Reagents Added to Solution			Cs^{137} Removal (%)
		K_2SO_4	$(NH_4)_2SO_4$	Na_2SO_4	
Al	2.6	3.0		10	99.4
2		3.0			99.95
Bl	2.6	4.5		10	99.2
2		4.5			99.91
Cl	2.6	2.0		10	98.8
2		2.0			99.94
Dl	2.6	3.0		1.5	99.8
2		3.0			99.998
El	2.6	3.0		15	99.7
2		3.0			99.998
Fl	2.6		3.0	15	99.8
2			3.0		99.993

Table 46. Removal of Radionuclides from Acid $Al(NO_3)_3$ Solution by Potassium Alum Precipitation

Conditions: See conditions as stated for removal of cesium, Table 45, pass E

Radionuclide	Per Cent Removed
Ce^{144}	0.04
Y^{91}	0
Sr^{89}	5.6
Zr^{95}-Nb^{95}	0.07
Ru^{106} (10 months old)	0.09

Heat Transfer and Energy Balance

In order to produce insoluble ceramic clinkers with fission product heat it is necessary to evaluate both the heat required by the sintering process and the heat available in the reactor fuel process waste. A balance of the heat available and the heat requirement must be obtained in each experiment. Since the power requirement for the ceramic clinker is fixed for a given mix, the only design variables are the heat lost during the experiment and the energy available in the waste solution.

Analysis of the heat experiments reported by the ceramicists indicated that clinkers could be produced with an energy application of 24.9 kwhr/gal of clinker. A thermochemical calculation of the energy required to sinter at 900°C, assuming no heat loss, showed that a clinker could be produced by using 12.3 kwhr/gal. A comparison of the calculated value and the experimental results indicated that about one-half the energy applied was lost or ineffective in sintering. Recent experiments in which the rate of heat addition was more realistic (that is, the highest power was applied initially, gradually decreasing with time until the experiment was completed) indicated that clinkers could be produced at 796°C with an energy application of 9.9 kwhr/gal of clinker, a value lower than the calculated value of 12.3 kwhr/gal.

Calculations of the power available for sintering in present-day waste solutions (assumed to be beta plus ½ gamma energy) indicate that small sintering experiments (furnace diameters less than 6 ft) cannot be performed with 90-day cooled wastes, since the heat losses per unit volume of clinker are greater for small clinkers. Table 49

shows the power required in the waste solution for various clinker sizes to hold the clinker at an equilibrium temperature of 900°C.

At the present time only rough calculations have been made of the heat losses during sintering. The problem is basically one of unsteady state heat flow and is further complicated by the geometry of the system and the operating heat losses. Experimental data have been collected and will be used in more extensive calculations of total and instantaneous heat losses.

Table 47. Activity of Lixivium from Preliminary Leaching Tests

Mix No.	Clay Material*	Counts/min/ml		
		426°C	638°C	800°C
47	Hector bentonite	465	18	26
48	Hector bentonite	551	61	30
49	Hector bentonite	538	28	0
50	Hector bentonite	10	285	362
51	Hector bentonite	77	56	1088
52	Hector bentonite	10	19	433
53	Cerclay	18	12	36
54	Cerclay	37	31	30
55	Cerclay	35	19	33
56	Cerclay	2	0	7
57	Cerclay	5	1	346
58	Cerclay	1	0	305
59	Cerclay	0	0	564
77	M. H. bentonite	71	3	0
78	M. H. bentonite	419	36	29
79	M. H. bentonite	350	0	7
80	M. H. bentonite	4	6	982
81	M. H. bentonite	12	64	2706
82	M. H. bentonite	10	20	623
83	Zeogel attapulgite	0	0	35
84	Zeogel attapulgite	0	4	845
85	Zeogel attapulgite	5	14	18
86	Zeogel attapulgite	47	0	0
87	Zeogel attapulgite	267	0	16
88	Zeogel attapulgite	45	0	1

*Activity of fission product waste solution used in preparation of clinkers was 23,000 counts/min/ml.

Sintering Furnace Off-Gases

The sintering process produces a complex of particulates ranging from approximately gas molecule size (1 Å) to 10 μ. The nature of the aerosol will vary with the changing temperature of the sintering materials. As the sintering material heats, water vapor and water droplets are evolved. Radioactive materials begin to appear in the aerosol when the temperature of the mass reaches 86°C, Table 50. After the boiling temperature is reached, the aerosol contains water droplets carrying both dissolved and insoluble particles.

The nature of the aerosol particulates evolved at temperatures greater than 100°C is not presently known. On the basis of experiments with sodium chloride it is known that a copious number of crystalline particles of about 0.05 μ are evolved at temperatures greater than 300°C. The particle size of the NaCl aerosol increases as the temperature of the solid salt material increases to 800°C. Particulates from the sintering furnace are expected to follow a similar pattern.

Reactive and nonreactive gases will be present throughout the sintering process. Of the reactive gases the first to appear is carbon dioxide, released during the mixing operation. Radioiodine will be present in the off-gases during the entire sintering operation, though the major part of the iodine will be volatilized below 200°C. Nitrate salts begin to decompose at 150°C, and oxides of nitrogen persist at 800°C. The important nonreactive gases present in the waste solution are Kr^{85} and Xe^{133}.

It is recognized that no single filtering agent can effectively remove this multiplicity of contaminants, thus suggesting the multibed air cleaner shown in Fig. 26, the components of which are sand, soda lime, and activated carbon. Dry sand is an effective filter for particulates. The efficiency of a sand filter depends upon (1) sand grain size and shape, (2) superficial air velocity (volumetric flow divided by filter cross-sectional area), and (3) sand bed depth.

If very moist aerosols are passed through a sand filter, water condenses in the filter voids and clogs the filter. Figure 27 shows the buildup of pressure at the inlet of a sand filter as it becomes

Table 48. Comparison of Calculated and Determined Chemical Composition of 700-, 750-, and 770°C-Sintered Clinkers

	Calculated* Composition (%)	Chemical Analysis		
		700°C Clinker Composition (%)	750°C Clinker Composition (%)	770°C Clinker Composition (%)
SiO_2	45.57	46.62	45.73	45.80
Al_2O_3	16.17	15.89	15.75	16.32
Fe_2O_3	5.20	4.35	4.98	5.17
CaO	11.06	10.07	11.86	12.02
MgO	2.88	3.11	5.02	3.00
Na_2O	12.04	12.15	14.03	13.15
K_2O	2.37	3.26	2.16	3.52
Other	4.71	4.55	0.47	1.02
Total	100.00	100.00	100.00	100.00

*Based on analysis of limestone and Conasauga shale.

Table 49. Power Required per Gallon of Dry Clinker to Maintain Equilibrium Temperature of 900°C for Various Surface-Area-to-Volume Ratios

Ratio, Area/Volume (ft^{-1})	Clinker Diameter (ft)	Clinker Thickness (ft)	Volume of Dry Clinker (gal)	Volume of Waste (gal)	Power Required per Gallon of Dry Waste (w)	Power Required per Gallon of Dry Clinker (w)
1	6	6	1268	2159	6.7	11.3
2	3	3	158.9	270.1	8.2	13.9
3	2	2	47.0	80.0	10.4	17.7
4	1.5	1.5	19.8	33.7	12.9	22.0
5	1.2	1.2	10.1	17.2	15.1	25.7
6	1.0	1.0	5.9	10.0	17.8	30.2
7	0.86	0.86	3.7	6.3	20.4	34.7
8	0.75	0.75	2.5	4.3	22.6	40.2
9	0.67	0.67	1.7	2.9	26.8	45.6
10	0.60	0.60	1.3	2.2	30.2	51.4

Table 50. Entrainment by Evaporation

Well		Condensate	
Temperature (°C)	Count (counts/min/ml)	Count (counts/min/ml)	DF*
90–100	856	1.340	6.39×10^2
86	8514	1.35	6.3×10^3
91	8514	2.47	3.44×10^3
95	8514	63.0	1.35×10^2

*DF (decontamination factor) = $\frac{\text{counts/min/ml in well}}{\text{counts/min/ml in condensate}}$

saturated with water. The sharp drop is indicative of channeling. By proper filter design the condensed water can be drained from the filter, thus maintaining the sand in an unsaturated condition.

Laboratory sintering experiments using Ru^{106} tracer show that the multibed filter functions in the following manner. Water condenses in the lower few inches of the filter and is drained to a sump beneath the filter. The evolved ruthenium is found both in the condensate and plated on the surface of the tube leading to the filter. No activity is found in the off-gas system after the filter. The data from these experiments are presented below.

	Activity (counts/min)
Initial waste	5.6×10^7
Final waste	4.4×10^7
Condensate	3.3×10^6
Ruthenium scrubber	0
Air cleaner	5.8×10^6
Tubing	2.9×10^6

Soda lime is an effective agent for removal of nitrogen oxides from gas streams. A soda lime bed (8-mesh) placed on the sand filter reduced the oxides of nitrogen concentration (nitrite) to approximately 10 ppm, as determined by bubbling through dimethylaniline. A 12-in.-deep bed of soda lime was not measurably more effective than a 4-in. bed. The 4-in. bed of soda lime was one-sixth the depth of the sand filter.

Radioiodine, when used as a tracer, condensed on the sand. As the sand was heated by the condensing water vapor, the iodine sublimed, moving slowly up the filter to the sand–soda lime interface where it remained. The distribution of iodine within the filter is shown in Fig. 28.

Activated carbon was included in the multibed air cleaner primarily to remove the initial surge of iodine. Since the iodine did not reach the activated carbon, its inclusion for iodine removal was not justified. However, the activated carbon did reduce the nitrogen oxides passing the soda lime to less than 1 ppm nitrites. For this reason the activated carbon was retained in the air cleaner.

"Adiabatic" Self-Sintering Experiment

One of the major problems in the laboratory study of self-sintering is the simulation of a fission product heat source. Many heating systems, varying from dielectric furnaces to Calrod immersion heaters, have been tried with little success. It appears that the best way to determine what effect fission product heating has on the properties of the clinker and the heat requirements is to experiment with actual wastes as the heat source.

One means of simulating fission product heating on a small scale (24-in.-dia clinker) with conventionally cooled reactor fuel process wastes would be to reduce the heat losses to as low a value as possible. This concept is the basis of "adiabatic" self-sintering. In this experiment the furnace would be equipped with a heat barrier to balance the heat lost through the furnace walls

(Fig. 29). The heat barrier would operate at a temperature below that of the clinker so that heat flow, if any, will always be from the clinker to the surrounding walls and insulation. Using 60-day cooled wastes the experiment should be completed in about 90 days, at which time the temperature of the clinker would be 900°C. The time required for the experiment would be increased, depending on the heat losses allowed in the furnace.

A prototype experiment has been designed in which Calrod heaters will be used to simulate the fission product heating, and equipment is being fabricated. This experiment will provide information for design calculations and equipment operation. Upon completion of this experiment a facility will be constructed for a true adiabatic experiment using a high-level waste solution including equipment for the collection and decontamination of the sintering off-gases.

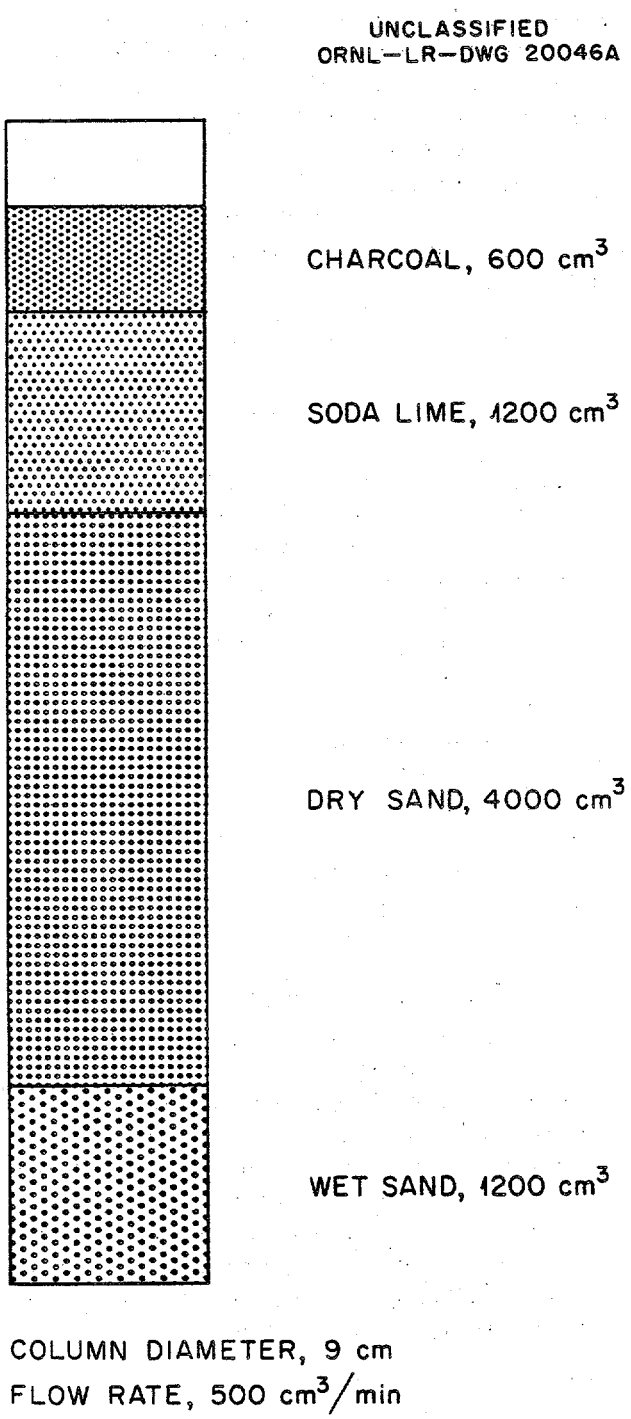

Fig. 26. Multibed Low-Velocity Air Cleaner.

Self-Sintering Experiment

It is anticipated that, when the adiabatic experiment has been completed, information will be

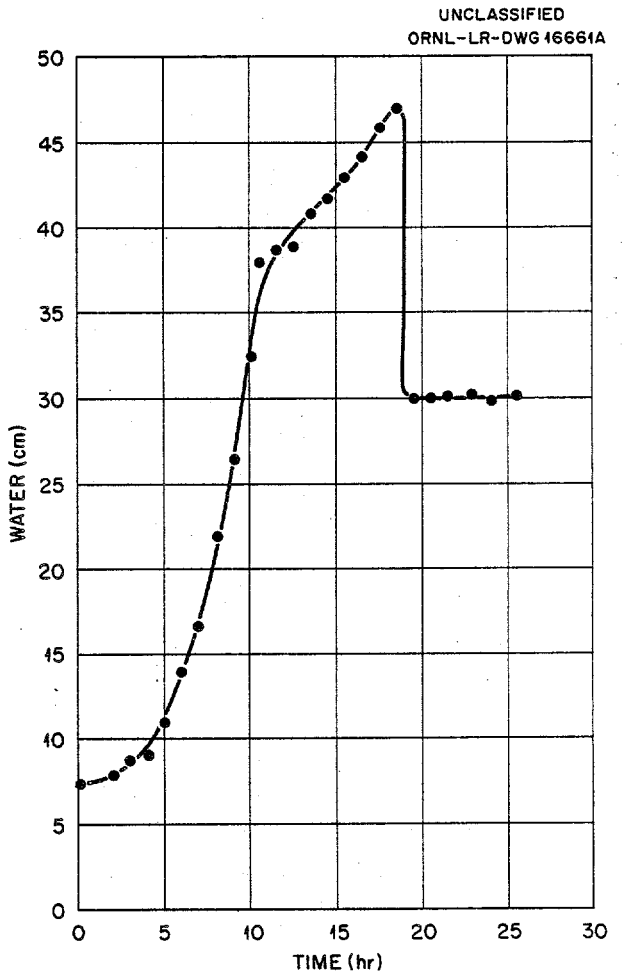

Fig. 27. Pressure Drop Across Sand Filter.

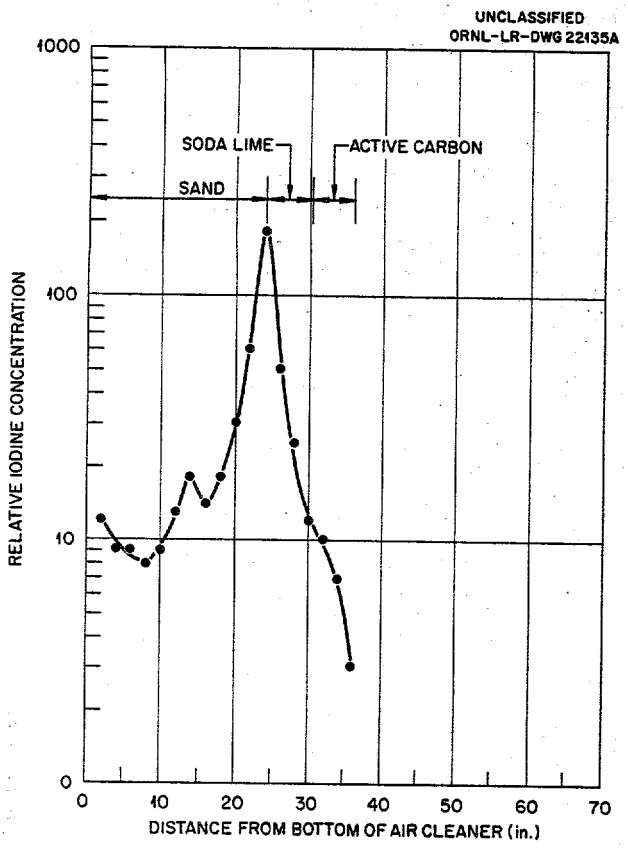

Fig. 28. Iodine-131 Distribution Within the Multibed Air Cleaner.

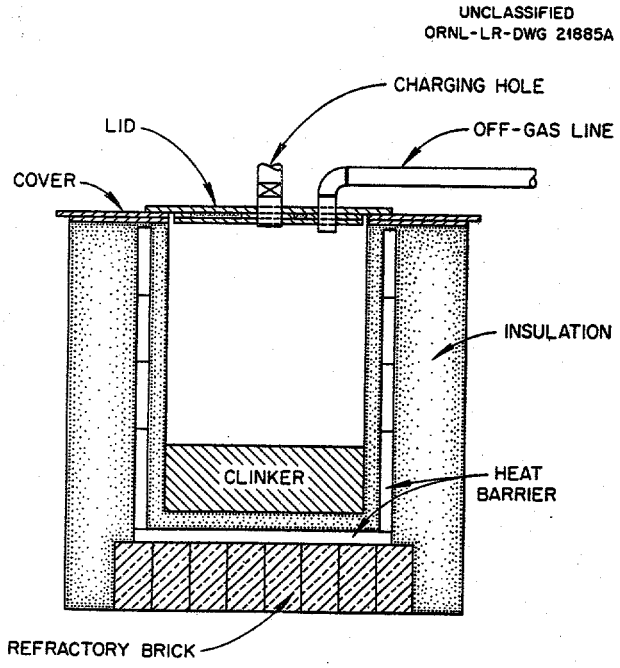

Fig. 29. Furnace for "Adiabatic" Self-sintering Experiment.

available to check the design of an experiment using high-level waste solution to provide the heat necessary for self-sintering; no heat barrier will be required. The experiment would use 30 gal of 6-day-cooled MTR fuel process waste and would produce a radioactive clinker 24 in. in diameter by 8 in. thick. The short cooling time (6 days) is required because of the increased heat losses per unit volume in small experiments; it does not mean that all self-sintering must be done with short-cooled wastes. A schematic diagram of the facility for the proposed experiment is shown in Fig. 30. The experiment and operating procedure have been described in a preliminary proposal to the AEC.[13]

Pilot Pit No. II

The construction of pilot pit No. II has been completed during the past year. Figure 31 is a schematic drawing of the complete system, including the 720-gal mixer, the sintering furnace, and the off-gas system. Figure 32 shows details of the immersion heater, and Fig. 33 is a view of the installation. Final hookup of power and instrument wiring and a comprehensive check of the installation remain to be done. The 6-in. pipe discharging from the mixer is for use in a test of mixer operation prior to the actual experiment.

The experiment to be carried out in this facility will utilize mix No. 15 (aluminum nitrate waste, shale, limestone, and soda ash) with a rate of power application corresponding to the decay of actual waste solution.

Evaluation of Ceramic Clinkers

A study of petrographic thin sections of clinker produced by sintering mix No. 15 at an average temperature of 790°C has shown that the clinker is glassy and vesicular. Further study and x-ray analysis have shown this material to be similar in appearance to the compound melilite (orthodisilicate mineral) but with some dissimilarities in the intensities and spacings in the x-ray patterns. Petrographic study of samples sintered at lower temperatures has shown that very few

[13] E. G. Struxness, *Experimental Self-Sintering of Reactor Fuel Process Wastes*, Health Physics Division, ORNL, November 20, 1956. Proposal to USAEC.

UNCLASSIFIED
ORNL-LR-DWG 21883A

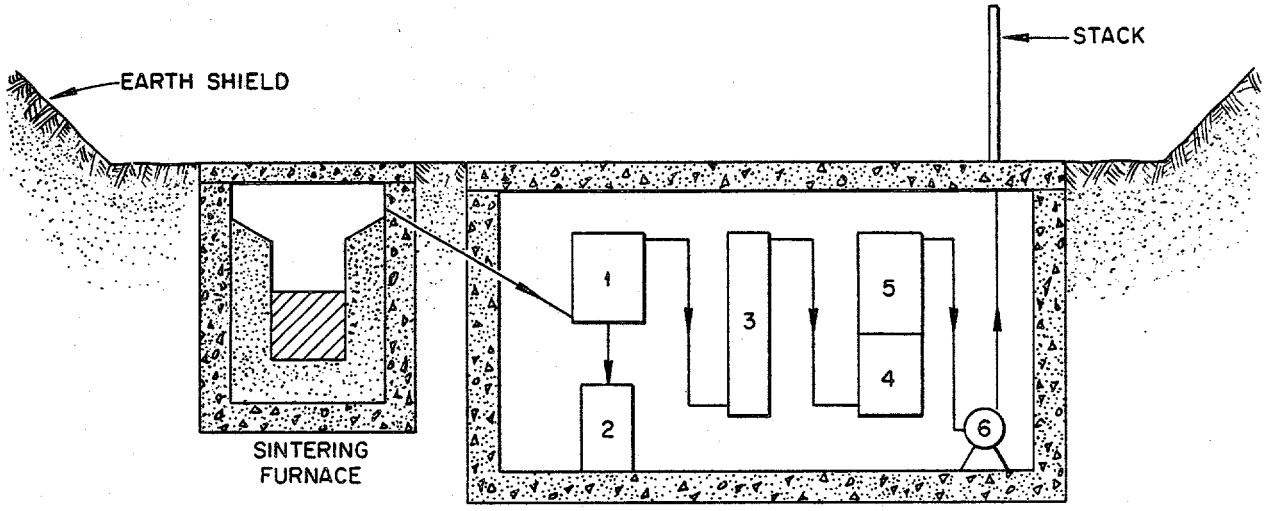

1 AIR-COOLED CONDENSER
2 CONDENSATE STORAGE
3 FIBERGLAS FILTER
4 HEATER
5 IODINE REACTOR
6 EXHAUSTER

Fig. 30. Schematic Diagram of Proposed Self-sintering Experiment.

UNCLASSIFIED
ORNL-LR-DWG 24798

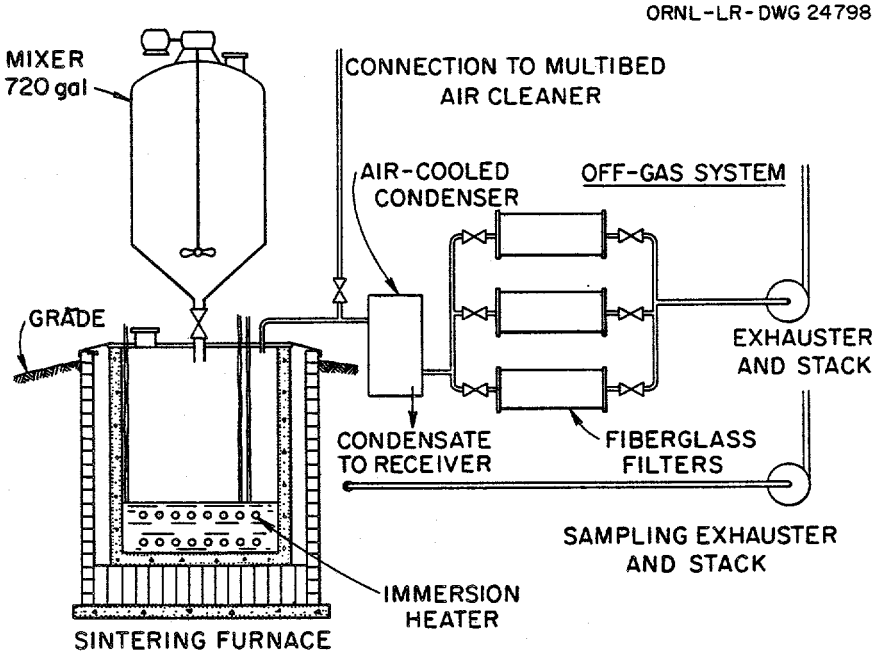

Fig. 31. Schematic Outline – Pilot Pit No. 2.

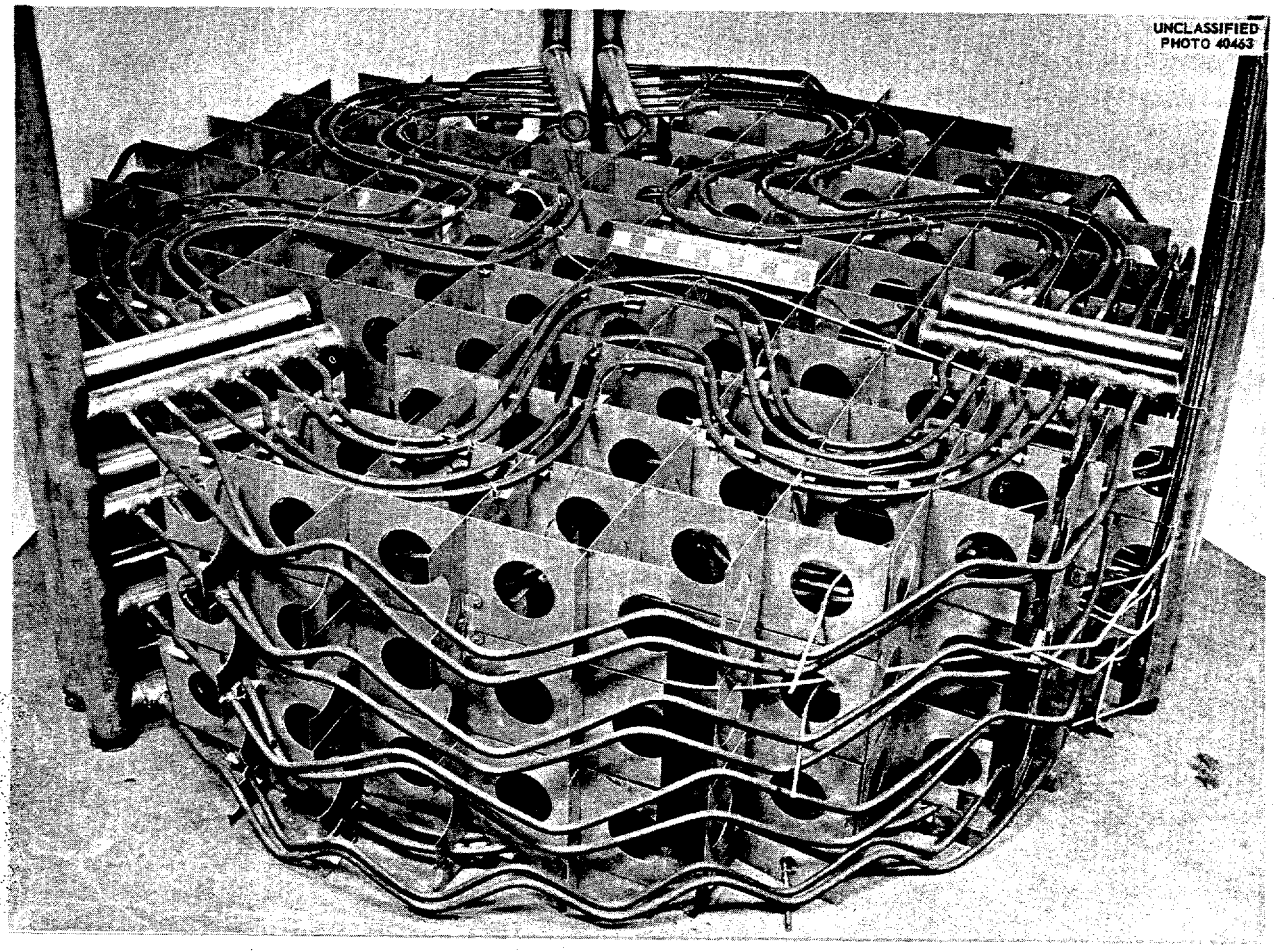

Fig. 32. Electric Immersion Heater Used in Pilot-Scale Sintering Experiment (Pilot Pit No. 2).

structural or chemical changes occur below 790°C. Photographs of the petrographic thin sections used in the above analysis are shown in Fig. 34.

Thermal mineralogy of clinkers formed by firing in laboratory muffle furnaces instead of sintering furnaces has shown that $CaCO_3$ and $NaNO_3$ are present at 426°C. By increasing the temperature to 638°C all traces of $NaNO_3$ and $CaCO_3$ were removed. Samples sintered at 800°C showed that an unidentified microcrystalline material and quartz were present and later consumed by a glass formed at about 1000°C. The glass material has an index of refraction of 1.550 indicating that some of the alumina and iron oxide has gone into solution. The differences in the samples formed in muffle furnaces and sintering furnaces merit further investigation.

Laboratory evaluation of the solubility and stability of experimentally produced clinkers has been initiated. The first stage of this investigation, determination of the solubility of the nonradioactive ceramic matrix (mix No. 15) in distilled water, is complete. Table 51 lists the solubility of 750 and 770°C clinkers as determined by static, boiling, and flowing leach tests.

Chemical analysis of the lixivium is in progress along with permeability, porosity, crushing-strength, and surface-area measurements of the clinkers.

Design and fabrication of a laboratory sintering furnace is complete for the production of clinkers tagged with mixed fission products. This equipment, operated at power levels representative of a decaying waste solution, will be used to produce samples for additional petrographic and leaching studies.

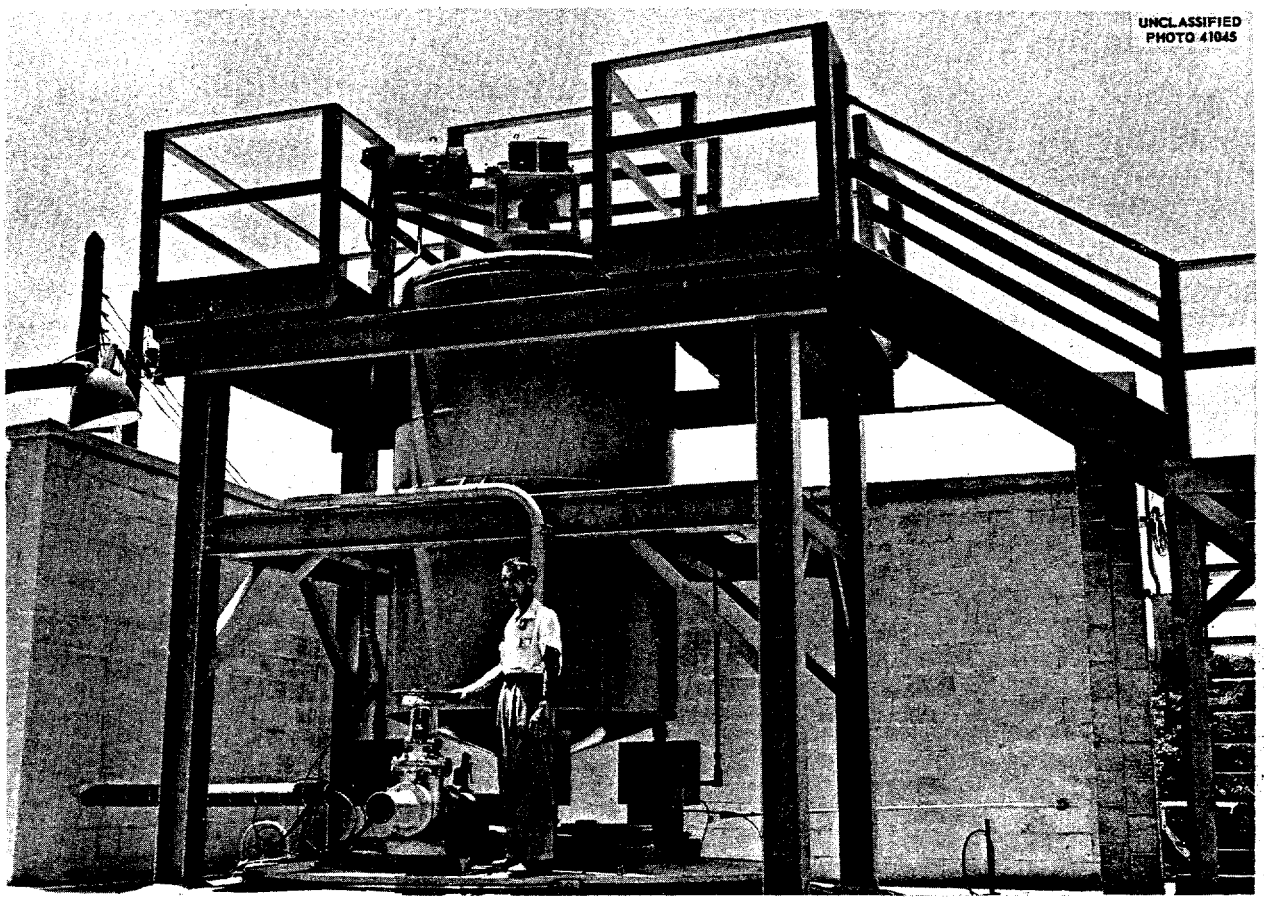

Fig. 33. View of Pilot Pit No. 2 Mixer and Shield.

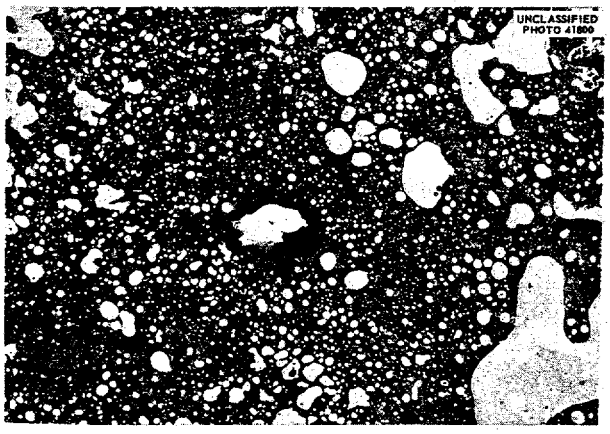

Fig. 34. Petrographic Thin Section of Ceramic Clinker (Courtesy E. Roedder, USGS).

DISPOSAL INTO GEOLOGIC STRUCTURES

W. de Laguna F. L. Parker

Disposal into Deep Wells

The study of the problem of disposal of radioactive wastes into deep wells has been confined to an attempt to determine the critical factors involved. Some geologists believe it is unlikely that untreated wastes can be injected into the ground at all, because acid aluminum nitrate waste forms a gelatinous precipitate when attempts are made to pass it through a sand column. Others believe the wastes to be considered for deep-well disposal might be the neutralized and aged Purex or Darex types, with which plugging of the well

Table 51. Results of Preliminary Static, Boiling, and Flowing Leach Tests of Mix No. 15

Sintering Temperature (°C)	Sample Description	Leach Test and Volume of Lixivium	Leach Interval	pH Change	Milligrams Removed per Gram of Sample Leached
750	1 in. cube	Static, 1000 milliters	4 weeks	+0.9	1.1
770	1 in. cube	Static, 1000 milliters	4 weeks	+0.7	0.9
750	No. 4 mesh	Static, 1000 milliters	4 weeks	+1.1	1.7
770	No. 4 mesh	Static, 1000 milliters	4 weeks	+1.0	1.5
750	No. 40 mesh	Static, 1000 milliters	4 weeks	+1.3	3.3
770	No. 40 mesh	Static, 1000 milliters	4 weeks	+1.2	3.1
750	No. 120 mesh	Static, 1000 milliters	4 weeks	+1.8	6.5
770	No. 120 mesh	Static, 1000 milliters	4 weeks	+1.6	6.0
750	1 in. cube	Flowing, 20 liters	1 week	0	120
770	1 in. cube	Flowing, 20 liters	1 week	+0.1	100
750	1.5 in. cube	Flowing, 20 liters	1 week	+0.1	130
770	1.5 in. cube	Flowing, 20 liters	1 week	+0.1	120
750	1 in. cube	Boiling, 1000 milliters	2 hours	+0.2	1.5
770	1 in. cube	Boiling, 1000 milliters	2 hours	+0.2	1.4
750	No. 4 mesh	Boiling, 1000 milliters	2 hours	+0.7	2.3
770	No. 4 mesh	Boiling, 1000 milliters	2 hours	+0.6	2.2
750	No. 40 mesh	Boiling, 1000 milliters	2 hours	+1.5	4.8
770	No. 40 mesh	Boiling, 1000 milliters	2 hours	+1.3	4.6
750	No. 120 mesh	Boiling, 1000 milliters	2 hours	+1.8	8.5
770	No. 120 mesh	Boiling, 1000 milliters	2 hours	+1.6	8.1

is less apt to be a problem, particularly after pretreatment by filtering and centrifuging.

The thermal problems appear to place severe restrictions on disposal in depth. This is particularly true if the disposal of waste that has had only a 100-day cooling period is considered. The problem is changed by several orders of magnitude, however, if the wastes are stored in tanks for ten years and then put underground. A more critical aspect of the thermal problem than age of the waste is the probability of concentration of the activity by adsorption on the solid matrix of the aquifer. This could localize the heat production, possibly at the base of the well. The fear that the well would turn into a geyser may be unjustified, for the well can be plugged, with concrete if necessary, so that it is stronger than the formation around it. High temperatures may be reached locally in depth, but the inference that this will force contaminated water up to the water table is not sound, for with any movement away from the hot core, the heat would be dissipated quickly. In fact, the high temperatures suggested by some are based on the assumption that the heat will be lost only by conduction; if there is any movement, as by convection, the heat which is so slowly produced can be carried away. It is difficult to foresee containment of the heat and dissipation of the activity except in the formation of a narrow passageway, such as a fracture, leading from an overheated storage chamber up to the surface. This might occur in a consolidated rock, but hardly in an unconsolidated sediment.

It is apparent that a practical solution of the deep-well disposal problem requires the close cooperation of engineers familiar with the technology of fuel element reprocessing, of petroleum engineers experienced in oil production, and of the geologists and hydrologic engineers of such organizations as the U.S. Geological Survey. Progress has been made in this direction, and there has been one formal discussion between representatives of the Atomic Energy Commission, the American Petroleum Institute, the Geological Survey, and the Laboratory.

Disposal into Salt Formations

The question of disposal into salt structures appears to be more of a direct engineering problem, and less of a general scientific problem, than disposal into deep wells. There is already sufficient information on the general location of suitable salt deposits in the United States, so that the question of site selection is largely one of choice, not of exploration. The nature of salt as a structural material is fairly well known, although tests to determine the effects of heat, pressure, radiation, and chemical interaction must be made. The only difficult structural problem is likely to be the slow plastic flow of heated salt with time. Cavities can be made in salt either by mining or by drilling down from the surface and dissolving out an opening. The second method has been used by the petroleum industry to store highly volatile liquids, and its feasibility in the absence of heat generation has been demonstrated.

A major problem of disposal into salt stems from the need to dissipate the heat generated by fission product decay. Mined openings may have certain advantages in this respect over openings made by solution. Mined openings may be made any shape, and more particularly into a series of parallel corridors between which would be sunken tanks, a pattern which would permit air to be blown over the tanks to cool the liquid in them. Similar rooms could also be used to store solid waste. Forced ventillation might be required to dissipate the heat generated.

SOIL DISPOSAL OF INTERMEDIATE-LEVEL WASTES

R. L. Blanchard (USPHS)
R. L. Bradshaw
K. E. Cowser
W. de Laguna
E. R. Eastwood
B. Kahn (USPHS)
F. L. Parker
G. G. Robeck (USPHS)
H. J. Wyrick

The preceding section deals with methods of disposal of high-level radioactive waste from nuclear reactors. An equally important problem is the disposal of much larger volumes of intermediate-level radioactive wastes that are associated with the operation of nuclear reactors and related chemical facilities.

Laboratory Soil Column Studies

The capacity of local shale for adsorbing cesium was obtained by passing a 0.1 *M* cesium solution with Cs^{137} tracer upward through water-filled shale columns until the activity of the effluent equaled that of the influent. The columns were washed with distilled water, and the cesium was leached with 6 *M* HCl. The amount of cesium adsorbed by the soil was determined by counting the radioactive cesium in the acid solution and is given in Table 52. The milliequivalents of cesium adsorbed

Table 52. Adsorption of Cesium on Dried Conasauga Shale

Soil Aggregate Size Range (U.S. Standard Sieve)			Weight of Soil (g)	Column Size		Flow Rate	Cesium Attached to Soil (meq/100 g)
Number Passing	Number Retained	Size (mm)		Diameter (cm)	Length (cm)		
20	40	0.84–0.44	30	2.5	12.5	0.1 ml/min	22.1
10	20	2.00–0.84	20	2.5	10	0.5 ml/min	22.5
8	10	2.38–2.00	10	2.5	2.5	1 ml/min	22.7
50	70	0.29–0.21	1	0.6	2.5	2 ml/hr	15.6
70	80	0.21–0.77	0.25	0.4	3.75	1 ml/hr	12.0

ranged from 22.1 to 22.7 per 100 g of soil and were independent of grain size between 8 and 40 mesh. Flow rates greater than 0.5 ml/min were too rapid, because the cesium adsorption of the apparently saturated soil increased upon standing. It was concluded that a satisfactory column for this work is that of 20 g of 10-to-20-mesh shale and a flow rate of 0.5 ml/min.

A laboratory column study of the behavior of waste solution passing through local soil was made by passing a sample of the overflow from waste pit No. 3 to No. 2 (collected on October 19, 1956) through a 2.5-cm-dia soil column of 20 g of 10- to 20-mesh Conasauga shale until the 15,750 ml of available solution was used. The gross gamma count rate of the effluent was taken from time to time, and analyses were made of the influent and effluent radioactive and nonradioactive constituents and of the radionuclides adsorbed on the drained and dried shale.

The gamma count rate of the effluent remained constant at approximately 15% of the influent count rate for the first 4.5 liters, then increased steadily to 95% of the influent count rate at 13 liters and remained between there and 100%. Values of effluent activity – the average of four values reported as count rates by the Analytical Chemistry Division and converted to disintegration rates by means of empirical counting efficiency factors – are listed in Table 53 and compared with influent activity.

The chemical composition of the effluent did not differ significantly from that of the influent. The effluent was 0.5 *M* in $NaNO_3$ and 0.2 *M* in NaOH, and contained 0.010 *M* Al^{+++}, 0.04 *M* SO_4^{--}, 0.03 *M* CO_3^{--}, and between 0.001 and 0.01 *M* of Ca^{++}, K^+, PO_4^{---}, and Cl^-.

After the upflow passage of the solution through the column, the shale was divided into two equal parts for the radiochemical analysis listed in Table 54. The radionuclides were identified by their characteristic radiations. A search for radionuclides other than the major long-lived fission products was made with a gamma spectrometer and indicated the presence of radionuclides of cobalt and antimony.

The preliminary results indicated in Table 54 suggest the following:

1. The capacity of the shale for adsorbing cesium – the major radionuclide in this waste solution – is approximately 3.4×10^8 d/min/g or 70 μc/lb.
2. Appreciable breakthrough of the adsorbable radionuclides occurs after 2 liters of solution have passed through 20 g of shale.

Table 53. Activity in Waste Solution After Passage Through Soil Column

Source of solution: overflow from pit No. 3
Collection date: October 19, 1956
Weight and size of column: 20 g of 10- to 20-mesh Conasauga shale, 2.5 cm in diameter

Radioelement	Activity of Influent (d/min/ml)	Activity of Effluent (d/min/ml)							
		0–2 Liters	2–4 Liters	5–6 Liters	7–7.5 Liters	9.3–11 Liters	11–13 Liters	14–14.5 Liters	15.70–15.75 Liters
Cesium	1,300,000	26,000	120,000	290,000	510,000	950,000	980,000	1,300,000	1,200,000
Ruthenium	210,000	210,000		220,000	210,000	230,000		220,000	210,000
Strontium	16,000	180		1,300	1,900	12,000		11,000	11,000
Rare earths + yttrium	15,000	4,200		5,300	5,900	12,000		10,000	10,000
Zirconium	1,800	990						510	
Niobium	28,000	1,600						1,700	
Cobalt	15,000	11,000						13,000	
Antimony	8,600	9,600						9,500	

Table 54. Activity Adsorbed on Soil Column from Waste Solution

Activity corrected for decay to January 30, 1957
Direction of flow: up
Weight of local Conasauga shale column: initial, 20.00 g
final, 20.66 g
Weight of portions after being split in two: top portion: 9.43 g
bottom portion: 11.23 g

Radioelement	Radionuclide	Activity in Units of 10^6 d/min/g		Total Activity Adsorbed on Column in Units of 10^7 d/min	Total Activity Applied to Column in Units of 10^7 d/min	Per Cent of Influent Activity Adsorbed
		Top Portion	Bottom Portion			
Cesium	Cs-Ba^{137}	320	340	680	2000	33
Ruthenium	Ru-Rh^{106}	1.1	1.5	2.8	330	0.9
Strontium	80% Sr^{90}	3.3	5.0	8.7	24	36
Trivalent rare earths + yttrium	96% Y^{90}	2.6	4.1	7.0	23	38
Cerium	Ce-Pr^{144}	0.62	1.2	1.9		
Zirconium	Zr^{95}	0.12	0.14	0.28	2.8	10
Niobium	Nb^{95}	3.4	4.8	0.86	14	2
Cobalt	Co^{60}	0.72	1.0	1.8	24	8
Antimony	Sb^{125}	0.010	0.014	0.025	14	0.2

3. Complete breakthrough of the cesium occurs after 13 liters of solution have passed through 20 g of shale.

4. Ruthenium and antimony passed through the soil without being appreciably absorbed; cobalt is poorly absorbed; zirconium and niobium are to a large extent unaccounted for, and were probably adsorbed on the glassware.

5. There are no apparent stable constituents that would serve to indicate when radioactive cesium is about to break through.

The first few liters of effluent from the soil column, which contained 90% Ru^{106}, 7% Co^{60}, and 3% Sb^{125}, were subjected to several precipitation and anion exchange procedures to attempt further decontamination. Antimony was completely precipitated as lead antimonate. The conversion of the ruthenium from its present apparently nonionic state to the RuO_4^{--} form was attempted by (1) heating the basic waste solution with $KMnO_4$ and (2) oxidizing at room temperature with NaOCl (ref 14). The solution heated with potassium permanganate was either stirred with anion resin to remove the ruthenate by adsorption, or ethyl alcohol was added to reduce both the manganese and the ruthenium to the insoluble dioxides. In addition to appreciable amounts of ruthenium, which contributes approximately 75% of the gamma count rate, gamma spectrometer studies indicate that almost all the Co^{60} and most of the Sb^{125} (the other noncationic radionuclides) are removed from solution. Some removal values obtained by the $KMnO_4$ treatment are given in Table 55. Additional removal of antimony was obtained by precipitating lead antimonate with 1 mg of antimony trichloride and 25 mg of lead acetate per 50 ml of waste solution.

The waste solution, oxidized with sodium hypochlorite, was treated with lead acetate to remove

[14] J. L. Howe and F. N. Mercer, *J. Am. Chem. Soc.* 47, 2926 (1925).

Table 55. Removal of Noncationic Radionuclides from Intermediate-Level Waste by $KMnO_4$ Treatment

Used 50 ml of solution, previously passed through soil column

Method	Treatment	Removal of Gross Gamma Activity (%)
A	Slurried with 1 g of Dowex-1 resin, twice in succession	14
B	Boiled with 25 mg of $KMnO_4$, slurried twice with 1 g of Dowex-1	48
C	Heated with 50 mg of $KMnO_4$, slurried twice with 1 g of Dowex-1 resin	76
D	Repeated (C) three times in succession	93
E	Repeated (C) twice, and precipitated lead antimonate	97
F	Mixed with 1.5 g of $KMnO_4$ + 3 ml of alcohol	58
G	Boiled with 0.75 g of $KMnO_4$ for 30 min and added 1.5 ml of alcohol	85
H	Boiled with 1.5 g of $KMnO_4$ for 30 min and added 1.5 ml of alcohol	89
I	Method (H) plus lead antimonate precipitation	92

the hypochlorite (as lead oxychloride), causing the formation of ruthenium dioxide, with absorption of this oxide on to the lead precipitate. Decontamination values given in Table 56 indicate that the gross ruthenium-cobalt-antimony removal increases with the standing time of the oxidized solution, as well as with the stirring time after the lead has been added, with the former being slightly more influential. Because of the advantages of the NaOCl treatment over that of $KMnO_4$ (no heating needed and higher decontamination), the NaOCl treatment will be combined with a soil column decontamination of the wastes in a larger-scale test of waste decontamination.

A study was made to determine the volumes of various ionic solutions needed to replace cesium ions (containing Cs^{137} tracer) sorbed on local Conasauga shale. Columns of shale were first saturated with cesium chloride solution, then washed with distilled water, and finally eluted with dilute solutions of alkali salts. The fractions of cesium washed from the soil by the different volumes of elutriant are given in Table 57. The results suggest that the rate of cesium elution is affected by the elutriant anion, as well as the kind of cation and the cation concentration.

Wastes Released to ORNL Pits

The volume of intermediate-level liquid wastes transferred to the pits through December 1956 and the estimated curies of Cs^{137}, Ru^{106}, and gross beta activity are shown in Table 58. The individual pit inventory separates the events of direct waste transfer and the overflow of waste between pits. The volume of waste overflow is based on staff-gage readings taken before and after the overflow period and rating curves that relate liquid stage to volume in terms of gallons.

As shown in the total pit inventory 5,600,000 gal of radioactive waste containing 58,000 curies of Cs^{137} and 15,000 curies of Ru^{106} has been discharged to the system of disposal pits (curies measured at time of discharge into pits). On the average, Cs^{137} and Ru^{106} account for 90% of the sample count rate, with the exception of those periods when special programs of operating procedures change the type and concentrations of the radionuclides present. During such periods I^{131} or the total rare earths are the major contributors of the radioactivity transferred to the pits. The concentration of Cs^{137} and Ru^{106} in the waste that is eventually overflowed to pit No. 4 is reduced by a factor of 4 to 5 due to occlusion in precipitates settling in pits No. 2 and No. 3, adsorption on the shale side walls of the pit, dilution, and decay.

The normal waste stream now released to the seepage pits contains, on the average, 16.3 mg/ml of sodium and 23.8 mg/ml of NO_3, which account for 70% of the total solids. The total waste to

Table 56. Removal of Noncationic Radionuclides from Intermediate-Level Waste by NaOCl Treatment

Used 25 ml of solution previously passed through soil column

Treatment				Removal (%)		
NaOCl, Milliliters of 5% Solution	Standing Time (hr)	pH	$Pb(C_2H_3O_2)_2 \cdot 3H_2O$ (milliliters of 150 mg/ml-soln)	Stirring Time in Hours		
				0.1	24	90
1	1	10	2	66	87	91
1	66	10	2	88	94	
1	24	10	2	81	91	93
1	24	10	1.5	79	88	91
1	6	10	3	83	88	
0.5	6	10	3	74	80	
0.5	6	10	1.5	56	69	76
1	0.5	7	2	47	49	51
1	0.5 (add 1 ml of 2 *M* NaOH)		2	55	69	75
1	0.5 (add 1 ml of 3 *M* NaOH)		2	51	62	74
1	0.5	10	3	78	79	81

Table 57. Elution of Cesium from Conasauga Shale Columns

Soil column weight: 20 g
Soil particle size: 10 to 20 mesh
Upflow rate of solution: 0.5 ml/min

Leach Solution	Cesium Replaced (%)					
	Volume of Leach Solution (ml)					
	50	100	200	300	400	1000
0.01 *M* NaCl	8	16	25	33	37	51
0.1 *M* $NaNO_3$	14	27	39	47	53	74
0.1 *M* CsCl	31	89	96			
Tap water	0.4	2.0				
1.0 *M* NaCl	52	75	90	97	98	
0.1 *M* NaCl	13	38	58	70	77	98
0.1 *M* NaOH	3	12	26	36		

pit No. 3 contained about 110 tons of sodium and 140 tons of NO_3, and the waste to pit No. 4 about 54 tons of sodium and 80 tons of NO_3.

Evaporation and Seepage

The loss of liquid from the waste pits is important when considering control of the system and forecasting the future requirement of number and size of additional pits. A balance must be effected between the amount of waste discharged to the pits and the loss of waste from the pits. The rate of seepage will influence the design of future pits.

The transport of liquid is governed by four parameters, which are (1) inflow of waste, (2) rainfall, (3) evaporation, and (4) seepage. The volume of waste transferred is obtained from the Tank Farm[15] records, and rain-gage records of rainfall are

[15] An underground storage facility at ORNL consisting of 8 concrete Gunite tanks with a total capacity of 1,105,000 gal.

Table 58. Radionuclides Transferred to Waste Pits

	Individual Pit Inventory*											
	Pit No. 2				Pit No. 3				Pit No. 4			
	Gal	Curies			Gal	Curies			Gal	Curies		
		Beta	Cs^{137}	Ru^{106}		Beta	Cs^{137}	Ru^{106}		Beta	Cs^{137}	Ru^{106}
	$\times 10^3$	$\times 10^2$	$\times 10^2$	$\times 10^2$	$\times 10^3$	$\times 10^2$	$\times 10^2$	$\times 10^2$	$\times 10^3$	$\times 10^2$	$\times 10^2$	$\times 10^2$
Waste pumped to pit	1241	160	142	65	4400	548	435	84				
Waste overflowed to pit	3163	89	109	21					1308	23	27	6
Waste overflowed from pit	−1308	−23	−27	−6	−3163	−89	−109	−21				
Net waste to pit	3096	226	224	80	1237	459	326	63	1308	23	27	6

Total System Inventory*				
	Gal	Curies		
		Beta	Cs^{137}	Ru^{106}
	$\times 10^3$	$\times 10^2$	$\times 10^2$	$\times 10^2$
Pit No. 2	3096	226	224	80
Pit No. 3	1237	459	326	63
Pit No. 4	1308	23	27	6
Total	5641	708	577	149

*All amounts are accumulative through December 1956. The values represent the summation of the curies present at the time of discharge; no correction has been made for radioactive decay.

obtained from the U.S. Weather Bureau (USWB). The volume of rainfall entering the pits can be estimated reliably from the inches of precipitation and the catchment area of the pits. As an example pit No. 3, having a catchment area of 21,400 ft^2, collected about 726,000 gal of precipitation from a total rainfall of 54.24 in. during 1956.

A joint study with the USWB is in progress to determine the liquid losses due to evaporation and seepage. Meteorological equipment installed adjacent to pit No. 3 includes thermocouples and anemometers supported at 2 and 8 m above the ground to determine air temperature and wind speed. Humidity is determined by a Foxboro dew cell at the 2-m height. Equipment in pit No. 4 includes a float-supported anemometer to obtain wind movement at the surface of the liquid in the pit, and float-supported and fixed thermocouples to obtain the liquid temperature profiles. Observations have been recorded since May 1956, and the data are being processed.

Preliminary results indicate that the daily loss due to seepage is 1000 gal from pit No. 3 and 3900 gal from pit No. 2, when the liquid stage in the pits fluctuates between 10 and 14 ft. The liquid stage in pit No. 4 is observed to fall at a near constant rate of 0.21 ft per day, due in large measure to seepage. As an example, between the stages of 7 and 8 ft, this amounts to 20,000 gal per day.

During 1956 pit No. 3 gained almost as much liquid from rainfall as it lost through evaporation and seepage. Consequently the pit system would have operated almost as efficiently without this pit. This conclusion was a factor in the decision to use pit No. 3 for the disposal of sludge from the new lime–soda ash process waste treatment plant. Pit No. 2 has a net annual loss of about a million gallons.

Hydrology of Pit Nos. 2, 3, and 4

Pit No. 3 failed because its location permits only a very slow rate of seepage. Generally, significant liquid movement in the Conasauga shale is confined to the many minute fractures which follow the bedding plane; movement across the strike is very slow as shown by actual operation of the pits. Movement to the west from the southern end of pit No. 3 is largely blocked by the water-table mound around pit No. 2. At the other end, movement to the west is into the head of a small valley where it must compete with surface and ground water flow from a hill. Movement to the east from the north end of the pit is also impeded by normal ground water movement. The greater part of the seepage from the pit is probably restricted to the belt between wells Nos. 56 and 57, an effective distance of only 150 ft across the strike.

The location of pit No. 2 is probably the most satisfactory of the three sites. The pit is far enough out on the spur so that it can leak east and west with little interference from natural drainage from the north, and the slopes of the water-table mound from the pit are steep enough so that the induced ground water and waste movements are fairly rapid. The pit is oriented more nearly across the strike, and probably leaks effectively in both directions out along the strike, except for the north end, where seepage to the east is impeded by the water-table mound around pit 3.

These are several reasons for the rapid leaking from pit 4, although their relative importance is not known. This pit is oriented directly across the strike so that liquid from it can move out unimpeded in both directions. The water-table gradients out from the pit are steep, in part because the natural water table was lower before the pit was built, and in part because the distance of waste movement underground is short. In operation, pits 2 and 3 are kept nearly full; consequently, a stable water-table mound has formed around them and the gradients and rates of flow are in equilibrium. Pit 4, on the other hand, is operated intermittently, waste being run into it as needed. In some cases the pit goes dry before the next inflow; in other cases several inflows are added within a few days or weeks before the pit is empty. In no case has the pit been partially filled long enough for equilibrium to be established.

The difference between the leakage rates of the three pits cannot be attributed entirely to the differences in topography; there appears to be, in addition, a difference in the transmissibility of the shale aquifer at the three sites. If it can be assumed that the pits leak dominantly along the strike, then seepage to the east from pit No. 3, as mentioned above, is largely confined to a belt 150 ft wide. The water-table gradient here, parallel to the strike, is about 0.2 (20 ft in 100). There is probably some leakage to the west through a belt of shale about 100 ft wide where the gradient is estimated to be 0.1. If the pit leaks 1000 gal a day, the transmissibility, T, of the aquifer around pit 3 is given by

$$T[(150 \text{ ft} \times 0.2) + (100 \text{ ft} \times 0.1)] = 1000 \text{ gal per day},$$

$$T \times 40 \text{ ft} = 1000 \text{ gal per day},$$

$$T = 25 \text{ gal per day per foot}.$$

Similarly, pit No. 2 appears to leak to the west through a belt 200 ft wide, and to the east through a belt 150 ft wide. The gradient in both of these belts is roughly 20 ft in 100. In 1956, the pit leaked at an average rate of 3900 gal a day, so that

$$T(350 \text{ ft} \times 0.2) = 3900 \text{ gal per day},$$

$$T \times 70 \text{ ft} = 3900 \text{ gal per day},$$

$$T = 56 \text{ gal per day per foot}.$$

On March 25, 1957, the date of the water-table contour map shown in Fig. 35, the water table around pit No. 4 was briefly in equilibrium. At this time the pit was leaking at a rate of 16,500 gal a day, and this flow passed out through two zones, each about 200 ft wide, in which the water table gradients were roughly 15 ft in 100.

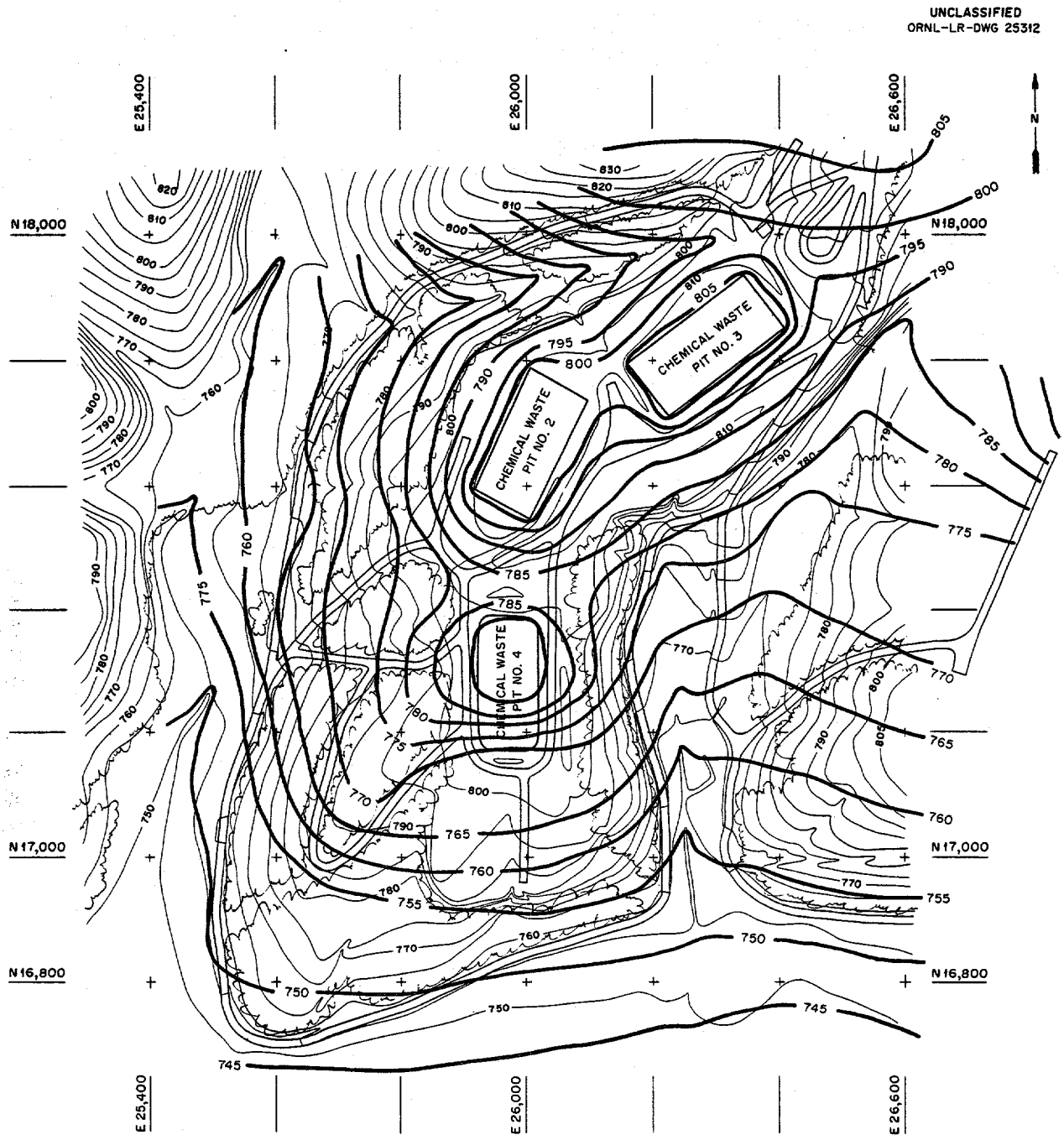

Fig. 35. Water Table Contour Map – March 25, 1957.

$$T(400 \text{ ft} \times 0.15) = 16{,}500 \text{ gal per day} ,$$

$$T \times 60 \text{ ft} = 16{,}500 \text{ gal per day} ,$$

$$T = 275 \text{ gal per day per foot} .$$

The detailed pattern of seepage from the pits is difficult to define, and the water-table gradients are rough approximations. It may not be correct to apply simple concepts of ground-water movement to pit No. 4, since it leaks at the same rate at the same pit stage even when ground-water conditions are somewhat different, suggesting that other factors control its rate of seepage. However, there is a strong suggestion that the shale is more permeable at the southern end of the ridge near pit No. 4 than it is to the north near pit No. 3. There are several reasons which may account for this. The ridge was formed by the erosion of the two small valleys that border it, so that the southern end of the ridge was formed first. Natural ground-water movement, therefore, has occurred for a longer time at the southern end, and, since natural underground drainage here was more nearly parallel to the strike, the movement may have been more vigorous than to the north, the location of pit No. 3. There does not appear to be any lithologic difference in the shale itself which would account for the apparent difference in permeabilities.

There are very real differences in the structure of the shale under the three pits. Under pit No. 3, the shale in general dips evenly to the south although there is a small open anticline at the north end of the pit so that the beds at the north end dip gently north. No study was made of the shale under pit No. 2. The adjacent beds appear to dip to the south at 30 to 40 deg, and there are no folds or faults apparent. The shale under pit No. 4, however, is isoclinally folded. The belt of intense deformation starts abruptly at the north edge of the pit. The southern edge of the belt is less clearly defined, but appears to lie about 50 ft south of the south end of the pit. The belt of tightly folded rock extends approximately along the strike east and west for at least 500 ft in each direction. It is possible that this tight folding has resulted in a more permeable pattern of fracturing along the strike, although there is good evidence that the permeability across the strike is very low at the south end of the pit.

One conclusion is inescapable, namely, that there are likely to be important differences in the operating characteristics of pits located in topographically similar sites. A consideration of the topography can provide necessary but not sufficient conditions for the choice of a satisfactory site. Core drilling, pressure testing, and test pumping do not provide sufficient information with which to predict pit operation prior to construction and use. An alternative would be to test the pit with water before filling it with waste.[16]

Extent of Underground Dispersion

To assess the movement and dilution of the wastes from the pits and hence the safety of the operation to the environment downstream from the pits, 55 wells totaling 5500 ft have been drilled around the waste pits. From well sampling data the radioactive materials moving out of the pits have been determined to be largely Ru^{106}, with smaller amounts of the complexed ions of Co^{60} and Sb^{125}. Nitrates are predominant in the contaminated wells.

The rate of movement of wastes from pits No. 2 and No. 3 is 2 to 4 ft per day along the strike and 0.4 to 0.8 ft per day across the strike, and from pit No. 4 the rate is 10 to 30 ft per day along the strike and 0.1 to 1.5 ft per day across the strike. In Fig. 36 is shown a map of the concentration of the radionuclides in the wells surrounding the pits. The activity has spread primarily to the east and west, confirming the hydrologic and geologic findings which suggested that the most rapid movement would be along the strike of the formation. The flow out of pit No. 4, which has been the most intensively studied, indicates that south of the pit there is very little movement across the strike. Figure 37 shows this more strikingly where wells 84 and 105 are along the strike, and well 93 is across the strike. With the greatest movement of waste along the strike, a part of the activity finds its way into the two small streams draining the pit area.

The vertical pattern of the waste movement from the pits is traced by logging observation wells with the well probes shown in Fig. 38. The trailer-mounted probes consist of halogen-type G-M tubes and a preamplifier mounted in an aluminum housing. The remaining units are scintillation probes containing sodium iodide crystals, photomultiplier

[16] E. G. Struxness *et al.*, *HP Semiann. Prog. Rep. Jan. 31, 1955*, ORNL-1860, p 13–18.

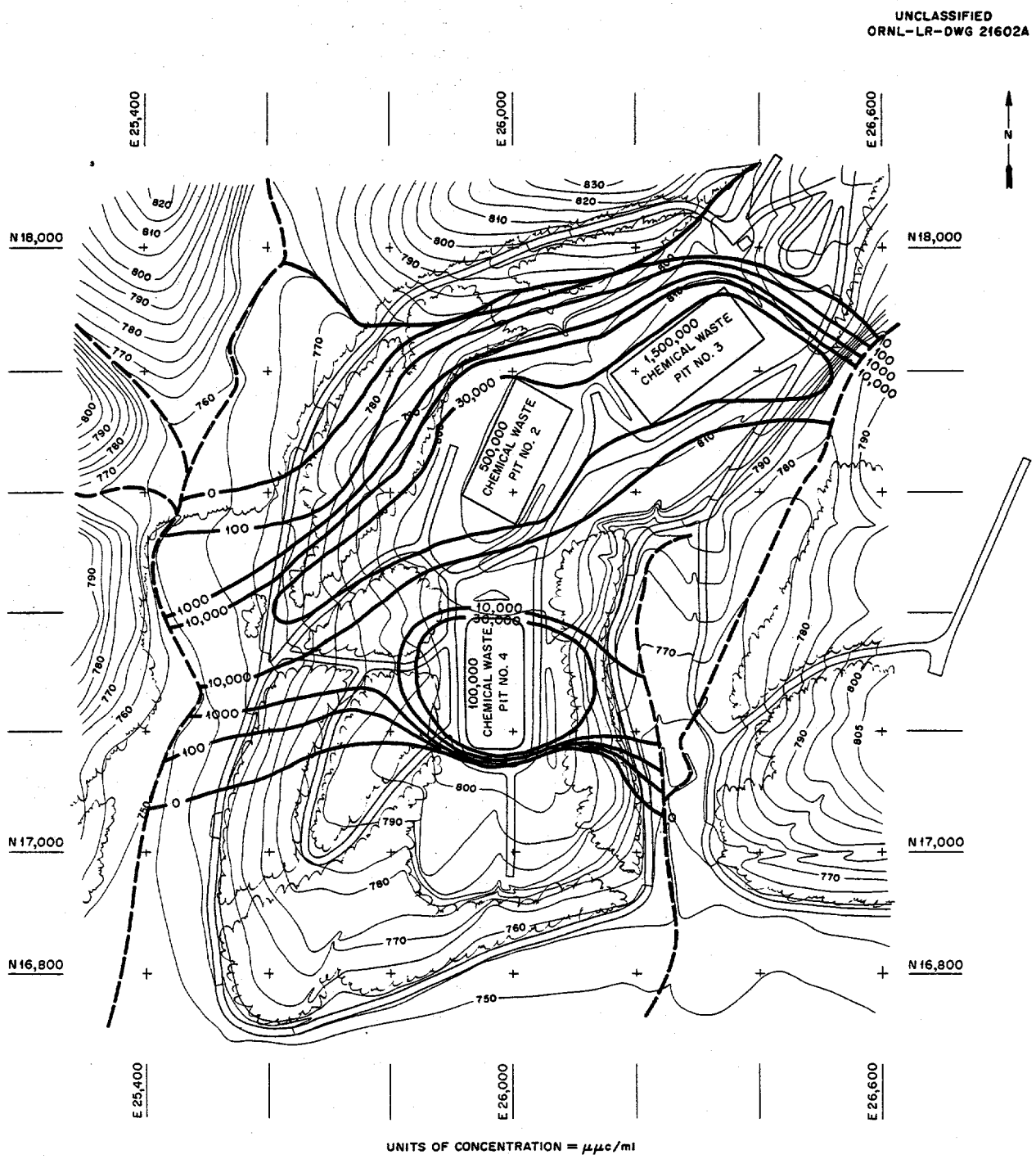

Fig. 36. Lateral Dispersion of Radioactive Wastes from ORNL Pits (Feb. 1957).

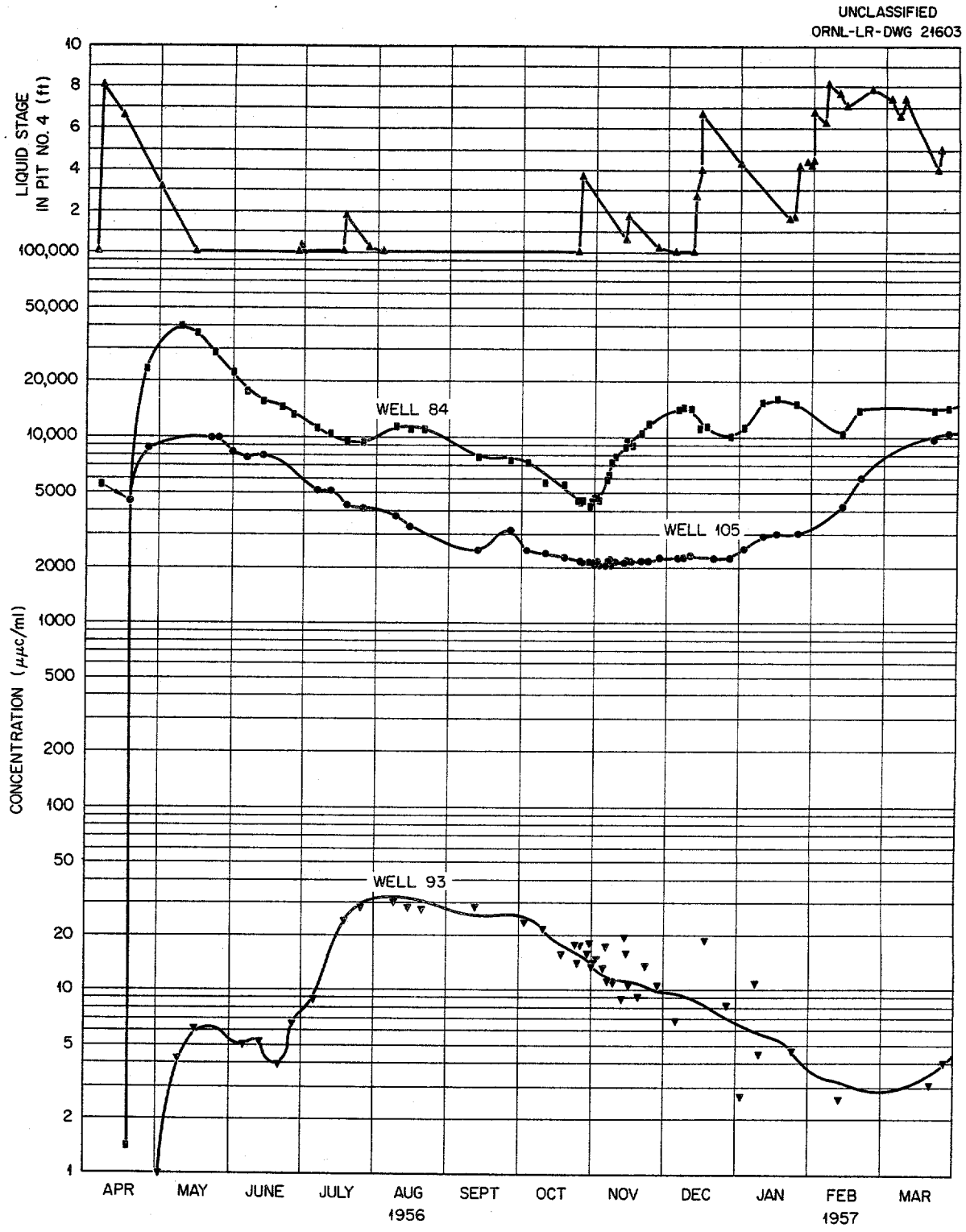

Fig. 37. Activity of Well Samples.

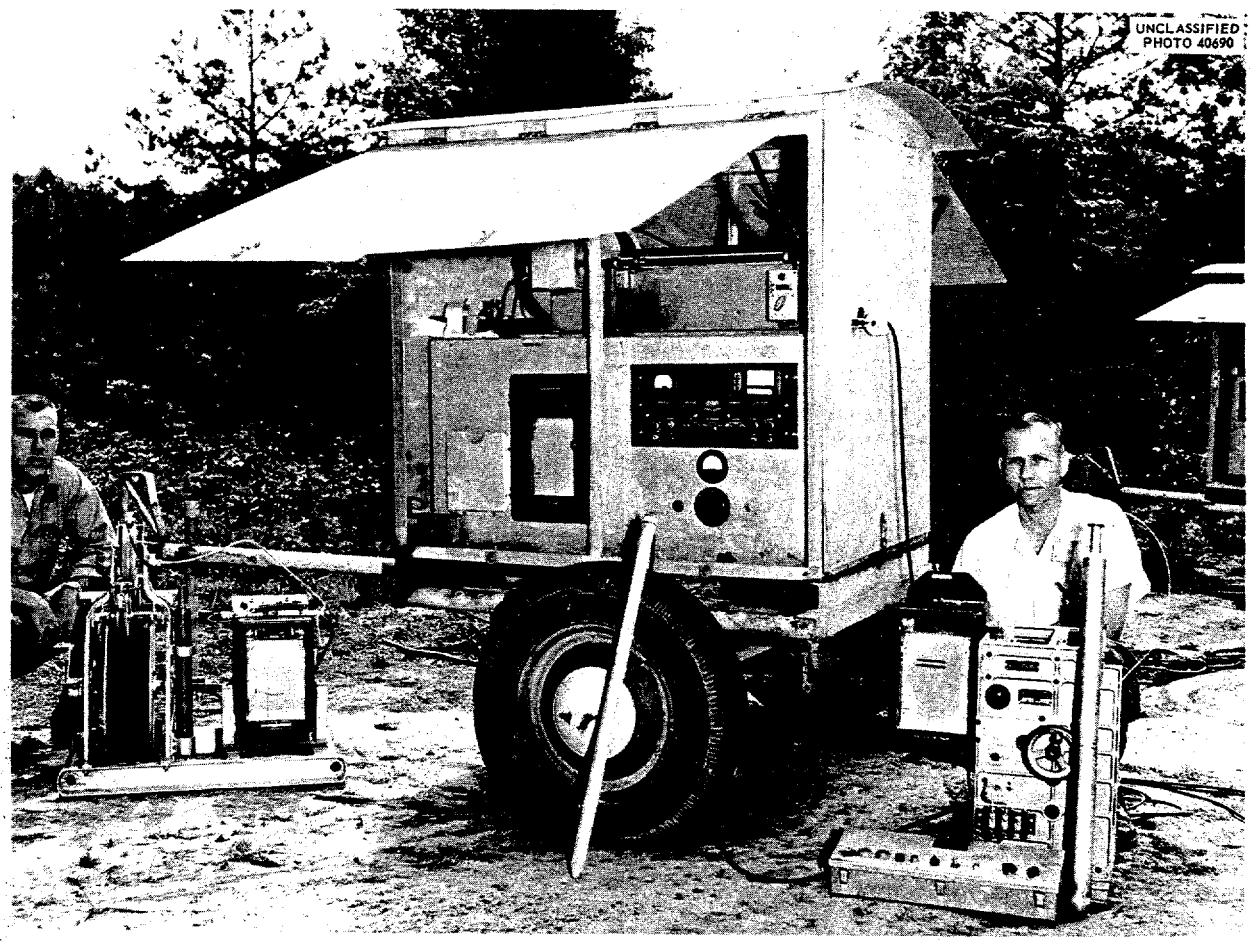

Fig. 38. Well Probing Equipment.

tubes, and pertinent electronics. The probe on the right was designed by the New York Office, AEC, and the other unit was developed by the Denver Office, U.S. Geological Survey. By calibrating the equipment in a 6-in.-dia aluminum container filled with solutions of Ru^{106}-Rh^{106}, it was determined that the sensitivity of the two scintillation units (crystal size $1\frac{1}{8}$ by $1\frac{1}{2}$ in.) and a 6-in. G-M tube was about 1×10^{-5} μc per milliliter, and a 2-in. G-M tube about 3×10^{-4} μc per milliliter.

Results of logging the grouted wells support the hypothesis that waste seeping from the pits will travel primarily through the weathered shale.[17] As shown in Fig. 39 activity penetration below pit No. 4 has virtually ceased upon reaching the more consolidated shale, a depth of 19 ft.

Disposal in Surface Streams

The rates of flow in the streams receiving radioactive contaminants are measured continuously and periodic samples are collected for analysis to determine the total transport of waste constituents. From the short-term record obtained thus far, it is noted that grab samples from the streams do not give a true picture of the amount of activity passing into the White Oak Creek system. In Fig. 40 it is observed that there is a rapid change in the concentration of activity in the streams as the flow of water changes, while the total activity per unit time remains relatively constant. The waste seeps out of the pit at a rate depending upon the liquid-level in the pit and the slope of the

[17] E. G. Struxness *et al., HP Semiann. Prog. Rep. July 31, 1956*, ORNL-2151, p 26, esp 32.

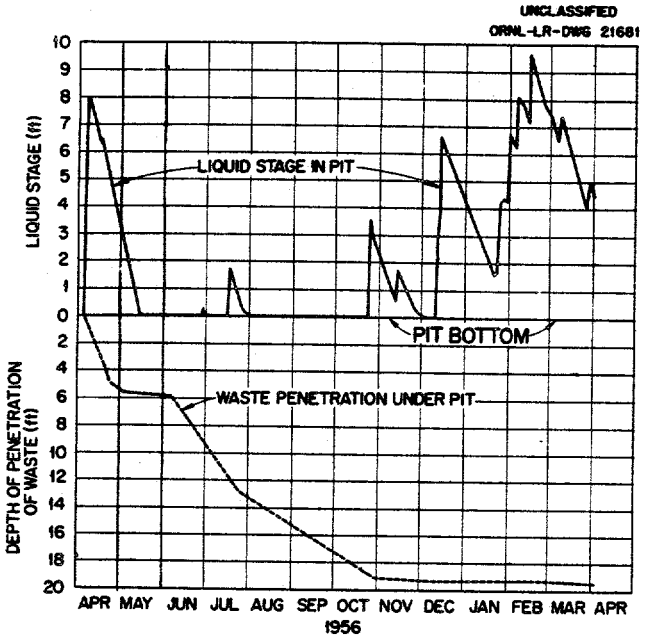

Fig. 39. Movement of Radioactive Wastes Under Pit No. 4.

water table. These change rather slowly except for overflows of waste into the pit. Therefore, it is assumed that the amount of activity entering a stream over a period of time is uniform but that the concentration changes rapidly depending upon the weather conditions and the flow in the stream.

Cesium-137 has reached the streams in quantities too minute to be detected by gamma ray spectrometry and radiochemical analysis but has been detected in trees in the immediate environs. At the present time the amount of Ru^{106} discharged from White Oak Lake and diluted in the Clinch River is less by a factor of 10^6 than the MPC value given in Handbook 52.

Selection of Future Disposal Sites

There are two factors to consider in selecting any waste disposal site: cost and safety. In Oak Ridge disposal operations to date, much basic information has been lacking and the emphasis has been on out-of-pocket costs. After some years of study and operation, there is still little information on environmental hazards, and apparently no well-considered analysis of the many factors which constitute the *total* cost. Where operations irrevocably condemn land for centuries it is not sufficient merely to consider the day-to-day operating cost. At the present time, therefore, areas selected for future disposal sites cannot be regarded as final and to so select areas is justified only because the work of the Laboratory currently required planning for land utilization.

The site requirements for safe and cheap disposal of liquid waste into seepage pits are more precise and restrictive than those for burial-ground disposal of solid waste. Therefore, the seepage pit requirements must come first. Both the burial grounds and the pits are probably safer if located in the Conasauga shale. However, since the topographic requirements for these two types of disposal are somewhat different, there should not be competition for the same land. An exception is that each operation will be cheaper and more convenient if the respective sites are located closer to the Laboratory and to such facilities as roads and power lines. Liquid wastes are transported more cheaply and more safely by pipeline than by tank truck, while solid wastes must be transported by truck in any case. Once the truck is loaded, it costs little to travel a few extra miles. The pipeline, however, is expensive to build and difficult to relocate. The seepage pits, therefore, should be located as near the Laboratory as possible and so grouped as to reduce the length of pipeline required and the number of monitoring installations. The burial grounds can be more remote and scattered.

Burial-Ground Requirements. – A good burial-ground site would be a wide area of flat well-drained land, underlain by a soil soft enough to be handled easily by earth-moving machinery and yet solid enough to stand firmly in steep cuts if necessary. It should not be subject to flooding either by surface water or by the ground water, since water is the transport medium.

Unfortunately, no such site exists in the ORNL area. All the geologic formations and soils in this area are relatively impermeable and drain so slowly that wide flat areas have poor ground-water drainage. In any large, flat area the depth to the water table, after a wet winter or spring, is likely to be so shallow as to be a hindrance to safe ground disposal.

The varying depth to water in the burial sites used so far has not been studied except at burial ground No. 3 in Bethel Valley,[18] some 3000 ft

[18] G. De Buchananne, chap. 5, "Hydrologic Features," p 5 in *Geologic Conditions at the Oak Ridge National Laboratory Area Relative to the Disposal of Radioactive Wastes* by P. B. Stockdale, ORO-58 (Aug. 1, 1951).

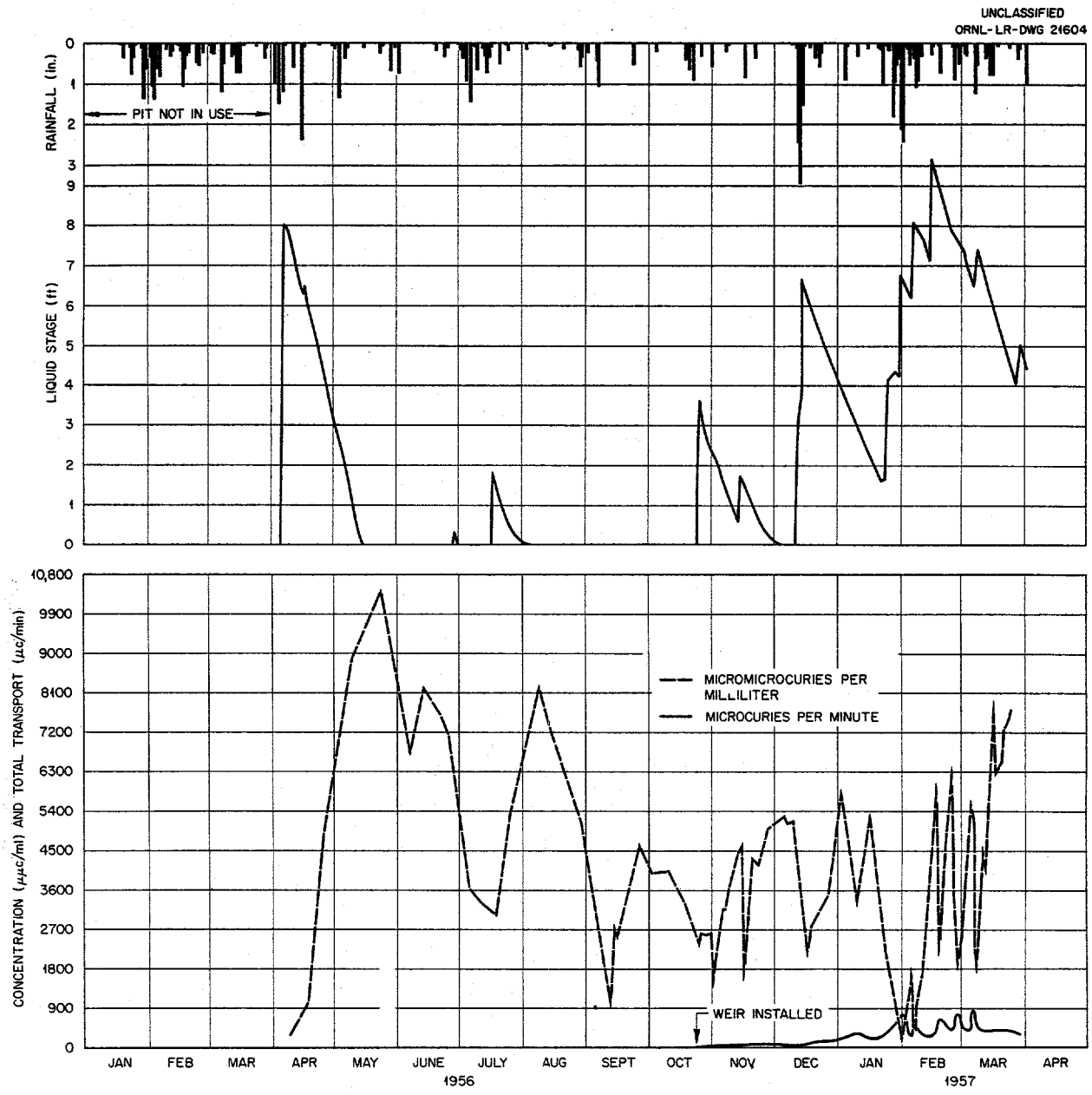

Fig. 40. Concentration and Transport of Radioactivity Past Stream-Monitoring Station.

southwest of the Laboratory area. This site was abandoned largely as a result of this study. It is probably true that this site and similar sites underlain by the Chickamauga limestone are undesirable, but this has not been proven. In particular, the magnitude and nature of the hazard have not been fully assessed to determine the suitability of such sites for the disposal of low-level solid wastes. No study has been made of the presently active burial site in shale in Melton Valley; the site appears to be better than the others abandoned and no obvious difficulties have been encountered. The Melton Valley site is considered as an operating model here and can serve as a basis for comparison. It is indicated on Fig. 41, part of a detailed topographic map of Melton Valley.

Several topographically and geologically similar areas are shown in Fig. 42. Three of these are in the same belt of shale, area A is at the head of Melton

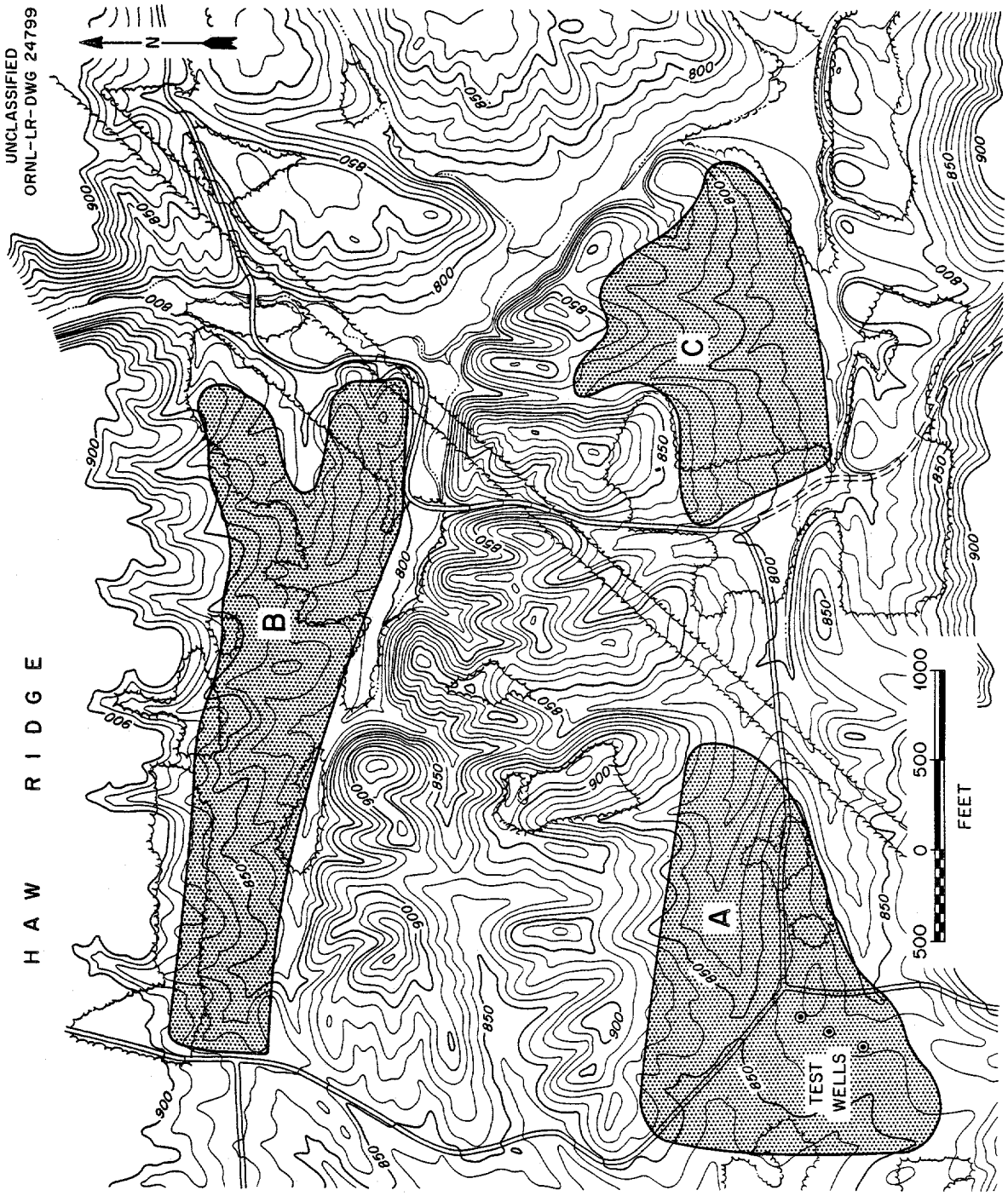

Fig. 41. Operating Disposal Sites and Suggested Areas for Radioactive-Waste Disposal.

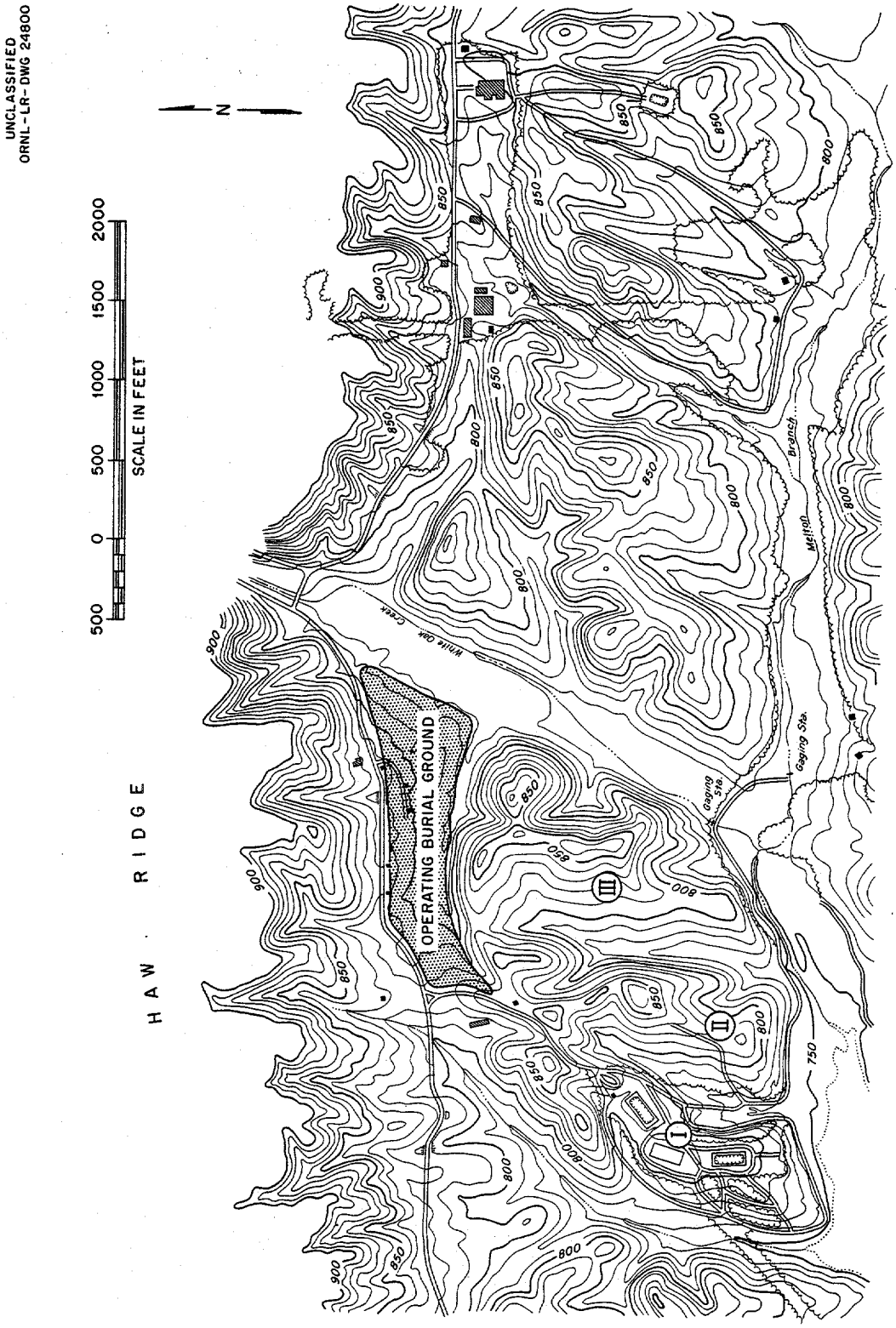

Fig. 42. Suggested Areas for Disposal of Liquid and Solid Radioactive Wastes.

Valley and extends over into the head of Bearden Creek, areas B and C are entirely in the valley of Bearden Creek. Three test wells were put down in area A about two years ago when the site was under consideration for the disposal of liquid wastes. In the spring, the depth to water in these wells is about 10 ft so that seepage pits could not be operated easily, but much of the area might be suitable for a burial ground if shallow trenches were used. More wells and observations would be needed here to determine the limits of prudent operation and also to determine the nature and thickness of the soil cover. The Conasauga shale in this area is more calcareous than under the present burial ground and shallow beds of limestone may restrict the depth of trenches. Area B lies to the north and is probably underlain by the same red noncalcareous shale as the present burial ground. The western end is steeper than the land presently in use and may be a little less convenient to work. The eastern end is relatively flat and, in part, poorly drained. Area C appears to be most similar to the site of present operations, although the shale is probably somewhat more calcareous.

These are the best sites in the belt of Conasauga shale located south of the Laboratory. A modest study of all three areas would furnish information of considerable value. Burial operations in these areas would require stream gaging and sampling on lower Bearden Creek, since their drainage does not go into the presently monitored water at White Oak Lake. Continued operation in the White Oak Lake drainage area would also be desirable in that the lake provides an element of safety. The safety features of the lake, however, are of more value to control a sudden release of liquid from a tank or seepage pit, and are not an important factor in the selection of a site for burial of solid wastes. Another objection to the use of the water shed of Bearden Creek is the need to keep this unique area free of contamination so that extended ecological studies will be possible.

The largest potential-burial ground area, however, is in another belt of the Conasauga shale north of the Laboratory in Bear Creek Valley. There is a large area here topographically suitable for burial of solid waste, and the water table in this valley should be studied to define the extent of usable ground.

Geologically, the practice of digging trenches is not good, as it lowers the solids toward the water table and places them in a poorly drained, but still leaky tank. The solid wastes soak in a mixture of ground water and rain water for much of the winter, but are left high and dry in the fall when the water table drains down. The adsorptive capacity of the soil for virtually all of the fission products is so great that the method may be quite safe, but there appears to be some justification for a study of other methods than trench burial. Any resulting change in burial practice might change the requirements for burial-ground site selection.

ORNL Seepage Pit Requirements. – Seepage pits for the disposal of intermediate-level liquid waste have been in operation in Melton Valley for several years, and despite their many defects, will have a limited but valuable function for some time to come. Study of the present pits has suggested valid criteria for the selection of future sites.

The Conasauga shale appears to be the only local formation that should be considered for liquid waste disposal. The reasons for this have been given at length elsewhere.[19] The present pits are in the gray calcareous shale of the Conasauga formation. Pits located in the red noncalcareous shale or in mixed limestone and shale will have somewhat different operating characteristics.

The pits should be located in areas where the normal depth to the water table is 30 or 40 ft. Where this depth is less, 15 to 20 ft, it is unlikely that the rate of seepage will be rapid enough to make the cost of the operation attractive. This depth-to-water requirement is best met on the crests of ridges running south into Melton Valley from Haw Ridge on the north. The length of the pit should extend from northwest to southeast across the strike of the shale so as to cut the maximum number of bedding planes. The slope of the sides of the ridge should not be so steep as to intercept the uplifted water table which will extend out from the pit after it is in operation. A side-hill slope of 20 ft in 100 is perhaps the limit for safe operation, and a slope of 30 ft in 100 has

---

[19] W. de Laguna, *Sanitary Engineering Aspects of the Atomic Energy Industry. A Seminar Sponsored by the AEC and the Public Health Service, Held at the Robert A. Taft Engineering Center, Cincinnati, Ohio, Dec. 6–9, 1955*, TID-7517(Pt. Ib), p 426–456.

been known to lead to trouble; this value, however, will vary from site to site, and each pit should be tested with water as it is built. Construction and operation will be easier if the top of the ridge is flat. A sloping ridge crest will require modification of the present simple pit design.

A part of the Melton Valley topographic map is shown in Fig. 41. The present operating pits are shown at I. The next ridge to the east, II, will probably be the site of the next disposal pit. The topography here is favorable, and four test wells have shown a depth to the water table of about 40 ft. Still farther east, ridge III is also topographically suitable, although the steep eastern slope may require that the pit be located 50 or 100 ft west of the ridge crest. East of White Oak Creek there are several suitable ridges, although test wells and a study of ground-water conditions would be required before any decision could be made. East of the area shown in Fig. 41 the topography is less favorable and the pits would have to be smaller and more scattered. Present understanding of the problem suggests that the best area for waste disposal pits extends about 2 miles east of the present operating pits. The results of studies to date suggest that this area should be reserved for future disposal of intermediate-level liquid waste.

RADIATION DOSIMETRY

G. S. Hurst

DOSIMETRY APPLICATIONS

C. C. Sartain J. A. Auxier
G. S. Hurst
Health Physics Division

T. V. Blosser
ORNL Applied Nuclear Physics Division

Ichiban Project

Introduction. – The ultimate objective of the Ichiban Project[1] is the determination of the absorbed doses of fast neutrons and gamma radiation received by survivors of the nuclear bombing of Hiroshima and Nagasaki. The Atomic Bomb Casualty Commission (ABCC) has accumulated a large amount of medical data in Hiroshima and Nagasaki over a ten-year interval, and has been conducting investigations of the location of survivors, which, with the new techniques of dosimetry for nuclear tests developed at ORNL,[2] should make possible the dose evaluation for many of the survivors. Because the tolerance of man to radiation has been based almost entirely on data for radiation effects on animals, the normalization of these data to man is extremely important, and the atomic bomb survivors offer by far the best existing means for such normalization.

In the spring of 1956 a survey team was formed and sent to Japan to study Japanese building practices and the records of the ABCC in order to determine the feasibility of the dose evaluation. The team included representatives of ORNL, US-AEC, USAF-SAM, and LASL. The team findings were most encouraging and the Ichiban Project was initiated.

Determination of Angular Distribution of Weapons Radiation. – An important basic step in the determination of the dose received by A-bomb survivors is the measurement of the angular distribution of the radiation from nuclear devices as a function of distance from the explosion. This step is necessary for determining shielding by any structure, and is especially important when many structures are closely spaced as they are in Japanese cities.

A system of collimators for field use was designed and tested in the Laboratory before its construction on a field scale. Over-all considerations led to the design shown in Figs. 43 and 44. This system employs a water-tank unit which is basic to both neutron and gamma measurements and into which appropriate inserts are placed: lead inserts for gamma collimation, and water-containing inserts for fast neutron collimation. Inserts were also made in more than one angular opening. The water tank is necessary for the gamma collimators in order to prevent the fast neutrons from reaching the lead and producing gamma rays, by inelastic scattering, which would lead to spurious results, particularly for the case of small solid angles subtended in a direction away from the blast.

The neutron collimators were tested in the Laboratory by using Po-Be sources and the absolute tissue dosimeter.[3] The gamma units were tested with Co^{60} sources and the SID.[4] A technical report of the collimator tests performed in the Laboratory is being prepared.

The production collimators were sent to the Nevada Test Site (NTS) for the 1957 summer test series where successful measurements are in progress; however, sufficient data for presentation are not available at this time.

Radiation Attenuation by Japanese Houses. – Attenuation measurements on existing Japanese houses have been made by ORNL personnel in conjunction with work of the Liaison Pool (see "Liaison with ABCC," this report). These measurements were "poor slab geometry" and were made with a radium-gamma source and a Landverk electroscope. The averages of many determinations are listed in Table 59 and include attenuation measurements made on roofs, inside walls, and exterior walls. Not shown here are

[1] A joint ORNL, USAF-SAM, AEC, LASL Program. The word "Ichiban" is Japanese for "A," "No. 1," "The most," "Greatest."

[2] G. S. Hurst *et al.*, *Rev. Sci. Instr.* 27, 153–156 (1956).

[3] G. S. Hurst, *Brit. J. Radiol.* 27, 353–357 (1954).

[4] J. A. Auxier, G. S. Hurst, and R. E. Zedler, *The Single Ion Detector for Gamma Dosimetry in Mixed Fields of Fast Neutrons and Gamma Rays* (to be published).

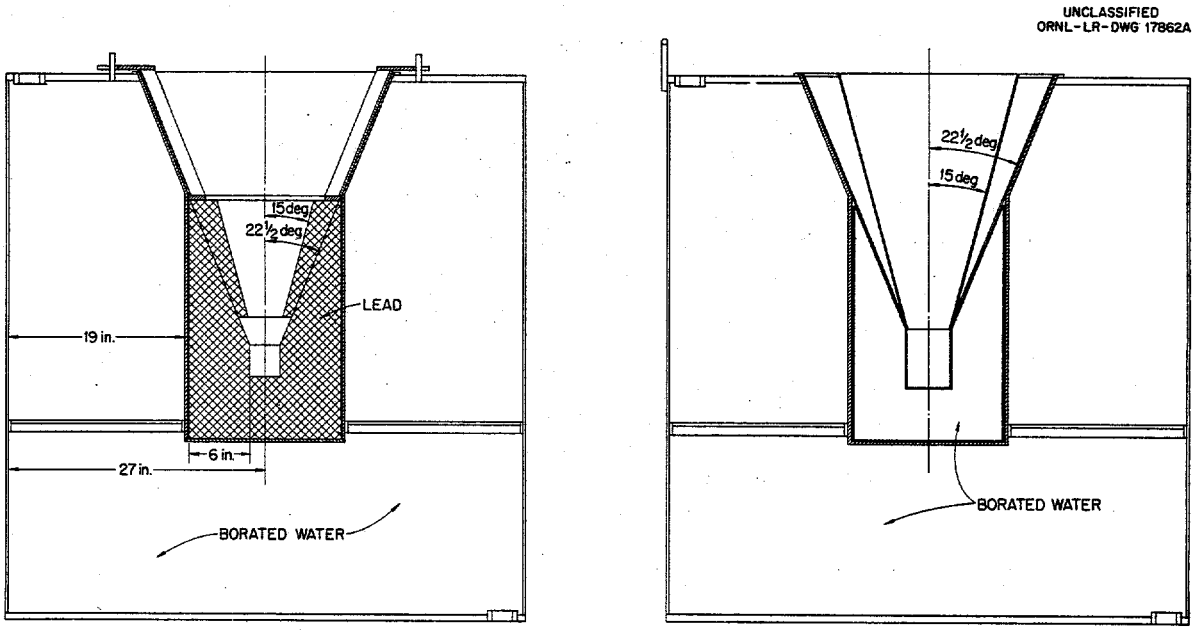

Fig. 43. Cross-sectional View of Collimator with Gamma and Neutron Inserts.

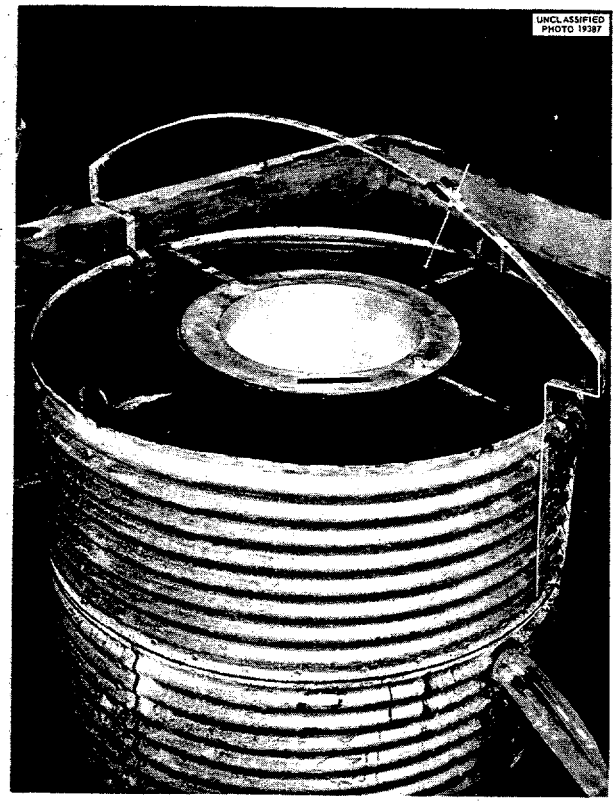

Fig. 44. Laboratory Prototype for Testing Purposes.

Table 59. Radium Gamma Attenuation by Japanese House Components

Components	Attenuation for Ra γ (%)	
	Hiroshima	Nagasaki
Outside walls	18	22
Inside walls	24	22
Standard tile roof	20	31
Concrete tile roof	13	
Thatched roof	7	

several miscellaneous measurements, including those for thin (1.6 mm) glass doors and windows and for paper doors, all of which provide sensibly zero attenuation for gamma radiation.

Some attenuation measurements are under way in the field (NTS) using the collimators. Plane slabs of building materials are in some cases placed over the collimator openings in order to determine attenuation factors. Radiation shielding by light frame structures will also be determined on a limited scale.

Further attenuation measurements are also under way in the Laboratory. A mockup of a house wall is being studied for neutron attenuation, since it was most inconvenient to attempt this measurement in Japan. This study has not progressed far enough for the data to be presented here.

A program is being planned for more comprehensive shielding studies of Japanese type houses and components. This study should be made at the Tower Shielding Facility at ORNL in early 1958, after the NTS data have been analyzed. Such a study would be especially useful in that any angular distribution found in the field studies could be mocked up rather readily at that facility, and comprehensive dosimetry accomplished for both neutrons and gamma radiation with much greater economy and convenience than at NTS.

Liaison with ABCC. – In order to realize the objectives of the Ichiban Program, the dosimetry data which are accumulated through experimentation and calculation must be closely coordinated with the medical records of the ABCC. In order to effect this communication, there has been established a Liaison Pool which has, in addition to communication, the following specific objectives:

ABCC records should be reviewed so that
1. data can be obtained on buildings and shielding,
2. location and fate of individuals in buildings can be determined,
3. medical facts may be obtained for correlation with absorbed dose,
4. expansion of the ABCC Shielding Survey Program can be recommended when desirable.

Bomb-burst data should be collected on the following:
1. burst height (with error),
2. location of ground zero (with error),
3. weather conditions at time of burst, including temperature, humidity, atmospheric pollution, and barometric pressure.

Three-dimensional pictures, from stereophotographs and other sources, should be used so that the extent, if any, to which multiple shielding of one house by another altered the spectrum and reduced the quantity of radiation absorbed by individuals located indoors.

Physical measurements on existing houses should be performed so that average values, with standard deviations, of the following quantities can be determined:
1. density of roof material,
2. thickness of roof material,
3. density of wall material,
4. thickness of wall material,
5. mass absorption coefficient of wall material,
6. mass absorption coefficient of roof material.

Dosimetry and biostatistics should be correlated.

These objectives are being accomplished with considerable success. Most of the attenuation measurements to be done in Japan, the weather data, and burst locations have been made and/or analyzed satisfactorily. The important "three-dimensional" conception of the two cities just before the bombings has been emphasized to the ABCC shielding group and some drawings have already been made which demonstrate the feasibility of making such drawings for the area containing most of the exposed population. These drawings are based on prebombing and postbombing aerial photographs, on the sketches in the shielding histories, and on interviews with survivors concerning their immediate neighbors. Various checks were devised to estimate the reliability of the interview histories and the Liaison Pool personnel were surprised at the vividness and conciseness of the accounts of the situations at the time of bombing; situations which had to be recalled after some 12 intervening years.

The high quality of the data collected by the ABCC and the splendid cooperation of the group gives assurance of project success.

PHYSICS OF TISSUE DAMAGE

H. P. Yockey

In recent years the discovery has been made that the biochemical specificity of proteins is carried, largely at least, in the exact order of 20 amino acid residues. This specificity is believed to be under genetic control recorded in the exact order of four kinds of nucleotides in deoxyribonucleic acid (DNA). Gamow was the first to realize that such a situation has vast resources of mathematical problems and possibilities. He attempted to solve the problem of finding the code which related the 4-letter DNA alphabet and the 20-letter protein alphabet. This has not yet been done satisfactorily, partly because of the small number of protein sequences known.

This discovery leads to further possibilities of treating the living organism as a communication system by applying ideas, recently developed by Shannon,[5] which compose a new mathematical discipline; namely, information theory. The role of noise in the genetical specificity message and its relation to survival has been investigated in this laboratory. It has been shown that it is possible to give a general treatment of survivorship from this point of view.

These considerations lead to the notion that death is the result of decay of information content in the DNA of a cell. That is, it is not so much the destruction of a molecule as the destruction of its ability to carry genetical specificity that leads to death. The agent by which this is accomplished assumes a role of secondary importance.

A symposium on information theory in Health Physics and Radiobiology was held in Gatlinburg, Tennessee, October 29–31, 1956. The papers contributed at this meeting, as well as those stimulated by it, will be published by Pergamon Press.

The program with the Clevite Research Center was initiated by a pilot experiment. Suitable cuts of Rochelle salt, $(NH_3)\ H_2PO_4$ (ADP), KH_2PO_4 (KDP), and $NaClO_3$ were prepared. The frequency constant and the dielectric constants were measured at Clevite. Samples of these crystals were irradiated at low temperature in the LITR and returned at room temperature to Clevite. Definite changes in these constants were found and the proper range for irradiation time was determined.

The principal experimental difficulty rested in the problems involved in remounting the crystals. Accordingly, holders have been designed and are being built which will hold the crystal during the entire course of its use.

Clevite is currently preparing suitable cuts of crystals of the above materials for lower temperature irradiation and annealing studies. The crystals will be irradiated at ORNL at low temperature and returned at low temperature to Clevite for measurements during annealing to destruction (i.e., 250°C for $NaClO_3$).

[5]C. E. Shannon, *Mathematical Theory of Communication*, University of Illinois Press, Urbana, 1949.

THEORETICAL PHYSICS OF DOSIMETRY

J. Neufeld R. H. Ritchie
W. S. Snyder

Validity of the Bohr-Lamb Criterion

The Bohr-Lamb criterion[6] is based on the assumption that an ion when passing through matter is stripped of all its orbital electrons that have velocities smaller than the translational velocity of the ion. This criterion is not based on any rigorous theoretical arguments and its order of accuracy has never been determined, partly because it was correlated with statistical atomic models which represent merely a rough approximation.

In this investigation an attempt has been made to establish the possible accuracy of the Bohr-Lamb criterion by using, instead of a statistical model, the very reliable data on ionization potentials of various ions obtained by Lisitzin.[7] The Lisitzin data are based on a study of various sequences of isoelectronic systems and provide values for electronic orbital velocities that are of a relatively high order of accuracy. These values have been used in order to correlate the Bohr-Lamb criterion with experimental data. The results show that the Bohr-Lamb criterion is only applicable to fission fragments and not to lighter ions. In order to remedy this situation, the procedure suggested by Knipp and Teller[8] was followed, and two empirical parameters, γ_L and α_L, were introduced. They are defined as follows:

$$\gamma_L = \frac{v_L}{V}, \qquad \alpha_L = \frac{Z_L^{*(1)}}{Z_{av}^*},$$

where V and Z_{av}^* represent the velocity and the average charge of a moving ion; v_L is the velocity of the most loosely bound electron having a binding charge $Z_L^* = Z_{av}^*$, and Z_L^* is the binding charge that corresponds to the most loosely bound electron having velocity $v_L = V$. (The values v_L and $Z_L^{*(1)}$ have been determined from graphs based on the computations of Lisitzin.)

[6]N. Bohr, *Phys. Rev.* 58, 654 (1940); W. E. Lamb, Jr., *Phys. Rev.* 58, 696 (1940).

[7]E. Lisitzin, *Soc. Sci. Fennica, Commentationes Phys.-Math.* 10, No. 4 (1940).

[8]J. Knipp and E. Teller, *Phys. Rev.* 59, 659 (1941).

The numerical values of γ_L and α_L corresponding to all available measurements of ions of various velocities were determined. The results fail to show any regularity in the behavior of these parameters as a function either of the ionic species, or of the ionic velocity, or of the surrounding medium. After a survey of the literature covering the last 16 years has been made, no definite opinion regarding the accuracy of the Bohr-Lamb criterion has been reached. This may be due to the paucity of experimental data or to the lack of uniformity in the quality of various measurements made on ionic charges and velocities.

A Quantum Theory of the Dielectric Constant

In order to treat the complex many-body problem of the interaction of conduction electrons in solids Lindhard[9] and Hubbard[10] have independently developed a quantum theory of the dielectric constant of metals. Their treatments are essentially semiclassical in that they treat the electric field in the medium as classically prescribed, although the electronic motion in the solid is treated by quantum perturbation theory.

The present work is concerned with a generalization of the work of the above-mentioned authors, in which the concept of a prescribed field is unnecessary, and the interaction of charged particles with the plasma is made consistent in the sense of first order perturbation theory. The generalization allows one to treat very simply such problems as the interaction of fast electrons with plasma electrons and the correlation energy of electrons in plasma. The second topic will be treated in a subsequent paper, while results for the first one will be given here.

[9] J. Lindhard, *Kgl. Danske Videnskab, Selskab, Mat.-fys.* 28, No. 8 (1954).

[10] J. Hubbard, *Proc. Phys. Soc.* (*London*) A68, 976 (1955).

[11] D. Bohm and D. Pines, *Phys. Rev.* 92, 609 (1953).

The very elegant field quantization methods of Bohm and Pines[11] have been applied to plasma problems by Bohm and Pines, and by others. However, inherent in their approach is a wave-vector cutoff procedure, that is, a mathematical device which divides the region of collective interaction of plasma electrons from the region of individual interactions. Separate treatments are necessary in the two regions. In the present theory collective and individual interactions are treated on an equal basis, and the wave-vector cutoff treatment is unnecessary.

The Hartree one-particle wave equation for the ith electron in the plasma may be written

$$(1)\quad [H_0 - e\phi(\vec{r},t)]\,\psi_i(\vec{r},t) = i\hbar\frac{\partial}{\partial t}\psi_i(\vec{r},t)\ ,$$

where ϕ is the self consistent electric field in the medium[11] and H_0 is the unperturbed hamiltonian. (In this treatment all electronic motion is assumed to be non-relativistic so that only the instantaneous coulomb field need be considered.) Since first-order perturbation theory is employed throughout this theory, it may be assumed that an external field will induce transitions in the plasma and that the electric field due to these transitions will be proportional to the inducing field. Hence, the $\vec{k},\omega$ Fourier component of an external charge density $q(\vec{r},t)$ may be written

$$(2)\qquad \epsilon_{\vec{k}\,\omega}\, k^2 \phi_{\vec{k}\,\omega} = 4\pi q_{\vec{k}\,\omega}\ ,$$

which is a generalization of Poisson's equation. This equation will be taken as the definition of the generalized dielectric constant $\epsilon_{\vec{k}\,\omega}$.

The wave function of the ith electron in terms of free electron momentum eigenfunctions is now expanded and solved for the coefficients of the expansion by first-order time-dependent perturbation theory.

For an incident electron of momentum k_i, the probability of interaction, $d\tau$, per cm of path in the plasma is

$$(3) \qquad d\tau = \frac{m^2 e^2 k_f}{\pi \hbar^3 k_i} \frac{d\Omega}{k^2} \operatorname{Im}\left(\frac{1}{\epsilon^*_{\vec{k}\omega}}\right), \quad \left| \begin{array}{l} \vec{k} = \vec{k}_i - \vec{k}_f \\ \omega = \dfrac{\hbar}{2m}(k_i^2 - k_f^2) \end{array} \right.$$

where $\vec{k}_f$ is the final momentum of the incident electron, and $d\Omega$ is an element of solid angle about the direction of the final momentum vector. The interaction probability $d\tau$ is a function of θ, the angle between $\vec{k}_i$ and $\vec{k}_f$, and $\hbar\omega$, the energy lost in the interaction.

Within the approximation of small damping and for an incident electron whose velocity is large compared with the maximum Fermi velocity in the gas, the imaginary part of the dielectric constant of a degenerate Fermi-Dirac electron gas may be written,

$$(4) \qquad \operatorname{Im}\left(\frac{1}{\epsilon^*_{\vec{k}\omega}}\right) = \frac{\gamma\omega_p^2\omega}{\left[\omega^2 - \left(\omega_p^2 + \dfrac{\hbar^2k^4}{4m^2} + \dfrac{3\hbar^2}{5m^2}k_f^2k^2\right)\right]^2 + \gamma^2\omega^2},$$

where k_f is the maximum Fermi momentum in the plasma, and γ is the damping constant. This term shows a sharp resonance when the energy loss, ΔE, has the value

$$\Delta E = \hbar\omega_{res},$$

where

$$\omega_{res}^2 = \omega_p^2 + \frac{3}{5}\frac{\hbar^2}{m^2}k_f^2k^2 + \frac{\hbar^2}{4m^2}k^4,$$

which is the relation between energy loss and momentun transfer which was found experimentally by Watanabe[12] and was explained on the basis of plasma dispersion by Watanabe and Kanezawa. We may now integrate over ω and find

$$(5) \qquad d\tau(\theta) = \frac{me^2\omega_p^2}{2\pi\hbar^3}\frac{k_f}{k_i}\frac{d\Omega}{k^2}\frac{1}{(\omega_{res})},$$

[12]H. Watanabe, *J. Phys. Soc. Japan* 11, 112 (1956).

where

$$k^2 = k_i^2 + k_f^2 - 2k_i k_f \cos\theta ,$$

and

$$k_i^2 = k_f^2 + \frac{2m}{\hbar}(\omega_{res}) ,$$

which agrees with the result obtained by the author[13] using a semi-classical impact treatment which is valid when $\theta \ll 1$.

Now when the momentum loss $\hbar k$ is large compared with all initial momenta in the plasma, it may be shown that

$$\text{(6)} \qquad \text{Im}\left(\frac{1}{\epsilon^*_{\vec{k}\omega}}\right) = \frac{\gamma\omega_p^2\omega}{\left(\omega^2 - \frac{\hbar^2k^4}{4m^2}\right)^2 + \gamma^2\omega^2} .$$

Substituting this into Eq. 3 and using the conservation of energy and momentum we find

$$\text{(7)} \qquad d\tau = \frac{8\pi Ne^4}{m^2v^4}\,\frac{\cos\theta\, d\theta}{\sin^3\theta} ,$$

which is just the formula for Rutherford scattering of electrons on free electrons expressed in a reference frame in which the struck electrons are initially at rest.

It is of some interest to treat the case of the dielectric constant of an assembly of isolated one-electron atoms such as hydrogen gas with the density low enough so that the overlap of electrons on different atoms can be ignored. If it is assumed that only longitudinal electric forces are operative, it may be shown that the dielectric constant is

$$\text{(8)} \qquad \epsilon_{\vec{k}\omega} = 1 + \frac{m\omega_0^2}{\hbar k^2}\sum_n \frac{2\omega_{0n}\left|\left\langle e^{i\vec{k}\cdot\vec{r}}\right\rangle_{0n}\right|^2}{\omega_{0n}^2 - (\omega + i\gamma)^2} ,$$

where

$$\omega_0^2 = \frac{4\pi Ne^2}{m} ,$$

N is the atomic density in the medium,

$\left\langle e^{i\vec{k}\cdot\vec{r}}\right\rangle_{0n}$ is the matrix element for the $0 \longrightarrow n$th transition,

ω_{0n} is the frequency associated with this transition.

This is a simple generalization of the Kramer-Heisenberg formula. Calculating the interaction probability of a fast electron of initial velocity v and final momentum k_f, we find that the energy loss associated with the $0 \longrightarrow n$ transition occurs at the value

[13] R. H. Ritchie, *Phys. Rev.* 106, 874 (1957).

$$\Delta E = \hbar\omega_{res} = \hbar\left(\omega_{0n}^2 + \frac{2m\omega_0^2\omega_{0n}}{\hbar k^2}\left|\left\langle e^{i\vec{k}\cdot\vec{r}}\right\rangle_{0n}\right|^2\right)^{1/2}, \tag{9}$$

which shows a shift in energy loss due to coulomb interactions between atoms in the medium. When the momentum change $\vec{k}$ of the incident electron is large the second term is small compared with the first. Then the energy loss is just $\hbar\omega_{0n}$, the value appropriate to an isolated atom. The angular distribution in this case becomes

$$d\tau(\theta) = \frac{m^2e^2\omega_0^2}{\pi\hbar^3 v}\frac{k_f\,d\Omega}{k^4}\left|\left\langle e^{i\vec{k}\cdot\vec{r}}\right\rangle_{0n}\right|^2, \tag{10}$$

which is just the Born approximation for the scattering of fast electrons by isolated atoms.

When the momentum change $\vec{k}$ is not so large that the second term may be neglected, we may write

$$d\tau(\theta) = \frac{m^2e^2\omega_0^2}{\pi\hbar^3 v}\frac{k_f\,d\Omega}{k^4}\frac{\omega_{0n}\left|\left\langle e^{i\vec{k}\cdot\vec{r}}\right\rangle_{0n}\right|^2}{\omega_{res}}. \tag{11}$$

If k is so small that only the first term in the expansion of the matrix element is important, we may write

$$d\tau(\theta) = \frac{me^2\omega_0^2}{2\pi\hbar^2 v}\frac{k_f\,d\Omega}{k^2}\frac{f_{0n}}{\sqrt{\omega_{0n}^2 + f_{0n}\omega_0^2}}, \tag{12}$$

where f_{0n} is the oscillator strength of the $0 \longrightarrow n$th transition. This formula is identical with one which may be derived by classical methods[12] and leads to a formula which may be written for small scattering angles θ in the form

$$d\tau(\theta) = \frac{e^2}{2\pi\hbar v^2}\frac{\omega_0^2 f_{0n}}{(\omega_{0n}^2 + f_{0n}\omega_0^2)^{1/2}}\frac{d\Omega}{\left[\theta^2 + \frac{1}{\omega_E^2}(\omega_{0n}^2 + f_{0n}\omega_0^2)\right]}, \tag{13}$$

where ω_E is $mv^2/2\hbar$.

If the expansion of the matrix element of the exponential function is carried to the next order in k^2, a parabolic connection between energy loss and angular deviation of the incident electron is found, just as in the plasma case.

EXPERIMENTAL PHYSICS OF DOSIMETRY

R. D. Birkhoff H. H. Hubbell
T. E. Bortner W. G. Stone
J. S. Cheka
Health Physics Division

R. L. Blanchard L. W. Johnston
AEC Fellows in Radiological Physics

Electron Attachment in Mixtures Containing Oxygen

O_2-N_2 Mixtures. – For the case of O_2-N_2 mixtures, it has been reported[14] that α, the probability of electron capture per cm of travel and per mm Hg of O_2 pressure, depends on the pressure of O_2 and the pressure of N_2. The empirical results are described by the following equation:

$$\alpha_e = Af_1P + Bf_2P + Cf_1Pf_2P,$$

where f_1P is the pressure of O_2, f_2P is the pressure of N_2, and A, B, and C are experimentally determined constants.

In order to explain the above pressure dependance the following model was postulated. The first step is the formation of O_2^{-*} (vibrationally excited O_2^-) according to the reaction,

$$O_2 + e^- \longrightarrow O_2^{-*}$$

The O_2^{-*} may be stabilized by any of the reactions:

(1) $O_2^{-*} \longrightarrow O_2^- + h\nu$

(2) $O_2^{-*} + O_2 \longrightarrow O_2^- + O_2^*$

(3) $O_2^{-*} + N_2 \longrightarrow O_2^- + N_2^*$

(4) $O_2^{-*} + O_2 + N_2 \longrightarrow O_2^- + O_2^* + N_2^{-*}$

or the electron may be spontaneously re-emitted by the reaction,

$$O_2^{-*} \longrightarrow O_2 + e^-$$

Assigning life times λ_1 and λ_2 to reactions (1) and (5) respectively, and rate constants C_1, C_2, and K for reactions (2), (3), and (4) respectively, it is seen that α depends on pressure as follows:

$$\alpha_T = \left(\frac{\lambda_1 + C_1f_1P + C_2f_2P + Kf_1Pf_2P}{\lambda_1 + C_1f_1P + C_2f_2P + Kf_1Pf_2P + \lambda_2} \right) \times \beta$$

where β is the cross section for the formation of O_2^{-*} by electron impact. At low pressures λ_2 predominates in the denominator and if λ_1 has the particular value 0, the equation for α_T reduces to the form required by experiment α_e. At high pressure $\alpha_T \longrightarrow \beta$, that is, α is independent of pressure. From the data, $(C_1/\lambda_2)\beta$, $(C_2/\lambda_2)\beta$, and $(K/\lambda_2)\beta$ can be determined. The theory of Bloch and Bradbury[15] gives $\lambda_2 = 10^{10}$ sec^{-1}, and the experiments of Bradbury[16] may be tried for β since in his work he found α to be pressure independent. Using these results one may calculate C_1 and C_2, and these may be translated to cross sections by means of the equations,

$$C_1 = n\sigma_1 v \text{ and } C_2 = n\sigma_2 v,$$

where n is the number density of molecules at 1 mm Hg pressure, σ_1 and σ_2 are cross sections in cm^2, and v is the mean velocity of the O_2^{-*} ion. The results for various values of E/P (v·cm^{-1}·mm^{-1}) are compiled in Table 60.

The major difficulty of the above model is in the values of σ_1 which are some 100 times a gas kinetic cross section. This large value may be because of incorrect values for either λ_2 or β. Further experimentation to attempt to find β is in progress.

O_2-Argon Mixtures. – Values of α for O_2-A mixtures are shown in Fig. 45. This behavior of α can be understood without difficulty. The attachment reaction which is involved is

$$O_2 + e \longrightarrow O^- + O$$

since in argon at these E/P values the electron energy is great enough to dissociate the O_2 molecule (dissociation energy of O_2 is 5.09 v, appearance of O^- is energetically possible at electron energy of 3.1 v).[17]

---

[14] G. S. Hurst *et al.*, *HP Semiann. Prog. Rep. July 31, 1956*, ORNL-2151, p 43.

[15] F. Bloch and N. E. Bradbury, *Phys. Rev.* 48, 689 (1935).

[16] N. E. Bradbury, *Phys. Rev.* 44, 883 (1933).

[17] L. B. Loeb, *Basic Processes of Gaseous Electronics*, p 428, University of California Press, Berkeley, 1955.

Table 60. Summary of Coefficients for $N_2 + O_2$

E/P ($v \cdot cm^{-1} \cdot mm^{-1}$)	β ($cm^{-1} \cdot mm^{-1}$)	$(C_1/\lambda_2)\beta$ ($cm^{-1} \cdot mm^{-1}$)	σ_1 (cm^2)	$(C_2/\lambda_2)\beta$ ($cm^{-1} \cdot mm^{-1}$)	σ_2 (cm^2)	$(K/\lambda_2)\beta$ ($cm^{-1} \cdot mm^{-3}$)
0.2	0.281	4.5×10^{-3}	9.6×10^{-14}	1.4×10^{-4}	3.0×10^{-15}	2.2×10^{-5}
0.4	0.217	2.4×10^{-3}	6.6×10^{-14}	5.0×10^{-5}	1.4×10^{-15}	7.6×10^{-6}
0.6	0.177	1.5×10^{-3}	5.1×10^{-14}	2.9×10^{-5}	0.98×10^{-15}	2.4×10^{-6}
0.8	0.140	1.5×10^{-3}	6.4×10^{-14}	1.8×10^{-5}	0.77×10^{-15}	7.0×10^{-7}

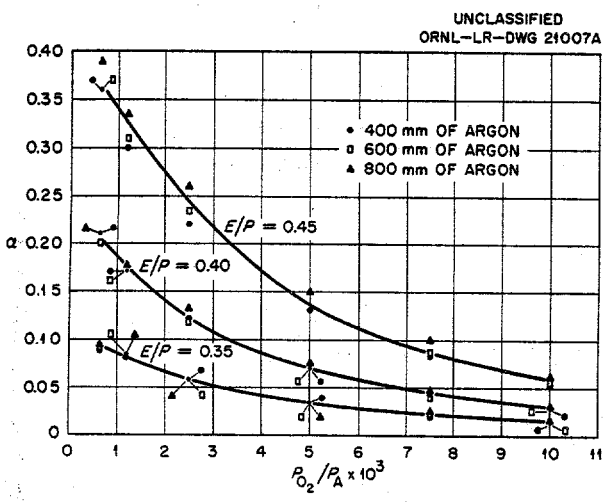

Fig. 45. Dependence of α on the Concentration of Oxygen in Argon for Indicated Argon Pressures.

Figure 45 shows that as E/P decreases, α decreases, and since a decrease in E/P must be associated with a decrease in the mean agitation energy, α (in this region of electron energies) decreases with energy. Electron agitation energy depends on the reduced electric field, E/P, and the nature of the gas. In argon there are no excitation levels less than 10 v; consequently, electrons may be accelerated by the field to energies up to 10 v while making only elastic collisions with argon atoms. When O_2 is added to argon, the mean electron energy is decreased because electrons make inelastic collisions with O_2. Therefore for a fixed argon pressure, α will decrease with increasing values of P_{O_2}/P_A. On the other hand, if P_{O_2}/P_A is fixed, the electron agitation energy will not depend on total pressure, hence α should not depend on P_A. Therefore, the only assumption which must be introduced in order to understand all the data in Fig. 45 is that the agitation energy of electrons in argon is decreased by the addition of O_2.

The Spherical Condenser as a High Transmission Particle Spectrometer

The inverse square electric field between two concentric charged spheres provides a focussing of the charged particles which leave a point source on the inner sphere. Several representative trajectories are shown in Fig. 46. The electric field is adjusted so that monoenergetic particles, emitted tangent to the inner sphere, will follow the surface of the inner sphere (i.e., have circular trajectories) until they emerge from the spectrometer into a field-free region after having gone through a central angle ϕ. Particles making an angle α initially with the tangent plane follow elliptical paths as shown. As the angle α is increased, the displacement of the trace from the inner sphere at an angle ϕ increases until a maximum is reached, whereupon the trace begins to return and finally reaches the inner sphere. The bunching of trajectories at the central angle ϕ suggests the introduction of a slit at this position in order to give the arrangement energy selectivity without sacrificing transmission. A counter placed along the line joining the source and center of the spheres intercepts the trajectories after they emerge from the region between the spheres.

The analysis of the transmission, resolution, and line profile shape of this spectrometer have been carried out both graphically, for ϕ between 120 and 160 deg, and analytically, in small angle approximation for ϕ between 160 and 180 deg, and the results agree well with each other. In order

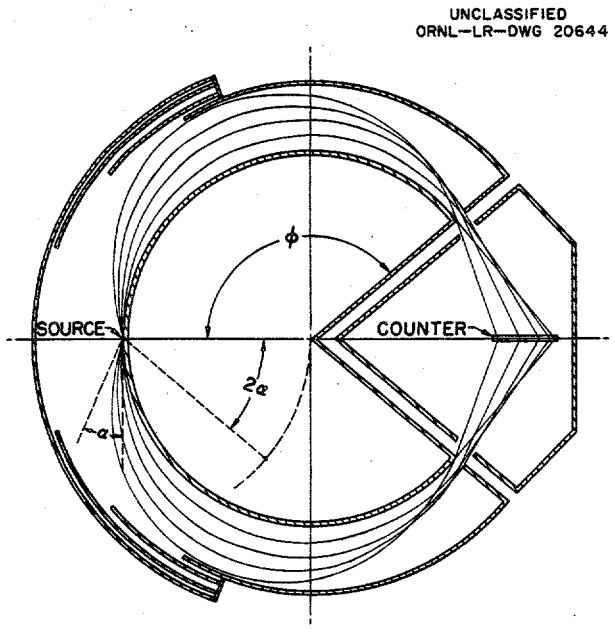

Fig. 46. Cross-sectional View of Spherical Condenser Spectrometer.

to construct the trajectories graphically, use is made of the fact that the total energy (kinetic plus potential) of a particle in an inverse square field is proportional to the length of the major axis of the ellipse. For a major axis of fixed length (monoenergetic particles), with one focus at the center of the spheres, the other focus must lie on a circle which has the source as its center and which passes through the center of the spheres. For a take-off angle α, the included angle between the source-center line and the source-focus line will be 2α as shown. The ellipses are drawn as follows: fix the ends of a fine wire at the foci; place a pencil in the loop at the source position (vertex of the angle 2α); move the pencil, constrained by the wire, to trace out the ellipse. A set of ellipses for various angles α is thus obtained corresponding to the trajectories of monoenergetic particles. The transmission of the apparatus is then

$$T = \tfrac{1}{2} \sin \alpha_{max} , \quad (1)$$

where α_{max} is the angle for which the trajectory just touches the inner sphere after a central angle ϕ. The transmission defined here is the fraction of all monoenergetic particles emitted by the source which can get through the slit.

Trajectories may be drawn for particles of other energies in a similar way except that the foci are located at the center of the spheres and on a circle about the source but not passing through the center (not shown). Resolution and line profile shapes are obtained from these traces.

The analytical solution is obtained from the equation of the ellipse.

$$r = \frac{\cos^2 \alpha}{1 - \cos \phi + \cos \alpha \cos(\phi + \alpha)} \quad (2)$$

where r and all subsequent spatial parameters are in units of the inner sphere radius. It is easily shown that

$$\alpha_{max} = \frac{\pi - \phi}{2} , \quad (3)$$

and hence that the transmission is

$$T = \frac{1}{2} \cos \frac{\phi}{2} . \quad (4)$$

The width of the slit may be found from the value of α for which the trajectory is at its maximum displacement from the inner sphere at ϕ. This value of α is given by

$$\tan \alpha_{max\ displ} = \frac{1}{2} \cot \frac{\phi}{2} , \quad (5)$$

and a substitution of this value of α in Eq. 2 yields the radius of the outer slit edge.

The inner sphere constitutes the inner edge of the slit and it may be necessary to use spherical anti-scatter shells, located on equipotentials, for the inner sphere similar to those shown on the outer sphere.

After passing through the slit the trajectories are straight lines which come back to the counter on the axis at a distance τ from the center of the spheres where

$$\tau = \frac{\cos^2 \alpha}{1 - \cos \phi - \cos^2 \alpha} . \quad (6)$$

A postaccelerating voltage may be placed across the gap between the conical surfaces where the trajectories emerge from the deflecting field.

Figure 47 shows the line profile at $\phi = 170$ deg. The abscissa δ is the per cent deviation in energy from the energy for which a trace with $\alpha = 0$ is a

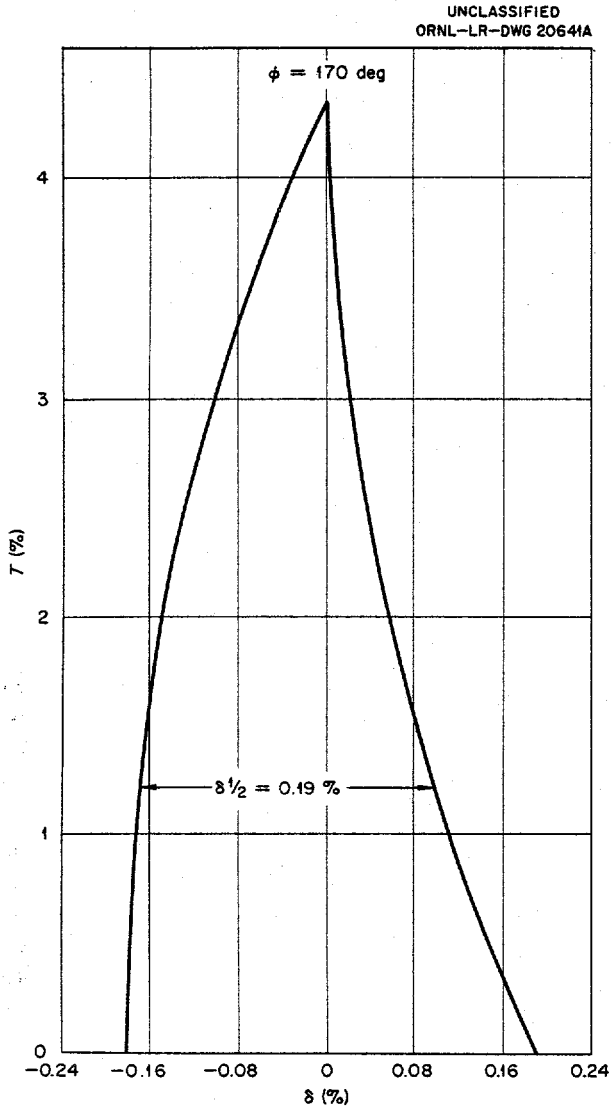

Fig. 47. Line Profile for Point Source and $\phi = 170$ deg.

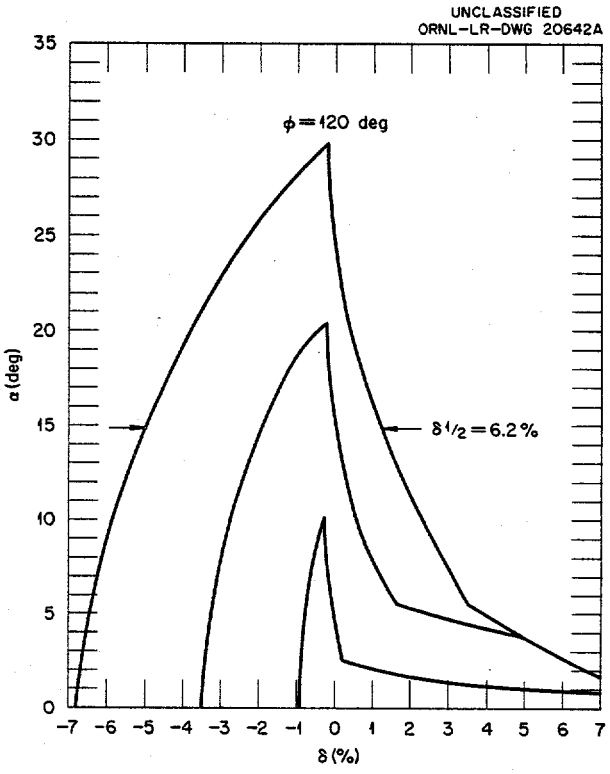

Fig. 48. Line Profile for Point Source and $\phi = 120$ deg.

circle. The energy resolution $\delta_{1/2}$ is 0.19% (momentum resolution 0.095%) and the transmission is 4.4%. For higher transmission a smaller ϕ is necessary, and line profiles for $\phi = 120$ deg are shown in Fig. 48. The ordinate is the increment in α in degrees which can contribute to a given energy component δ. Because the incremental α is very nearly equal to the transmission in per cent, this profile differs only slightly from the profile having the transmission as ordinate. The highest curve is the profile to be expected when the slits are placed as discussed above; the lower curves result when the inner edge of the slit does not coincide with the inner sphere but is moved progressively outward. The resolution is improved in the lower curves, but the transmission suffers and the line profile develops an undesirable tail. Thus if high resolution is desired, a value of ϕ near 180 deg should be chosen rather than a narrowing of the slits at a smaller ϕ.

Figure 49 is a plot of transmission, resolution, and the ratio of the two as a function of ϕ. The energy resolution in per cent is given by

$$\delta_{1/2} = \frac{(\pi - \phi)^2}{16} \times 100 \,, \tag{7}$$

provided $(\pi - \phi)$ is a small angle. Actually the equation holds rather well for ϕ as small as 120 deg.

The performance of this type of electrostatic spectrometer may be contrasted favorably with the Purcell type,[18] which had a transmission of about 1% at an energy resolution of 0.2%, and the more

[18] E. M. Purcell, *Phys. Rev.* 54, 818 (1938).

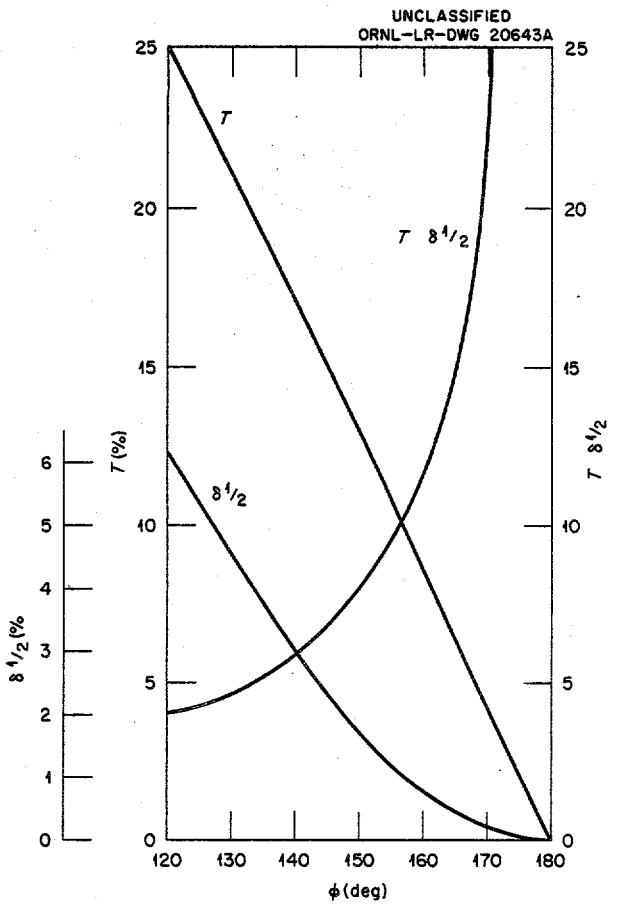

Fig. 49. Transmission, Resolution, and Figure of Merit of Spectrometer as a Function of the Angle ϕ.

recent versions of the Purcell instrument by Browne *et al.*,[19] where $T = 0.025\%$ and $\delta_{1/2} = 0.2\%$, and by Kobayashi[20] where $T = 3.4\%$ and $\delta_{1/2} = 1.3\%$. Allison and Weyl[21] have built a spectrometer with $\phi = 180$ deg, which has $T = 0.4\%$ and $\delta_{1/2} = 1.2\%$.

The characteristics of this type of spectrometer when the source is of finite extent are currently being investigated. Preliminary results indicate that the transmission and resolution for point sources on the inner sphere, but as much as 5% off the symmetry axis, differ only slightly from the values for point sources on the axis. Thus the spectrometer should have a very high luminosity (product of transmission and source area) as well as high transmission.

The spectrometer may be useful as a low energy x-ray spectrometer using a photoelectric radiator at the source position. X rays moving to the left in Fig. 46, from the center to the radiator, eject photoelectrons having an angular distribution peaked in the lateral direction (i.e., into the angular aperture of the spectrometer). Thus the spectrometer is ideally suited to detecting these electrons.

The Preparation of Thin Uniform Sources for a Beta-Ray Spectrometer

As the measurements of beta spectra have been extended to lower energies, thinner sources have been required in order to avoid distortion of the spectra by scattering and absorption of the radiation in the source. The effect of a thick source is generally noted as an apparent increase in the number of beta rays present at low energy, and as an apparent broadening of internal conversion lines.

Two of the most common methods of source preparation are the evaporation of a radioactive liquid on the source backing and the deposition of the source material by vacuum evaporation. The first method, although simple and rapid, produces generally a very nonuniform source with the activity concentrated in a ring. For this method variations in uniformity of deposition of the order of 400% were obtained by densitometer measurements of radioautographs of various sources. The addition of insulin to the source carrying liquid reduced the departure from uniformity to the order of 140%. Typical radioautographs are shown in Fig. 50.

The other commonly used method, vacuum evaporation, produces uniform sources but is very wasteful of the activity, most of it appearing on the vacuum evaporator instead of the source backing. Decontamination of the evaporator adds to the time and cost of source preparation by this method.

The source backings used here were a sandwich of two different organic films with a total thickness of about 30 $\mu g/cm^2$. Formvar was used because of its mechanical strength, and polystyrene was used in order to render the backing more resistant to acids. Metallic films of about 30 $\mu g/cm^2$ were vacuum evaporated onto the backings to make them

[19] C. P. Browne, D. S. Craig, and R. M. Williamson, *Rev. Sci. Instr.* 22, 952 (1951).

[20] Y. Kobayashi, *J. Phys. Soc. Japan* 8, 440 (1953).

[21] K. Siegbahn, *Beta- and Gamma-Ray Spectroscopy*, North-Holland Publishing Co., Amsterdam, 1955.

UNCLASSIFIED
PHOTO 40254

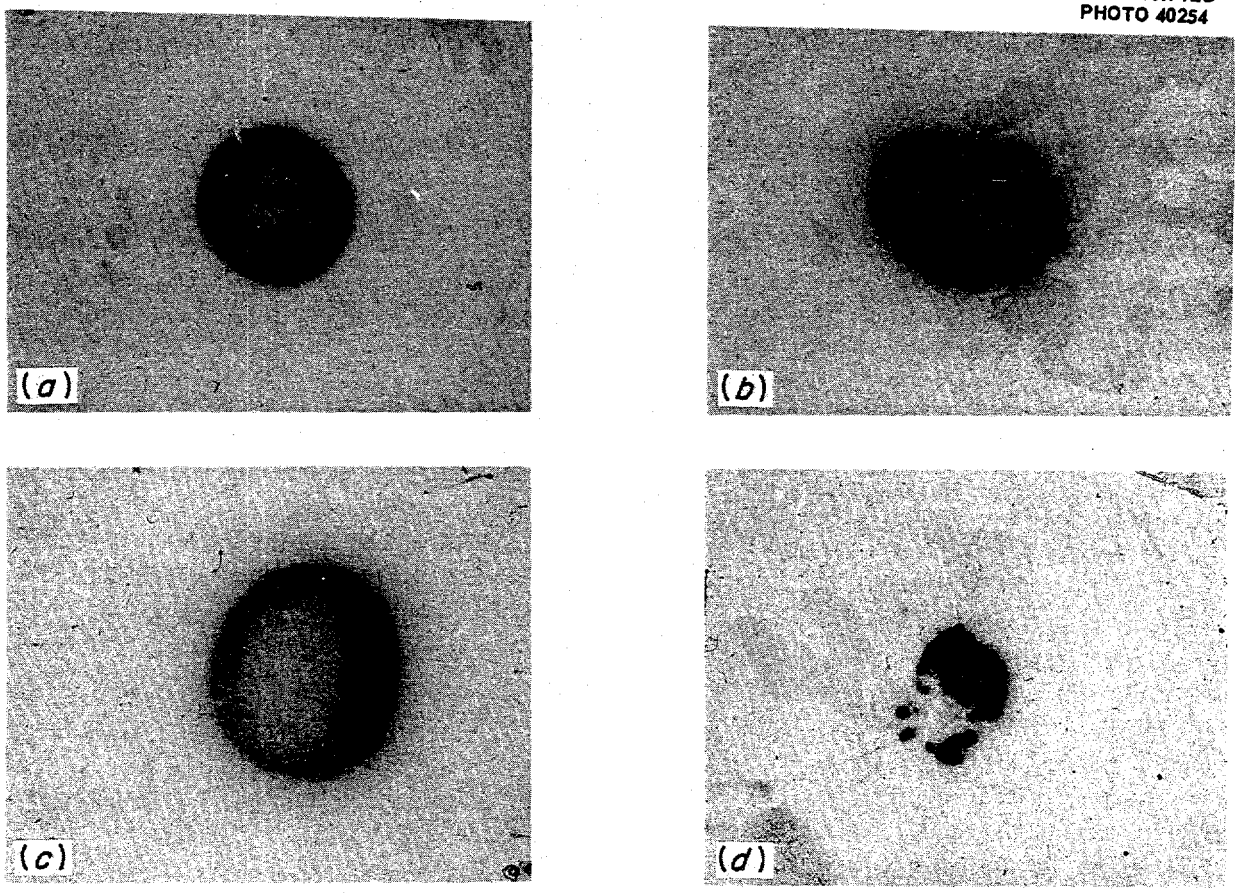

Fig. 50. Autoradiographs of Depositions by Evaporation. (*a*) Evaporation of Ru^{106} with insulin by mixing, (*b*) evaporation of Ru^{106} with insulin by wetting, (*c*) evaporation of Ru^{106} by partial evaporation, and (*d*) evaporation of Ce^{144}.

electrically conducting in order to ground the source electrically.

Two additional methods of source preparation were studied in an attempt to improve the uniformity of deposition. The first method took advantage of the unique properties of radiocolloids. The second method involved electrodeposition of the source material.

Even though the solubility product is not reached, a radiocolloidal suspension, in contrast to an inert colloidal suspension, may be adsorbed, filtered, and centrifuged, and will even settle out of solution solely by the action of gravity. Advantage may be taken of the last named property by placing a portion of the radioactive solution on the source backing and exposing it to an atmosphere of either hydrogen sulfide or ammonia in order to form a colloidal suspension of an insoluble sulfide or hydroxide. Table 61 lists the radionuclides used and the per cent of deposition obtained after an exposure time of 2½ hr. Figure 51 shows the radioautographs of sources of Ce^{144} and Hg^{203} prepared by this method. The variation in the uniformity of the radioautographs ranged from 30% to 40%. This constitutes a considerable improvement over the liquid evaporation method, although the per cent deposited is below that achieved in the other method.

Also, by using a reducing metal as the vaporized metal conducting film on the source mounting, a large number of radionuclides can be reduced, and will then be adsorbed onto the remaining conducting film.

Care must be taken to halt the reaction before the film is completely dissolved. Table 62 lists the radionuclides prepared by this method and the

Table 61. Per Cent Deposited by Radiocolloid Precipitation

Radionuclide	Deposited in NH_3 Atmosphere (%)	Deposited in H_2S Atmosphere (%)
Phosphorous-32	9.5	
Scandium-46	20.4	
Selenium-57	1.4	36.7
Cobalt-60	1.5	12.1
Yttrium-91	32.4	
Ruthenium-106	11.2	34.0
Silver-110	65.6	50.0
Indium-114	1.4	13.4
Cerium-144	28.2	
Iridium-192	4.4	3.0
Mercury-203	27.1	82.0

per cent deposited on both the source mounting and on the glass container. The solution was stirred continuously and the time to reach maximum deposition varied from 3 to 8 hr. Adsorption was obtained also from the nonreducing metals gold and copper as a result of the peculiar properties of radiocolloids noted above. Figure 51 shows radioautographs of sources prepared by this method. Variations in uniformity of deposit of only 1.5% were noted.

In the electrodeposition method, the gold source-grounding film was used as the cathode in an electrolytic cell. The solution was stirred continuously with a platinum rod which served also as the anode. Depositions were carried out for about three hours in a 0.1 *M* acid electrolyte at a potential of about 3 v and with a cell current of 20 to 50 ma. Results are summarized in Table 63. The depositions were found to be uniform within 3 to 8% for the various sources.

Sources were prepared also with no external emf applied to the cell. Magnesium was chosen as the

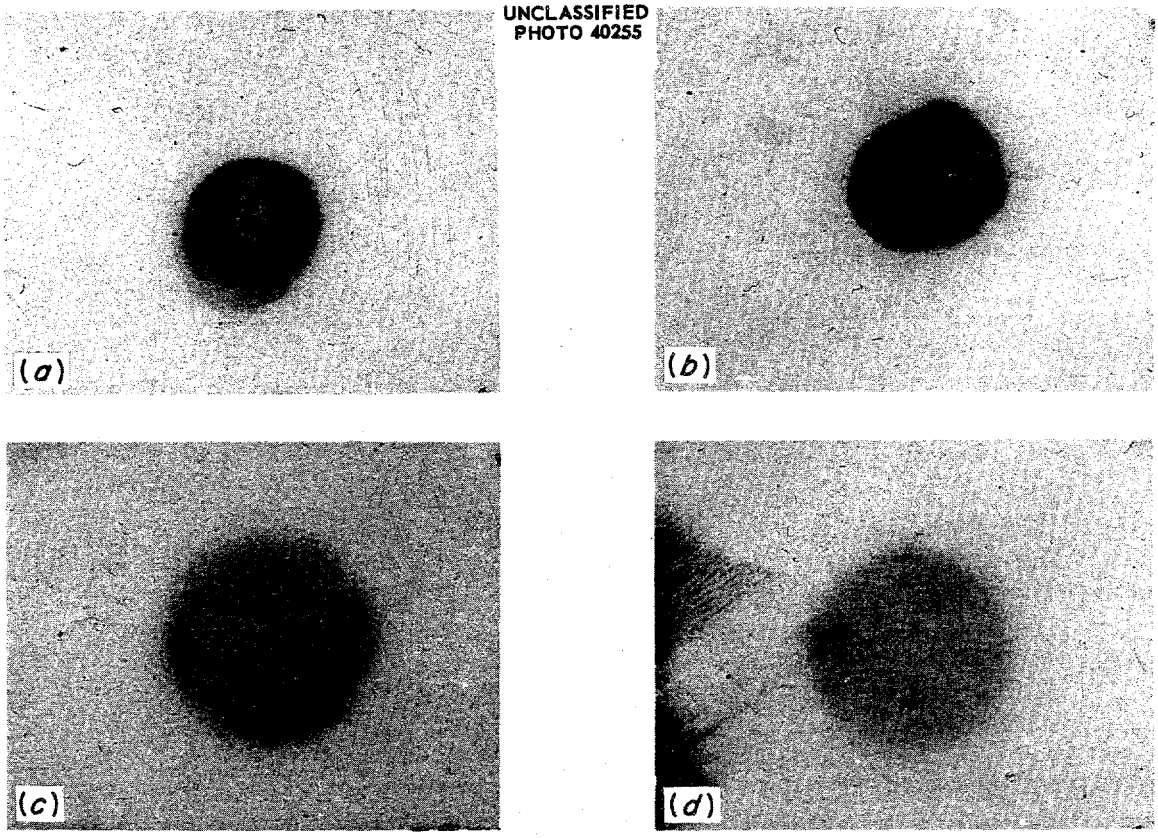

Fig. 51. Autoradiographs of Radiocolloidal Depositions. (*a*) Cerium-144 deposited on Formvar in an NH_4OH atmosphere, (*b*) mercury-203 deposited on Formvar in an H_2S atmosphere, (*c*) mercury-203 deposited on gold by reduction in 0.1 *M* HNO_3, and (*d*) silver-110 deposited on gold by reduction in 0.1 *M* HNO_3.

Table 62. Source Prepreparation by Reduction and Radiocolloid Adsorption

Isotope	Steel (%)	Magnesium (%)	Aluminum (%)	Gold (%)	Copper (%)
Cobalt-60					
Adsorbed on metal	0.10	67.4	0.24	0.15	0.19
Adsorbed on tube	0.19	2.82	0.00	0.06	0.13
Chromium-51					
Adsorbed on metal	0.338	37.43	0.27	0.61	4.25
Adsorbed on tube	0.138	3.56	0.04	0.26	13.24
Indium-114					
Adsorbed on metal	2.36	31.27	0.326	3.14	23.20
Adsorbed on tube	0.96	10.31	0.29	5.64	35.08
Iridium-192					
Adsorbed on metal	0.97	69.05	1.39	0.61	4.33
Adsorbed on tube	0.38	2.70	0.08	0.22	0.56
Mercury-203					
Adsorbed on metal	65.30	22.49	44.92	99.94	64.33
Adsorbed on tube	6.05	4.24	4.24	1.36	4.14
Ruthenium-106					
Adsorbed on metal	9.21	72.51	48.06	8.50	36.34
Adsorbed on tube	10.71	0.80	1.24	5.50	14.52
Selenium-75					
Adsorbed on metal	42.10	75.39	42.83	1.09	15.05
Adsorbed on tube	6.55	5.25	15.26	1.11	4.69
Silver-110					
Adsorbed on metal	18.37	64.94	72.42	87.15	92.02
Adsorbed on tube	36.52	11.45	11.21	4.51	2.16

Table 63. Electrodeposition by an Applied emf

Radionuclide	Chemical Form	Solution	emf (v)	Current (ma)	Time (hr)	Per Cent Deposited
Ruthenium-106	$RuCl_3$	0.1 *M* HCl	3.8	55	3.5	62.1
Silver-110	$AgNO_3$	0.1 *M* HNO_3	2.8	20	3.0	92.2
Mercury-203	$Hg(NO_3)_2$	0.1 *M* HNO_3	3.0	20	3.0	94.4
Cobalt-60	$CoCl_2$	0.1 *M* HCl	2.9	55	4.0	1.4
Indium-114	InCl	0.1 *M* HCl	3.4	50	3.0	33.1
Chromium-51	$CrCl_3$	0.1 *M* HCl	2.8	40	4.5	14.6
Gold-198	$AuCl_3$	0.1 *M* HCl + HNO_3	4.0	40	4.0	95.4
Iron-59	$FeCl_3$	0.1 *M* HCl	3.2	55	3.0	1.9
Cobalt-60	A Co complex	Prepared electrolyte	4.2	14	4.0	91.1
Iron-57	$FeCl_2$	Prepared electrolyte	5.0	40	5.0	94.8

anodic material and the gold film constituted the cathode. The results are given in Table 64. Autoradiographs of sources prepared by this method are shown in Fig. 52. Variations in uniformity of about 5% were noted.

As a check on the source uniformity achieved with an external emf, a source of Au^{199} was prepared and the spectra of the internal conversion lines from the 207.8-, 158.5-, and 49.6-kev gamma rays were taken. With the Health Physics beta spectrometer operating at a momentum resolution of 0.25%, no broadening in line profile was noted at energies as low as 35 kev. The conversion spectrum from the 158.5-kev gamma ray is shown in Fig. 53.

Response of an Anthracene Scintillation Counter to 10- to 120-kev Electrons

The use of anthracene as a scintillation detector in beta spectrometry and dosimetry is based on the large pulse height, short decay time, and low response to x radiation found for this material. A search of the recent literature as summarized in Table 65 reveals a lack of information on resolution obtainable from thin bare crystals at energies below 120 kev. In addition there is considerable disagreement as to the linearity of pulse height with incident energy at the lower energies. The work described below represents an effort to obtain data on the response of anthracene which would be useful in low-energy electron spectroscopy. A more complete account of the studies herein described is available.[22]

Electrons from a 3MP1 electron gun were accelerated down a six-section accelerator which has been previously described.[23] After passing through a $\frac{3}{8}$-in.-dia hole in a lead baffle, the electrons traveled a distance of 60 cm in a field-free tube, passed through another $\frac{3}{8}$-in. collimator and struck the bare anthracene crystal. Use of the drift tube reduced the background count rate with the gun off to about 4 counts/min. An aluminum reflector in the form of a truncated cone surrounded the crystal as shown in Fig. 54. The crystal was secured (with silicone grease) onto the window of a selected RCA 6199 photomultiplier tube. The multiplier signal fed into a linear amplifier, single-channel analyzer,[24] and scaler. The amplifier was rated by the manufacturer to give a pulse with a rise time of 0.2 μsec and decay time of 0.8 μsec.

Two crystals were made from commercial material, machined to $\frac{3}{8}$-in. diameter and cleaved on both faces so that the final thicknesses were 0.060 and 0.011 in., respectively.

Typical pulse-height distributions are shown in Fig. 55. The noise background in the photomultiplier at room temperature masked the pulses

[22] L. W. Johnston *et al.*, *Response of the Anthracene Scintillation Counter to Low Energy Electrons*, ORNL-2298 (April 16, 1957). A preliminary report was given at the Southeastern Section Meeting of the American Physical Society, April 4, 1957; see *Bull. Am. Phys. Soc.* 2, Series II, 279 (1957).

[23] A. W. Blackstock, R. D. Birkhoff, and M. Slater, *Rev. Sci. Instr.* 26, 274 (1955).

[24] The amplifier and analyzer were Atomic Instrument Co. Models 218 and 510, respectively.

Table 64. Electrodeposition by Internal Electrolyses

Radionuclide	Chemical Form	Electrolyte	Time (hr)	Per Cent Deposited
Ruthenium-106	$RuCl_3$	0.01 *M* HCl	8.0	95.7
Silver-110	$AgNO_3$	0.01 *M* HNO_3	5.0	98.7
Mercury-203	$Hg(NO_3)_2$	0.1 *M* HNO_3	8.0	97.3
Cobalt-60	$CoCl_2$	0.1 *M* HCl	8.0	90.1
Indium-114	InCl	0.1 *M* HCl	3.0	98.6
Iron-59	$FeCl_3$	0.1 *M* HCl	6.0	99.2
Chromium-51	$CrCl_3$	0.1 *M* HCl	5.0	97.3
Gold-198	$AuCl_3$	0.1 *M* HCl	5.5	97.8

UNCLASSIFIED
PHOTO 40253

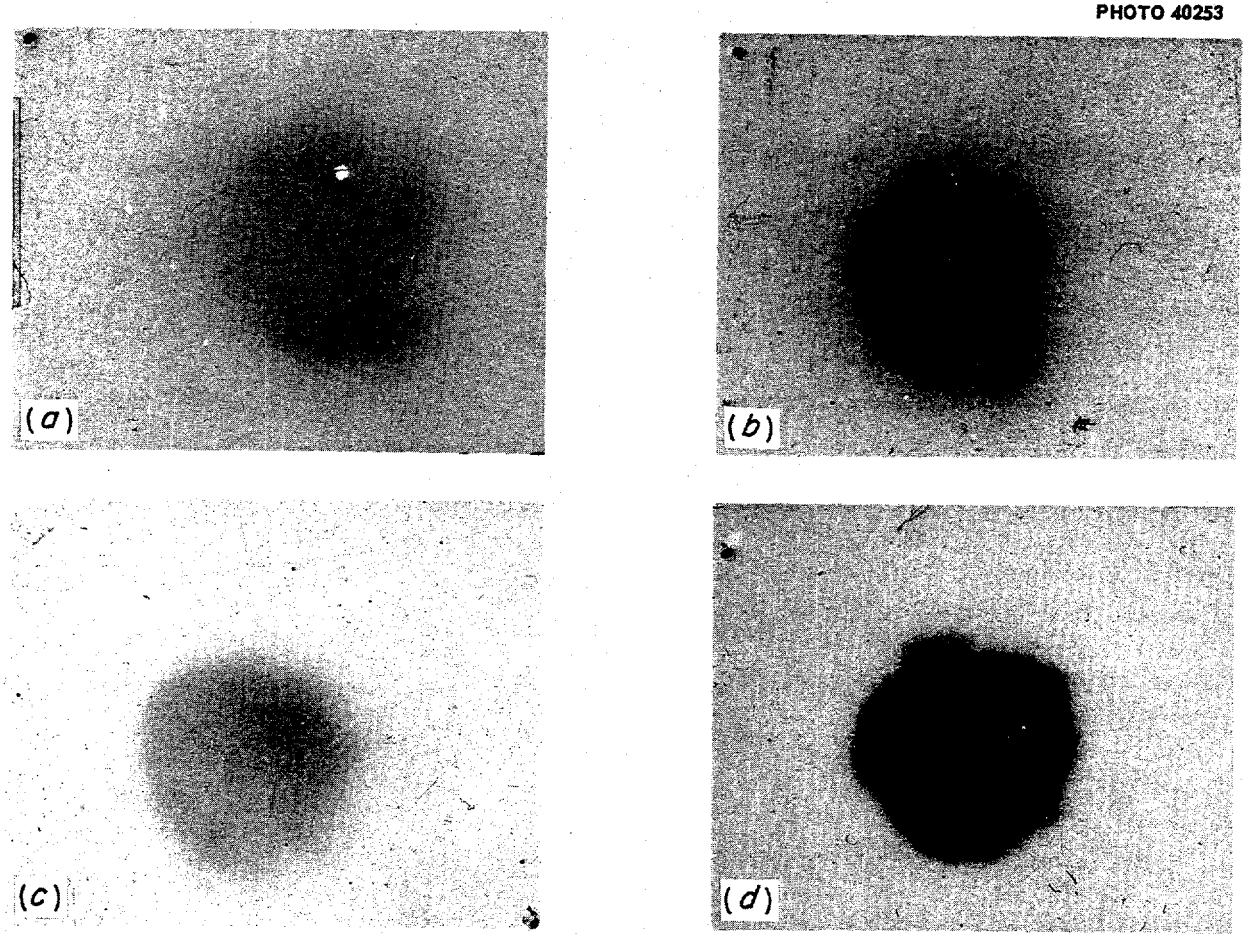

Fig. 52. Autoradiographs of Electrodeposition. (*a*) Mercury-203 electrodeposited on gold, (*b*) ruthenium-106 electrodeposited on gold; 4 v, 55 ma in 0.1 *M* HCl, (*c*) indium-114 internally electrodeposited on gold in 0.1 *M* HCl, and (*d*) gold-198 internally electrodeposited on gold in 0.1 *M* HCl.

below about 10 kev. The pulse height at the peak of each curve was determined by extrapolating the sides of the distribution until they intersected.

Figure 56 is a plot of the pulse height at the maximum of the distribution vs electron energy for the 0.060-in. crystal. The curve is linear within experimental error, and the least squares line through the points intersects the energy axis at 4.5 kev. A similar curve for the 0.011-in. crystal has an intercept of 3.5 kev. The pulse height distributions were found to be approximately Gaussian of the form

$$G(h) = C \exp\left[-\frac{\alpha^2(H-h)^2}{a^2}\right],$$

where $G(h)$ is the counting rate at some pulse height; C is the maximum counting rate of the distribution which occurs at pulse height H; α^{-1} is the slope of the pulse height at the maximum of the distribution vs energy curve; and $2a/\alpha$ is the full width of the distribution at C/ϵ. It can be shown[21] that $a^2 = 2K(E - i)$ where E is the electron energy, i is the intercept of the pulse height at the maximum of the distribution vs energy curve, and K is a constant having units of kev per photoelectron. K may be interpreted as the amount of electron energy absorbed in the crystal necessary to produce a photoelectron at the photocathode.

The average values of K for all the data were 1.47 ± 0.09 kev/photoelectron and 1.32 ± 0.13

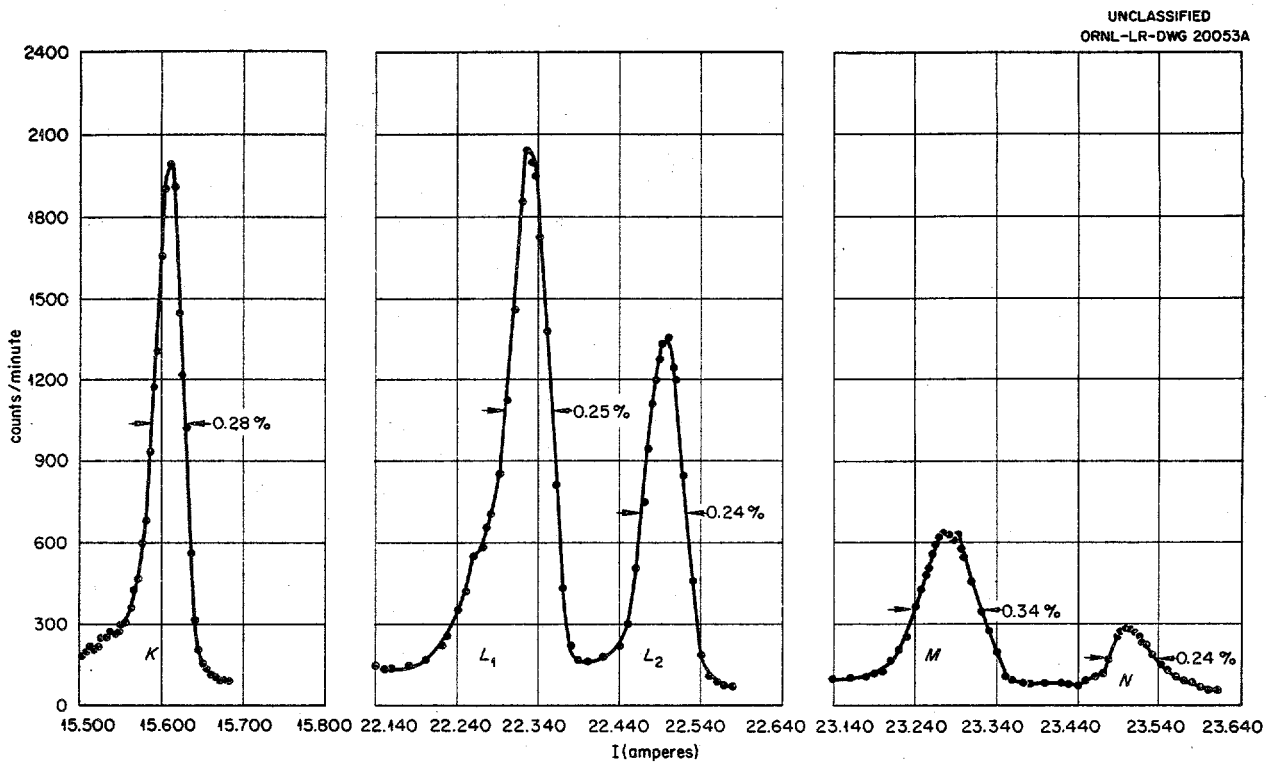

Fig. 53. The Internal Conversion Lines of the 159-kev Gamma Ray of Hg^{199}.

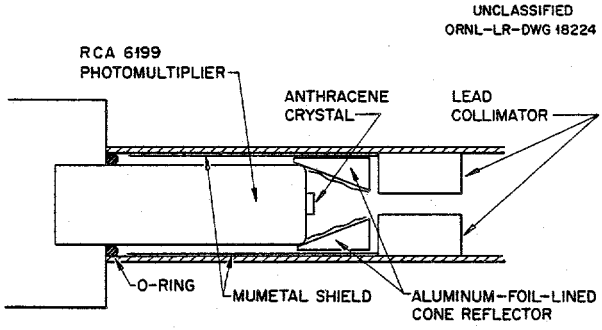

Fig. 54. Scintillation Counter Arrangement.

kev/photoelectron for the 0.060- and 0.011-in. crystals, respectively. The values of the constant a^2, which measures the resolution, were plotted in Fig. 57 for the 0.060-in. crystal. The curve for the 0.011-in. crystal was similar. The curves are linear within experimental error, indicating that a theory of the pulse-height spread based on

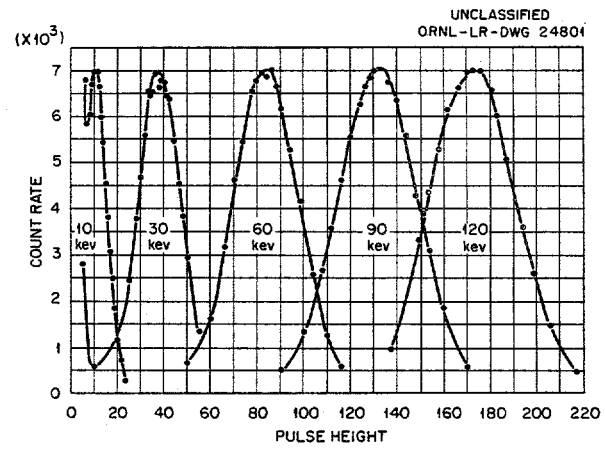

Fig. 55. Typical Pulse-Height Distribution for Electrons Incident on Bare Anthracene Crystals on an RCA 6199 Photomultiplier. The 10-kev curve was taken with the 0.011-in.-thick crystal. The rest were taken with the 0.060-in. crystal.

Table 65. Summary of Existing Data

Observer	Source of Radiation	Photomultiplier	Type of Pulse Analyzer	Foil Cover
Hopkins[a]	β-ray spectrometer	RCA 5819	Integral	Yes
Taylor *et al.*[b]	Pulsed electron gun	RCA 5819	Integral	Not stated
Robinson and Jentschke[c]	k-capture x rays	RCA 5819	Differential	Yes
Fowler and Roos[d]	X-ray tube	RCA 5819	Differential	Not stated
Birks and Brooks[e]	X-ray tube	EMI 5060	Differential	Not stated
Present work	Electron gun	RCA 6199	Differential	No

	Crystal Thickness (cm)	Energy Range Studied (kev)	Linearity of Response with Energy	Resolution Studies
Hopkins	1.29	30–1900	Linear above 125 kev	Yes
	2.50	800–3200	Linear above 125 kev	Yes
Taylor *et al.*	0.25	0.5–624	Linear above 100 kev	No
Robinson and Jentschke	1.00	9–24	Linear within error	No
Fowler and Roos	0.2	10–40	Linear within error	No
Birks and Brooks	0.2	6–30	Linear within error	No
Present work	0.028 and 0.15	10–120	Linear within error	Yes

[a] J. I. Hopkins, *Rev. Sci. Instr.* 22, 29 (1951); *Phys. Rev.* 77, 406 (1950).
[b] C. J. Taylor *et al.*, *Phys. Rev.* 84, 1034 (1951).
[c] W. H. Robinson and W. Jentschke, *Phys. Rev.* 95, 1412 (1954).
[d] J. M. Fowler and C. E. Roos, *Phys. Rev.* 98, 996 (1955).
[e] J. B. Birks and F. D. Brooks, *Proc. Phys. Soc. (London)* 69B, 721 (1956), and references therein.

the statistical variation in the number of photoelectrons produced at the cathode of the photomultiplier satisfactorily represents the present data.

The shape of any of the pulse-height distribution curves may be closely approximated by a Gaussian except at the base of the distribution where the experimental distribution is somewhat wider. The results presented here may be contrasted with Hopkins' data[25] taken at higher energies which yielded a value of K of 3.3 kev/photoelectron and an intercept, i, of 25 kev. These differences are probably attributable to the effect of Hopkins' cover over the crystal and greater thickness of the crystal, and the differences between crystal and reflector geometry. Other factors which could explain the disagreement with Hopkins' results are the differences in photocathode and crystal efficiences.

INSTRUMENT RESEARCH

F. J. Davis
G. S. Hurst
J. A. Auxier
P. W. Reinhardt
E. B. Wagner

The Single Ion Detector for Gamma Dosimetry in Mixed Fields of Fast Neutrons and Gamma Rays

The miniature dosimeter for measuring gamma radiation in the presence of fast neutrons[26] has been developed and improved. Designated SID

[25] J. I. Hopkins, *Rev. Sci. Instr.* 22, 29 (1951); *Phys. Rev.* 77, 406 (1950).

[26] F. J. Davis *et al.*, *HP Semiann. Prog. Rep. July 31, 1956*, ORNL-2151, p 64.

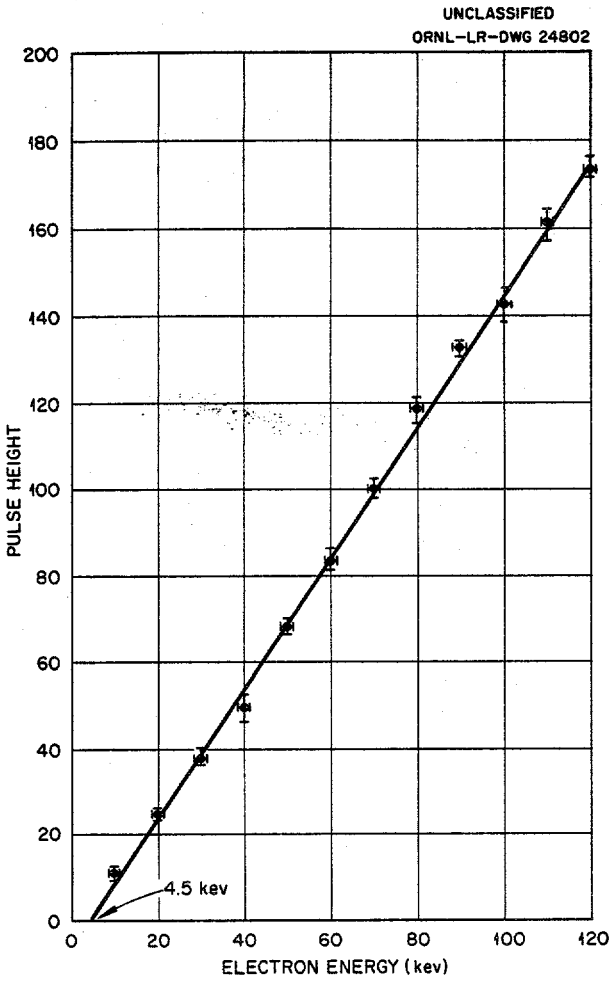

Fig. 56. Peak Pulse Heights vs Electron Energy for Electrons Incident on a Bare Anthracene Crystal 0.060 in. Thick.

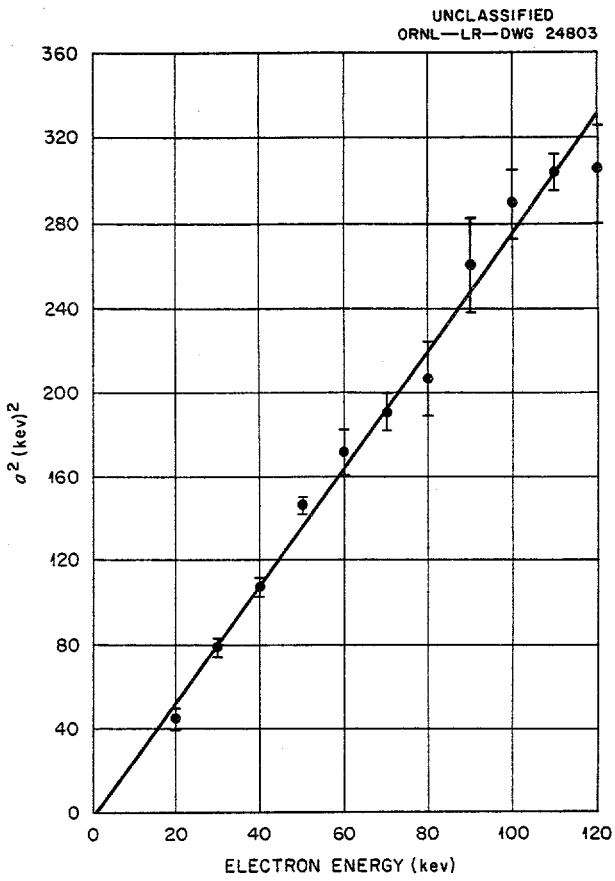

Fig. 57. Plot of a^2 vs Electron Energy for the 0.060-in. Anthracene Crystal. The a/α is the half width of any pulse-height distribution at $1/e$ of its maximum.

(single ion detector), the counter is now commonly filled with isobutane for improved stability. It was determined that the amount of energy imparted to the hydrogen contained in such a minute quantity of isobutane by fast neutrons could be neglected. The energy response has been explored by using a constant voltage x-ray machine to compare the response of the counter with that of a thin wall Victoreen r-meter. With a decrease of the effective energy of x rays below 200 kev, the response of the counter was found to increase. An aluminum anode was substituted for the stainless steel one with the result that the low energy response improved. By addition of tin foil around the counter, the response was made to approximate closely that of the r-meter down to an effective x-ray energy of about 80 kev. Figure 58 depicts the energy response for several thicknesses of tin.

A study of the response of the SID as a function of wall material has been completed. Figure 59 shows a ring of counters that were identical except for the wall material (cathode). All counters were interconnected by a common filling tube to insure uniform gas pressure in each counter, and a source holder was located accurately in the center of the ring. A typical family of pulse-height distribution curves are shown in Fig. 60 for carbon, aluminum, copper, tin, and lead walls. A comprehensive analysis of these data has not been completed.

Advances in the Standard Proportional Counter Method of Fast Neutron Dosimetry

The proportional-counter method for measuring fast-neutron dose in the presence of gamma radiation has been considerably improved through (1) re-

design of the proportional counter, (2) a study of the behavior of the counter for various filling gases, and (3) development of a more convenient form of the electronics necessary for pulse integration and dose read-out.

The pulse integrator is the simple 4-stage binary type[27] which gives an accuracy of ±5% over the energy range of 0.5 to 14 Mev. Through the use of preset timers, decade scalers, and neon lamp decimal points, the dose rate may be read directly in mrad/hr. The first model of a working instrument is shown in Fig. 61.

The instrument is suitable for radiobiological, neutron-physics, shielding, and radiation-protection research.

Improvements in Threshold Detector Counting

Fission-Foil System. – As a result of the increased demand for measurements of neutron spectra and dose determinations with threshold detectors using sulphur, gold, and fission foils, several improved techniques have been developed. Increased sensitivity could obviously be accomplished if the detector sample were increased in size; however, since the world's supply of Np^{237} is probably less than 50 g, an attempt must be made to increase the sensitivity by means of increasing the counting efficiency.

[27] F. M. Glass and G. S. Hurst, *Rev. Sci. Instr.* **23**, 67–72 (1952).

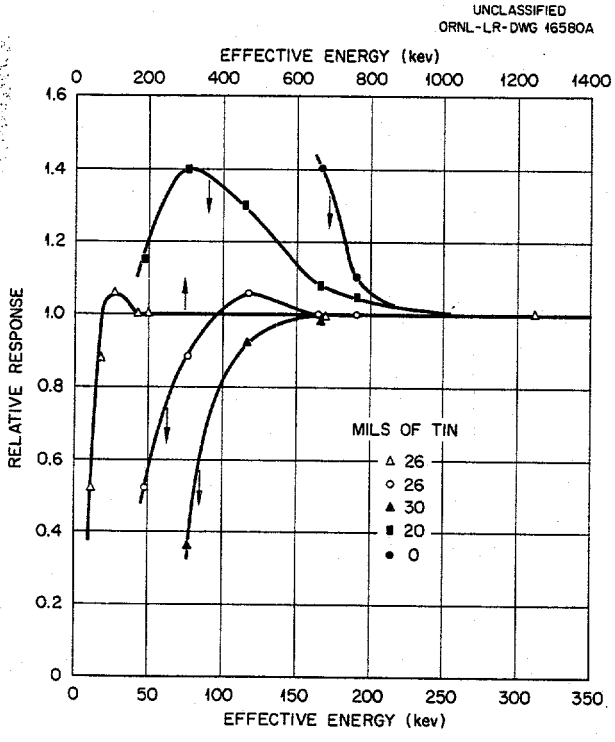

Fig. 58. Energy Response for Several Thicknesses of Tin.

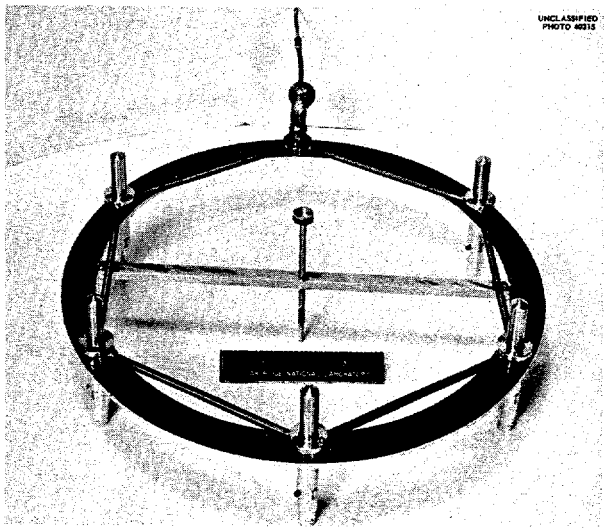

Fig. 59. A Ring of Detectors for Measuring the Relation of Response to Cathode Material.

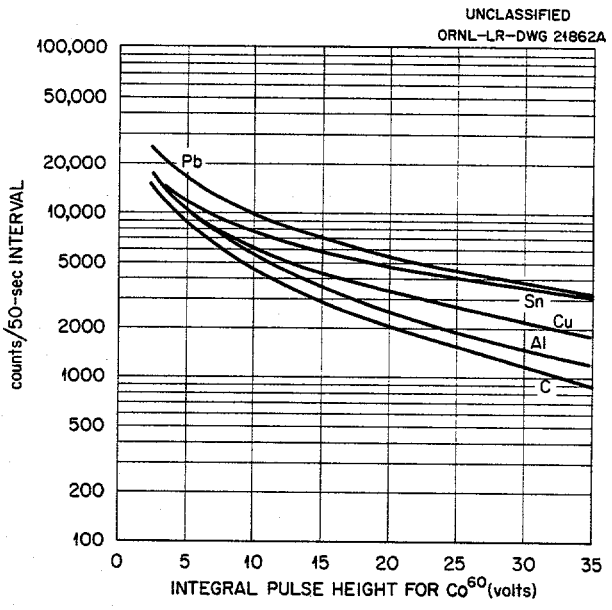

Fig. 60. Integral Pulse-Height Curve; Counter Voltage – 520, Gain – 47,500.

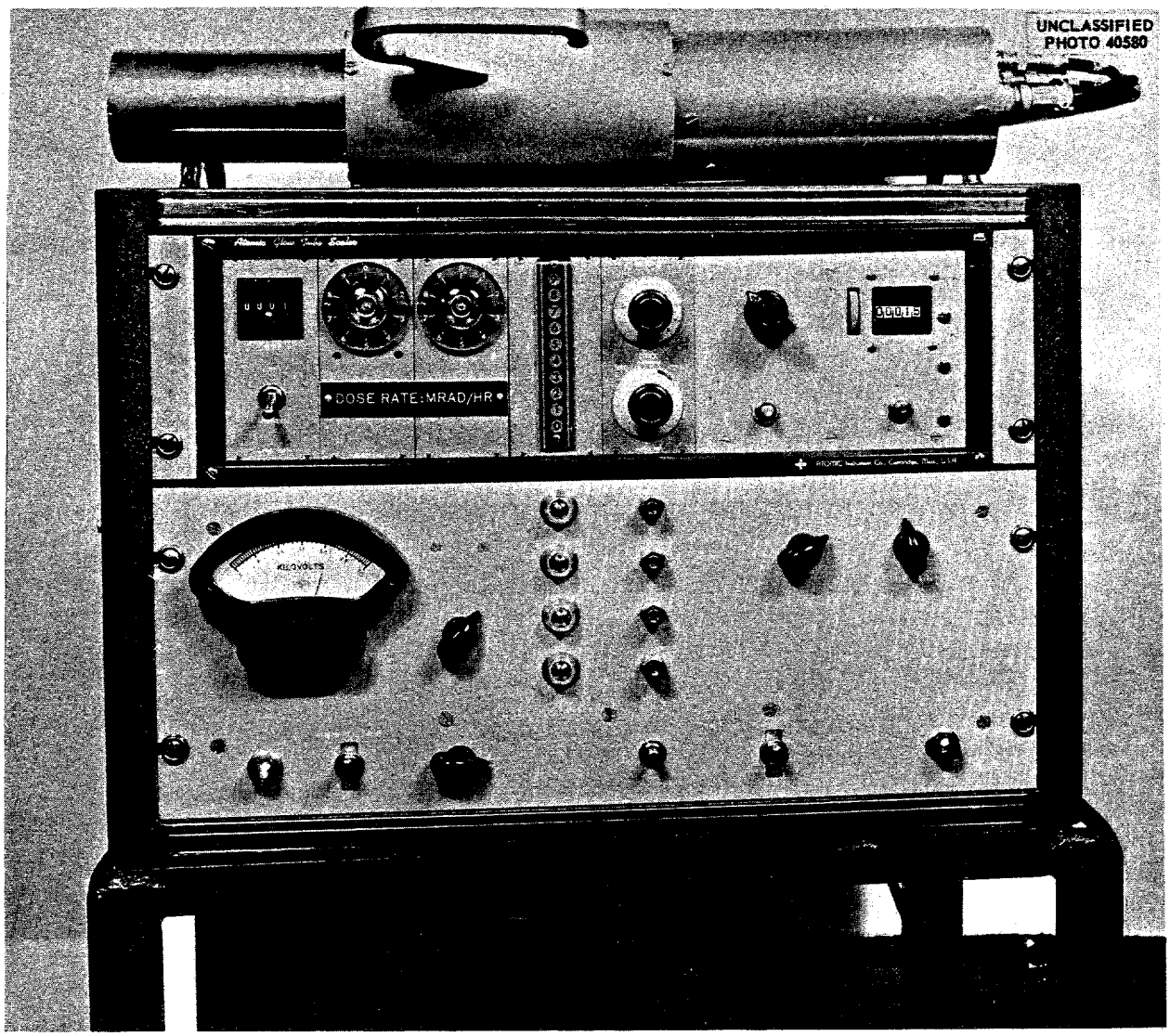

Fig. 61. The Radsan.

In the original method described by Hurst et al.[28] the fission foils were counted on a 1 × 1½-in. NaI-crystal gamma counter. In order to improve the sensitivity two 4-in.-dia by 2-in.-thick NaI crystals are now used on each side of the foil. A diagram of the present arrangement is shown in Fig. 62. A ⅝-in. lead filter now replaces the ⅛-in. brass filter previously used. The increased filtering is especially effective in reducing the natural soft-gamma background of Np^{237}.

The procedure used to determine the optimum setting of the discriminator was to maximize the quantity $S/\sqrt{B}$, where S is the count resulting from sample irradiation and B is the background count rate before irradiation. The discriminator setting thus determined to be optimum was at a level accepting pulses originating from gamma rays above 0.66 Mev. This choice was influenced by the convenience of using the 0.66-Mev gamma ray of Cs^{137} as a monitoring source. The over-all gain in efficiency of counting was a factor of 12.4 at 1 hr after irradiation and 15.6 at 12 hr after irradiation.

[28] G. S. Hurst *et al.*, *Rev. Sci. Instr.* 27, 153 (1956).

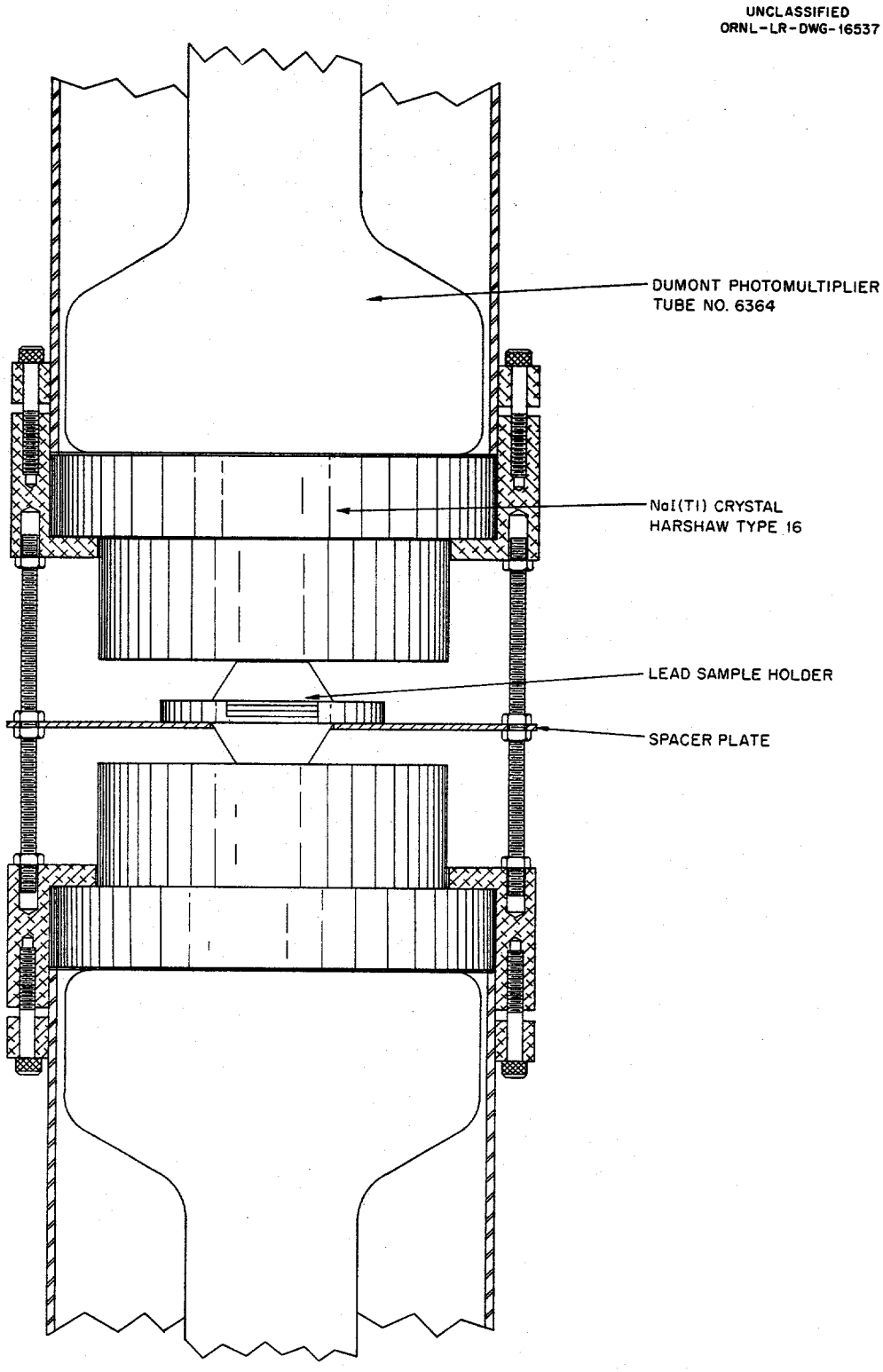

Fig. 62. Fission Foil Scintillation Counter.

Since one of the main troubles of a scintillation counting system is drifts in gain, an automatic monitoring system was developed to obviate this difficulty. A block diagram giving the basic components of this system is shown in Fig. 63. Each time a sample foil is changed, a Cs^{137} source is automatically placed in the foil-counting position. This activates a servomotor which adjusts the high voltage supplying the photomultiplier tubes so that the count rate is corrected to a predetermined value. The predetermined count rate is chosen to be that count rate for which the greatest change of count rate with discriminator setting occurs. In other words, the servomechanism adjusts the gain of the system so that the discriminator accepts pulses equivalent to the cutoff point of the 0.66-Mev gamma ray of Cs^{137}. Since this predetermined count rate of the Cs^{137} is particularly sensitive to gain setting, the servo only has to maintain this count rate to within 10% in order to maintain the count rate of the fission foils to within 1%. Ordinarily the servo system can maintain the count rate of the Cs^{137} to within 1 or 2%.

In the older technique of counting, an automatic timer was used to cut off the count at a predetermined time. This timer utilized a synchronous motor with clutches and relays. As a result of slippage of clutches, etc., the method was found to be unreliable in short counting times of the order of 1 min; therefore, a timing scaler has been substituted for the synchronous motor. The timing scaler simply counts the cycles of the 60-cycle ac supply and, when set to a predetermined count, cuts off the counting scaler so that it counts over a time interval accurate to within one cycle. Thus it has been found convenient to refer to count rates as counts per kilocycle rather than counts per minute.

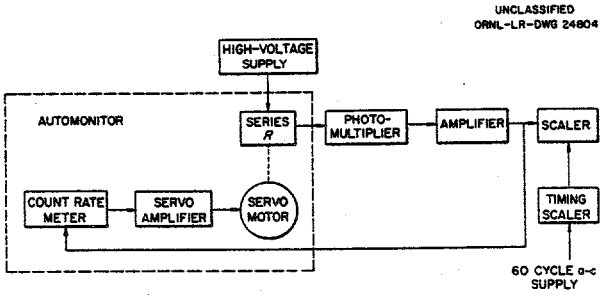

Fig. 63. Block Diagram Showing Automatic Monitoring System.

In order to correct for the decay of the fission-foil gamma count rate with time, it has been found advantageous to record the correction factors at 1-min intervals on an Esterline-Angus (EA) recorder tape. The tape is then run through an EA recorder and the correction factors read off while the foils are counted. This eliminates the necessity for recording the elapsed time since irradiation and then converting this time to decay factors.

Previously, when Np^{237} fission foils were being counted, it appeared that the count rate did not decay at the same rate as the count rate for Pu^{239} fission foils during the first several hours after irradiation. One reason is that Np^{238}, which decays with a 2.1 day half life, emits gamma rays of the order of 1.0 Mev. By counting the Np foils a second time, approximately two days after irradiation, the amount of activation due to neutron capture can easily be calculated. This effect has been reduced by placing cadmium and indium foils between the fission foils. It was further noticed that the U^{238} foils did not decay as fast as Pu^{239} but did decay faster than Np^{237}, suggesting that a shift in the yield of the fission products may be the phenomenon being observed. In order to test this a U^{235} foil was irradiated and its decay curve followed. It was found that the deviations from the Pu^{239} decay rate were in the same direction as the deviations from the Np^{237} decay rate and roughly twice as much. This indicated that the shift in the fission product yield curve with mass number was affecting the decay curves. The lowest curve in Fig. 64 shows the variation with time of the ratio of Pu^{239} fission gamma rays to those of U^{235} as measured by our counting system. The other two curves Pu^{239}/Np^{237} and Pu^{239}/U^{238} are calculated curves obtained by assuming the effect to be proportional to the difference in atomic weight, that is, one-half and one-fourth the deviation from unity, respectively. The greatest deviation appears to be in the neighborhood of 4 hr after irradiation and the ratio approaches unity about 14 hr after irradiation. The curve was not followed for longer periods of time. In studying the Hunter-Ballou[29] curves for the fission products most prominent at 4 hr after irradiation and emitting gamma rays more energetic than 0.66 Mev, it appears that Te^{133}, Y^{92}, I^{135}, Rb^{88}, and Kr^{87}

[29] H. F. Hunter and N. E. Ballou, *Nucleonics* 9(5), C-4 (1951).

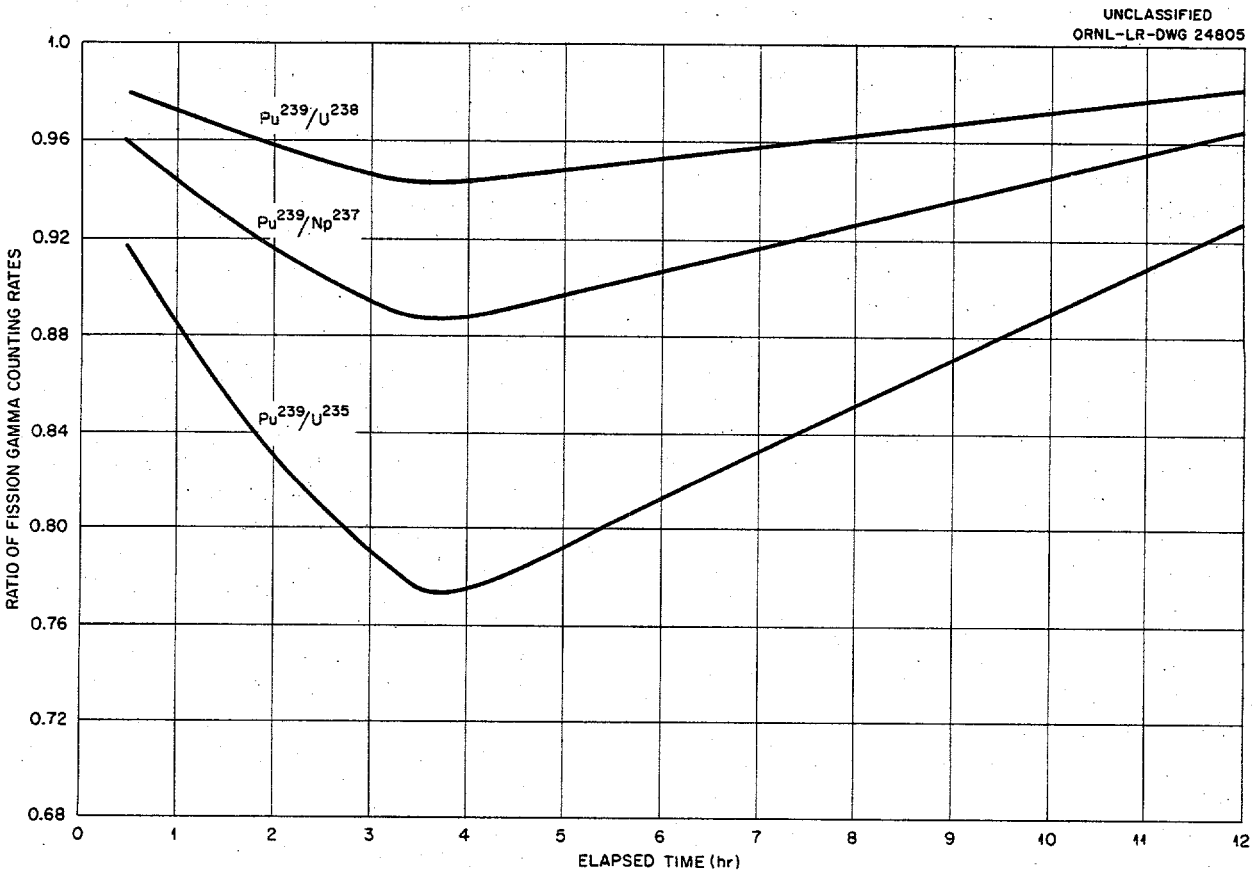

Fig. 64. Variation of the Decay Rates of the Fission Gammas from Pu^{239}, U^{238}, Np^{237}, and U^{235}.

would be shifted so as to increase their relative yield in going from Pu^{239} to U^{235}, while only La^{141} would be shifted to decrease its relative yield. The yield of Cs^{138} being on the peak of the yield curve would probably remain about the same. This then at least qualitatively indicates the changes in the decay curves in the right direction.

Sulfur Counting. – Until recently, determination of the number of neutrons having energies greater than 2.5 Mev by counting the 1.71-Mev beta rays from the $S^{32}(n,p)P^{32}$ reaction has been limited by the area of the sulfur sample. Although larger sulfur samples could be used, larger counters would be required, and counter backgrounds would be increased accordingly. A simple method for removing the P^{32} from the sulfur has been developed, making it possible to increase the sensitivity of a given detection system manyfold without increased counter background.[30]

Phosphorus-32 is removed from sulfur by first melting an exposed sulfur sample in an aluminum dish; a hot plate operated at a low temperature is adequate. The sulfur is then ignited and allowed to burn out leaving the P^{32} attached to the aluminum dish. It has been found that very pure sulfur is required for a complete sulfur burn out.

For counting purposes the sulfur is burned in a 0.001-in.-thick aluminum dish 1½ in. in diameter and ½ in. deep. After the burning operation the sides of the dish are folded down forming a 1½-in. disk which is counted on the scintillation counter shown in Fig. 65. For increased counter geometry, a lead reflector 1 in. in diameter and ⅛ in. thick is placed on top of the aluminum disk. The counting geometry of the system was found to be 61%, when the counting bias was chosen to be just sufficient

[30] F. J. Davis *et al.*, *HP Semiann. Prog. Rep. July 31, 1956*, ORNL-2151, p 93.

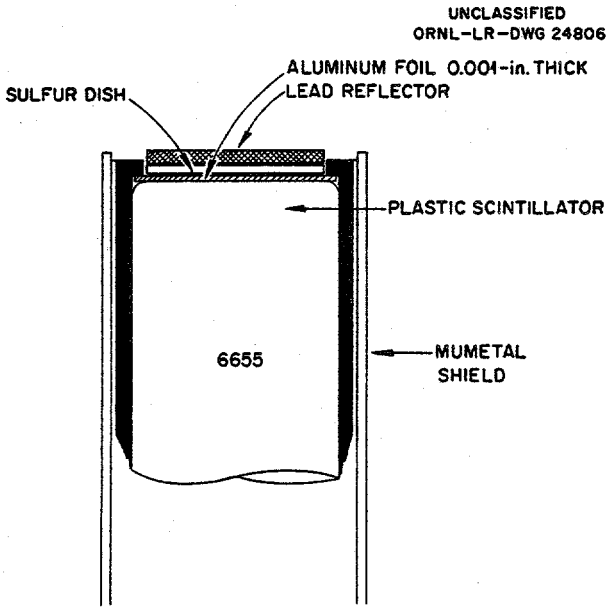

Fig. 65. Scintillation Counter Assembly for Counting P^{32}.

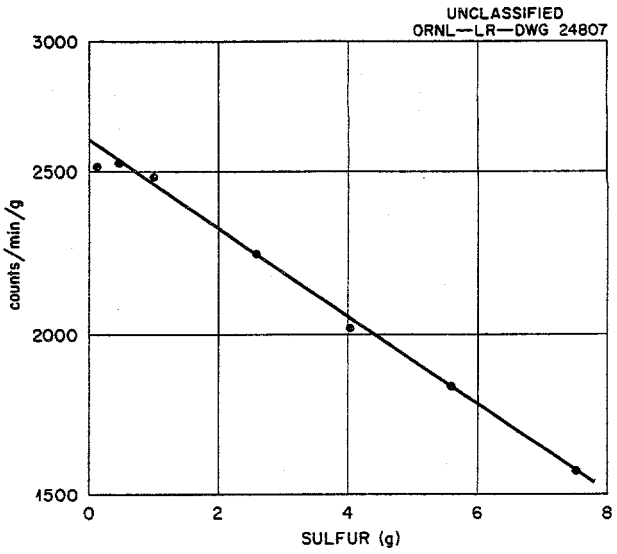

Fig. 66. Extrapolated Activity of P^{32} in Sulfur.

to exclude photomultiplier noise. A natural-uranium source is used to standardize the counter.

To determine the P^{32} yield, various amounts of activated sulfur were spread uniformly in aluminum dishes and counted. In Fig. 66 is shown a plot of counts per minute per gram vs grams of sulfur. The extrapolated zero thickness count is 2605 counts·min^{-1}·g^{-1}. When this amount of sulfur was burned out, a count of 2395 counts·min^{-1}·g^{-1} was obtained giving a P^{32} yield of 92%. For further verification of the P^{32} yield, a quantity of P^{32} was spread over the surface of a standard sulfur pellet, and the pellet placed with the active side face down in an aluminum dish and counted. The sulfur was then turned active side up and melted and burned as previously described. The sides of the dish were folded, and the dish placed on the counter with an unactivated sulfur pellet on top to reproduce the same counting geometry. The yield determined by this method was 93.5%. The latter method is considered more accurate since both counts are taken with identical geometry and higher counting rates could be used to reduce the statistical error. Applying the 61% counting geometry to the 93.5% yield, one obtains a geometry of 57% of the total P^{32} disintegrations for a given burned out sulfur sample. An exposure of the standard 1½- by ⅜-in. pellet which weighs 21 g to 10^{10} neutrons above the 2.5-Mev threshold gives a count rate of 848 counts/min. When burned, the count rate is 15,773 counts/min or 750 counts·min^{-1}·g^{-1}. A recent exposure at the Tower Shielding Facility gave a count rate of 210 counts/min for a standard burned pellet or 10 counts·min^{-1}·g^{-1} for a total neutron dose of 1.0 rep. These counting rates are to be compared to the background of 30 counts/min for the scintillation detector.

Calibration Cross Sections. – Since publication of the threshold detector article,[31] several changes have been made in the neutron cross section of the various detectors. All the cross sections discussed here are values given in BNL-325 (ref 32). The fission cross section for Pu^{239} is 720 barns at thermal energy,[33] but at room temperature the non-$1/v$ correction is 1.075; thus the adopted cross section is 774 barns. The $S^{32}(n,p)P^{32}$ reaction is calibrated by activation of P^{31} with thermal neutrons; the cross section for the latter is 0.19 ± 0.03 barns. Note that BNL-325 recommends the absorption cross section as being more reliable for this case (ref 31).

---

[31] G. S. Hurst *et al.*, *Rev. Sci. Instr.* 27, 153 (1956).

[32] D. J. Hughes and J. A. Harvey, *Neutron Cross Sections*, BNL-325 (July 1, 1955).

[33] D. J. Hughes and J. A. Harvey, *Heavy Element Cross Sections Presented at Geneva August 1955*, Addendum to BNL-325 (July 15, 1955).

The adopted fission cross sections for Pu, U, and Np in the fast neutron region remain the same as those already published.[30] The cross sections of the $S^{32}(n,p)P^{32}$ shown in Fig. 67 are "smoothed out" of values taken from BNL-325 (ref 31). Since the cross section changes with energy, it was weighted by the fission spectrum[34] to determine an effective value. This effective value depends on the adopted threshold in the following way:

$$\sigma_{eff} = \frac{\int_0^\infty n(E)\sigma(E)\,dE}{\int_{E'}^\infty n(E)\,dE},$$

where $n(E)$ is the spectral distribution function, $\sigma(E)$ is the cross section for the $S(n,p)P^{32}$ reaction, and E' is the threshold energy when $E' = 2.0$ Mev, $\sigma_{eff} = 0.173$ barns; and when $E' = 2.5$ Mev, $\sigma_{eff} = 0.229$ barns. The latter is adopted for a fission spectrum.

Calibration Measurements. – The entire threshold detector system was calibrated by irradiating Au, Pu^{239}, and P^{31} with thermal neutrons. Gold samples were exposed both at the Los Alamos Water Boiler and in the water column at the top of the ORNL graphite reactor. It was found that the fluxes in the two reactors were in good agreement; however, the ORNL value had been determined by comparison with the flux in the X-10 Standard Graphite Pile.[35] The flux in the X-10 Standard Pile is an "absolute flux" which should be converted to an "activation flux." When this is done, the flux values in the Los Alamos Water Boiler and the X-10 Standard Pile are reduced by the factor 1/1.128.

Table 66 gives the relative sensitivity and background counts of the foils.

One kc equals $16\frac{2}{3}$ sec. Results from the Tower Shielding Facility gave a dose of 54.2 rads using

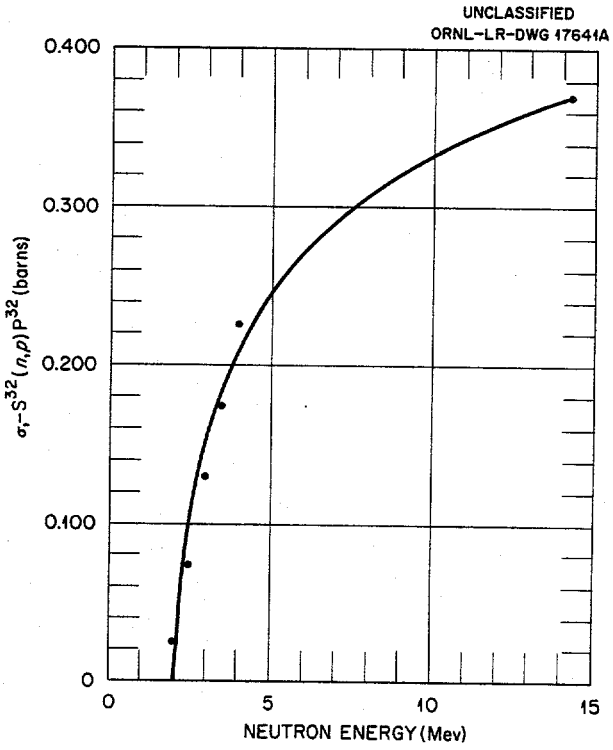

Fig. 67. Cross Section for $S^{32}(n,p)P^{32}$ Smoothed Out from BNL-325 Values.

[34] L. Cranberg *et al.*, *Phys. Rev.* 103, 662 (1956).

[35] E. D. Klema, R. H. Ritchie, and G. McCammon, *Recalibration of the X-10 Standard Graphite Pile*, AECD-3590 (Oct. 17, 1952).

Table 66. Relative Sensitivity and Background Counts of Various Foils

	Total Background (counts·kc^{-1}·g^{-1})	Counts·kc^{-1}·g^{-1} for 10^{10} neutrons/cm^2 at 1 hr After Exposure	Counts·kc^{-1}·g^{-1} for 10 rad Godiva neutrons at 1 hr After Exposure
Au	14	9360	
Pu	900	4390	1600
Np	700	3300	1100
U	400	1190	200
S "burned"	8	210	15

threshold detectors as compared to 53.8 rads as measured with a proportional counter. Spectrum measurements made at Godiva compared to values given by Rosen[36] and normalized for Pu are given in Table 67.

It appears that either the mass or cross section for Np is in error.

Table 67. Ratio of Threshold Detector Value to Rosen's Value

	Run 1	Run 2
Pu	1.00	1.00
Np	1.23	1.14
U	1.11	0.91
S	0.95	0.95

[36] L. Rosen, *Proc. Intern. Conf. Peaceful Uses Atomic Energy Geneva, 1955* 4, 97 (1956).

EDUCATION, TRAINING, AND CONSULTATION

E. E. Anderson

AEC FELLOWSHIP PROGRAM

E. E. Anderson M. F. Fair

The present group of 26 AEC Fellows in Radiological Physics and 1 Air Force trainee completed their year of graduate study at Vanderbilt University in June. The records for the year show that 70% of the group earned an average of B or better. The group is now at ORNL for training in Applied Health Physics and is taking a ten-week course in Reactor Engineering. Ten of the group have been granted a six-month extension of their Fellowship and will work on research problems either at ORNL or at Vanderbilt University to complete the requirements for the MS degree. The AEC Fellows for the 1957–1958 program were selected in March, and the group of 29 will enroll at Vanderbilt University in September.

OTHER ACTIVITIES

E. E. Anderson M. F. Fair
K. Z. Morgan

Two Air Force officers have been at the Laboratory for a six-month course in Health Physics including extensive training in Applied Health Physics. One officer from Fort McClellan, Alabama, spent one month in Applied Health Physics training, and two civilians from Wright-Patterson Air Force Base had a two-week training period in Personnel Monitoring.

K. Z. Morgan presented a 12-hr course in Health Physics as a part of the course "Nuclear Energy Fundamentals for Industry" offered at North Carolina State College.

A 10-hr Health Physics lecture series was presented for the Chemical Technology Division. Two courses in Mathematics were conducted for the Laboratory Apprentice Training Program. Lecture and discussion periods on particular phases of Health Physics were given for:

1. The ORNL Orientation Program,
2. MIT Practice School,
3. REED,
4. Y-12 Development Group,
5. ORINS Radioisotope Techniques Course,
6. ORINS UT-AEC Military Veterinary Radiological Health Course.

One member of the Section spent approximately 2½ months in the Division of Biology and Medicine, Washington, D.C., working primarily on the Education and Training Programs of the Division of Biology and Medicine.

A special short course in Health Physics Fundamentals will be presented from January 20 to March 14, 1958, to fill an immediate need to supply personnel who have some understanding of the nature, scope, and magnitude of health physics problems. Students will be selected in a manner that will render maximum value to the AEC, with applications from the AEC and its major contractors receiving primary consideration. Applicants should be actively engaged in health physics, industrial hygiene, or related fields, and must be on the payroll of the sponsoring organization.

PUBLICATIONS

E. D. Arnold, ed., ORNL CF-57-2-20 (Feb. 11, 1957) (classified).

J. A. Auxier and G. S. Hurst, "A Fast Neutron Insensitive Gamma Dosimeter," *Proceedings of the Health Physics Society, University of Michigan, June 25–27, 1956, Ann Arbor, Michigan* (April 1957).

S. R. Bernard, J. R. Muir, and G. W. Royster, "The Distribution and Excretion of Uranium in Man," *Proceedings of the Health Physics Society, University of Michigan, June 25–27, 1956, Ann Arbor, Michigan,* (April 1957).

S. R. Bernard and E. G. Struxness, *A Study of The Distribution and Excretion of Uranium in Man: An Interim Report,* ORNL-2304 (June 4, 1957).

S. R. Bernard, B. R. Fish, J. R. Muir, and B. L. Harless, *Fitting Linear Combinations of Exponentials to Human Uranium Excretion Data,* ORNL-2364 (to be published).

R. D. Birkhoff, R. H. Ritchie, and J. S. Cheka, "The Spherical Condenser as a High-Transmission Particle Spectrometer," *Bull. Am. Phys. Soc.* Series II 2(4), 174 (1957).

R. L. Blanchard, B. Kahn, and R. D. Birkhoff, "Preparation of Thin, Uniform Sources for a Beta-Ray Spectrometer," *Bull. Am. Phys. Soc.* Series II 2(5), 279 (1957).

T. E. Bortner, G. S. Hurst, and W. G. Stone, "Drift Velocities in Some Commonly Used Counting Gases," *Rev. Sci. Instr.* 28(2), 103–108 (1957).

T. E. Bortner and G. S. Hurst, "Apparatus for Measuring Electron Attachment," *Bull. Am. Phys. Soc.* Series II 2(5), 280 (1957).

T. J. Burnett, "Air Pollution Aspects of Power Reactors," *Eng. Progr. Univ. Florida* vol X, No. 9 (1956).

T. J. Burnett, "Reactors, Hazard vs Power Level," *Nuclear Sci. and Eng.* 2, 382–393 (1957).

J. S. Cheka, "A Neutron Film Dosimeter," *Proceedings of the Health Physics Society, University of Michigan, June 25–27, 1956, Ann Arbor, Michigan* (April 1957).

R. J. Davis, V. L. Sheldon, and S. I. Auerbach, "Lethal Effects of Gamma Radiation upon Segments of a Natural Microbial Population," *J. Bacteriol.* 72(4), 505–10 (1956).

H. F. Howden, "Investigations on Sterility and Deformities of *Onthophagus* (Coleoptera, Scarabaeidae) Induced by Gamma Radiation," *Ann. Entomol. Soc. Am.* 50(1), 1–9 (1957).

H. H. Hubbell, Jr., R. M. Johnson, and R. D. Birkhoff, "Beta-Sensitive Personnel Dosimeter," *Nucleonics* 15(2), 85–9 (1957).

H. H. Hubbell, Jr., R. D. Birkhoff, and R. M. Johnson, *Pocket Ion Chambers for Beta Radiation Dose,* ORNL-2158 (April 26, 1957).

F. N. Huffman, J. S. Cheka, B. G. Saunders, R. H. Ritchie, and R. D. Birkhoff, "Spatial Distribution of Energy Absorbed from an Electron Beam Penetrating Aluminum," *Phys. Rev.* 106, 435 (1957).

G. S. Hurst and T. E. Bortner, "Electron Attachment in O_2-N_2 Mixtures," *Bull. Am. Phys. Soc.* Series II 2(5), 280 (1957).

Interdivisional Committee on Waste Treatment and Waste Disposal (E. D. Arnold, J. O. Blomeke, K. E. Cowser, W. de Laguna, A. T. Gresky, I. R. Higgins, W. J. Lacy, C. D. Watson, R. J. Morton, Secretary, E. G. Struxness, Chairman), ORNL-2266 (Feb. 11, 1957) (classified).

L. W. Johnston, R. D. Birkhoff, J. S. Cheka, H. H. Hubbell, and B. G. Saunders, *Response of the Anthracene Scintillation Counter to Low Energy Electrons,* ORNL-2298 (April 16, 1957).

L. W. Johnston, R. D. Birkhoff, J. S. Cheka, H. H. Hubbell, and B. G. Saunders, "The Response of the Anthracene Scintillation Counter to Monoenergetic Electrons," *Bull. Am. Phys. Soc.* Series II 2(5), 279 (1957).

B. Kahn, E. R. Eastwood, and W. J. Lacy, *Use of Ion Exchange Resins to Concentrate Radionuclides for Subsequent Analysis*, ORNL-2321 (May 31, 1957).

B. Kahn, B. K. Smith, C. P. Straub, "Determinations of Low Concentrations of Radioactive Cesium in Water," *Anal. Chem.* **29**, 1210 (1957).

B. Kahn and A. Goldin, "Radiochemical Procedures for the Identification of the More Hazardous Nuclides," *J. Am. Water Works Assoc.* **49**, 767 (1957).

H. L. Krieger, B. Kahn, and C. P. Straub, *Removal of Fission Products from Reactor Wastes*, ORNL-2297 (May 24, 1957).

W. J. Lacy and D. C. Lindsten, "Removal of Radioactive Contaminants from Water by Ion Exchange Slurry," *Ind. Eng. Chem.* **49**, 1515 (1957).

W. J. Lacy and W. de Laguna, "Methods of Preparing Radioactive Cations for Tracing Ground Water," *Science* **124**, 402 (1956).

W. J. Lacy and D. C. Lindsten, "Removal of Radioactive Materials from Contaminated Water by Ion Exchange Slurry," *Abstracts of Papers, 130th Meeting Am. Chem. Soc., Atlantic City, N. J., September 16 to 21, 1956*, p 110.

D. C. Lindsten, W. J. Lacy, H. N. Lowe, A. L. Donahew, and R. Rodriguex, "Ion Exchange for the Removal of Radionuclides from Water," *Salty Dog IX* (in press) (1957).

H. N. Lowe, W. J. Lacy, B. F. Surkiewicz, and R. F. Jaeger, "Destruction of Microorganisms in Water, Sewage, and Sewage Sludge by Ionizing Radiations," *J. Am. Water Works Assoc.* **48**(11), 1363–72 (1956).

H. N. Lowe, W. J. Lacy, B. F. Surkiewicz, and R. F. Jaeger, "Gamma Ionizing Radiation for the Sterilization of Water and Sewage," *Salty Dog VIII*, ERDL (in press) (1957).

H. J. Moe, T. E. Bortner, and G. S. Hurst, "Ionization of Acetylene Mixtures and Other Mixtures by Pu^{239} α-Particles," *J. Phys. Chem.* **61**, 422 (1957).

K. Z. Morgan, "Health Physics," *American Institute of Physics Handbook* (ed. by D. E. Gray), p 250–57, McGraw-Hill, New York, 1957.

K. Z. Morgan, "Instruments for Measuring Radiations," *Encyclopedia of Instrumentations for Industrial Hygiene* (ed. by C. D. Yaffee, D. H. Byers, and A. D. Hosey), p 937–47, University of Michigan, Ann Arbor, Michigan., 1956.

K. Z. Morgan, "Maximum Permissible Internal Dose of Radionuclides: Recent Changes in Values," *Nuclear Sci. and Eng.* **1**(6), 477–500 (1956).

K. Z. Morgan, "Tables of Maximum Permissible Exposure to Nuclear Radiations," *Handbook of Biological Data* (ed. by W. S. Spector), p 469–70, W. B. Saunders, Philadelphia, 1956.

R. J. Morton, K. E. Cowser, F. L. Parker, and E. G. Struxness, *An Evaluation of the Studsvik Plan*, ORNL CF-57-2-87 (Feb. 14, 1957).

J. Neufeld and W. S. Snyder, "Dependence of the Average Charge of an Ion on the Density of the Surrounding Medium," *Bull. Am. Phys. Soc.* Series II **2**(1), 70 (1957).

R. H. Ritchie, "Plasma Losses by Fast Electrons in Thin Films," *Bull. Am. Phys. Soc.* Series II **2**(5), 287 (1957).

R. H. Ritchie, "Plasma Losses by Fast Electrons in Thin Films," *Phys. Rev.* **106**(5), 874–81 (1957).

R. H. Ritchie and A. Y. Sakakura, "Asymptotic Expansions of Solutions of the Heat Conduction Equation in Internally Bounded Cylindrical Geometry," *J. Appl. Phy.* **27**(12), 1453–59 (1956).

C. J. Rohde, Jr., "A Modification of the Plaster-Charcoal Technique for the Rearing of Mites and Other Small Arthropods," *Ecology* 37(4), 843–44 (1956).

C. C. Sartain and H. P. Yockey, "Cryostat for Reactor Irradiation of Samples," *Bull. Am. Phys. Soc.* Series II 2(3), 157 (1957).

W. S. Snyder, "The Variation of Neutron Dose with Neutron Energy and Geometry," *Proceedings of the Health Physics Society, June 25–27, 1956, Ann Arbor, Michigan* (April 1957).

W. S. Snyder and J. Neufeld, "On the Passage of Heavy Particles Through Tissue," *Radiation Research* 6(1), 67–78 (1957).

W. S. Snyder and J. Neufeld, "Vacancies and Displacements in a Solid Resulting from Heavy Corpuscular Radiation," *Phys. Rev.* 103(4), 862–64 (1956).

I. H. Tipton, M. J. Cook, R. L. Steiner, J. M. Foland, K. K. McDaniel, and S. D. Fentress, *Methods of Collection, Preparation and Spectrographic Analysis of Human Tissues*, ORNL CF-57-2-2 (Feb. 28, 1957).

I. H. Tipton, M. J. Cook, R. L. Steiner, J. M. Foland, K. K. McDaniel, and S. D. Fentress, *Spectrographic Analysis of Normal Human Tissue from Dallas, Texas*, ORNL CF-57-2-3 (Feb. 28, 1957).

I. H. Tipton, M. J. Cook, R. L. Steiner, J. M. Foland, K. K. McDaniel, and S. D. Fentress, *Spectrographic Analysis of Normal Human Tissue from Miami, Florida*, ORNL CF-57-2-4 (Feb. 28, 1957).

A. C. Upton, K. W. Christenberry, G. S. Melville, J. Furth, and G. S. Hurst, "The Relative Biological Effectiveness of Neutrons, X Rays, and Gamma Rays for the Production of Lens Opacities: Observations on Mice, Rats, Guinea-Pigs, and Rabbits," *Radiology* 67(5), 686–96 (1956).

H. P. Yockey, "An Application of Information Theory to Physics of Tissue Damage," *Radiation Research* 5(2), 146–55 (1956).

R. E. Yoder and F. M. Empson, "Experimental Sand Filters for Airborne Radioactive Particulates," *Public Works* (in press).

R. E. Yoder and F. M. Empson, "The Effectiveness of Sand as a Filter Medium," *Proceedings of Am. Ind. Hyg. Assoc., April 20–26, 1957, St Louis, Missouri* (in press).

PAPERS

S. I. Auerbach

The Soil Ecosystem and Waste Disposal to the Ground, Symposium on Radio-Ecology, Meeting of American Institute of Biological Sciences, August 28, 1956, University of Connecticut, Storrs.

S. I. Auerbach and H. F. Howden

Studies in a Drained Radioactive Contaminated Lake Basin. I. Productivity of the Pioneer Biota and Its Uptake of Sr^{90} and Cs^{137}, Ecological Society of America, December 28, 1956, New York.

S. I. Auerbach and M. Engelmann

Effects of Gamma Radiation on Population Growth in Collembola, Fourth Annual Meeting Entomological Society of America, December 27–30, 1956, New York.

R. D. Birkhoff

Experiments with Cavities, Health Physics Society Annual Meeting, June 17–19, 1957, Pittsburgh, Pennsylvania.

R. D. Birkhoff, H. H. Hubbell, Jr., and R. M. Johnston

Design and Calibration of Pocket Personnel Dosimeters for Beta Radiation, Radiological Society of North America, December 2–7, 1956, Chicago, Illinois.

R. D. Birkhoff, L. W. Johnston, J. S. Cheka, H. H. Hubbell, Jr., and B. G. Saunders

The Response of the Anthracene Scintillation Counter to Monoenergetic Electrons, American Physical Society, April 4–6, 1957, Lexington, Kentucky.

R. D. Birkhoff, R. H. Ritchie, and J. S. Cheka

The Spherical Condenser as a High Transmission Particle Spectrometer, American Physical Society, April 25–27, 1957, Washington, D. C.

R. L. Blanchard, B. Kahn, and R. D. Birkhoff

Summary paper of R. L. Blanchard's Master's thesis research work, *The Preparation of Thin, Uniform Sources for a Beta-Ray Spectrometer,* at the American Physical Society, April 4–6, 1957, Lexington, Kentucky.

W. J. Boegly

The Sintering of Reactor Wastes: Problems Associated with the Formation of Ceramic Clinkers, Working Meeting on Fixation of Radioactivity in Stable, Solid Media, June 19–21, 1957, Johns Hopkins University, Baltimore, Maryland.

T. E. Bortner

An Apparatus for Measuring Electron Attachment, Health Physics Society Annual Meeting, June 17–19, 1957, Pittsburgh, Pennsylvania.

T. E. Bortner and G. S. Hurst

An Apparatus for Measuring Electron Attachment, American Physical Society, April 4–6, 1957, Lexington, Kentucky.

T. J. Burnett

A Scale of Permissible Radiation Exposure as Dictated by Various Degrees of Emergency, U. S. Naval Air Development Center, April 1957, Johnsville, Pennsylvania.

Reactors, Hazard vs Power Level, American Nuclear Society; December 10–11, 1956, Washington, D. C.

K. E. Cowser and F. L. Parker

Soil Disposal of Radioactive Wastes Criteria and Techniques of Site Selection and Monitoring, Health Physics Society Annual Meeting, June 17–19, 1957, Pittsburgh, Pennsylvania.

F. M. Empson

Summary of Air Cleaning Activities at ORNL, Fifth AEC Air Cleaning Seminar, June 24–27, 1957, Harvard University, Boston, Massachusetts.

B. R. Fish

Practical Applications of Analog Computer to the Analysis of Distribution and Excretion Data, Health Physics Society Annual Meeting, June 17–19, 1957, Pittsburgh, Pennsylvania.

L. Hemphill

Experimental Evaluation of Ceramic Clinkers, Working Meeting on Fixation of Radioactivity in Stable Solid Media, June 19–21, 1957, Johns Hopkins University, Baltimore, Maryland.

H. F. Howden and S. I. Auerbach

Some Effect of Gamma Radiation on the Reproduction of Trogoderma sternale *(Coleoptera: Dermestidae),* Fourth Annual Meeting Entomological Society of America, December 27–30, 1956, New York.

G. S. Hurst

Advances in Mixed Radiation Dosimetry, Health Physics Society Annual Meeting, June 17–19, 1957, Pittsburgh, Pennsylvania.

Attachment of Electrons in O_2-A and O_2-N_2 Mixtures, Health Physics Society Annual Meeting, June 17–19, 1957, Pittsburgh, Pennsylvania.

Measurement of Dose from Coexisting Neutron and Gamma Radiation, Fifth Tripartite Instrumentation Conference, October 22–26, 1956, Upton, New York.

G. S. Hurst and T. E. Bortner

Electron Attachment in O_2-N_2 Mixtures, American Physical Society, April 4–6, 1957, Lexington, Kentucky.

L. W. Johnston, R. D. Birkhoff, J. S. Cheka, H. H. Hubbell, and B. G. Saunders

The Response of the Anthracene Scintillation Counter to Monoenergetic Electrons, American Physical Society, April 4–6, 1957, Lexington, Kentucky.

B. Kahn

Methods for Determining the Absorption of Radioactive Materials by Soils and Sediments, 84th Annual Meeting American Public Health Association, November 15, 1956, Atlantic City, New Jersey.

B. Kahn and A. S. Goldin

Radiochemical Procedures for the Identification of the More Hazardous Radionuclides, Nuclear Science and Engineering Congress, March 11–14, 1957, Philadelphia, Pennsylvania.

B. Kahn, E. Eastwood, and W. J. Lacy

Use of Ion Exchange Resins to Concentrate Radionuclides for Subsequent Analysis, American Chemical Society Meeting, December 6–8, 1956., Memphis, Tennessee.

W. J. Lacy

Effects of Ion Exchange Parameters on the Removal of Strontium and Stable Calcium from Aqueous Solutions, American Chemical Society Meeting, December 6–8, 1956, Memphis, Tennessee.

W. J. Lacy and D. C. Lindsten

Removal of Radioactive Contaminants from Water by Ion Exchange Slurry Agents, 130th Meeting American Chemical Society, September 1956, Atlantic City, New Jersey.

W. J. Lacy and W. de Laguna

Removal of Radionuclides from Water by Polyelectrolytic Coagulation of Shale, 131st Meeting American Chemical Society, April 7–12, 1957, Miami, Florida.

K. Z. Morgan

Health Physics, Eighth Annual Nuclear Science Seminar, December 6, 1956, Oak Ridge, Tennessee.

Health Physics and Its Application to Research and Industry, Advanced Atomic Energy Course for Management, March 6, 1957, Gatlinburg, Tennessee.

Internal Dose from Short-Lived Radionuclides, Shorter-Term Biological Hazards of a Fallout Field Symposium, December 14, 1956, Washington, D. C.

Methods of Estimating the Medical Exposure to Ionizing Radiation, Joint Meeting of ICRP-ICRU-UN Task Group, April and May 1957, Geneva, Switzerland.

Recent Changes in Maximum Permissible Exposure Values, 1957 Nuclear Congress, March 12, 1957, Philadelphia, Pennsylvania.

Recent Developments in Values of Maximum Permissible Internal Dose, Health Physics Division Information Meeting, October 26, 1956, Oak Ridge, Tennessee.

Review of Japanese Dosimetry Program, Japanese Dosimetry Meeting, January 8, 1957, Oak Ridge, Tennessee.

Status of Internal Dose Problem, Health Physics Society Annual Meeting, June 17–19, 1957, Pittsburgh, Pennsylvania.

R. J. Morton

The Engineer's Need for Ecological Research in Problems of Reactor Waste Disposal, Symposium on Radiation Biology, Meeting of American Institute of Biological Sciences, August 27, 1956, University of Connecticut, Storrs.

J. Neufeld

Dependence of the Average Charge of an Ion on the Density of the Surrounding Medium, American Physical Society, January 30–February 2, 1957, New York.

F. L. Parker

Tracers in Hydrological Studies, 38th Annual Meeting of the American Geophysical Union, April 29–30, 1957, Washington, D. C.

F. L. Parker and K. E. Cowser

The Use of Soils in the Disposal of Reactor Fuel Reprocessing Wastes, American Nuclear Society Meeting, June 10–12, 1957, Pittsburgh, Pennsylvania.

R. H. Ritchie

Plasma Losses by Fast Electrons in Thin Films, read by title, American Physical Society, April 4–6, 1957, Lexington, Kentucky.

C. C. Sartain

A Review for the Physics Teacher of Recent Work on the Relation Between Radiation Disordering and the Aging Process, American Physical Society, April 4–6, 1957, Lexington, Kentucky.

C. C. Sartain and H. P. Yockey

Cryostat for Reactor Irradiation of Samples, American Physical Society, March 21–23, 1957, Philadelphia, Pennsylvania.

W. S. Snyder

Calculation of Radiation Dose, Health Physics Society Annual Meeting, June 17–19, 1957, Pittsburgh, Pennsylvania.

E. G. Struxness, W. J. Boegly, and L. Hemphill

The Sintering of Reactor Wastes: Experimental Formation of Inert Ceramic Clinkers Designed to Retain Fission Products, American Nuclear Society Meeting, June 10–12, 1957, Pittsburgh, Pennsylvania.

H. P. Yockey

A Treatment of Aging, Thermal Killing, and Radiation Damage by Information Theory, Symposium on Information Theory in Health Physics and Radiobiology, October 29–31, 1956, Gatlinburg, Tennessee.

An Explanation of the Nature of Aging and Radiation Damage by Use of Information Theory, Health Physics Society Annual Meeting, June 17–19, 1957, Pittsburgh, Pennsylvania.

An Information Theory Treatment of the Destruction and Emergence of Order, American Physical Society, January 30, 1957, New York.

Information Theory and New Ideas in Health Physics, American Nuclear Society, December 10–11, 1956, Washington, D. C.

Mathematical Implications of the Genetic Specificity of Deoxyribonucleic Acid, Health Physics Information Meeting, October 25, 1956, Oak Ridge, Tennessee.

R. E. Yoder and F. M. Empson

A Multibed Low Velocity Air Cleaner, Fifth AEC Air Cleaning Seminar, June 24–27, 1957, Harvard University, Boston, Massachusetts.

The Effectiveness of Sand as a Filter Medium, American Industrial Hygiene Association Meeting, April 21–26, 1957, St. Louis, Missouri.

LECTURES

E. E. Anderson

Biological Effects of Radiation, Chemical Technology Division, Isolation Laboratory, ORNL, January 4, 1957, Oak Ridge, Tennessee.

Health Physics, REED Orientation Seminar on Power Reactors, July 10, 1957, Oak Ridge, Tennessee.

Health Physics Lecture Series, Chemical Technology Division, ORNL, September 11, 13, 18, 1956, Oak Ridge, Tennessee.

Nuclear Physics Review, Eighth Annual Nuclear Science Seminar, November 27, 1956, Oak Ridge, Tennessee.

Principles of Health Physics, Radioisotope Techniques School, Oak Ridge Institute of Nuclear Studies, August 17, September 14, November 2, 1956, Oak Ridge, Tennessee.

Radiation Hazards and Current Practices in Radiation Protection, presented to the following groups:

1. Division of Science and Mathematics, Fort Valley State College, April 16, 1957, Fort Valley, Georgia.
2. Physics Colloquium, Southern Illinois University, March 28, 1957, Carbondale.
3. Physics Department, University of Cincinnati, March 29, 1957, Cincinnati, Ohio.
4. Sigma Xi Society, University of Georgia, April 15, 1957, Athens.

Radiation Protection, presented to the following groups:

1. Men's Club, Bearden Methodist Church, October 16, 1956, Bearden, Tennessee.
2. Oak Ridge Institute of Nuclear Studies, Museum Division, August 15, 1956, Oak Ridge, Tennessee.

The Health Physics Profession, Physics Department, University of Rochester, October 1956, Rochester, New York.

Why Health Physics? Stable Isotopes Division Seminar, ORNL, December 11, 1956, Oak Ridge, Tennessee.

S. I. Auerbach

Ecological Problems of Health Physics, Seminar, Department of Physics, Vanderbilt University, May 16, 1957, Nashville, Tennessee.

R. D. Birkhoff

Spectral Distribution of Electron Flux in a Radioactive Medium, ORINS-ORNL Traveling Lecture, Vanderbilt University, December 5, 1956, Nashville, Tennessee.

K. E. Cowser

Waste Disposal Research at ORNL, Lecture at Vanderbilt University to AEC Fellowship students, February 13, 1957, Nashville, Tennessee.

D. A. Crossley, Jr.

Current Status of Research on American Chigger Mites, Seminar, Department of Zoology and Entomology, University of Tennessee, April 2, 1957, Knoxville.

F. M. Empson

Status of Pilot Pit No. 2, Applied Health Physics Seminar, February 6, 1957, Oak Ridge, Tennessee.

M. F. Fair

Civil Defense, presented to the following groups:

1. East Tennessee Association of Osteopathic Physicians and Surgeons, January 27, 1957, Morristown.
2. Knoxville Executive Women's Club, March 12, 1957, Knoxville, Tennessee.
3. Kiwanis Club Luncheon, April 4, 1957, Cleveland, Tennessee.

Health Physics, presented to the following groups:

1. Massachusetts Institute of Technology Practice School students, September 19, 1956; February 7, 1957, Oak Ridge, Tennessee.
2. Veterinary Radiological Health Course, sponsored by UT-AEC Experiment Station, September 24, October 8, 1956, Oak Ridge, Tennessee.

Health Physics Lecture Series, Chemical Technology Division, ORNL, September 25, 27, October 2, 4, 9, 11, 1956, Oak Ridge, Tennessee.

Health Physics Monitoring, Radiobiology Course, sponsored by the Biology Division of ORNL for Biology Division personnel, December 9, 1956, Oak Ridge, Tennessee.

Nuclear Physics Lecture Series, personnel in the Health Physics Division, September 27, October 4, 11, 18, 25, 31, November 8, 15, 29, December 6, 13, 1956, Oak Ridge, Tennessee.

Principles of Health Physics, Radioisotope Techniques School, Oak Ridge Institute of Nuclear Studies, January 18, February 15, May 10, June 7, July 5, 1957, Oak Ridge, Tennessee.

Radiation Fallout, Roane County Medical Association, February 26, 1957, Oak Ridge, Tennessee.

Radiological Protection Problems, Houston City Health Department, January 10–11, 1957, Houston, Texas.

K. Z. Morgan

Applied Problems in Health Physics at Oak Ridge National Laboratory, Health Physics Department, Atomic Energy Research Establishment, May 6, 1957, Harwell, England.

Control of Radiation by the Health Physicist, U.S. Naval Medical School, October 16, 1956; March 11, 1957, Bethesda, Maryland.

Health Physics, U.S. Naval Air Development Center, November 15, 1956, Johnsville, Pennsylvania.

Internal Exposure, Vanderbilt University, February 25–26, March 4–5, 1957, Nashville, Tennessee.

Maximum Permissible Exposure to Ionizing Radiation, Dennison University, January 14, 1957, Granville, Ohio; University of Kentucky, January 15, 1957, Lexington; Medical College of Virginia, February 21, 1957, Richmond.

Radiation Tolerances (series of six lectures), North Carolina State College, July 9–14, 1956, Raleigh.

Problems in the Applications of Health Physics. Berea College, February 18, 1957, Berea, Kentucky.

C. C. Sartain

Some Current Research in Health Physics, 3161st Research and Development Group, U.S. Army, August 8, 1956, Oak Ridge, Tennessee.

E. G. Struxness

Waste Disposal, Toxicology, etc., Lectures at Vanderbilt University to AEC Fellowship students, April 15–16, 22–23, 1957, Nashville, Tennessee.

H. P. Yockey

A Discussion of Actual Reactor Accidents, Lecture to ORSORT students, ORNL, May 16, 1957, Oak Ridge, Tennessee

Information Theory in Biology, Donner Laboratory, University of California, April 24, 1957, Berkeley.

Radiation Damage and Aging, Lecture at Vanderbilt University to AEC Fellowship students, April 11, 1957, Nashville, Tennessee.

Science and Information Theory, Chemistry Division, ORNL, November 28, 1956, Oak Ridge, Tennessee.

Solid State Research in Health Physics, Solid State Conference, ORNL, April 16, 1957, Oak Ridge, Tennessee.

Understanding Radiation Effects, Lions Club, January 14, 1957, Kingston, Tennessee.

R. E. Yoder

A Review of Sand Filter Development at ORNL, Applied Health Physics Seminar, February 6, 1957, Oak Ridge, Tennessee.